

**Morphometric analysis of taxonomy,
evolution, autecology and homology in
ozarkodinid conodonts**

Thesis submitted for the degree of

Doctor of Philosophy

at the University of Leicester

by

David Owen Jones BSc (Bristol)

Department of Geology

University of Leicester

September 2006

UMI Number: U601152

All rights reserved

INFORMATION TO ALL USERS

The quality of this reproduction is dependent upon the quality of the copy submitted.

In the unlikely event that the author did not send a complete manuscript and there are missing pages, these will be noted. Also, if material had to be removed, a note will indicate the deletion.



UMI U601152

Published by ProQuest LLC 2013. Copyright in the Dissertation held by the Author.
Microform Edition © ProQuest LLC.

All rights reserved. This work is protected against
unauthorized copying under Title 17, United States Code.



ProQuest LLC
789 East Eisenhower Parkway
P.O. Box 1346
Ann Arbor, MI 48106-1346

Morphometric analysis of taxonomy, evolution, autecology and homology within ozarkodinid conodonts

by

David Owen Jones

Abstract

A rigorous understanding of conodont element morphology is fundamental to virtually every aspect of conodont research, yet the complexity of morphological variation within elements presents a challenge for qualitative approaches. To address this problem, a suite of new morphometric protocols has been developed and applied to two conodont taxa.

Analysis of the conodont '*Ozarkodina*' *excavata* has enabled development of a new quantitative methodology to objectively discriminate between morphologically similar elements occupying different positions within the conodont skeleton. The methodology differentiated elements with a success rate comparing favourably to expert discrimination, and has application not only in identifying homology in collections of isolated elements, but also in taxonomy. The hypothesis that '*O.*' *excavata* is monospecific has also been tested, and the discovery of significant morphological discontinuities between spatiotemporally separated populations strongly suggests that multiple species are currently accommodated within this taxon. The protocols also have potential to permit repeated and objective identification of biostratigraphically useful morphologies. A natural population of '*O.*' *excavata* has been examined, elucidating population structure, survivorship and element and apparatus growth within this taxon at a level of detail exceptional even for conodont studies.

Evolutionary and taxonomic hypotheses have been tested in the conodont genus *Pterospathodus*, using a long, densely and evenly sampled stratigraphic sequence. This has revealed few discontinuities within measured variables through time, highlighting the difficulties of objective taxonomic division of an anagenetic continuum. Apparent directional evolutionary trends are partially confirmed, but analysis is hindered by the inability to identify immature elements and separate ontogenetic and evolutionary change. This study has quantified evolutionary rates in conodonts for the first time.

The methods and results presented here have the potential to catalyse comprehensive morphometric analysis of conodonts using these widely applicable protocols and refine the existing qualitative framework around which our understanding of conodont morphology is currently based.

Contents

Abstract	i
Contents	ii
Acknowledgements	iii
Introduction	1-4
Chapter one: New morphometric protocols for analysing morphological variation in conodont elements	5-32
Chapter two: Application of new morphometric protocols in identification of element homology in conodonts	33-53
Chapter three: Testing species hypotheses in conodonts – multivariate morphometric analysis of ' <i>Ozarkodina</i> ' <i>excavata</i>	54-78
Chapter four: Testing species hypotheses in conodonts – outline analysis of ' <i>Ozarkodina</i> ' <i>excavata</i>	79-103
Chapter five: The autecology of an ozarkodinid conodont	104-131
Chapter six: Morphometric analysis of evolutionary rate and pattern in the conodont <i>Pterospathodus</i>	132-164
Conclusions	165-166
References	167-177
Appendix 1: CD of data in Excel spreadsheet	

Acknowledgements

First of course, I wish to express my deepest gratitude to my supervisors Dr Mark Purnell and Professor Dick Aldridge, for all their invaluable advice and discussion, and for their tolerance of my shortcomings.

Second, I would like to express my thanks to all those who have helped me in this work by providing me with access to material: Jim Barrick (Texas), Peter von Bitter (ROM), Lennart Jeppsson (Lund), Peep Männik (Tallinn), Giles Miller (NHM); to others who advised me in lab preparation techniques: Kathy David (ROM), Andrew Swift (Leicester); and to those to who provided advice on quantitative issues: Norm MacLeod (NHM), Alistair McGowan (NHM), Abigail Brown (NHM). Thanks also to Philip Gingerich (Michigan) for providing me with his program for analysing evolutionary rates and pattern; to fellow postgraduate Dave Cornwell, for writing an automated file formatting program; and to Dave York of the Department, for producing several items of customised equipment.

Finally, I'd like to thank my parents for their encouragement and understanding over the past four years.

Introduction

Conodonts are an extinct group of early vertebrates (Aldridge and Purnell 1996, Donoghue et al. 2000, Donoghue et al. 1998), represented by one of the best fossil records of any group of organisms (Foote and Sepkoski 1999). Because of this, conodonts represent an invaluable palaeobiological tool: they constitute the premier biostratigraphic group for the Palaeozoic (Higgins and Austin 1985, Sweet and Donoghue 2001); they offer an unparalleled opportunity to study evolutionary rates, patterns and processes within early vertebrates; and by virtue of their phylogenetic position, conodonts are ideally placed to elucidate the sequence and timing of character acquisition within the vertebrate clade (Purnell 2001). The conodont fossil record consists primarily of microscopic tooth-like structures known as elements. Natural bedding plane assemblages preserving these elements in approximate life position have demonstrated that these structures formed the conodont skeleton, which functioned as an oropharyngeal feeding apparatus within the animal (Aldridge et al. 1993, Purnell and Donoghue 1997; see Figure 1).

This work deals exclusively with “complex” conodonts; those with skeletons composed of multiple element types that generally display obvious morphological differentiation. Although element morphology varied greatly between these taxa, current evidence from natural assemblages suggests that the configuration and composition of the skeleton was relatively conservative (Purnell and Donoghue 1998), particularly within the order Ozarkodinida. Figure 1 shows the 15-element apparatus architecture of a typical ozarkodinid conodont, using the biological anatomical notation of Purnell et al. (2000). The rostral portion of the apparatus, towards the front of the animal, is formed by a pair of M elements and a bilaterally symmetrical set of S elements. The S elements are numbered S_0 – S_4 from the centre outwards and comprise a single, axial S_0 element and a pair each of S_1 , S_2 , S_3 and S_4 elements, symmetrical across the midline of the animal. The caudal region of the skeleton, behind the M and S elements, is formed by two pairs of bilaterally opposed P elements: the P_2 pair rostrally and the P_1 pair caudally.

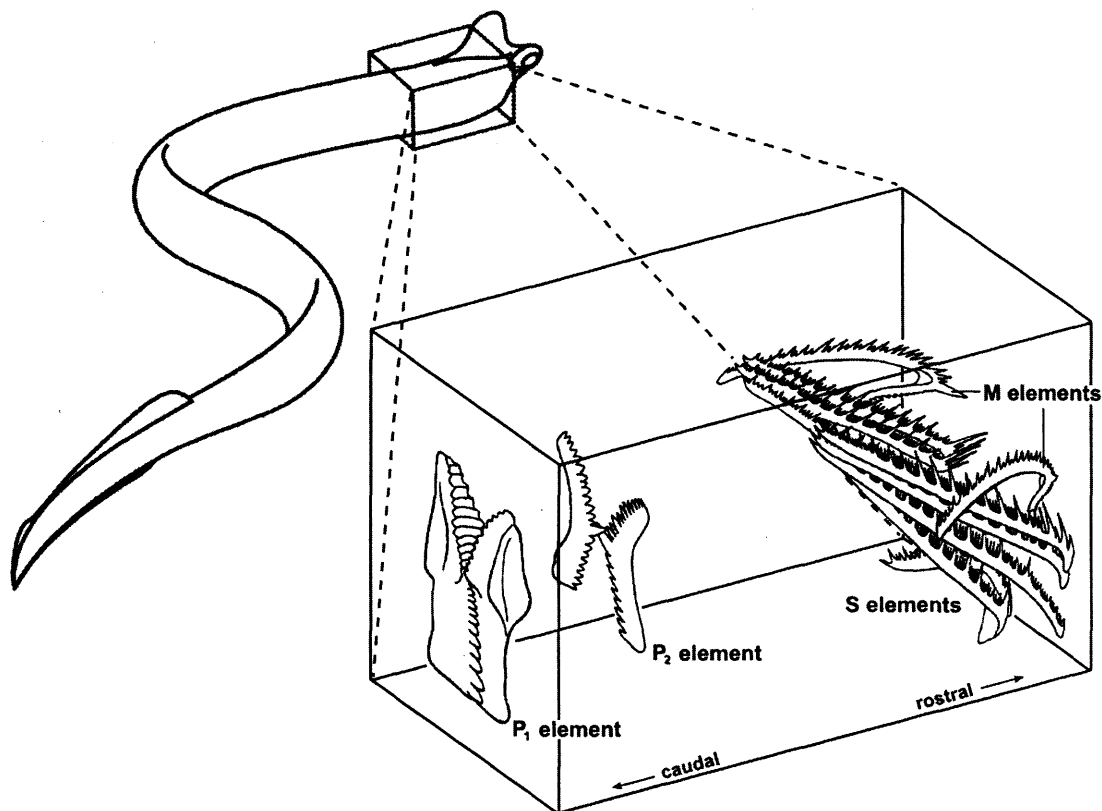


Figure 1: Diagram of a conodont illustrating skeletal architecture. Modified from Aldridge and Purnell (1996).

A rigorous understanding of conodont element morphology is obviously fundamental to virtually every aspect of conodont research. Yet despite recent advances in our knowledge of conodonts, our understanding of element morphology remains dominantly qualitative. Coupled with the subtlety and complexity of morphological variation exhibited by conodont elements, this leads to subjective conclusions regarding taxonomic schemes, biostratigraphic zonation and interpretation of evolutionary patterns, based entirely upon expert opinion. Furthermore, such an arbitrary framework renders the rigorous testing of taxonomic or evolutionary hypotheses difficult or impossible. Some conodont workers have acknowledged this (e.g. Barnett 1971, Klapper 1985).

Attempts have been made previously to address the shortcomings of traditional approaches by utilising morphometrics, but these studies are few; most date from the mid 1980s to mid 1990s, and at present comparatively little morphometric analysis is being conducted on conodonts. This, despite the ever increasing ease of applying morphometrics to fossils, thanks to more sophisticated hardware together with numerous commercial and freely downloadable image-analysis programs. Clearly, the potential contribution of morphometrics to the analysis of conodont element morphology has clearly yet to be realised.

The primary aim of the current work is to address this issue: first, by developing a set of standardised, straightforward morphometric protocols that can be easily applied by any conodont worker; and second, to utilise these protocols to analyse two conodont taxa,

'*Ozarkodina*' *excavata* (Branson and Mehl 1933) and *Pterospathodus* (Walliser 1964), thus demonstrating efficacy of the protocols at capturing patterns of morphological variation within conodont elements. These two taxa were selected because they display apparently contrasting evolutionary patterns: '*O.*' *excavata* appears not to vary systematically through time, but instead represents a single species displaying stasis; however *Pterospathodus* appears to exhibit one of the best examples of prolonged directional evolution within conodonts. The disparate morphological patterns displayed by these two taxa provide an ideal testing ground for the new protocols, which have, as the results presented herein demonstrate, contributed substantially to our understanding of these species' morphology.

However, during the course of this work, the taxonomy of '*O.*' *excavata* has been revised, with material belonging to this species reassigned to the new genus *Wurmiella* (Murphy et al. 2004). From the outset, it seems necessary to provide justification for the continued use of the name '*Ozarkodina*' *excavata* here. First, the revision has not received universal acceptance; although rigorous phylogenetic analysis does raise questions over the generic assignment of '*O.*' *excavata*, it finds no support for Murphy et al.'s (2004) taxonomic scheme (see Donoghue et al. in review). Second, questions remain as to the validity of even establishing a new name, since others may have priority (R. J. Aldridge pers. comm. 2006). Third, the majority of workers continue to use '*Ozarkodina*' *excavata* to refer to material belonging to this species, so for clarity of communication it seems preferable to continue using the nomenclature that was established in the literature at the beginning of this project. Moreover, the results presented here cast doubt on the accepted view that '*O.*' *excavata* represents a single species (see chapters three and four), so reassignment of all material belonging to this taxon to a new name seems premature. Regardless of these justifications, the revision is acknowledged by placing '*Ozarkodina*' within quotation marks when referring to '*O.*' *excavata* (following the recommendations of Bengtson 1988).

In the first chapter, the hitherto unacknowledged theoretical and practical difficulties in applying morphometrics to conodonts are reviewed. A suite of new, standardised morphometric protocols designed to characterise morphological variation within conodont elements and address these problems, is outlined. The variables measured are described and illustrated in detail, and justification is given for their use. The remaining chapters apply these protocols to analyse element morphology in '*O.*' *excavata* and *Pterospathodus*.

Chapter two examines element homology, through analysis of discrete elements and elements from natural assemblages belonging to '*O.*' *excavata* from the Eramosa Lagerstätte (Silurian, Wenlock) in southern Ontario. Tests revealed inaccuracy and inconsistency in expert discrimination of morphologically similar P₁ and P₂ elements. This could significantly hinder our understanding of conodont phylogenetics, element and apparatus evolution and

palaeoecology. A method has been developed of analysing the data acquired using the protocols to discriminate discrete P₁ and P₂ elements based on morphology alone with a level of accuracy and precision favourably comparable to that of expert differentiation. The ability of the methodology to objectively discriminate between morphologically similar elements also holds obvious promise of taxonomic application.

In two chapters, the hypothesis that '*O.*' *excavata* is monospecific is tested; first using traditional morphometrics (Chapter three), and then by applying outline analysis (Chapter four). The results of both chapters demonstrated that significant morphological differences exist between spatiotemporally discrete populations of '*O.*' *excavata*, and reveals that the characters separating them are functional. This strongly suggests that multiple species are currently accommodated within '*O.*' *excavata*. Trends of increasing P element differentiation through time were also indicated, and the ability of the analyses to repeatedly and objectively identify discrete groupings at different stratigraphic levels offers promise of biostratigraphic application.

Chapter five examines the autecology of '*O.*' *excavata*, by analysing elements from the Eramosa Lagerstätte. The hypothesis, based on taphonomic evidence, that the Eramosa Lagerstätte preserves a single population of '*O.*' *excavata*, was strongly supported by comparison of size distributions with populations of extant animals. This enabled biologically rigorous analysis of autecology within the species. Cluster analysis has revealed size groupings interpreted as generational cohorts, which were used as the basis of a survivorship analysis. This analysis suggested increasing mortality rates through time, and allowed comment regarding the nature of growth within elements. Apparatus ontogeny was demonstrated to be isometric, supporting current hypotheses of conodont element function and feeding strategies.

In Chapter six the protocols are applied to an anagenetic lineage of *Pterospathodus*, to test existing evolutionary and taxonomic hypotheses, using the longest, most densely and evenly sampled stratigraphic sequence yet analysed quantitatively in conodonts. This has revealed few discontinuities within measured variables through time, suggesting that whilst taxa currently identified within *Pterospathodus* may have biostratigraphic value, their biological reality is uncertain. Apparent directional evolutionary trends were partially confirmed, but analysis is hindered by the inability to identify and exclude immature elements from the analyses and thereby separate ontogenetic and evolutionary change. Evolutionary rates of have been quantified in conodonts for the first time.

Chapter two is ready for publication and has been formatted for the journal *Paleobiology*. Appendix one is a CD of raw data used in the analyses, and is best accessed through Microsoft Excel.

Chapter one: New morphometric protocols for analysing morphological variation in conodont elements

Introduction

Despite the importance of conodonts and the volume of work focussed on them, no comprehensive morphometric work has been conducted on the clade. Previous studies have had rather narrow aims, and ranged from simple biometric work to more sophisticated outline analyses. Significantly, they have had a wide variety of goals, demonstrating the utility and flexibility of morphometrics: these include analysis of size distributions (e.g. Jeppsson 1976), examining ontogeny and survivorship (Armstrong 2005, Tolmacheva and Löfgren 2000, Tolmacheva and Purnell 2002), testing hypotheses of feeding mechanisms (Purnell 1993, 1994), taxonomy and species recognition (Croll and Aldridge 1982, Croll et al. 1982, Girard et al. 2004b, Klapper and Foster 1986, 1993, Ritter 1989, Sloan 2003), identifying biostratigraphically useful morphologies (Barnett 1972, Lambert 1994, Murphy and Cebecioglu 1984, Murphy and Springer 1989), uncovering ontogenetic patterns (Murphy and Cebecioglu 1986), investigating evolutionary trends (Barnett 1971, Girard et al. 2004a, Murphy and Cebecioglu 1987, Renaud and Girard 1999, Roopnarine et al. 2004) and assessing different morphometric techniques themselves (MacLeod and Carr 1987). Nevertheless, the potential of morphometric analysis of conodonts that is suggested by these studies has yet to be fully realised. This chapter outlines new, standardised morphometric protocols, with wide cross-taxon application, which aim to exploit this potential, by providing a means of comprehensively quantifying and analysing conodont element morphology.

Data acquisition: theoretical considerations

The effective incorporation of biological homology is generally considered key to the power of landmark-based morphometrics, as outlined for example by Bookstein (1991 p. 56). Biological homology is identified through morphological and topological similarity of structures shared with a common ancestor, and thus justifies comparability among these structures in different individuals (Smith 1988; see Purnell et al 2000 for a discussion of homology in the conodont skeleton).

Unfortunately, biological homology is difficult to incorporate when analysing features within conodont elements, owing to their growth pattern (Donoghue 1998, Donoghue et al. in review). Element growth is indeterminate, so that the number of potential landmarks varies

widely, even between elements of a similar size and ontogenetic stage. Furthermore, element growth is accretionary, with the element increasing in size through apposition of apatite lamellae, making empirical identification of homologous landmarks difficult. Consequently, only two types of homologous landmarks, defining biologically homologous structures, can be relocated consistently in euconodont elements: both mark features of the basal cavity, the first its apex, the second its distal extremities. Both types of landmark represent developmentally significant locations: the apex of the basal cavity marks the point of initiation of element growth; the distal extremities of the cavity are the points of incremental addition of crown and basal body tissue along the axis of growth (i.e. the distal tips of the enamel-dentine interface (Sansom 1996)). Moreover, these landmarks occur only along the lower surface of the element. Purely landmark-based approaches are thus unable to capture a comprehensive picture of conodont element morphology.

Although biological homology cannot easily be incorporated into measurements of conodont elements, morphological and topological equivalence between measures can be maintained using other approaches. Several outline techniques have previously been used to analyse conodonts. Ultimately, all deal with coordinate-point data in a similar way, differing primarily in the form of this output (MacLeod 2002), but producing comparable results (Rohlf 1986). Outline analyses have been criticised for not incorporating biological homology (Bookstein et al. 1982), yet non-reliance on landmarks is a major advantage when analysing forms where it is difficult or impossible to identify biological homology (Crampton 1995, Foote 1989, MacLeod 1999, Velhagen and Roth 1997). Indeed, standard eigenshape analysis (Lohmann 1983, Lohmann and Schweitzer 1990) has been used to analyse non-biological structures, such as the form of alpine valleys and sedimentary grain shape (MacLeod 2002); here of course there is no biological homology, yet useful shape information was gained from these analyses. Elliptic Fourier Analysis (EFA, Ferson et al. 1985, Giardina and Kuhl 1977, Kuhl and Giardina 1982) has also been used to analyse conodont morphology to good effect (e.g. Renaud and Girard 1999), as have some less standard outline techniques (e.g. Klapper and Foster 1986). Eigenshape analysis has yet to be applied to conodonts, despite the fact that extended eigenshape (EES) analysis (MacLeod 1999) can utilise the landmarks at the terminals of the basal cavity, which EFA cannot: this landmark-registering allows biological homology to be incorporated. Both Elliptic Fourier and EES analysis were used in this work to examine shape in conodont elements. Standard eigenshape analysis was also used in Chapter two, where the homologous landmarks at the extremities of the basal cavity could not be reliably identified on some specimens because they required coating with ammonium chloride for imaging.

Traditional multivariate techniques (the application of multivariate analyses to simple biometrics variables such as distances, angles, ratios, etc. (Marcus 1988)) can also be utilised but have several drawbacks in comparison with landmark-based approaches. For example, they do not incorporate biological homology as effectively as landmark-based methods (Bookstein 1991), so that measured variables must have sufficient topological equivalence to ensure biological comparability from element to element. Furthermore, in the absence of a landmark-based framework (e.g. truss analysis), these traditional approaches tend to sample forms in an unsystematic, arbitrary way and thus cannot be used to recover the original form (Strauss and Bookstein 1982). However, traditional multivariate techniques do have major strengths. First, they are applicable to incomplete elements, so maximising sample sizes (an important advantage when analysing fossil material) and minimising bias towards well preserved material (Ritter 1989). Second, they can be easily applied by non-experts in morphometrics, which is an obvious benefit. Finally, because the number of traditional measurements theoretically obtainable from '*O.*' *excavata* and *Pterospathodus* is limited by the morphological simplicity of their elements, characters were not selected *a priori* as those arbitrarily deemed to be most informative (unlike many previous studies); every theoretically valid measurement was made. The patterns of morphological variation revealed by morphometric analyses of these measurements could then be evaluated in terms of their taxonomic utility or potential biological significance.

Data acquisition: empirical protocol

A standard extraction method was suitable for obtaining conodont elements from lithologies with a significant calcareous component (see Stone 1987 for review of techniques). Rock samples were placed in acid baths containing buffered acetic acid conforming to the recommendations of Jeppsson et al. (1985) and left for one to two weeks, depending on the quantity of material generated as the rock dissolved. Samples were suspended above the base of the bath in a perforated container, to speed the reaction and allow elements to fall undamaged to the bottom. Once sufficient material had accumulated, samples were removed from the baths, and the contents of the bath sieved through 1 mm and 63 μm mesh sieves. Spent acid was re-used as buffer.

The 63 μm -1 mm fraction was then sieved gently with warm water for 10-15 minutes, to remove any remaining clay, washed into a filter paper and placed in an oven to dry completely. The un-dissolved material and >1mm fraction were placed into fresh buffered acid and the process repeated until the rock was entirely dissolved or reached a point where little or no further dissolution would occur.

The Eramosa lithology required an extra stage of preparation owing to the large organic content of the rock; when sieved residues were placed into the oven to dry, the organics became consolidated into a solid mass that would have required further mechanical breakdown, leading to element damage. Therefore, after sieving, samples were placed in sodium hypochlorite (NaOCl) to oxidise the organics (Kathy David, pers. comm.). The residues required at least a week immersed in NaOCl , with gentle agitation each day. After this time, the residue was sieved for around 20 minutes, washed into filter paper and allowed to dry in air for no more than twenty-four hours (otherwise consolidation would still occur). The residue was then returned to fresh NaOCl and the cycle repeated until the water passing through the sieve cleared within minutes of starting to sieve.

Once residues had dried, a heavy liquid separation with tribromomethane (CHBr_3) was used to fractionate the residue. After flushing with acetone ($(\text{CH}_3)_2\text{CO}$) and drying, elements were removed from the heavy fraction under the microscope and placed in ten-well black-field slides, one element to a well. This ensured that each element could be easily re-located. Elements were photographed on the slide (black-field slides produced superior images to white-field slides). Elements within assemblages required ammonium chloride coating for imaging (Cooper 1935).

Images were acquired using a Qimaging Evolution Micropublisher 3 Color digital CCD camera mounted on a Leica Wild M8 light microscope. Magnification was fixed such that a 2048×1536 pixel image captured a field of view approximately 7×3 mm in size, the

maximum able to accommodate all elements at constant magnification. This apparatus is faster, cheaper and easier than scanning electron microscopy (SEM) imaging. Although image quality decreases marginally when photographing smaller elements, this can be overcome in principle by increasing the magnification for these elements, but time constraints prevented this. Specimens were illuminated with both a ring source, to avoid shadows, and directed fibre optic lighting, to maximise incident light. Polarising filters were required to eliminate the obscuring glare of reflected light. Images were captured as “tif” files within Media Cybernetics ImagePro Plus® (version 4.5) software on a PC. The images were then cropped to remove empty space around the elements, which reduced the final image size.

Despite the clarity of the resulting images, some enhancement (as defined by Bengtson (2000)) was still required before measurements could be made. This was kept to a minimum, to avoid introducing visual artefacts into an image. A HiGauss filter was applied within ImagePro Plus, which proved superior to the unsharp mask generally used for increasing image sharpness (Bengtson 2000), enhancing fine details without introducing excess noise. Slight adjustment of image brightness and contrast was also occasionally required, particularly on darker coloured elements (equivalent to CAI 4-5). Wherever image clarity following enhancement was poor enough to introduce uncertainty into the measures, the original element was re-checked.

All multivariate measures were obtained using the commercially available ImagePro Plus software. Eigenshape analysis was conducted using Adobe Photoshop® (version 7.0) for outline generation, Rohlf's digitising (tpsDig, version 1.37 (2003b)) and file manipulation (tpsUtil version 1.26 (2003a)) software and MacLeod's EES program (1999). Elliptic Fourier analysis was undertaken using PAST (Hammer et al. 2001). Measurements were insensitive to orientation in the x-y plane of the slide; however, orientation of this plane with respect to the z-axis does have an effect on the measures, so was kept as constant as possible through use of a universal stage, which allows independent tilting of the x-y plane within the z-axis. This stage is more sophisticated than Barnett's (1970) design, and allows finer control of specimen orientation.

Measurements were taken from digital images on-screen, ensuring greater accuracy and precision compared with conventional direct ocular graticule measures. A stage micrometer was photographed and used to calibrate within ImagePro Plus software. A data collection protocol combining manual and semi-automatic procedures was adopted. Working speed for the traditional measures is around three minutes per element, from imaging to data entry into a spreadsheet; for the outline analysis, it is about ten minutes per specimen.

Multivariate analysis

Since there are potentially several methods for measurement of some element features, the protocols used are discussed below to justify the particular approach adopted here. Tables 2 and 3 provide a summary of all the variables measured. Figures 5-11 illustrate the variables. Not all variables outlined below were utilised in this work, but they are included since the aim of this chapter is to provide a standardised protocol for measuring elements; the specific measurements used in each chapter are briefly described and illustrated therein. Element fragments lacking a cusp were not considered, to avoid measuring different parts of the same element. Biological anatomical notation (Purnell et al. 2000) is used for the work on '*Ozarkodina*' *excavata*. Traditional notation is used in the *Pterospathodus* work because the hypotheses tested therein are framed within this scheme. All measurements were obtained from images acquired for the purpose; illustrations from publications were not used (cf. Sloan 2003), to avoid potential bias resulting from uncertainty over details of preparation, orientation, etc. Raw measurement data used in this work are given in Appendix 1.

Length measurements

Length measures were acquired using a technique based on symmetric or median axis analysis. First used for representing outlines by Blum (1973) and later elaborated by Straney (1988), this technique internalises the outline of a 2D shape using symmetric points. These are the centres of circles that contact the margin of a shape tangentially at two or more points. A line drawn through these points forms the symmetric axis of that shape, representing a description of the object's outline. It is something of a justification from precedence that Bookstein (1991) and Velhagen and Roth (1997) used the technique in the analysis of jaw shape. A variant on median axis analysis was used in this work, with the circumference of the circles defined by two inter-denticle nadirs and the tangent point to the aboral margin (e.g. Figure 9), where a nadir is defined as the point of contact between the free tips of adjacent denticles or between denticle tip and cusp. If damage or wear made the position of the nadir uncertain, the measurement was not taken. This modified technique is fast, easy and accurate. It is important to emphasize that these are not triple point circles *sensu stricto*, since they frequently extend outside the element margin; to distinguish them, they are referred to here as anchored circles, and their centres denoted as anchored points.

The measurement line for process length is drawn from the cusp anchored point, through the anchored point of the penultimate denticle, to the distal terminus of the process. This line provides an effective and intuitive median of upper and lower margins from which

to garner data. Each process of an element was measured separately in '*Ozarkodina*' excavata P elements, and from this three other measures can be automatically obtained: total length as the sum of the processes, inter-process angle (see below) and the total length from dorsal to ventral tip (used in Chapter five).

The precision of the anchored circle technique in comparison with using linear measures constrained directly by the geometrically homologous points was tested as follows:

1. A camera lucida drawing of an '*O.*' excavata P element was opened in ImagePro Plus.
2. Points were placed on the nadirs on either side of the cusp, and on the nadirs on either side of the penultimate denticle on the ventral process.
3. Twelve additional points were then placed in arbitrary positions around the ventral cusp nadir.
4. Thirteen anchored circles were drawn for the cusp, each using a different point around the ventral nadir, and also the nadir itself. The centres of these circles were marked.
5. One anchored circle was drawn for the penultimate denticle.
6. Lines were drawn from the centre of each cusp circle to the centre of the terminal circle. The length of these lines was recorded (see Table 1, column 2).
7. Thirteen lines were then drawn directly from each of the points around the ventral cusp nadir to the terminal nadir of the penultimate denticle. The length of these lines was recorded (see Table 1, column 1).
8. The two sets of thirteen lines corresponded, such that the line from a circle anchored by a given cusp point was paired with the line drawn directly from that same point.
9. The same procedure was repeated for the anchored circle measurements, but varying two points: those on both sides of the cusp (see Table 1, column 3).

Varying the positions of the anchoring points mimics the situation when measuring elements where the placement of anchoring points is unclear. Yet even when two of the anchoring points were uncertain, using anchored circles still produced more precise measurements than a simple line. Thus, the use of anchored circles acts to reduce measurement error.

Direct linear measure	Anchored circle (one point varying)	Anchored circle (two points varying)
0.216	0.241	0.237
0.214	0.242	0.236
0.213	0.243	0.233
0.212	0.245	0.234
0.210	0.246	0.236
0.209	0.248	0.235
0.208	0.248	0.234
0.218	0.251	0.234
0.216	0.248	0.239
0.214	0.247	0.236
0.209	0.243	0.235
0.207	0.242	0.233
0.205	0.239	0.231
mean = 0.211 s.d. = 0.004	mean = 0.245 s.d. = 0.003	mean = 0.235 s.d. = 0.002

Table 1: Line lengths showing mean and standard deviation of repeat linear measures used to test accuracy of anchored circle protocol. Values are in millimetres.

On ‘*O.*’ *excavata* $S_{3/4}$ elements, total length was taken from the centre of the cusp anchored circle to the distal-most nadir, rather than to the terminus of the element (see Figure 7-8). This was because the element terminus is frequently formed by the final denticle, which projects backwards almost parallel to the process. This denticle is often broken, which would have prevented measurement of the process. The protocol was applied in all S elements.

M element lateral process length was measured on the assemblages from the Eramosa Lagerstätte (see Chapter five). This was measured as the distance between the centre of a circle anchored at the nadir between cusp and proximal-most denticle, and tangential to the basal cavity margin and cusp margin, to the distal terminus of the process (see Figure 6). This was specifically to obtain length data to examine apparatus ontogeny, and is justified because in assemblages, M elements are all flattened, and thus the measurement is far less influenced by process curvature. The measurement was not taken in isolated specimens because the markedly different degree of curvature in different specimens would have rendered the measurement non-standardised.

Uncertainties in cusp identification (see below), and therefore the positioning of the associated anchored circle, meant that the processes were not measured separately in *Pterospathodus*. Instead, total length was obtained with a single line along the long axis of the element from ventral to dorsal tip, constrained by two distal anchored circles. The disadvantage in this is that incomplete elements cannot be measured: if the total length line cannot be anchored, the other measures that are relative to it cannot be measured (see Figure 10).

Inter-process angle measurement

Because the anchored circles are affected by both the oral and aboral margins of an element, the difference in height between proximal and distal parts of a process, often observed in carminate elements (such as in classic 'O.' *excavata* P₁ element morphology), will concomitantly drag the circle centre up or down, resulting in different inter-processes angles than would be obtained from direct measurement of the aboral margin. This effect should be borne in mind when interpreting the results, as they will not always be directly comparable to inter-processes angles measured along the aboral margin, as used by some previous workers (e.g. Barnett 1971). Moreover, in P elements where the aboral margin is curved, as is often the case in 'O.' *excavata*, this approach avoids the ambiguity of placing straight lines along a curved margin to measure the arching of the element. Obviously the anchored circle technique does not capture information regarding the angular relationship between the oral and aboral margins; however, this shape information can be obtained using outline analysis (discussed later). Within the framework of this study, however, the measure is being used to analyse the *processes*, for which it does provide an appropriate measurement. Inter-process angle was not measured in *Pterospathodus* because of uncertainties in cusp identification (see below) and because the P₁ element is relatively straight.

Cusp base width

Appositional growth of the element crown may lead to incorporation into the cusp of the denticles adjacent to it. This will vary with ontogeny, and the consequent vertical shifting of the nadirs between the cusp and adjacent denticles is expected to render measurement of cusp base width relatively noisy. This should be taken into consideration when interpreting results. Although within the context of strict biological anatomical notation (Purnell et al. 2000), this measurement would be designated cusp height in P elements, and cusp length in S_{1/2} elements, cusp width seems a more intuitive term; hence it is used for all elements here. The cusp could not be reliably identified in *Pterospathodus* elements owing to its frequent morphological similarity to the denticles and difficulty in locating the basal cavity apex, and so was not measured.

Process height

This was measured only on those 'O.' *excavata* element types where height did not change dramatically along the length of a process (see Figures 5, 7 and 8). Some variation in height along the process is always present however, so a mean height was used. Where possible, this was an average of five measurements, but occasionally of four or three when damage, or in the case of assemblages, matrix, obscured the nadirs.

Widest point of element and relative position of widest point along element

These variables were measured in *Pterospathodus* elements, since it is a character that has been used previously in descriptions of *Pterospathodus* morphology (e.g. Männik and Aldridge 1989). The widest point of the element (see Figure 10) is affected by denticle fusion, so this measure is expected to be somewhat noisy.

Denticle packing

Denticle packing was used as morphometric variable by Croll and Aldridge (1982) and Croll et al. (1982), and also for 'O.' *excavata* by Murphy and Cebecioglu (1986), as a measure of denticle number per unit length. The protocol for the denticle packing measure was designed to take account of the differing structures of the elements. In 'O.' *excavata* elements, the distance along the bases of four denticles was measured, from nadir to nadir (see Figures 5, 7-10). This number of denticles was chosen as a compromise. It is small enough to minimise to effect of curvature in M elements, where a length measure along the base of the denticles is a chord between two points on a curved line, artificially inflating the denticle packing value by varying amounts depending on element curvature. It is also small enough to allow measurements of a statistically large sample of element fragments. It is large enough to gain informative data from those fragments that were measured. Moreover, it also allows more consistency in measurements between isolated elements and assemblage elements: in assemblages the M elements are typically crushed flat, so that the more denticles that are included, the less comparable is the estimate of the packing to the isolated elements. The nadir between the cusp and the first denticle was avoided since this denticle frequently shows fusion to the cusp in P elements, so denticle packing was measured from the next nadir distally (e.g. see Figure 5). Element types with specimens possessing large numbers of denticles were used to examine the accuracy of the measure in estimating the denticle packing along the length of the element, as follows:

1. Isolated elements were selected from samples of different ages and localities, each with seven or more denticles.
2. A line was drawn from the nadir between first and second denticles, to the next nadir along.
3. Another line was drawn, from the same origin, to the second nadir along.
4. This process was repeated down the length of the element, and repeated for all elements sampled.
5. The denticle packing was calculated for all lines and plotted in the graphs below. Each datum on the graph represents the packing value obtained for the number of denticles included in the measure, indicated on the abscissa. The points connected by each line represent single elements.

Figures 1-4 show that when fewer than four denticles are included, denticle packing may deviate markedly from the value obtained when the entire denticle row is included. Generally, however, packing values have stabilised at four denticles, i.e. packing values calculated from four denticles are representative of denticle packing for the element. However, this is frequently not the case for $S_{3/4}$ elements. Owing to the increasing denticle width along the denticle row in $S_{3/4}$ elements, no measurement except the entire denticle row will accurately capture the denticle packing for the element. Yet as noted above, the high frequency of breakage typically prevents measurement of the entire element. So, although this measure may not be representative of the denticle packing for the element, it does standardise between each type of element.

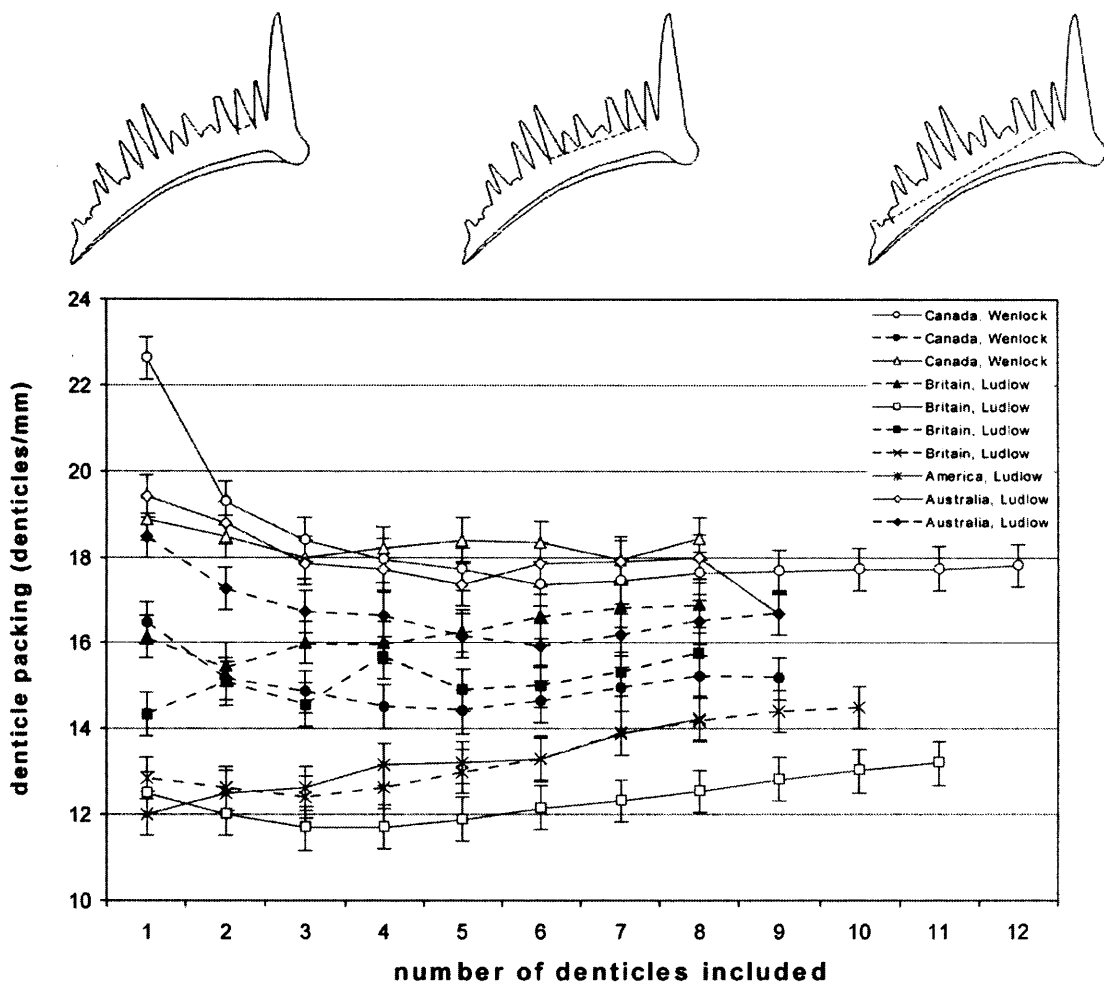


Figure 1: Lateral process denticle packing (LPDP) for ‘O.’ excavata M elements from various samples, with varying numbers of denticles included in the measure. The concave upward configuration of most of the lines reflects the concave nature of the element: increasing process curvature produces an increasingly oblique view of the element bases, which mimics the effect of increasing packing values and reducing the denticle base width. Diagrams atop the above graph illustrate measurements on an element (British, Ludlow), when one, six and twelve denticles were included. This technique was used on all element types. Different elements have different numbers of denticles: hence the lines are different lengths. The absolute difference in packing values between each element reflects inter-sample variation in the values.

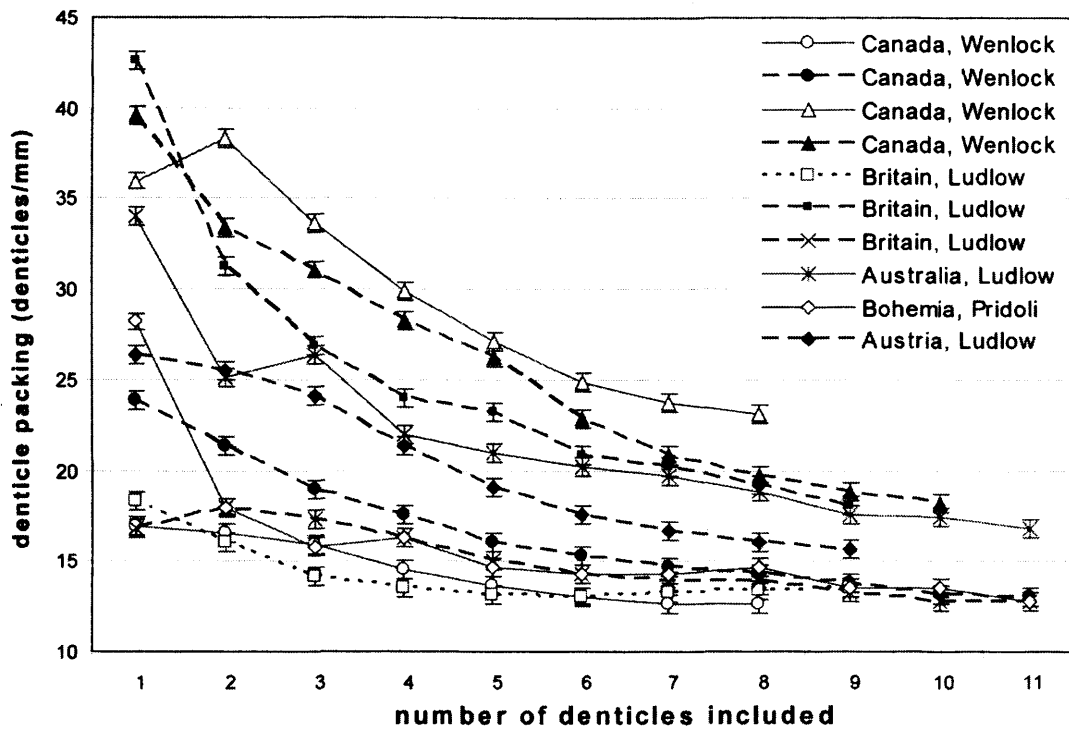


Figure 2: Posterior process denticle packing (PPDP) for ‘*O.* excavata $S_{3/4}$ elements from various samples, with varying numbers of denticles included in the measure. The exponential configuration of the lines reflects the increase in denticle base width along the process, concomitantly lowering the packing value.

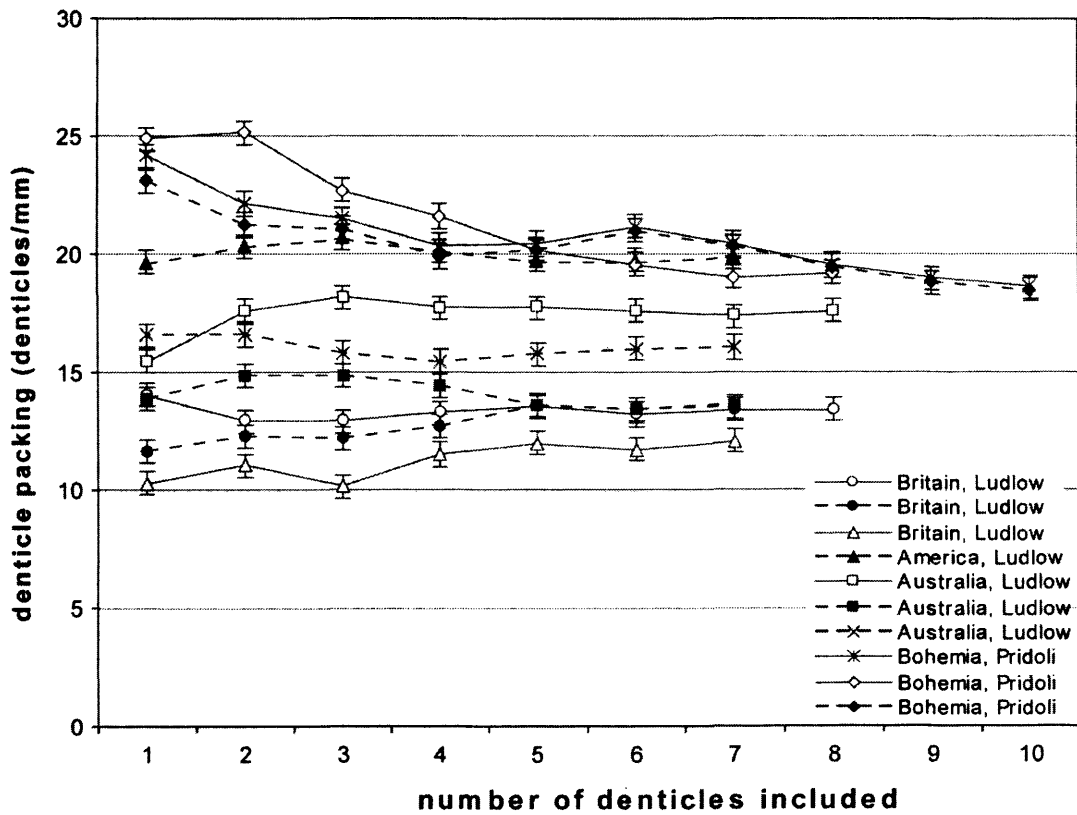


Figure 3: Ventral process denticle packing (VPDP) for ‘*O.* excavata P_1 elements from various samples, with varying numbers of denticles included in the measure.

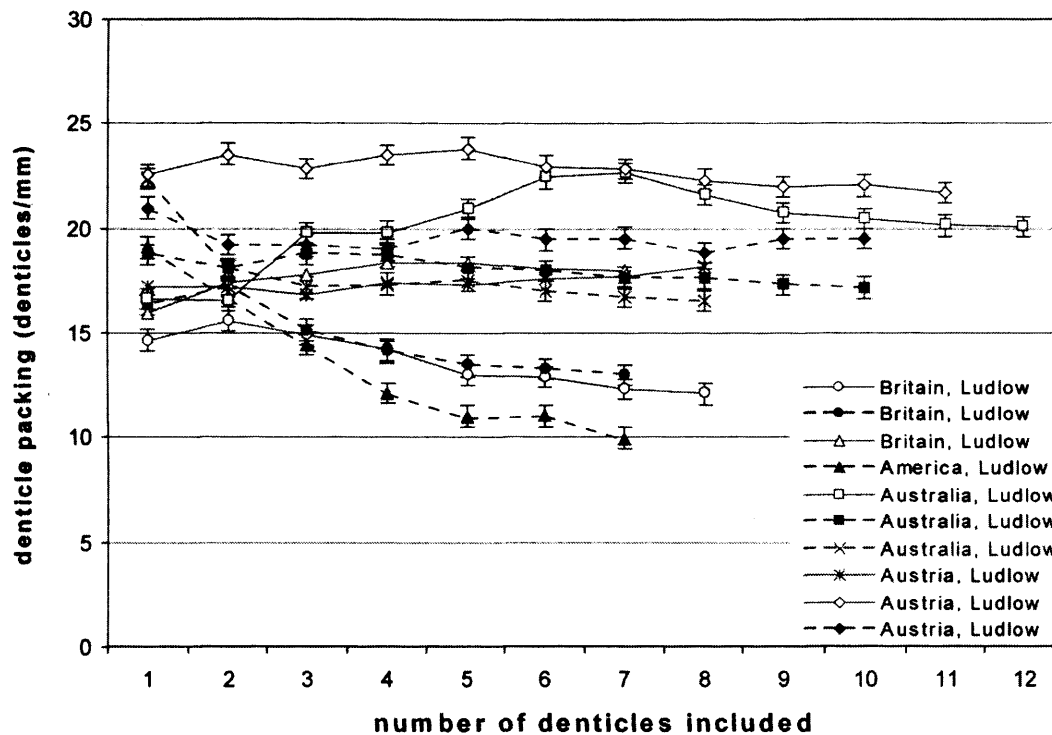


Figure 4: Dorsal process denticle packing (DPDP) for ‘*O.* excavata P₂ elements from various samples, with varying numbers of denticles included in the measure.

The morphology of *Pterospathodus* necessitated a slightly different technique for measuring denticle packing. Since the cusp in *Pterospathodus* elements could not be reliably identified (see above), the packing line was measured from the distal-most inter-denticle nadir, proximally. As with ‘*O.* excavata, the measurement line spanned four denticles. However, because denticles on the ventral process slope steeply downwards, measurement along their bases did not reflect their packing in an informative way. To compensate for this effect, the packing values were taken parallel to the total length line (see Figure 10). To a lesser extent, a similar morphology of denticulation pattern is present on the ventral processes of ‘*O.* excavata P elements and so this provides an opportunity to experiment with an alternative technique that could feasibly be applied to ‘*O.* excavata in the future. It furthermore avoids the difficulty of placing the terminals of the packing line when denticles are broken and the position of the nadirs consequently ambiguous.

Denticle number

Enumeration of denticles is occasionally problematic owing to the element growth pattern (Donoghue 1998). Initially, incipient denticles are produced, which, with further growth, develop sufficiently to be counted. Such nascent denticles have previously been coded as ½ (Tolmacheva and Löfgren 2000), but this begs the question of what counts as half a denticle. However, the problem will only become acute with smaller elements where a

difference of a single denticle can represent a major proportion of the total number. This is therefore more an interpretive caveat than a limitation on the usefulness of the measure.

Lateral process length

Lateral process length was measured only on *Pterospathodus* elements. In the absence of any homologous landmarks internal to the outline to mark the proximal terminus of the distance measure, the distance filter in the ImagePro Plus software was used. This filter calculates the distances of pixels within the outline of an object to that outline. A distance map of the object is created, where pixels are assigned a greyscale value based on the shortest distance from each pixel to the outline, in pixels (see Figure 11). Although not quite equivalent to median axis analysis, this filter internalises the element outline in an analogous way, and is ideal for providing topologically homologous points within branching structures (e.g. conodont elements with processes) for obtaining standardised measurements

Name	Abbreviation	Description	Elements measured
Ventral process length	VPL	Linear distance from the cusp anchored point to the distal process terminus, measured along a line passing through the anchored point of the penultimate denticle.	P ₁ , P ₂
Dorsal process length	DPL		P ₁ , P ₂
Anterolateral process length	ALPL		S _{1/2}
Posterior process length	PPL		S _{3/4}
Lateral process length	LPL	Linear distance from centre of circle anchored at the nadir between cusp and proximal-most denticle, and tangential to the basal cavity margin and cusp margin, to the distal terminus of the process.	M
Total length	TL	Sum of dorsal and ventral processes lengths.	P ₁ , P ₂
Inter-process angle	IPA	Angle between the dorsal and ventral process length lines (for P elements) or between the anterolateral and posterolateral process length lines (for S _{1/2} elements).	S _{1/2} , P ₁ , P ₂
Cusp base width	CBW	Linear distance between inter-space nadirs immediately adjacent to cusp.	S _{1/2} , P ₁ , P ₂
Anterolateral process height	ALPH	Mean of a series of linear distances, each measured along lines running aborally from the inter-space nadirs to the aboral margin, and orthogonal to the aboral margin.	S _{1/2}
Posterior process height	PPH		S _{3/4}
Lateral process height	LPH		M
Ventral process denticle packing	VPDP	Linear distance from the inter-space nadir proximal but one from cusp, along the base of four denticles distally. The value is divided by four to calculate the average denticle width of the process.	P ₁ , P ₂
Dorsal process denticle packing	DPDP		P ₁ , P ₂
Lateral process denticle packing	LPDP		M
Anterolateral process denticle packing	ALPDP		S _{1/2}
Posterior process denticle packing	PPDP		S _{3/4}

Ratio of cusp base width : mean denticle base width for ventral process	CBW:VPDW	Ratio of cusp base width to mean denticle width.	P ₁ , P ₂
Ratio of cusp base width : mean denticle base width for dorsal process	CBW:DPDW		P ₁ , P ₂
Ventral process denticle number	VPDN	Enumeration of denticles on the process.	P ₁ , P ₂
Dorsal process denticle number	DPDN		P ₁ , P ₂

Table 2: Summary of morphometric variables measured on ‘O.’ excavata elements. Variables are illustrated in Figures 5-9.

Name	Abbreviation	Description
Total length of element	TL	Linear distance from ventral to dorsal margin, measured along a line passing through the anchored points of penultimate ventral and dorsal denticles.
Width at widest point	WWP	Linear distance from oral-most inter-denticle nadir to the aboral margin of the element, orthogonal to the TL line.
Relative position of widest point along element	VDHP:TL	Ratio of the distance between the WWP line and ventral margin of element (indicated by PWP line in figure 10) and TL line, measured orthogonal to TL line.
Ventral process denticle packing	APDP	Linear distance along four denticles, measured from the distal-most inter-denticle nadir proximally, orthogonal to the TL line.
Dorsal process denticle packing	PPDP	
Denticle number	DN	Enumeration of denticles on the element.
Lateral process length	A/PLPL	Linear distance along median line of the process in distance map.

Table 3: Summary of morphometric variables measured on *Pterospathodus* P₁ elements. Variables are illustrated in figures 10-11.

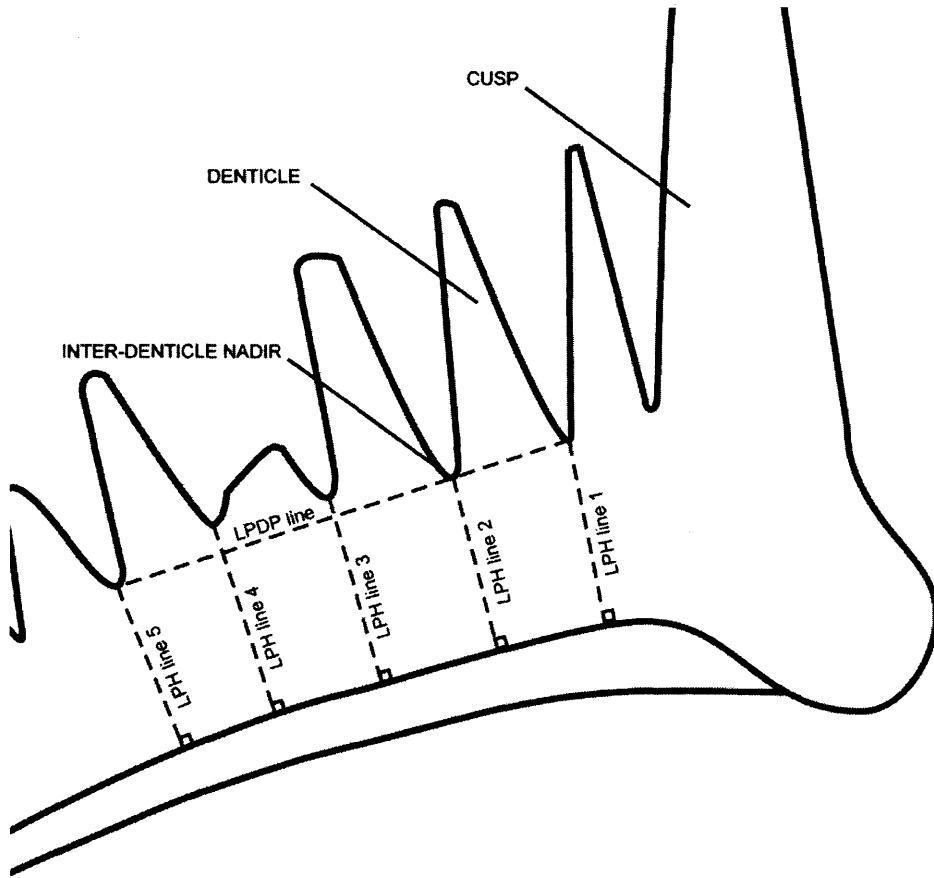


Figure 5: '*O.* excavata M element in medial view. Dashed lines represent the measures as outlined in Table 2. See Table 2 for key to abbreviations.

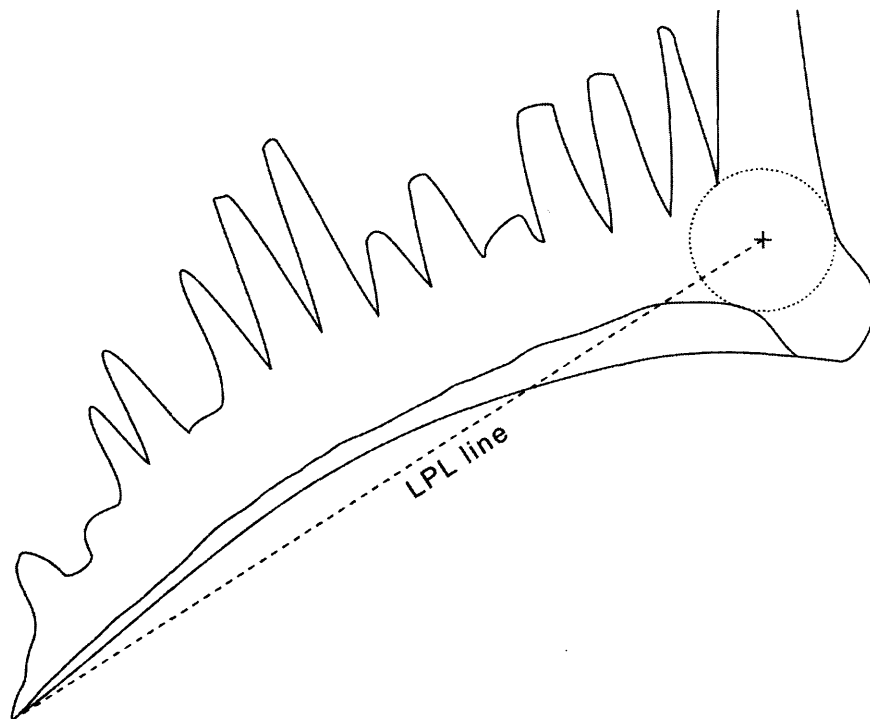


Figure 6: '*O.* excavata M element in medial view. Dashed line represents the measures as outlined in Table 2. See Table 2 for key to abbreviations.

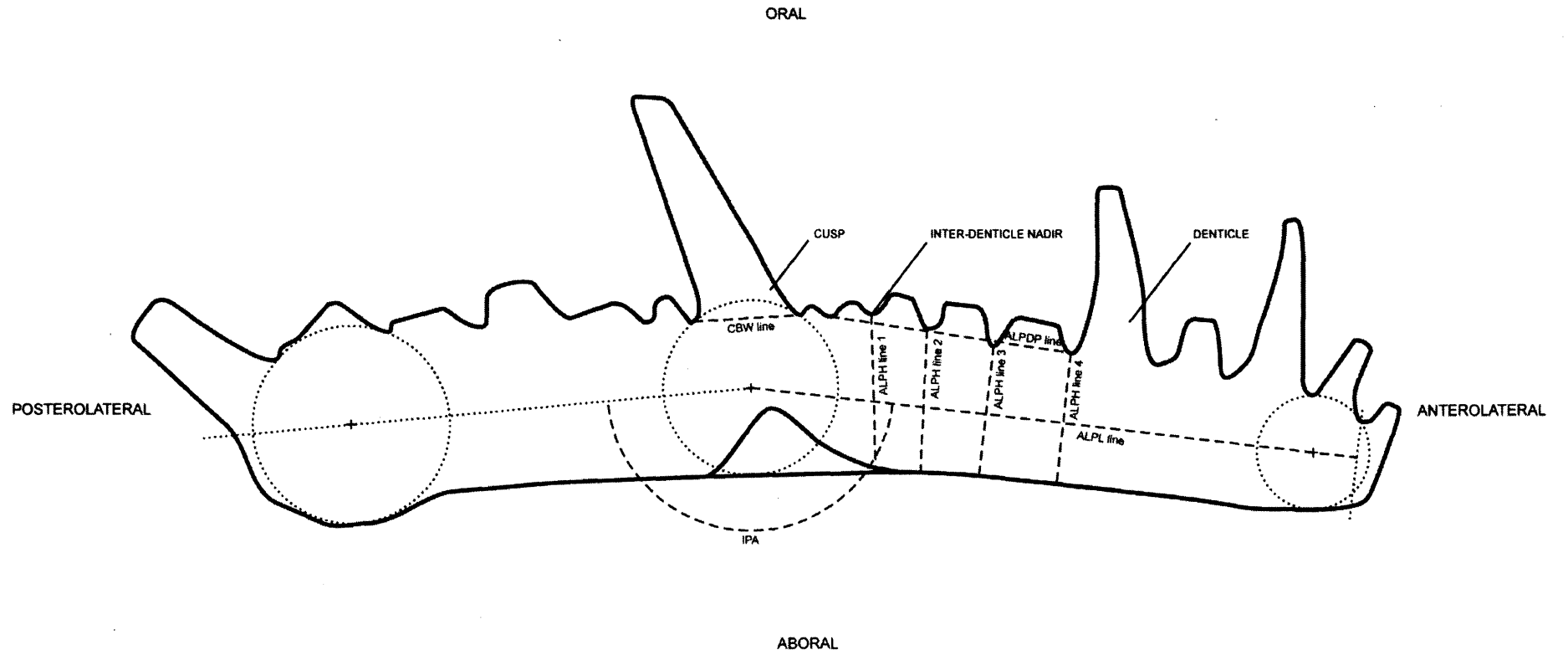


Figure 7: 'O'. excavata $S_{1/2}$ element in medial view. Anchored circles are dotted. Dotted lines are illustrative guide lines for process length and IPA measures. Dashed lines represent the measures, as outlined in Table 2. See Table 2 for key to abbreviations.

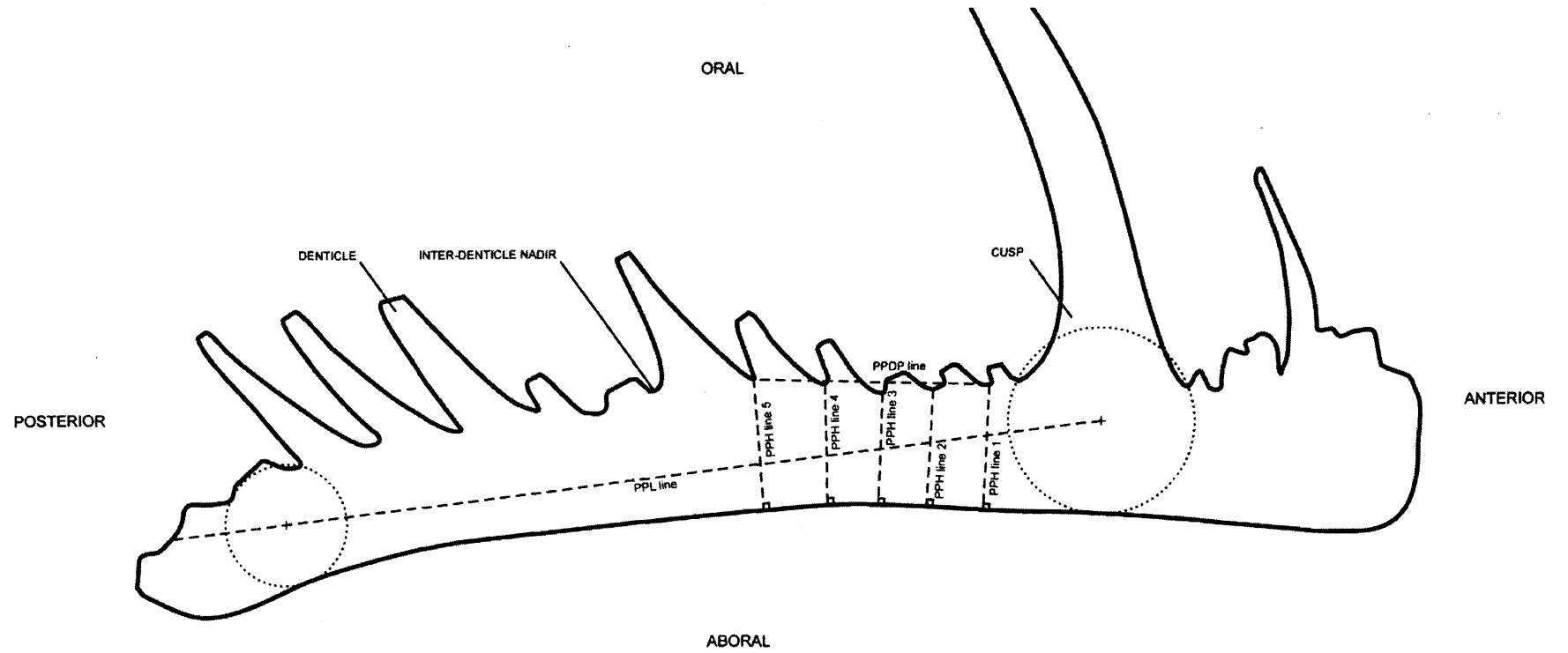


Figure 8: '*O*'. *excavata* $S_{3/4}$ element in medial view. Anchored circles are dotted. Dashed lines represent the measures, as outlined in Table 2. See Table 2 for key to abbreviations.

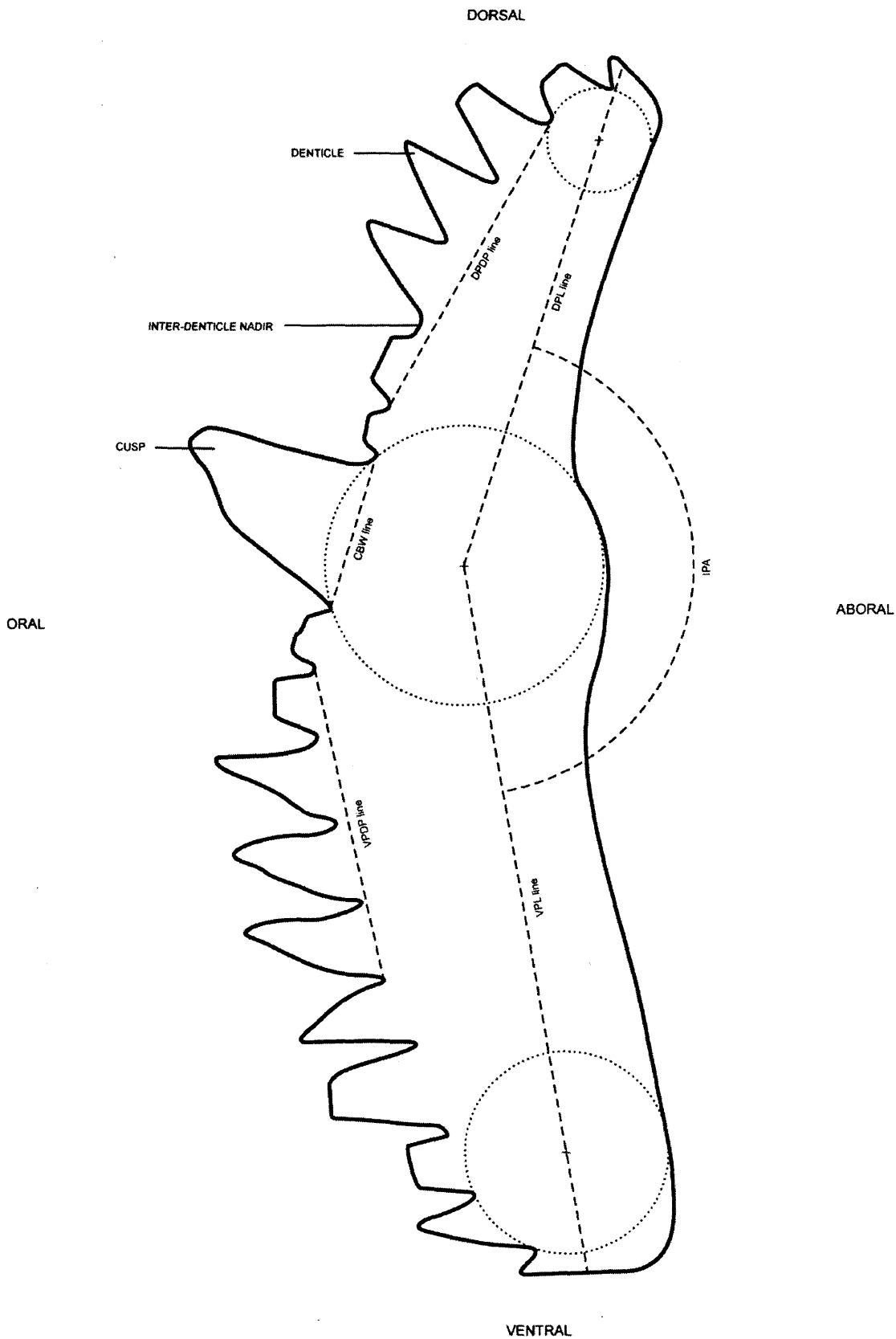


Figure 9: '*O.*' *excavata* P₁ element in rostral view. Measures are identical for P₂ elements. Anchored circles are dotted. Dashed lines represent the measures, as outlined in Table 2. See Table 2 for key to abbreviations.

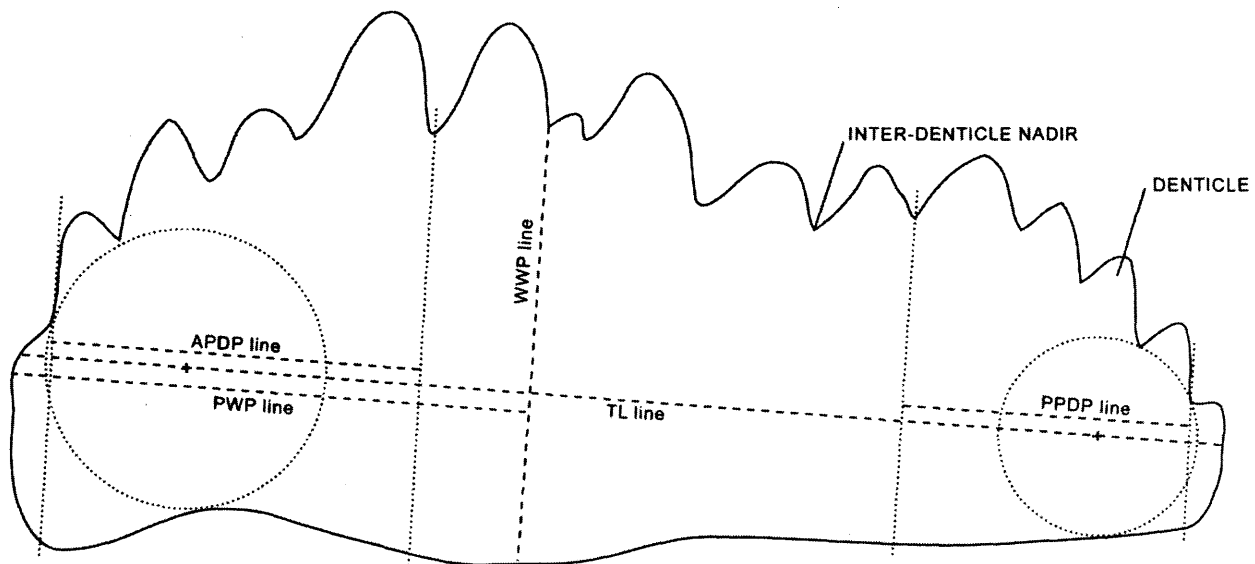


Figure 10: *Pterospathodus* P₁ element in lateral view. Anchored circles are dotted. Dotted lines are illustrative guide lines for DP lines, perpendicular to the TL line, as shown. Dashed lines represent the measures, as outlined in Table 3. See Table 3 for key to abbreviations.

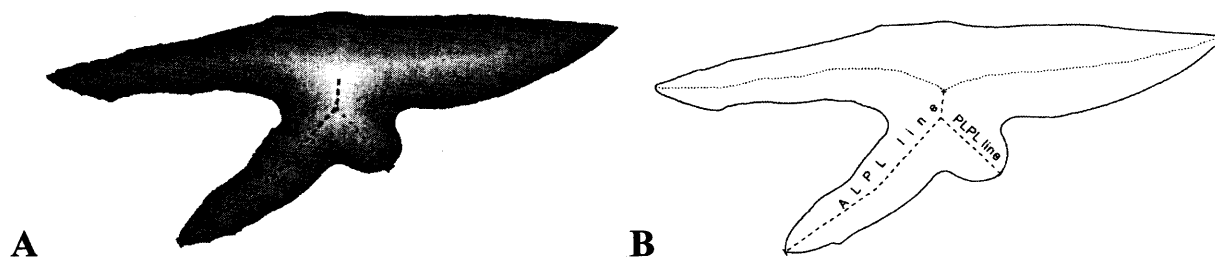


Figure 11: A) Distance map of *Pterospathodus* P₁ element in oral view, showing positioning of measurement lines along median axis of map; B) outline of *Pterospathodus* P₁ element, to more clearly illustrate measurement lines.

Outline analysis

Outline analysis has been utilised several times to investigate conodont element shape. Klapper and Forster (1986) digitised the outlines of the oral surfaces of *Palmatolepis* P elements, divided the outline into segments, took the mean of all the angles between each pair of coordinates within each segment, and used this as their raw data. Their results demonstrate that this is effective, although there are drawbacks with the method. The technique is sensitive to orientation because it measures absolute and not relative angles between coordinates on the outline; different numbers of points were used for different elements, so size changes could not be constrained effectively; the curvature of the outline varied in different segments, so that the mean angle was not always an informative measure of the angle along that segment; and no landmarks were used to register the outline. Klapper and Foster (1993) addressed the first and last of these problems – the former by orientating the posterior and anterior tips of the element to a linear guide, the latter by adding extra landmarks – but the others remain.

In a series of papers again focussing on *Palmatolepis*, Renaud and Girard (1999), Girard et al. (2004a) and Girard et al. (2004b) used elliptical Fourier analysis effectively to examine the shape of the oral surface of P elements. However, as with Klapper and Forster's studies above, Girard and co-workers used the anterior terminus of the element as proxy for the landmark at the terminus of the basal cavity. The two are frequently not the same in either '*O.*' *excavata* or *Pterospathodus*, and so this assumption should be treated with caution in all species. Also, in many carminate elements (including '*O.*' *excavata* and *Pterospathodus*) the denticle row overhangs the ventral margin in places, so that it is impossible to acquire a viable outline. Pictures of platform elements used in past analyses (e.g. Sloan 2003) also show this, yet the resultant effect on the outline is not considered.

Sloan (2003) compared different methods of acquiring and analysing outline data from various conodont taxa. Strangely, neither eigenshape nor Fourier analysis was applied; instead, several "non-standard" outline approaches were tested. Consequently, inverse Fourier functions and the modelling capabilities of eigenshape analysis could not be utilised to produce graphical representations of shape differences, and the results were presented as non-intuitive line plots. Moreover, few elements were figured, making it difficult to relate the results of the analyses back to the original specimens.

The open outline analysis of Roopnarine et al. (2004) used a cubic spline to describe the basal margin of *Wurmiella* P₁ elements, but restricting the analysis to the basal margin assumes that the most useful information is present in this region. This may be true from a taxonomic perspective (e.g. Murphy et al. 1981), but this is exactly the kind of unsystematic sampling of form for which traditional methods are criticised. Indeed, no shape analysis of the

complete rostral (*'O.' excavata*)/lateral (*Pterospathodus*) profile has been conducted prior to this work, which recognises that useful shape variability may be present in areas of the element hitherto not considered.

Outline analysis compensates for the uneven sampling of form that frequently results from traditional measures; particularly the inability of these measures to capture information regarding the width and general curvature of the element. In so doing outline analysis can provide a better measure of the overall shape of the element. Elliptic Fourier analysis (EFA, Ferson et al. 1985, Giardina and Kuhl 1977, Kuhl and Giardina 1982), eigenshape (ES) analysis (Lohmann 1983, Lohmann and Schweitzer 1990) and extended eigenshape (EES) analysis (MacLeod 1999) of the rostral profile of *'O.' excavata* and lateral profile of *Pterospathodus* P elements were conducted. Utilising several techniques allows their comparative efficiency at characterising shape variation to be assessed, and may produce complementary results (e.g Sloan 2003). For this study, the following procedure was applied for outline analysis. The procedure is described for *'O.' excavata*, using biological anatomical notation, but the procedure is identical for *Pterospathodus*.

Outline preparation

The outline of the P₁ element's rostral surface was prepared for digitisation in Adobe Photoshop. Denticles and cusp are frequently worn, broken or absent, and so required elimination from the outline: a mask was drawn around the top of the element, from nadir to nadir, and the denticles and cusp obscured. The dashed line in Figure 12 illustrates the path of this mask, creating the oral portion of the element outline. Although denticle fusion affects the smoothness of this line, in most cases it was insufficient to prevent the general shape of the element from being captured. The positions of the terminals of the basal cavity were marked on (represented by points labelled V and D in Figure 12) and the contrast of the image was increased to delineate the base of the element, producing a silhouette. The thick line in Figure 12 represents this aboral portion of the element outline.

Occasionally, small irregularities on the outline, such as mineral encrustation, required elimination. The outline was extended across these irregularities parsimoniously, using a straight line produced with a polygonal mask. This retouching, defined by Bengtson (2000) as adding what was not in the original image, is understandably advised against in most instances: for example where the fine details of internal features are of interest. It is not problematic in this situation where only the general form of the outline is under investigation and retouching is limited. Many elements were still not used if even such simple interpolation

of the outline was considered unjustified. An automated “action” can be set up in Photoshop to complete the final enhancements:

1. Application of a Gaussian blur filter, radius 1.2 pixels, to smooth the outline and reduce digitisation noise. The filter decreases the frequency of irregularities in the outline by averaging the pixels next to the hard edge. The radius dictates the area of pixels sampled for this averaging.
2. Rotation of the silhouette by 90° anticlockwise so that the ventral basal cavity terminus is in the top right hand corner, to maintain geometric equivalence during digitisation. If the ventral process of the element initially faced left, then the image was horizontally flipped.
3. Conversion of the image to greyscale to conserve memory. The image was then saved as a “tif” file.

Outline digitisation

The silhouette file was opened within the tpsDig software (Rohlf 2003b). Starting at the ventral basal cavity terminus (V) the outline was digitised anticlockwise to 200 Cartesian (x, y) coordinates and the dorsal basal cavity terminus (D) landmark registered. The data were saved as a tps file. The number of coordinates used determines how closely the digitisation follows the outline, and consequently how much of the original detail in the outline will be fed into the outline analyses: more points results in lower signal to noise ratio. For any outline analysis that involves this kind of digitisation, the initial choice is somewhat arbitrary. The 200 value was selected after first considering other workers’ choice (e.g. Klapper and Foster 1986), and then using a degree of trial and error. If too many points are included, variation from small irregularities swamps the signal; too few points results in major features being lost, such as the curvature of the aboral margin. Adjusting the outline tolerance during the EES analysis (see below) further fine-tunes the degree of shape variation incorporated in the analysis. Similar refinement can be achieved in EFA by varying the number of harmonics incorporated into the final principal components analysis (PCA): the higher the number of harmonics, the greater the detail incorporated.

Outline analysis

Both ES analysis and EFA were conducted within PAST, on the coordinate data. The Fourier coefficients from the EFA were further subjected to a PCA, also within PAST. Coefficients for all ten Fourier harmonics produced by PAST were used as variables in the

PCA. For the EES analysis, the coordinates were converted to extended phi coordinates within MacLeod's (1999) EES software. The extended phi coordinates were input to the extended eigenshape analysis program (MacLeod 1999). Tolerance was set at 99%: the lower the percentage, the less closely the outline is traced, so that noise is partitioned out, and subtle features are progressively removed. Interestingly, the first feature to be lost at lower values was the curvature of the basal margin: at 95% tolerance it was rendered straight in all but the most arched P_2 elements. This demonstrates that important shape information is not restricted to the basal margin (contra Roopnarine et al. 2004).

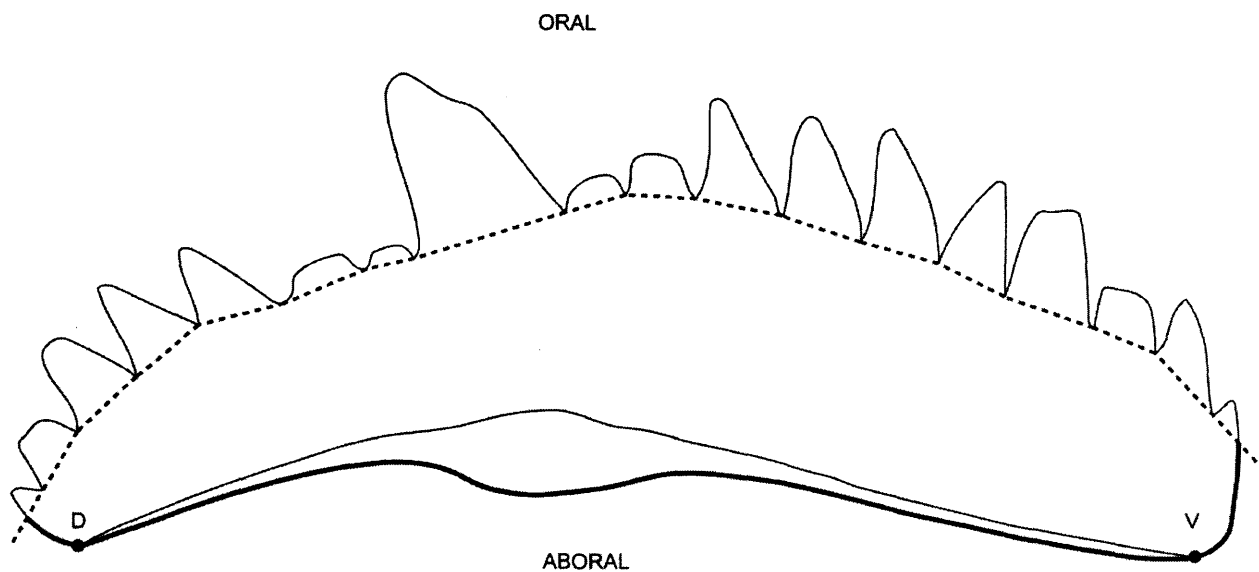


Figure 12: '*O.* excavata P_1 element in rostral view. Dashed line illustrates path of mask to obscure denticles, delineating oral margin of element outline to be analysed. Thick line represents aboral margin of outline. Points V and D mark the positions of the landmark points on the ventral and dorsal terminals of the basal cavity.

Analysis of error

The frequent omission of discussions of error has beset many previous morphometric studies of conodonts. Barnett (1971) made no mention of it but subsequently (Barnett 1972) controlled for error to some extent, stating vaguely that 2-3 operators measured some specimens several times. Error in Barnett (1972) was quoted as $\pm 1-2^\circ$ for angular measures and $\pm 0.01\text{mm}$ for linear measures. Croll et al. (1982) went no further than simply asserting that their technique was operator independent. Klapper and Foster (1986) constrained error by re-digitising fifteen specimens; however, it seems this was conducted once only, and not by different operators. Tolmacheva and Purnell (2002) quoted error at less than $10\mu\text{m}$ for their linear measures. No consideration of error was given in any other studies of conodont morphometrics.

Three potential sources of significant operator error were identified in this study: systematic error in calibration within ImagePro Plus was assessed through repeat calibrations of stage micrometer images; errors in linear and angular measures from inconsistencies in orientation of the x-y plane were assessed by multiple re-acquisitions of images for an element, with the stage adjusted afresh each time; pure measurement inconsistencies were assessed by repeat measurements of one linear and one angular measure on one image. For each of these analyses of potential errors, repeat measures were obtained by one operator, with measurements taken days apart to minimise bias from recall. Results are shown in Table 4.

	Calibration error	Orientation error (linear)	Orientation error (angular)	Measurement error (linear)	Measurement error (angular)
Replications	50	12	12	12	12
Mean	0.842 $\mu\text{m}/\text{pixel}$	0.24 mm	127.5°	0.117 mm	147.7°
Standard deviation	0.008 $\mu\text{m}/\text{pixel}$	0.001	0.477	0.005	0.761
Error	$\pm 0.03 \mu\text{m}/\text{pixel}$	$\pm 0.004 \text{ mm}$	$\pm 1.8^\circ$	$\pm 0.005 \text{ mm}$	$\pm 2.2^\circ$

Table 4: Statistics from repeat measures made within ImagePro Plus to assess error. Error values are based on the difference between mean and the upper/lower value of the range, whichever produces the larger value. Linear orientation error was assessed using an Eramosa ‘*O.*’ excavata M element (specimen no.: M-1-1), because this element type is the most three-dimensionally curved and so its measurements are most prone to error of this kind. Angular orientation error was assessed using an Eramosa ‘*O.*’ excavata S₀ element (specimen no.: S₀-1-8), this element also being three-dimensionally curved but unlike the M element, allowing an angular measure. Measurement error was assessed through measurement on an image of an Eramosa ‘*O.*’ excavata P₁ element (specimen no.: P-1-2A). An image of a small element of lower resolution was selected so as to maximise the potential error and obtain a “pessimistic” estimate.

Chapter two: Application of new morphometric protocols in identification of element homology in conodonts

Abstract.—Accurate hypotheses of primary homology within conodont skeletal elements are vital for most aspects of conodont research. However, morphological similarity of elements occupying different positions within the conodont skeleton can result in erroneous hypotheses of homology within collections of discrete elements. The Eramosa Lagerstätte of Ontario (Silurian, Wenlock) preserves both isolated skeletal elements and natural assemblages of articulated conodont skeletons. The latter provide a topological context within which to test hypotheses of element homology. Blind testing of qualitative discrimination of P₁ and P₂ elements of 'Ozarkodina' excavata from the Eramosa Lagerstätte by experienced workers revealed inaccuracy and inconsistency in distinguishing P element type. Using new, standardised morphometric protocols, the efficacy of characters used in traditional qualitative identification of P element homology for distinguishing P element types was tested individually using element pairs from articulated skeletons. No single variable achieved satisfactory discrimination success. Discriminant Function Analysis (DFA) of P₁ and P₂ elements from articulated skeletons revealed significant morphological differences between the two P element types. A combined sample of discrete and natural assemblage P elements was subjected to Principal Components Analysis (PCA). This produced a good multivariate discrimination of P element type: over 95% of natural assemblage P elements were correctly assigned; discrete elements were clearly separated. Eigenshape (ES) analysis and elliptic Fourier analysis (EFA) were also used to examine homology. EFA proved most effective at distinguishing P₁ and P₂ elements within natural assemblage elements, and produced comparable results to the PCA of multivariate measures. These results demonstrate the efficacy of the new morphometric protocols used, which hold promise of broad application to other conodont taxa where identification of element homology in collections of isolated specimens is problematic.

Introduction

Accurate hypotheses of primary homology between conodont elements are integral to most aspects of conodont research (Purnell and Donoghue 1998, Purnell et al. 2000). Element homology can only be identified unequivocally if skeletal architecture is fully understood (Barnes et al. 1979, Purnell 1993, Purnell et al. 2000). However, the configuration of the apparatus can only be determined from natural assemblages and fused clusters; within collections of discrete elements, interpretations of element homology are reliant largely upon morphological criteria (Purnell 1993). Since the conodont fossil record is dominated by disarticulated skeletal elements, problems can arise when elements occupying different positions within the conodont skeleton display similar morphologies. This is exemplified in the fossil Konservat-Lagerstätte of the Eramosa Member (Silurian, Wenlock) on the Bruce Peninsula of southern Ontario, which preserves both articulated conodont apparatuses and isolated skeletal elements. Several conodont species are represented in the Eramosa Lagerstätte but the fauna is dominated by 'Ozarkodina' excavata (Branson and Mehl 1933). Examination of 'O.' excavata apparatuses from the Eramosa Lagerstätte has revealed individuals whose P₁ and P₂ element morphology appears remarkably similar (von Bitter and Purnell 2005; see Figure 1 for examples).

Within collections of isolated conodont elements, which represent the bulk of the conodont fossil record, inaccurate identification of P element homology resulting from morphological similarity of P₁ and P₂ elements could have significant implications for our understanding of conodont palaeobiology and phylogenetics: it could introduce false hypotheses of primary homology into cladistic and other phylogenetic analyses, potentially obscuring hypothesised relationships between taxa (Hawkins et al. 1997); it could confound palaeoecological studies, for example by producing erroneous palaeoabundances (e.g. von Bitter and Purnell 2005) and masking true population structure; and it could confuse patterns of morphological evolution occurring within each element position (Purnell 1993). For example, previous interpretations of changing apparatus structure involving hypotheses of element loss or addition (e.g. Merrill and Merrill 1974) most probably result from morphologically similar elements occupying multiple positions within the apparatus. In cases such as 'O.' excavata, where the apparatus contains non-homologous but morphologically similar elements, it is clearly necessary to test hypotheses of conodont element homology and address these potentially significant biases.

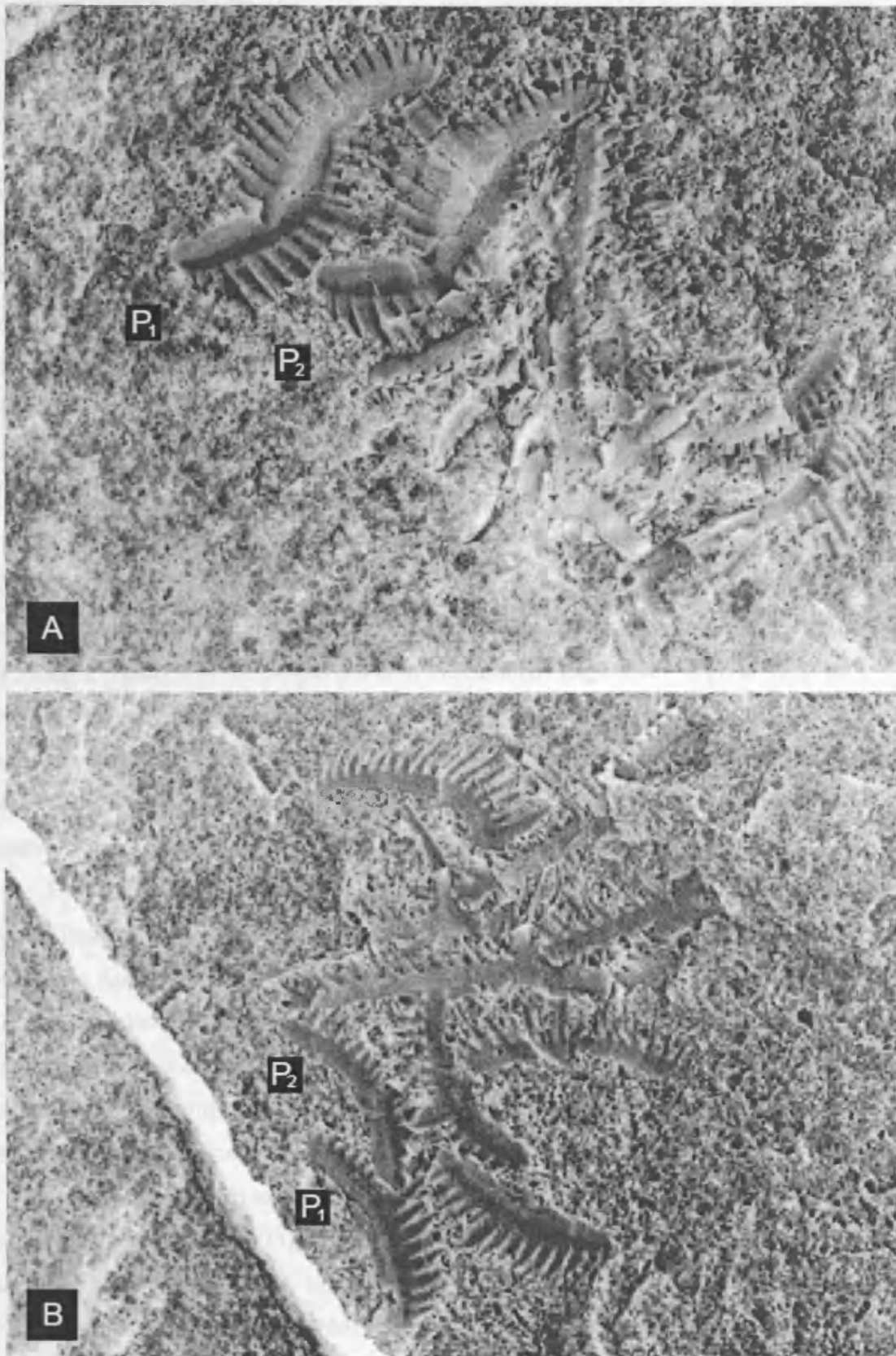


Figure 1: light micrograph of A) ROM assemblage 128 and B) ROM assemblage 144 after ammonium chloride coating, illustrating morphological similarity of P_1 and P_2 elements in 'O. excavata from the Eramosa Lagerstätte.

Material and Methods

This work is based on material from the Eramosa Lagerstätte. Most of the discrete elements and all of the articulated skeletons deriving from the lagerstätte were prepared at the Royal Ontario Museum (ROM), Toronto, and are housed in the ROM collections. Discrete elements were extracted using standard rock dissolution techniques, with some additional processing required owing to the nature of the Eramosa lithology (see Chapter one). Apparatuses were removed intact from bedding planes by undercutting with a small, carborundum-coated rotary blade on a Dremel electric tool (P. von Bitter personal communication 2006). Some isolated elements were acquired from two Eramosa sub-samples (of samples 01PB1 and 02PB1, see von Bitter and Purnell 2005) provided by the ROM and prepared at the Micropalaeontology laboratories in the Department of Geology, University of Leicester. These sub-samples were predominantly carbonate lithologies. Frequency of elements within the sub-samples of 01PB1 and 02PB1 respectively is approximately 96 kg^{-1} and 50 kg^{-1} . Preservation of elements within the Eramosa Lagerstätte is good: isolated specimens generally have complete processes, and frequently retain intact denticles; elements preserved in apparatuses are generally fragmented, but fragments remain correctly juxtaposed in most cases. All elements are pale amber in colour. Further details of the lithology, preservation and biota of the lagerstätte are given in von Bitter and Purnell (2005).

P elements from 33 articulated skeletons and 62 isolated P elements were measured. Element images from which data were acquired are provided in Appendix One. Raw data is tabulated in Appendix Two. Varying numbers of elements were measured from each skeleton, depending on element completeness and the number of elements unobscured by matrix; where feasible, matrix was carefully removed with a fine needle to provide better exposure. Nevertheless, measuring elements within natural assemblages remains difficult, limiting sample sizes. Elements on which preparation was conducted are recorded.

Data were acquired using the morphometric protocols outlined in Chapter one and Jones and Purnell (in press). Figure 2 illustrates the measured variables and the biological anatomical notation used in this work (Purnell et al. 2000). Table 1 provides descriptions of the measured variables and their abbreviations. Discriminant function analysis (DFA), a multivariate classification technique, was used for examining a priori groupings of elements, to test the discriminatory power of variables based on their capacity to correctly assign elements to known P element groupings. Hotelling's T^2 , a multivariate t-test, was used to test for significant differences between P_1 and P_2 elements. Because this is a parametric test applied to non-normally distributed data, only highly significant results were accepted as

justification for rejecting the null hypothesis, to minimise the risk of committing a Type I error (false rejection of the null hypothesis). Principal components analysis (PCA), a standard distribution-free ordination technique for reducing dimensionality in multivariate data and visualising and exploring data structure, was used where elements were not all grouped a priori. Spearman's rank correlation, a non-parametric test of correlation, was used to statistically assess patterns of co-variation between P₁ and P₂ elements. Two outline analyses were conducted on the rostral profile of the P elements (see Chapter one for methodology). Figure 3 illustrates the outline analysed. Sample size was limited because only elements with complete aboral margins could be included within the outline analyses, but 55 specimens of natural assemblage and discrete P elements were included. Owing to the necessity of coating the assemblages with ammonium chloride for imaging, landmark points at the terminals of the basal cavity could not be reliably identified. Thus, standard eigenshape analysis (Lohmann 1983, Lohmann and Schweitzer 1990) was utilised in place of the extended eigenshape analysis (MacLeod 1999) applied in other chapters. Although this means that the eigenshape results will not be strictly comparable, it does provide the opportunity to assess the efficacy of what is considered a less sophisticated technique (MacLeod 1999). The second outline analysis employed was elliptic Fourier analysis (EFA: Ferson et al. 1985, Giardina and Kuhl 1977, Kuhl and Giardina 1982). This produced forty Fourier coefficients, which were used as variables in a PCA. The PCA of the traditional multivariate dataset was based on a correlation matrix, because of the different units and scales of the variables, however the PCA of Fourier coefficients utilised a covariance matrix. In both DFA and PCA, missing data were dealt with using mean replacement; although unavoidable, this will have the effect of reducing variation within the dataset. Replacement was conducted within-groups: missing values for natural assemblage P₁, P₂ and discrete elements were replaced with means values for each group, rather than with mean values for all elements. All analyses were conducted in PAST version 1.44 (Hammer et al. 2001), SPSS version 14 and MINITAB version 14. Graphs were produced in Microsoft Excel and MINITAB version 14.

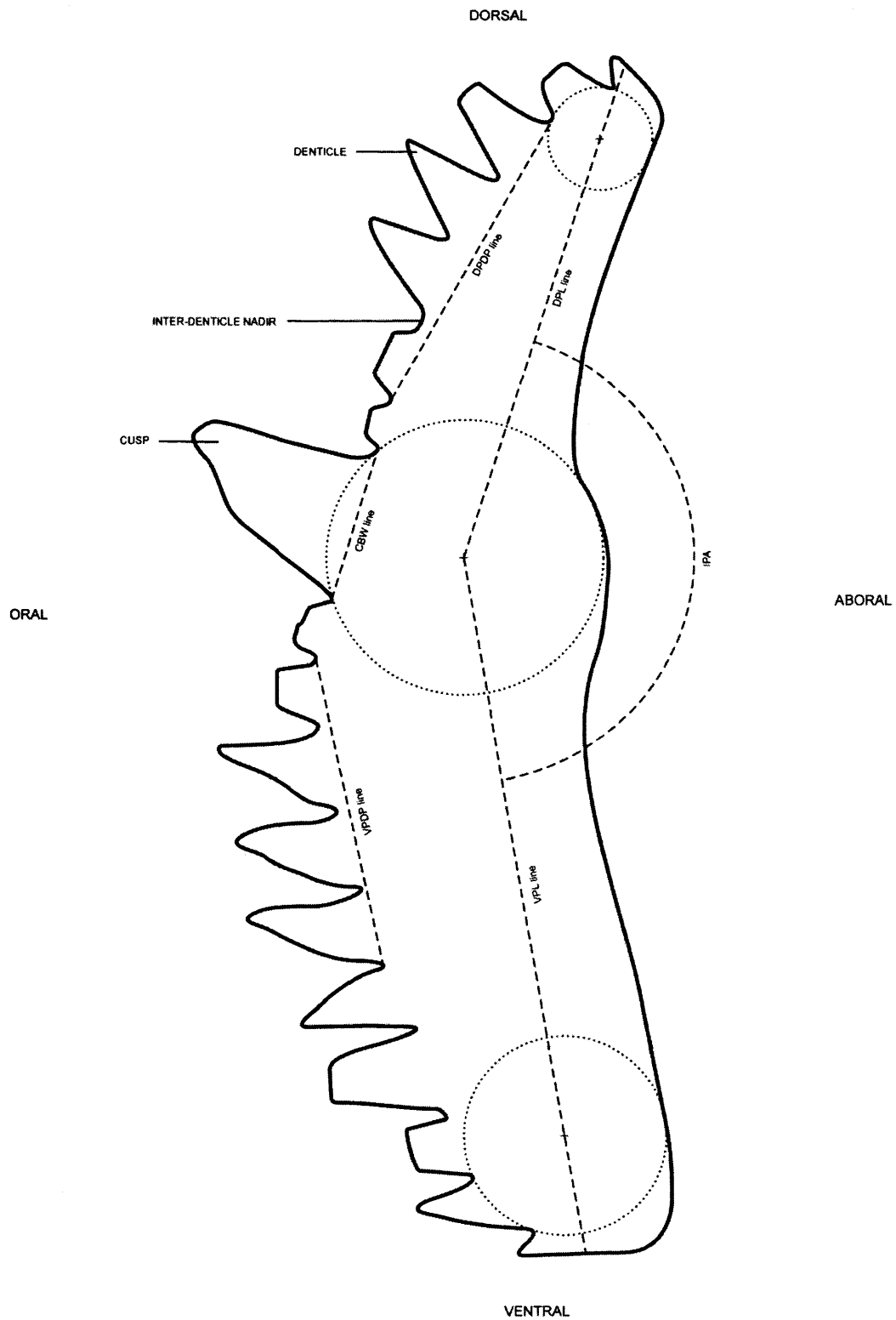


Figure 2: '*O.* *excavata* P₁ element in rostral view. Measures are identical for P₂ elements. Anchored circles are dotted. Dashed lines represent the measures, as outlined in Table 1. See Table 1 for key to abbreviations.

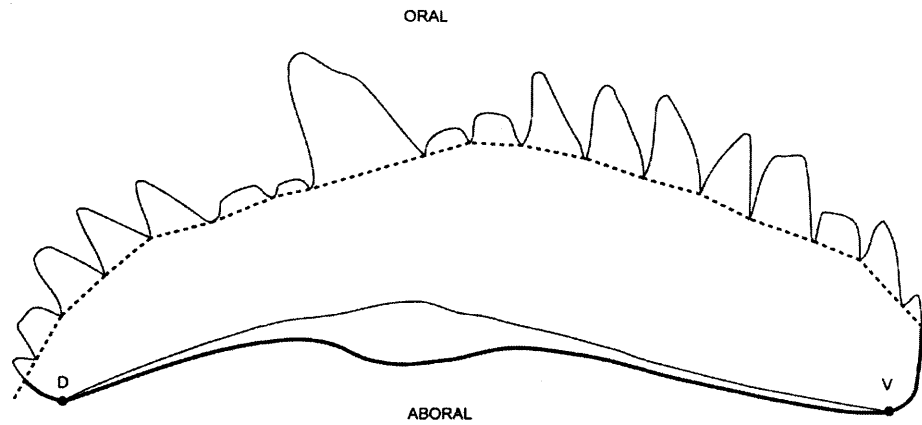


Figure 3: ‘O.’ excavata P₁ element in rostral view. Dashed line illustrates path of mask to obscure denticles, delineating oral margin of element outline to be analysed. Thick line represents aboral margin of outline.

Name	Abbreviation	Description
Ventral process length	VPL	Linear distance from the cusp anchored point to the distal process terminus, measured along a line passing through the anchored point of the penultimate denticle.
Dorsal process length	DPL	
Total length	TL	Sum of dorsal and ventral processes lengths.
Inter-process angle	IPA	Angle between the dorsal and ventral process length lines.
Cusp base width	CBW	Linear distance between inter-space nadirs immediately adjacent to cusp.
Ventral process denticle packing	VPDP	Linear distance from the inter-space nadir proximal but one from cusp, along the base of four denticles distally.
Dorsal process denticle packing	DPDP	The value is divided by four to calculate the average denticle width of the process.
Ratio of cusp base width : mean denticle base width for ventral process	CBW:VPDW	Ratio of cusp base width to mean denticle width.
Ratio of cusp base width : mean denticle base width for dorsal process	CBW:DPDW	
Ventral process denticle number	VPDN	Enumeration of denticles on the process.
Dorsal process denticle number	DPDN	

Table 1: Summary of morphometric variables measured on ‘O.’ excavata P₁ elements. Variables are illustrated in Figure 2. See Chapter one and Jones and Purnell (in press) for discussion of measured variables.

Qualitative Identification of Element Homology

The accuracy of qualitative differentiation based on morphology alone was first tested in a blind experiment. Nineteen images of P element pairs from apparatuses were cropped from their skeletons in Adobe PhotoShop, so as to obscure their topological context. These images were then presented to experienced conodont workers subscribed to the con-nexus listserv (<http://www.conodont.net>), who were asked to discriminate between P₁ and P₂ elements. Five people responded; of the 19 P element pairs, eight pairs were correctly identified by all workers, one pair was incorrectly assigned by all workers, and the remaining ten pairs had varying numbers of incorrect and uncertain identifications by different workers. Successful discrimination was related to individual experience: Silurian workers familiar with 'O. excavata' identified the most element pairs correctly, those working on other geological periods made the greatest number of inaccurate identifications. Although some workers correctly identified most elements, inconsistency between workers produced an overall success rate of 63%. In light of this between-worker inconsistency, the test was repeated using a further 12 images of discrete P elements, whose assignment was unknown, to test precision. This sample included specimens below the lower size range of the bedding-plane elements, to examine discrimination of younger individuals. A second group of five people responded, some of whom took part in the first test; 50% of these discrete P elements were assigned differently by different workers. The incidence of inaccuracy and inconsistency among even experienced researchers suggests that novice workers may often incorrectly distinguish P₁ and P₂ elements within 'O. excavata'. This bias will be more acute in taxa where P elements are less morphologically differentiated, for example within the prioniodinids (Purnell 1993).

Quantitative Identification of Element Homology

Because they preserve the elements of the conodont oropharyngeal apparatus in approximate life position, the natural assemblages preserved in the Eramosa Lagerstätte offer a unique opportunity to further examine and address the shortcomings of qualitative identification of element homology. By providing statistically large samples of 'O. excavata' P elements in topological context, and therefore with known assignment to P₁ or P₂ positions within the skeleton, the Eramosa Lagerstätte allows quantitative analysis of the morphological characters used by experienced workers to differentiate 'O. excavata' P elements, to test whether these characters provide an accurate and precise guide to distinguishing P₁ and P₂ elements in this species.

To determine how effective are the traditional characters used to differentiate P element types, several characters were selected and investigated individually. The characters were chosen based on discussions with an experienced conodont worker and on examination of illustrated specimens (Jeppsson 1969: Fig. 3, 1974: Plate 4, R. J. Aldridge, personal communication 2002). P element arching is commonly used to distinguish between P element types in 'O. excavata': P₁ elements are straight; P₂ elements are arched. Inter-process angles are used to capture this morphological information (see Chapter one and Jones and Purnell (in press) for methodology); straighter elements have larger inter-process angles, and arched elements have smaller inter-process angles. Another frequently used diagnostic character is cusp size: P₁ elements have smaller cusps than P₂ elements. It complete elements, cusp height is generally used. However, cusp height is difficult or impossible to measure because of both potential wear at the tip and breakage. Yet breakage equally confounds qualitative assessment of cusp height, and is often present in figured examples of 'O. excavata' P₂ elements (e.g. Jeppsson 1969); in these cases, the cusp base must be used to provide an indication of cusp size. Since cusp base width can be readily measured, it is used here as an alternative to cusp height. Finally, relative process length was also examined; P₁ elements generally have relatively longer ventral process, P₂ elements relatively longer dorsal processes.

Figure 4 plots each of the characters mentioned above for a P₁ and a P₂ element in each of a series of natural assemblages from the Eramosa Lagerstätte, to test the predicted patterns of co-variation within the skeleton used to recognise P element homology. The discriminatory rules are generally upheld for all characters. Figure 4A shows that most P₁ elements do have larger inter-process angles than the P₂ elements in each skeleton, producing a discriminatory success rate of 78%. Likewise, Figure 4B shows that most P₁ elements do have narrower cusp bases than P₂ elements, correctly discriminating 83% of P elements. Finally, Figure 4C shows the ratio of ventral:dorsal process lengths for P₁ and P₂ elements, revealing that the ratio for most P₁ elements is greater than one, indicating a relatively longer ventral process, and that for most P₂ is lower than one, indicating a relatively longer dorsal process, producing a 100% success rate in discriminating natural assemblage P₁ and P₂ elements. Results of Spearman's rank correlation are provided in Figure 4. For P₁ and P₂ elements within each natural assemblage, inter-process angle and ventral:dorsal process were not significantly correlated; however significant correlation was present in cusp base width for P₁ and P₂ elements within the natural assemblages.

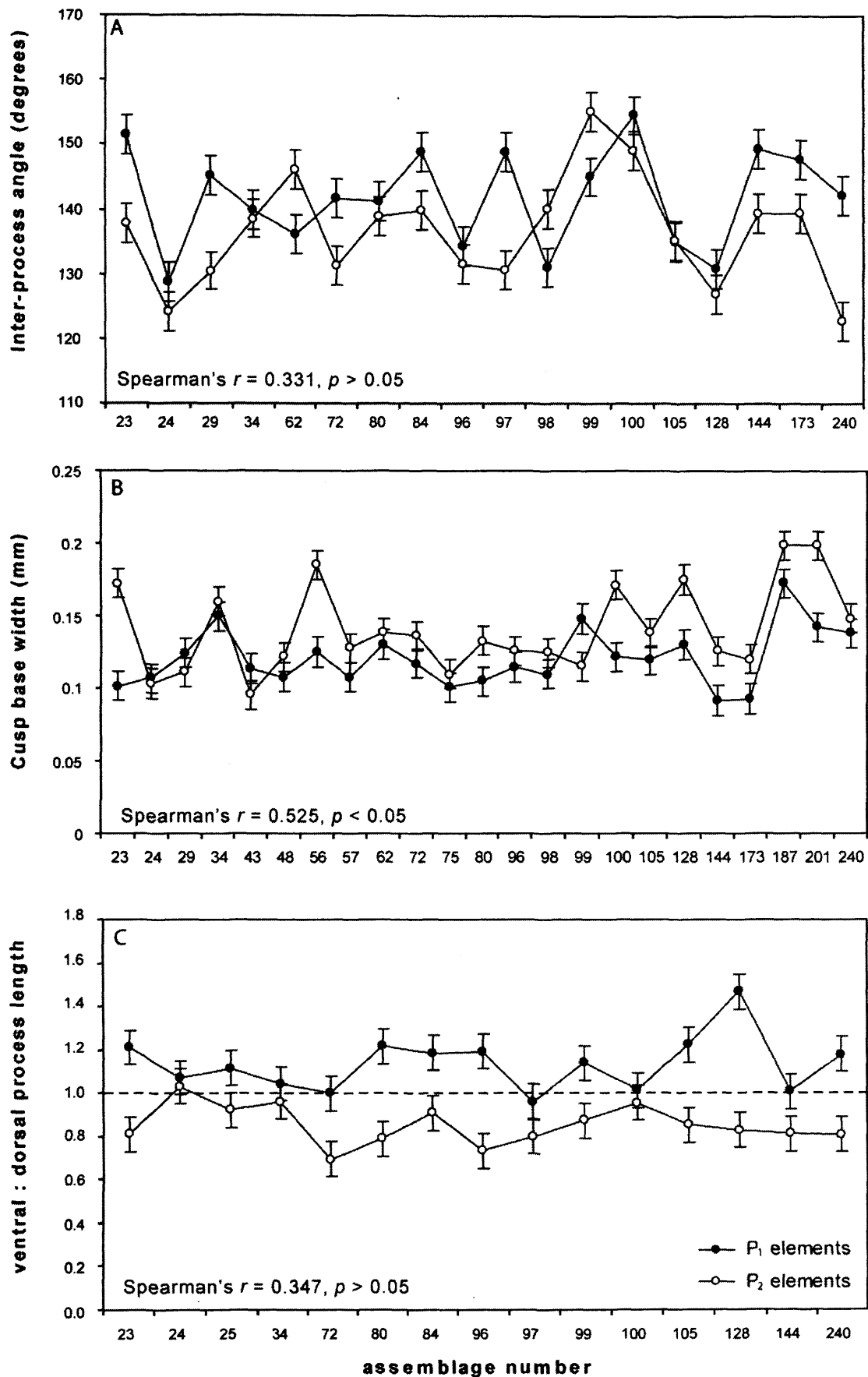


Figure 4: Plots of co-variation in A) inter-process angle, B) cusp base width and C) ventral:dorsal process length ratios for '*O. excavata*' natural assemblage P elements from the Eramosa Lagerstätte. Apparatuses are ordered according to sequence of discovery. Error bars based on spread of values produced by repeat measurements (see Chapter one).

Whilst Figure 4 shows that the relative values for the characters of P₁ and P₂ elements within each apparatus generally support their use in traditional discrimination, there is extensive individual variation in absolute character values between different apparatuses, and the r-values demonstrate that co-variation is frequently quite low. Moreover, the articulated skeletons sample only larger P elements; elements become increasingly distinct morphologically with growth, as evidenced by the general difficulty of taxonomic assignment of small/immature specimens, even morphometrically (e.g. Girard et al. 2004). Mature 'O.' excavata P elements might therefore be expected to be morphologically more distinct than juvenile individuals.

To search for a standard threshold value for dividing elements into P₁ and P₂ and to assess whether the characters are effective over a range of sizes, discrete elements and a set of 48 elements from articulated skeletons were ordinated, based on each of the three variables discussed above, against total length. These plots are shown in Figure 5. The P₁ and P₂ elements from natural assemblages do not form obvious groupings in any of the ordinations, although they do display some segregation based on ventral:dorsal process length. However, the distribution of isolated specimens appears continuous in all the plots; even for ventral:dorsal process length, they display no obvious discontinuities at which a discriminatory boundary between P₁ and P₂ elements could be drawn.

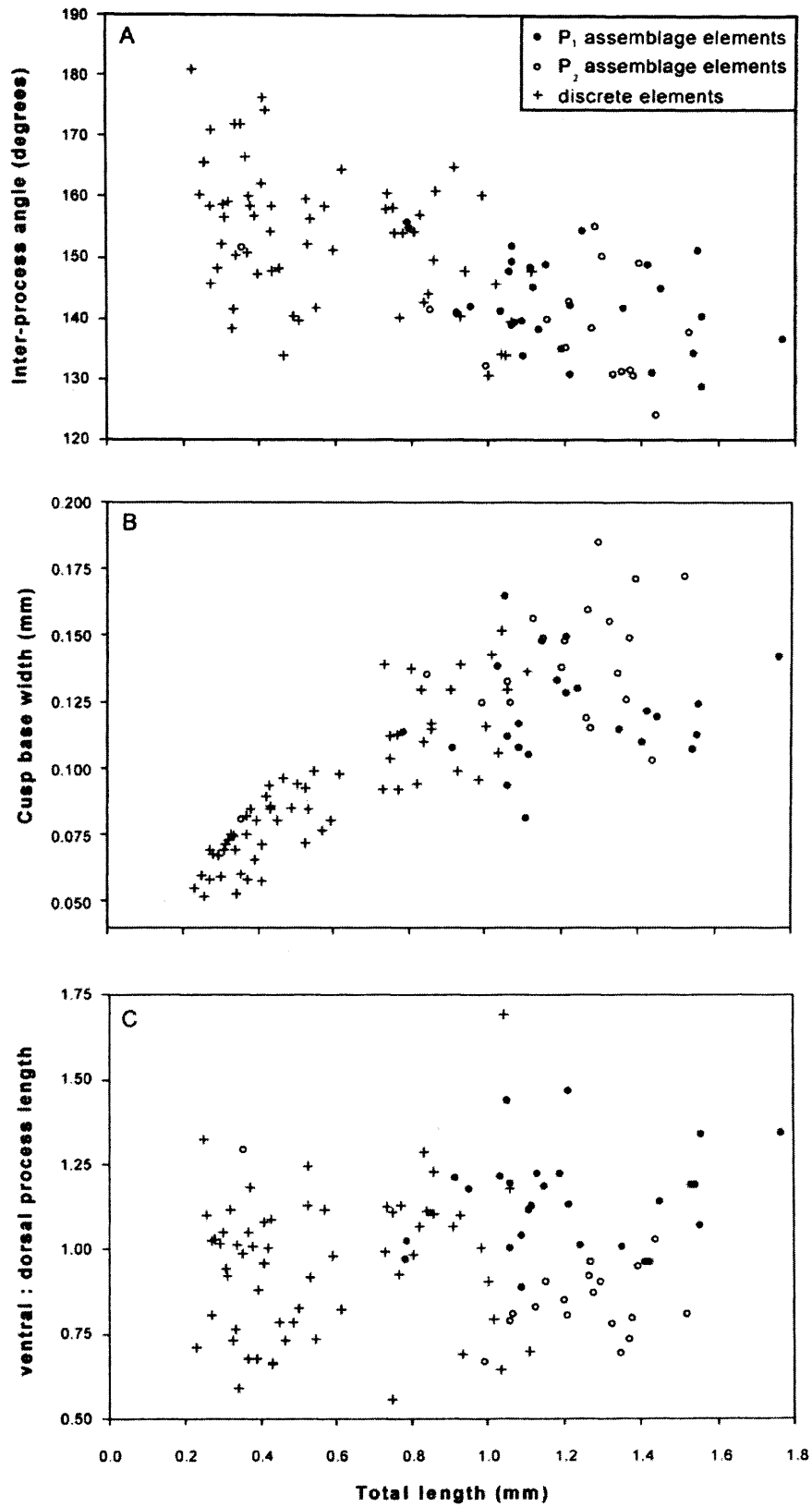


Figure 5: Bivariate plots of A) inter-process angle, B) cusp base width and C) ventral:dorsal process length for discrete and natural assemblage '*O.* excavata' P elements from the Eramosa Lagerstätte. Measurement error is as Figure 4.

Thus, Figures 4 and 5 show that ventral:dorsal process length provides the best single character discriminator of natural assemblage P₁ and P₂ elements. However, as might be expected, no single variable appears to represent an effective univariate discriminator of P₁ and P₂ elements amongst discrete element collections.

To determine if multivariate discrimination of P element type was more effective than univariate, P elements from articulated skeletons were analysed to test whether morphological differences between P₁ and P₂ could be detected, and to determine which variables characterised those differences. A discriminant function analysis (DFA) was conducted using ten measured variables (see Jones and Purnell (in press) for variable description). Ventral and dorsal process lengths were standardised to total length, so that relative differences were emphasized. The DFA was run twice. In the first run, a sample of 16 P₁ elements was taken from 16 articulated skeletons, and 15 P₂ elements from a different set of 15 skeletons, to maintain independence in the analysis. In the second, a larger set of 28 P₁ elements and 20 P₂ elements was examined (the same set used in the uni- and bivariate analyses above). Of these 48 elements, 16 of each type were sampled from articulated skeletons where both P elements were sampled. A greater proportion of P elements used in the blind test of natural assemblage specimens could be included in the second DFA, providing a better test of qualitative discrimination. Moreover, the pattern of clustering was virtually identical in both DFAs. Therefore, results from the DFA of the larger sample of 48 specimens (28 P₁ elements and 20 P₂ elements) are discussed below.

The DFA revealed significant morphological differences between P₁ and P₂ elements (Hotelling's $T^2 = 179$, $F = 46.2$, $p < 0.001$), and achieved a classification success of 100%, comparing favourably with expert discrimination. All specimens from the blind test on natural assemblage P elements were correctly assigned. The analysis also revealed which variables maximally separated the P element types: the relative length of dorsal and ventral processes of P₁ and P₂ elements proved the most powerful discriminator, with P₁ elements having relatively longer ventral processes, and P₂ elements possessing relatively longer dorsal processes. There was little input from other characters more commonly used in traditional qualitative differentiation, such as element arching and cusp size.

The same 48 P elements used in the DFA were then examined using a principal components analysis (PCA); PCA assumes no *a priori* clustering, so isolated elements could be included. Table 2 provides the eigenvalues for this PCA, along with the percent variation accounted for by the first three principal components. The relatively even distribution of variation across the principal components (PCs) probably reflects the limited co-variation between variables evident in Figure 4.

Although the first two principal components accounted for only 60% of the total variation within the sample, discrimination of P element type occurred entirely along PC-1 and PC-2, so PC-3 was not considered further. Figure 6 ordinated the elements in principal component morphospace based on eigenscores for the first two PCs. The P₁ and P₂ elements from the articulated skeletons form clearly separated fields. Only two P elements from natural assemblages are incorrectly assigned. The discrete elements are also well separated. A posteriori examination showed that three elements falling within the P₁ field (although in the area bordering the P₂ field) display classic P₂ morphology. Discrete specimens and elements from articulated skeletons also occupy different areas of morphospace in Figure 6.

The loadings in Table 3 indicate the amount of variance that each character contributes to the variance of each PC; how it “loads” upon each PC. The greater the loading value for a character (regardless of sign), the greater is its contribution to that PC axis. Since the boundary between P₁ and P₂ elements is oblique to the PC axes, the inset vector diagram in Figure 6 provides a better indication of which variables dominantly separate P₁ and P₂ elements. Table 3 also indicates whether a variable increases or decreases in value along a PC axis. A variable with a large positive loading will have a high value in elements with a high PC score, and a low value in elements with a low PC score. Conversely, a variable with a large negative loading will have a low value in elements with a high PC score, and a high value in elements with a low PC score.

Considering the loading values in Table 3 and the inset variable vector diagram in Figure 6 reveals that the variables and their directions of change correspond with the patterns identified and examined in the previous analyses. Natural assemblage P₁ elements have intermediate to high PC-1 and PC-2 scores, showing that they possess longer relative ventral processes, have higher inter-process angles and fewer denticles on the dorsal process. In contrast, natural assemblage P₂ elements have higher PC-1 and lower PC-2 scores, showing that they possess longer relative dorsal processes, and have lower inter-process angles and a larger number of denticles on the dorsal process. Although the PCA can separate P₁ and P₂ elements, and clear P element end-member forms exist, representing distinct P₁ and P₂ morphologies, there is a morphological gradation in the discriminatory variables along the PC axes. Thus, as apparent from Figure 4, P₁ and P₂ elements range from highly differentiated to virtually identical in morphology. Isolated P elements were assigned based on the results of the PCA and a DFA conducted on the PC-1 and -2 scores for these elements. This DFA produced over 93% correct discrimination.

PC	Eigenvalue	% variance Explained	cumulative % variance explained
1	328.659	34.852	34.852
2	267.641	28.382	63.234
3	135.123	14.329	77.563

Table 2: Eigenvalues, percent variance explained, and cumulative percent variance explained for the first three principal component axis from a PCA of 'O.' excavata discrete and natural assemblage P elements from the Eramosa Lagerstätte, Ontario.

Variable	PC-1 loading	PC-2 loading
VPL:TL	0.078	0.559
DPL:TL	0.14	-0.414
IPA	-0.426	-0.053
CBW	0.041	0.015
DPDP	-0.156	-0.474
VPDP	0.151	-0.253
CBW:VPDW	0.35	-0.216
CBW:DPDW	0.353	-0.303
VPDN	0.475	0.295
DPDN	0.521	-0.005

Table 3: Variable loadings on the first two principal components (PCs) from PCA of 'O.' excavata discrete and natural assemblage P elements from the Eramosa Lagerstätte, Ontario. See Table 1 for key to variable abbreviations. Figures in bold indicate the variables with the heaviest loading on that component.

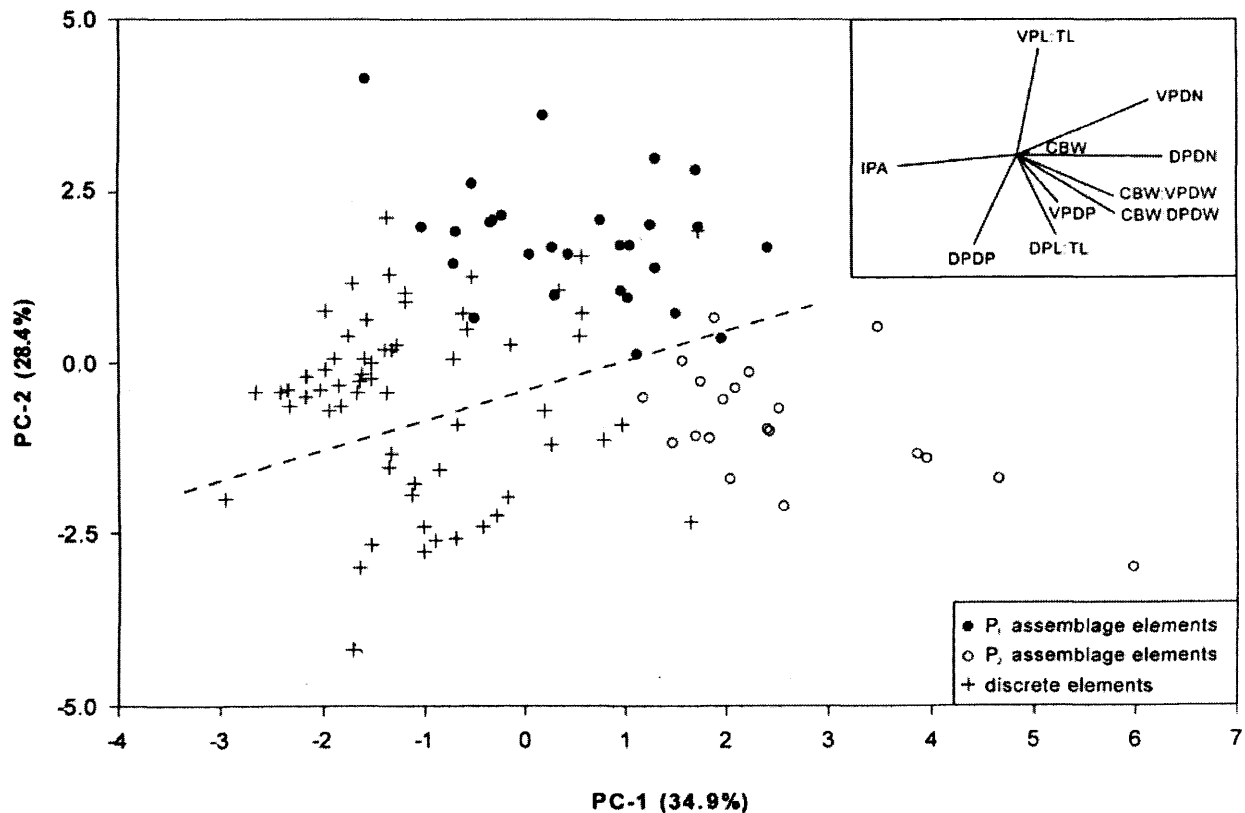


Figure 6: Biplot ordination of discrete and natural assemblage 'O.' excavata P elements from the Eramosa Lagerstätte on the first two principal components (PCs), based on eigenscores, with inset to illustrate vectors of variable loading relative to PC axes. Dashed line indicates approximate boundary between P₁ field (upper left) and P₂ field (lower right). See Figure 2 and Table 1 for key to variables.

Outline analysis was also undertaken to examine the general shape differences in the rostral profile associated with homology, and to determine whether more sophisticated outline techniques could also accurately discriminate P₁ and P₂ elements in 'O. excavata, as compared to traditional multivariate methods. Table 4 shows eigenvalues for the first three eigenshape vectors of the eigenshape (ES) analysis, and the percentage variance explained by each eigenshape. Ordinations of the element outlines in shape space, based on eigenscores, are shown in Figure 7. To aid visualisation and interpretation of the shape variation associated with each axis, eigenshape models are figured. These represent hypothetical shapes illustrating the pure shape variation occurring along each eigenshape axis. Figure 7 shows that eigenshape axis one (ES-1) is a contrast between arched and relatively narrow, long elements and wider, shorter and straighter individuals. The natural assemblage elements, known to be larger, cluster together on the right, and indeed ES-1 shows significant association with size (linear regression of ES-1 against TL: $r^2 = 0.504$, $p < 0.05$). This axis appears therefore to represent the increasing arching of elements through ontogeny, as detected by the traditional measures as distinguishers of P element type. Within the assemblage cluster, however, P₁ and P₂ elements are not discriminated. Eigenshape axis two (ES-2) captures far less shape differentiation, but the eigenshape models in Figure 7 suggest that elements with lower ES-2 values are more arched. There is limited indication of this on the graph: elements with lowest ES-2 values are P₂, those with the highest P₁, but sample size is too small to ascertain if this pattern is genuine. No differentiation between P element types or between discrete and natural assemblage elements appears present in ES-3, and little shape variation is manifest, so this axis is not considered further. No significance difference was found between P₁ and P₂ elements from articulated skeletons (Hotelling's $T^2 = 0.011$, $F = 0.696$, $p > 0.5$), and a DFA of ES scores produced only 59% correct discrimination between P element type in these specimens. Therefore, although standard eigenshape analysis has quantified important shape information within 'O. excavata P elements, it appears to be of limited utility in identifying homology within these elements.

ES	Eigenvalue	% variance Explained	Cumulative % variance explained
1	22.049	88.8	88.8
2	1.152	4.6	93.4
3	0.332	1.3	94.7

Table 4: Eigenvalues, percent variance explained, and cumulative percent variance explained for the first three eigenshape (ES) axes for 'O. excavata discrete and natural assemblage P elements from the Eramosa Lagerstätte.

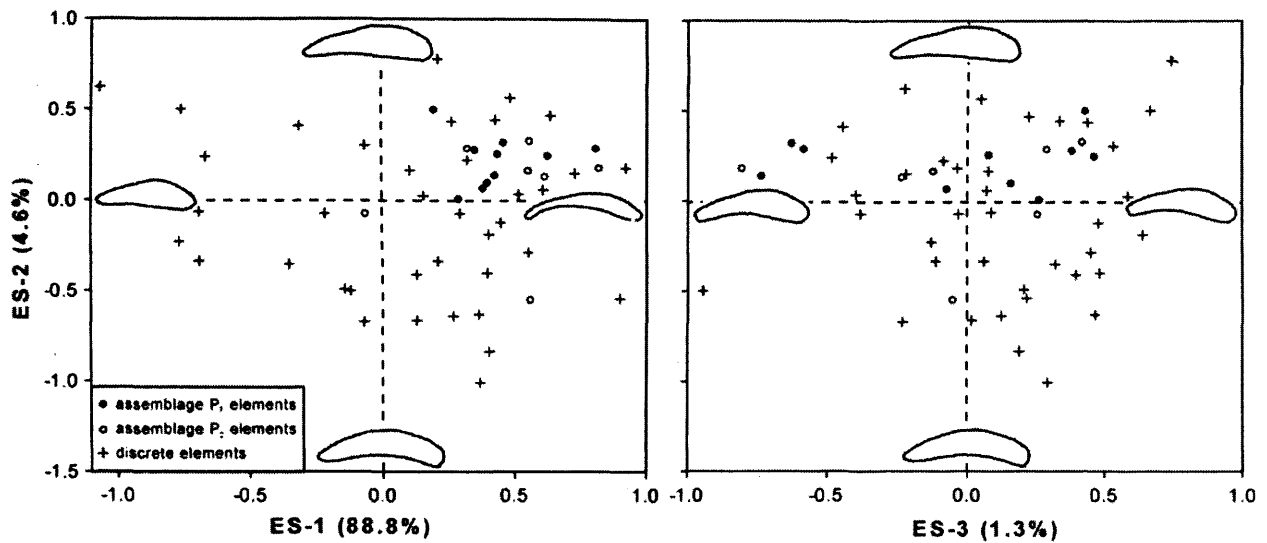


Figure 7: Ordination of discrete and natural assemblage ‘O.’ excavata P elements from the Eramosa Lagerstätte on the first three eigenshape (ES) axes, based on eigenshape scores. Outlines represent eigenshape models of shape change along each axis.

Table 5 shows eigenvalues for the first three principal components from the PCA of elliptic Fourier coefficients, and the percent variance explained by each. Although 88% percent of the variation within the sampled outlines captured by the EFA is explained by the first two principle components, PC-3 is also considered, as it also shows discrimination between P₁ and P₂ elements. Figure 8 shows the ‘O.’ excavata P elements ordinated on the first three PC axes, based on PC scores. To aid visualisation and interpretation of the shape variation associated with each axis, end-member elements are figured. Outlines were generated using the inverse Fourier function based on ten harmonics (the maximum number available in PAST; the more harmonics included, the greater the quantity of detail incorporated into the outline). The elements represented by these outlines are illustrated.

The end-member morphologies in Figure 8 show that variation along principal component one (PC-1) is similar to that of ES-1: a contrast between arched and relatively narrow, long elements and wider, shorter and straighter individuals. However, here the P element types are discriminated: isolated elements have high to intermediate PC-1 values, the natural assemblage P₁ elements intermediate values and the natural assemblage P₂ elements have low PC-1 values. PC-1 shows a stronger correlation with size than that of ES-1 (linear regression of PC-1 against TL: $r^2 = -0.733$, $p < 0.01$), and thus also appears to reflect the increasing curvature of elements through ontogeny. As is frequently the case in PCA, the first PC therefore appears to be capturing most of the size variation within the sample. Figure 8 shows that the second principal component (PC-2) seems to be capturing element length:width ratio, with some element of changing element curvature. Elements with high values are relatively short and wide, those with low values are relatively long and narrow.

This is an important aspect of shape undetectable by the traditional measures. Natural assemblage and discrete elements are not separated along PC-2. PC-3 again distinguishes P₁ and P₂ elements. The inflection point on the oral margin of PC-3 end-member outlines represents the approximate position of the cusp. In elements with low PC-3 values, which include the assemblage P₂ elements, this inflection point is positioned more ventrally than in elements with high PC-3 scores, which include the P₁ elements. Thus, the Fourier analysis appears to be capturing the differences in relative process length detected by the traditional analyses as a distinguisher of P element type. Natural assemblage and discrete elements are not separated along either PC-2 or PC-3, and there is no significant association with size on either PC axis (linear regression of PC-2 against TL: $r^2 = -0.053$, $p > 0.7$; linear regression of PC-3 against TL: $r^2 = 0.197$, $p > 0.1$), indicating PC-2 and -3 are capturing pure shape variation, independent of size. Significant differences were found between P₁ and P₂ elements from articulated skeletons (Hotelling's $T^2 = 0.271$, $F = 17.6$, $p < 0.001$), and a DFA of PC scores produced 100% correct classification of P element type in these specimens.

PC	eigenvalue	% variance explained	Cumulative % variance explained
1	0.006	71.7	71.7
2	0.001	16.9	88.7
3	0.0002	3.1	91.7

Table 5: Eigenvalues, percentage of variance explained and cumulative percent variance explained for first three principle components (PCs) from PCA of Fourier coefficients for 'O.' excavata discrete and natural assemblage P elements from the Eramosa Lagerstätte.

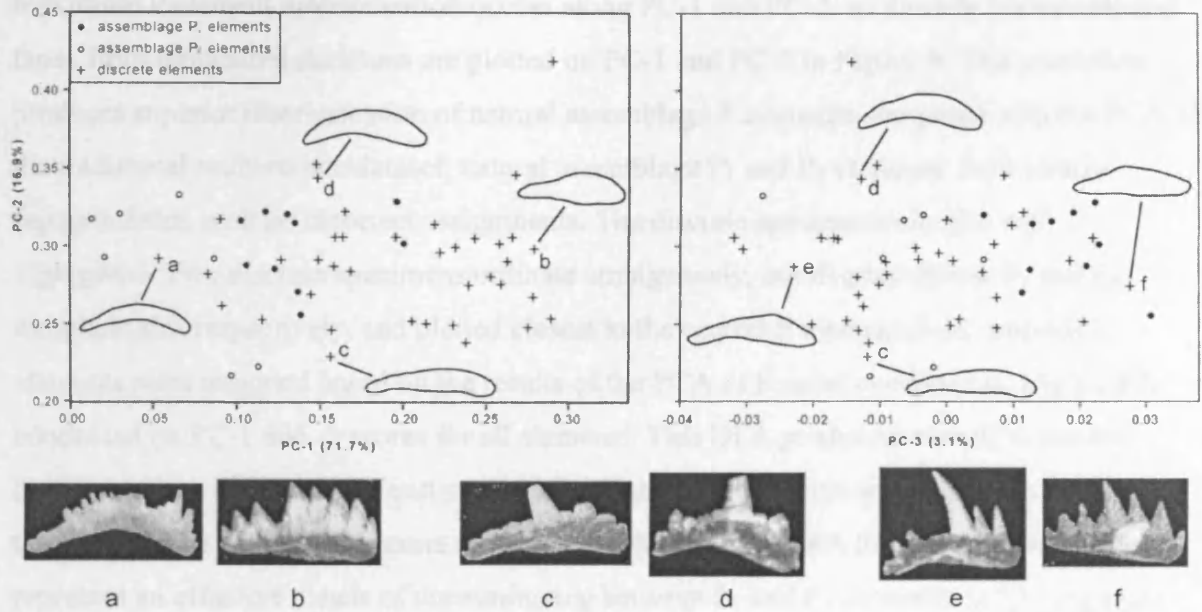


Figure 8: Ordination of discrete and natural assemblage 'O. excavata P elements from the Eramosa Lagerstätte on the first three principal component axes, based on PC scores from a PCA of Fourier coefficients produced by an EFA. End-member morphologies for each axis are illustrated by outlines and images of elements they represent.

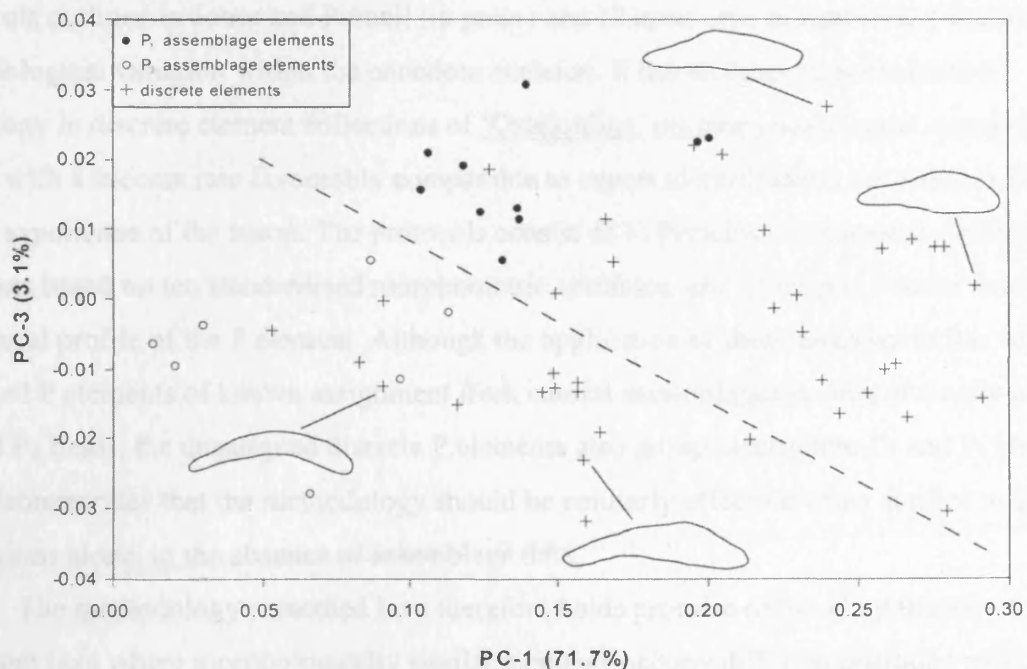


Figure 9: Ordination of discrete and natural assemblage 'O. excavata P elements from the Eramosa Lagerstätte on PC-1 and PC-3, based on principal component scores from a PCA of Fourier coefficients produced by an EFA. End-member morphologies for each axis are indicated by outlines. Dashed line indicates approximate boundary between P₁ field (upper right) and P₂ field (lower left).

Although important shape information regarding element width is captured by PC-2, maximum P element discrimination occurs along PC-1 and PC-3, so discrete P elements and those from articulated skeletons are plotted on PC-1 and PC-3 in Figure 9. This ordination produces superior discrimination of natural assemblage P elements compared with the PCA of the traditional multivariate dataset; natural assemblage P₁ and P₂ elements form clearly separate fields with no incorrect assignments. The discrete specimens are also well segregated. Two discrete specimens ordinate ambiguously, but display classic P₁ and P₂ morphologies respectively, and plotted closest to the correct P element field. Isolated P elements were assigned based on the results of the PCA of Fourier coefficients, and a DFA conducted on PC-1 and -3 scores for all elements. This DFA produced over 97% correct discrimination. The PCA of Fourier coefficients also concurs with discrimination by PCA of the multivariate dataset of discrete elements in 89% of cases. EFA therefore appears to represent an effective means of discriminating between P₁ and P₂ elements in 'O. excavata, potentially allowing reliable identification of homology within these conodont elements.

Conclusions

The results presented here clearly demonstrate the effectiveness of new morphometric protocols outlined in Jones and Purnell (in press) and Chapter one, in capturing patterns of morphological variation within the conodont skeleton. It has enabled identification of homology in discrete element collections of 'Ozarkodina excavata based upon morphology alone, with a success rate favourably comparable to expert identification, but requires little *a priori* experience of the taxon. The protocols consist of 1) Principal Component Analysis of P elements based on ten standardised morphometric variables, and 2) elliptic Fourier analysis of the rostral profile of the P element. Although the application of these analyses in this work has used P elements of known assignment from natural assemblages to unequivocally identify P₁ and P₂ fields, the unassigned discrete P elements also group clearly into P₁ and P₂ clusters. This demonstrates that the methodology should be similarly effective when applied to discrete collections alone, in the absence of assemblage data.

The methodology presented here therefore holds promise of broad application to other conodont taxa where morphologically similar elements occupy different positions within the skeleton; for example in many prioniodinids, where P elements frequently display even greater morphological similarity than that manifest in 'Ozarkodina excavata from the Eramosa Lagerstätte (Purnell 1993). Increasing the reliability of hypotheses of primary homology using these protocols will allow more rigorous cladistic analyses of conodonts, enable us to derive a clearer picture of morphological evolution within the conodont skeleton

and draw more accurate palaeoecological conclusions from collections of discrete specimens. Moreover, the ability of the methodology to determine quantitatively which variables discriminate between morphologically similar elements, providing more objective justification for selecting diagnostic characters, has obvious utility not just in establishing element homology, and also in taxonomy.

Although the multivariate analyses successfully separated P_1 and P_2 elements in 'Ozarkodina' excavata, they also quantify the qualitative observation that individuals vary in the degree of morphological differentiation between P_1 and P_2 elements within skeletons: some individuals possess P_1 and P_2 elements that are obviously different, some that are remarkably similar. Yet poorly and well differentiated P elements appear to represent end-members of a smooth continuum. This reflects a general morphological flexibility within and between the structural components of the P elements, also indicated by the low co-variation between variables in both the univariate analyses and Principal Component Analysis. The adaptive significance of this variation, which presumably reflects the degree of functional overlap between the two P element pairs, represents an important area for further research into developmental plasticity, specialisation and functionality within the earliest vertebrate feeding structures.

Chapter three: Testing species hypotheses in conodonts – multivariate morphometric analysis of ‘*Ozarkodina*’ *excavata*

Abstract

Conodonts are an extinct group of early vertebrates that possess an exceptionally good fossil record. This record has potential for numerous applications, including phylogenetics, palaeobiological investigation and evolutionary analysis. Exploiting this potential requires both rigorous delineation of conodont morphology and establishment of a stable taxonomic framework. Morphometric analysis provides an effective means of achieving these goals. A new standardised methodology for morphometric analysis, suitable for examining morphological variation within conodonts, is presented. It has been applied herein to the taxonomically problematic conodont species ‘*Ozarkodina*’ *excavata*, to test the hypothesis that this morphological variable taxon is monospecific. Using these morphometric protocols, significant morphological discontinuities have been identified within samples assigned to ‘*Ozarkodina*’ *excavata*. Analysis of these discontinuities in their spatiotemporal and biological context reveals significant differences between populations of ‘*Ozarkodina*’ *excavata* separated in space and time, suggesting that multiple species are currently accommodated within this taxon. The analysis additionally permits objective and repeatable recognition of biostratigraphically useful morphologies that may have broad utility in improving Silurian biozonation. The ability of the new protocols to effectively identify and discriminate morphologically distinct groups holds promise for wide across-taxon application.

Introduction

Conodonts are a large, extinct clade of stem gnathostomes, possessing a skeleton composed of phosphatic tooth-like elements, which formed an oropharyngeal feeding apparatus (Aldridge and Purnell 1996, Donoghue et al. 1998). The conodont fossil record consists dominantly of disarticulated elements; the huge abundance of these elements throughout the 300 million year span of the clade's existence has made them invaluable biostratigraphic tools for establishing and constraining relative ages in the geologic record (Higgins and Austin 1985, Sweet and Donoghue 2001). The exceptionally high quality of the conodont fossil record also offers an unparalleled opportunity to study evolutionary rates, patterns and processes within a vertebrate group. Additionally, by virtue of their phylogenetic position, conodonts have a key role to play in elucidating the sequence of character acquisition in the vertebrate clade (Purnell 2001).

Exploiting the palaeobiological potential of conodonts clearly requires a stable taxonomic foundation. However, conodont taxonomy is frequently problematic: as with many palaeontological studies, species boundaries must be delineated based solely on partial skeletal material that often displays extensive and complex morphological variation. Consequently, taxonomic hypotheses formulated on the basis of a qualitative understanding of conodont morphology are generally un-testable. This would seem an ideal problem for the application of morphometric analysis, and yet comparatively few studies have adopted such a quantitative approach to taxonomy.

Most previous morphometric investigations of conodont taxonomy have been based on outline analysis (e.g. Girard et al. 2004, Klapper and Foster 1986, 1993, Roopnarine et al. 2004): these are discussed in Chapter four, which deals with an extension of the methods presented here, but based on outline analysis. However, the earliest morphometric treatments of taxonomy were based around traditional morphological variables (lengths, angles, etc.) and multivariate analysis. Croll et al. (1982) and Croll and Aldridge (1982) developed and applied a methodology for acquiring measurements to characterise the P elements of *Ozarkodina* species. Although some of Croll et al.'s (1982) characters are of uncertain biological significance, their protocol did effectively detect clusters corresponding to these species. The statistical significance of the differences was not assessed. As Croll and Aldridge (1982) noted, their methodology was somewhat complex; however, importantly, they recognised the necessity of developing a standardised quantitative protocol for garnering morphological data from conodonts. The

elements examined in their study were not taxonomically assigned *a priori* and no blind tests were undertaken to assess the discriminatory power of the techniques when the specific assignment of the elements was unknown. Thus, the morphometric techniques provided a means to test existing qualitative schemes, rather than being presented as an alternative discriminatory tool.

In a morphometric study focussing on '*Ozarkodina*' *excavata*, Murphy and Cebecioglu (1986) examined the ontogeny of denticle packing in this species. They discovered that increase in denticle packing in a subspecies of '*O.*' *excavata*, *O. e. tuma*, followed a distinct ontogenetic trajectory, different to that of other '*O.*' *excavata* within their sample. Based on this, they raised *O. e. tuma* to species status. Recognising a species on the basis of a single variable is generally inadvisable (e.g. Willig et al. 1986), and Murphy and Cebecioglu's (1986) study is of limited value because the equations of the regression lines for the ontogenetic pathways were not provided, nor was the difference between the two trajectories tested for statistical significance.

Ritter (1989) examined the taxonomy of *Neogondolella mombergensis* to clarify its evolutionary mode and evaluate its biostratigraphic potential. He specifically tested characters on which previous authors had based taxonomic schemes purporting to identify multiple species within *N. mombergensis*. These characters were all traditional multivariate measures, and had questionable biological significance; perhaps unsurprisingly, Ritter (1989) found little support for the taxonomies based upon them, and only a single species could be identified within *N. mombergensis* by his morphometric analysis. Ritter (1989) noted particularly the inadequacy of a strictly typological approach to taxonomy when elements display continuously varying characters, because it requires arbitrary division of morphological continua; his morphometric analysis of *N. mombergensis* clearly highlights this difficulty.

The scarcity of morphometric treatments of conodont taxonomy makes it abundantly clear that the potential of rigorous quantitative analysis of conodont species hypotheses has yet to be fully realised. The work presented here aims to address this issue, by introducing a suite of new, standardised morphometric protocols with wide-across taxon applicability. These protocols have been used to test the hypothesis that morphological variation within the taxonomically problematic conodont species '*Ozarkodina*' *excavata* (Branson and Mehl 1933) is continuously distributed, with a view to assessing whether or not multiple species are currently accommodated within this taxon. The results also have potential biostratigraphic implications: '*O.*' *excavata* subspecies currently find very limited use in biozonation (e.g. Jeppsson and Aldridge 2000, Jeppsson et al. 2006), but the morphometric protocols outlined here hold promise of objective

and repeatable identification of biostratigraphically useful morphologies within conodont elements currently assigned to '*O.*' *excavata*.

The species concept and '*Ozarkodina*' *excavata*

The focus of this work is the conodont species '*Ozarkodina*' *excavata*. This species has a global distribution (Jeppsson 1974) and a stratigraphic range extending from at least the mid Silurian to the Early Devonian (Murphy and Cebecioglu 1986, Roopnarine et al. 2004), perhaps originating far earlier (Aldridge and Mabillard 1985, Cooper 1975, 1976, Jeppsson 1974). Most authorities currently consider '*O.*' *excavata* to be a single species displaying a high degree of continuous morphological variation, which appears not to vary systematically through time. However, the degree of morphological variation that can be included within '*O.*' *excavata* is uncertain (Jeppsson 1974). This problem is difficult to address using traditional methods of qualitative observation: the relative morphological simplicity of the elements within the '*O.*' *excavata* skeleton and the complex yet subtle variation they display has led to considerable subjectivity and inconsistency in determining the taxonomic boundaries of the species (Jeppsson 1974). These uncertainties surrounding the morphology and taxonomy of '*O.*' *excavata* make it an ideal choice of species for this application of the morphometric protocols: the goal of this work is to attempt to quantitatively test the hypothesis that the '*O.*' *excavata* hypodigm represents a single species (use of the term hypodigm follows Mayr et al. 1953: p.237, "A hypodigm is all the available material of a species").

Testing the morphological boundaries of a species raises the question of what a species is. In order to justify the approach to the specific problem of '*O.*' *excavata* some theoretical considerations of species concepts are required. In this work, a general species concept was chosen *a priori*, as recommended by Wiens (2004); hypotheses are framed and the results interpreted within this concept. Full discussion of the continuing debate over the various merits of different species concepts is beyond the scope of this work, but one fact seems unequivocal: despite implicit suggestions to the contrary by many authors (e.g., see contributions to Wheeler and Meier 2000) no single species concept is universally applicable. So rather than selecting a particular concept, and inevitably its associated conceptual baggage, a pragmatic approach is adopted, delineating species as follows.

Extinct and most extant sexually reproducing species are operationally identified through morphological features, or phenetic clusters in a quantitative sense (Sokal and Crovello 1970).

Yet such morphospecies are often implicitly, if not explicitly, considered as proxies for biological species (Benton and Pearson 2001). This is because biological species are composed of reproductively isolated populations (Mayr 1942, 1969) and the sharing of morphological characters is taken to indicate a shared, common gene pool. In this theoretical definition, biological species are deemed significant because this genetic coherence means that they approach closest to real entities or individuals (Baum 1998, Mishler and Donoghue 1982), in comparison with somewhat arbitrary supra-specific taxa.

Unfortunately, identification of biological species is not simply a question of discerning morphological differences; the use of morphology alone is frequently insufficient because often there is not an exact correspondence between morphological distinctiveness and reproductive isolation. Numerous instances of morphologically indistinguishable sibling species are now known in a range of animal groups (see Knowlton 1993 for a review of marine examples), and intra-specific differences can exceed those between species (e.g., Bell et al. 2002).

Polymorphisms such as ecophenotypy can also produce a range of morphologies within one species (e.g., Peijnenburg and Pierrot-Bults 2004). Moreover, delineating biological species is problematic because the biological species concept is ahistorical and emphasises intrinsic reproductive isolation mechanisms for species maintenance. Reproductive isolation is obviously impossible to test for in fossil populations, and the inapplicability of species concepts based around potential interbreeding is clear where populations are separated in time, perhaps by millions of years. Of course, in the case of fossils, determining where the boundaries between potential species may lie must be based on recognition of morphological discontinuities. But evaluating the biological significance of these discontinuities requires them to be interpreted within their spatial, temporal and ecological contexts. Only then can the likelihood that distinct morphologies represent reproductively isolated biological species be assessed.

Spatial information can be incorporated by considering the geographic distribution of morphologically distinct fossil populations; extrinsic spatial separation can prevent gene flow between populations, creating the potential for phenotypic differentiation. Moreover, such vicariance is easier to demonstrate in fossil populations than the intrinsic reproductive barriers required by the biological species concept. Environments will also vary across a species' geographic range, and any contrasting selection pressures that result will favour genetic and morphological divergence (the former enhancing reproductive isolation, the latter producing visible change) potentially reflecting the evolution of new species. Fine-scale spatial information can also aid in identifying migration events between local populations.

Initially, temporal information need only consist of whether a fossil population differs significantly in its morphology from those stratigraphically above or below, where all are initially considered to be the same species. Induction of these patterns explicitly as ancestor-descendent relationships through time is not necessary (but may be undertaken). Nevertheless, these patterns can be assessed to determine whether they would be most sensibly interpreted as the evolving sequence of populations forming a single species or, for example, as an anagenetic pathway, where one species evolves gradually into another. Other factors (sampling density, stratigraphic completeness, etc) will heavily influence any decision as to which of these alternative evolutionary-taxonomic scenarios is determined to be most probable.

Ecological and biological interpretations, including analysis of functional morphology to identify adaptive characters, are also required to better assess the taxonomic significance of observed differences, aiding for example, in the identification of confounding intra-specific variation caused by ontogenetic change or ecophenotypy. A population-based rather than strictly type-based approach to taxonomy is also utilised here. This is complementary to the application of quantitative analysis involving a large number of specimens and provides a clearer picture of the variation within the population by better constraining non-taxonomic aspects of variation. Moreover, previous morphometric studies have clearly demonstrated the pitfalls of strict typological taxonomy (e.g. Ritter 1989). If the morphological differences between a given population and the type specimens are statistically significant to a standardised level, this is justification for assigning those morphotypes to different species.

Based on the foregoing discussion, two levels of hypotheses have been formulated. The initial null hypothesis is that the morphological variation within the '*O.*' *excavata* hypodigm is continuously distributed, supporting the general consensus that the hypodigm is a single morphospecies. The alternative hypothesis is that morphological variation within the hypodigm forms discrete or overlapping clusters. If the null hypothesis is falsified and multiple morphological clusters are detected, then if the morphological clusters correspond to temporally and/or spatially discrete populations, and if characters that define them have adaptive biological significance, then the most parsimonious interpretation is that these populations represent separate species.

Materials and method

The primary focus of this study are elements from the '*O.* *excavata*' skeleton that are thought to have occupied the P₁ position. This is partly because P₁ elements are regarded as taxonomically useful (Sweet 1988), but particularly because this element has a comparatively large number of continuously varying features for measurement and is thus amenable to morphometric analysis. Consideration of multiple quantitative characters is advantageous in a taxonomic context (contra Murphy and Cebecioglu 1986), as it avoids the problem of dividing a sample into different phenetic clusters depending on which particular variable is being considered. This approach also means that correlations between characters are incorporated into the analysis; omission of such correlations can produce misleading results (Knowlton 1993, Willig et al. 1986). P₁ and P₂ elements were differentiated in many samples using protocols similar to those outlined in Chapter two. Other samples had well differentiated P₁ and P₂ elements, which did not require quantitative differentiation.

In order to capture as much of the potential variation as possible, the samples analysed included '*O.* *excavata*' elements from most of its spatiotemporal range (see Table 1). Assignment of these elements to '*O.* *excavata*' was based on published opinions and active input of conodont workers with experience in this taxon. The full data set is provided in Appendix 1. Original sample sizes ranged between nine and 44 elements. Inequality in sample size may mask differences in variance between samples, so samples were reduced through random sub-sampling, ensuring all samples contained between ten and 20 specimens (except for the poorly-preserved American topotype material).

Including such a "global" sample of the hypodigm produces an empirical morphospace for '*O.* *excavata*' within which individual samples lie. The use of empirical morphospaces has been criticised because of their potential instability with changing sample number and size; however, theoretical morphospaces, although more stable, are also problematic. For example, Villier and Eble (2004) have noted that theoretical morphospaces are dependent on *a priori* models of which variables (and usually a small number) best describe aspects of form, and this may result in unsatisfactory descriptions of object form. Following McClain et al. (2004), the robustness of the empirical morphospace with changing sample sizes was tested by also analysing the original, non-sub-sampled data set. Between the original (n = 536) and sub-sampled set (n = 454), eigenvalues were within 0.02 of each other, variance partitioning between components was identical, and variable loadings were all similar. This supports the interpretation

that the empirical hyperspace generated by the analysis does approach the stability of a theoretical morphospace.

Data were acquired using the morphometric protocols outlined in Chapter one and Jones and Purnell (in press). Figure 1 illustrates the measured variables and the biological anatomical notation used in this work (Purnell et al. 2000). Table 2 provides descriptions of the measured variables and their abbreviations. Principal components analysis (PCA) was used to analyse the data. PCA is a standard technique for reducing dimensionality in multivariate data and is also useful for visualisation and exploration of data structure. The samples were not subdivided *a priori* by locality or age, and PCA makes no assumptions that clusters are present within the data. A correlation matrix was used for the PCA because of the different units and scales of the variables. The total length variable was excluded owing to the strength of its correlation with several other variables; this allows it to be used as an independent variable for investigating potential ontogenetic patterns. Eight percent of the data were missing; this was handled through within-group mean replacement. Although unavoidable, this will reduce the variation within each sample. Canonical variates analysis (CVA), a multi-sample multivariate classification technique, was conducted on any groupings in the raw data indicated by the PCA, to optimise the clustering. Analyses was conducted in PAST Version 1.44 (Hammer et al. 2001) and SPSS Version 14. Graphs were produced in PAST and Microsoft Excel.

Locality	Age	Age data reference	N
Lithium, Missouri, USA	mid Ludlow	Boucot (1958); Rexroad and Craig (1971)	9
Broken River, Queensland, Australia *	Latest Silurian	A. Simpson pers. comm. 2005	11
Broken River, Queensland, Australia	mid Ludlow	A. Simpson pers. comm. 2005	20
Carnic Alps, Austria	Ludlow, mid Gorstian	Walliser (1964)	17
Muslovka Quarry, Bohemia	Upper Přídolí	Walmsley et al. (1974)	12
Netherton, Britain *	Ludlow, Ludfordian	Aldridge et al. (2000)	13
Ludlow, Britain	Ludlow, Ludfordian	Aldridge et al. (2000)	20
Hepworth, Ontario, Canada	Wenlock	von Bitter and Purnell (2005)	20
Pusku, Estonia	Llandovery, late Rhuddanian	P. Mannik pers. comm. 2005	20
Nyan 2, Gotland, Sweden	Ludlow, Ludfordian		15
Gerete 2, Gotland, Sweden (12)	Ludlow, Gorstian		20
Alsvik 7, Gotland, Sweden (11)	Ludlow, Gorstian		19
Alsvik 4, Gotland, Sweden (10)	Ludlow, Gorstian		20
Lilla Hallvards 3, Gotland, Sweden	Ludlow, Gorstian		20
Lukse 1, Gotland, Sweden (9)	Ludlow, Gorstian		20
Smiss 2, Gotland, Sweden	Ludlow, Gorstian		17
Snoder 1, Gotland, Sweden	Ludlow, Gorstian		20
Smissarvestrand, Gotland, Sweden (8)	Ludlow, Gorstian	L. Jeppsson pers. comm. 2004	20
Bodbacke 3, Gotland, Sweden	Ludlow, Gorstian	Jeppsson et al. (2006)	20
Urgude, Gotland, Sweden (7)	Ludlow, Gorstian		20
Sigdarve 1, Gotland, Sweden (6)	Wenlock, Homeric		20
Sudervik 2, Gotland, Sweden (5)	Wenlock, Homeric		16
Svarvare 3, Gotland, Sweden (4)	Wenlock, Homeric		20
Svarvare 1, Gotland, Sweden (3)	Wenlock, Homeric		20
Östergårde 2, Gotland, Sweden (2)	Wenlock, Sheinwoodian		20
Östergårde 1, Gotland, Sweden (1)	Wenlock, Sheinwoodian		20

469

Table 1: Locality, age and number of elements sampled (N) for each sample of ‘*O.*’ excavata P₁ elements analysed in this work. Swedish samples are ordered according to relative age at a series of intervals through the Ludlow and Wenlock. Numbers in brackets on left-hand column refer to sample notation in Figure 2 and in the text. Asterisks indicate which Australian and British samples were used in the analyses of spatially separated samples (see below).

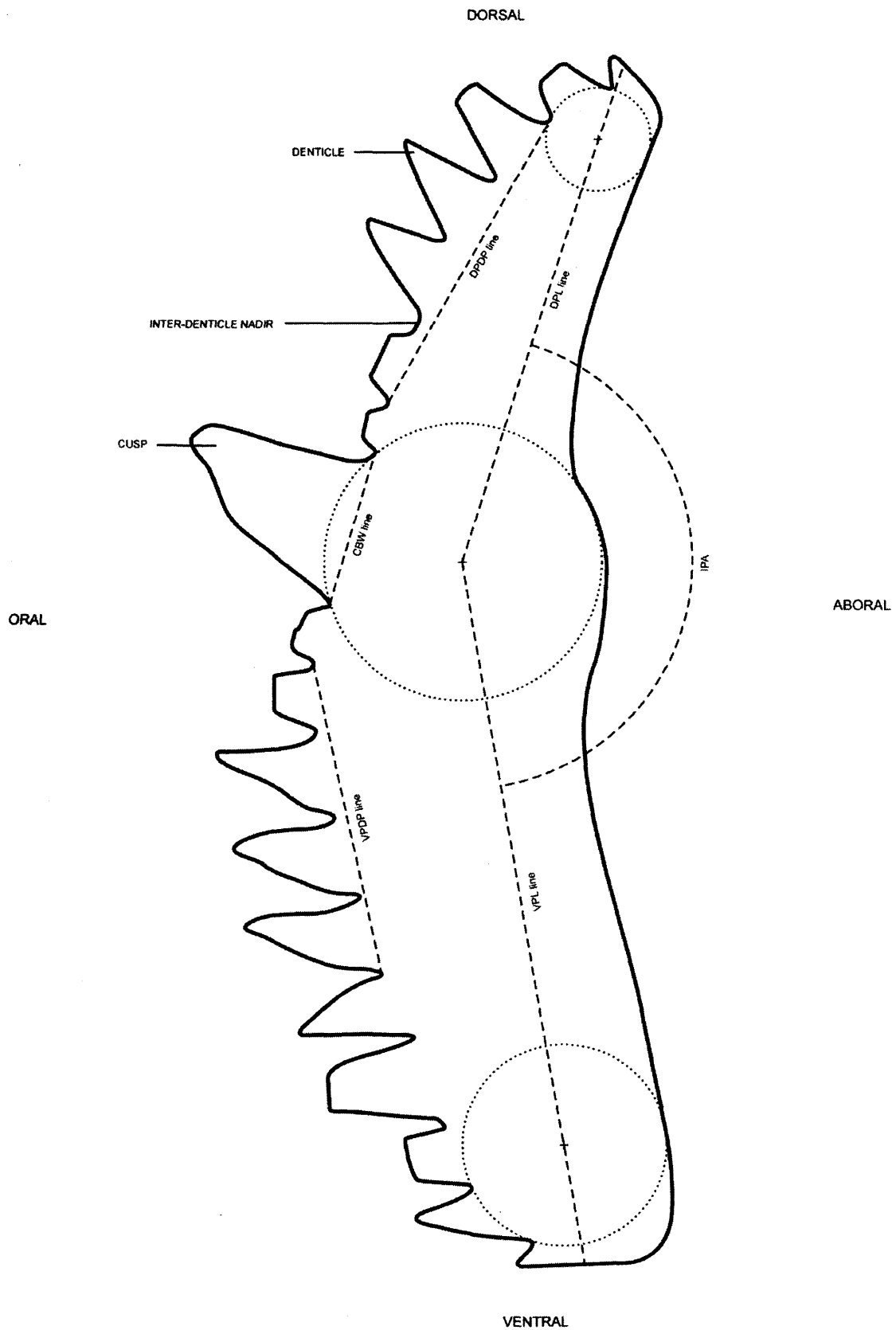


Figure 1: '*O. excavata* P₁ element in rostral view. Anchored circles are dotted. Dashed lines represent the measures used in the morphometric analysis, as outlined in Table 2. See Table 2 for key to abbreviations.

Name	Abbreviation	Description
Ventral process length	VPL	Linear distance from the cusp anchored point to the distal process terminus, measured along a line passing through the anchored point of the penultimate denticle.
Dorsal process length	DPL	
Total length	TL	Sum of dorsal and ventral processes lengths.
Inter-process angle	IPA	Angle between the dorsal and ventral process length lines.
Cusp base width	CBW	Linear distance between inter-space nadirs immediately adjacent to cusp.
Ventral process denticle packing	VPDP	Linear distance from the inter-space nadir proximal but one from cusp, along the base of four denticles distally. The value is divided by four to calculate the average denticle width of the process.
Dorsal process denticle packing	DPDP	
Ratio of cusp base width : mean denticle base width for ventral process	CBW:VPDW	Ratio of cusp base width to mean denticle width.
Ratio of cusp base width : mean denticle base width for dorsal process	CBW:DPDW	
Ventral process denticle number	VPDN	Enumeration of denticles on the process.
Dorsal process denticle number	DPDN	

Table 2: Summary of morphometric variables measured on ‘*O.*’ excavata P₁ elements. Variables are illustrated in Figure 1. See Chapter one and Jones and Purnell (in press) for discussion of measured variables.

Results and discussion

Multivariate analysis of morphological variation in the ‘O.’ excavata hypodigm

To test the hypothesis that variation within the ‘O.’ *excavata* hypodigm is continuously distributed, the multivariate data set (ten variables, 26 samples considered to belong to the ‘O.’ *excavata* hypodigm: see Table 1), was subjected to a principal components analysis (PCA). The eigenvalues and variance partitioning for the principle components are shown in Table 3. The first three components accounted for over 76% of the total variation within the hypodigm, and so only these components are considered further. The variance is however rather evenly distributed between these components. This probably reflects the large range of conflicting variation that has been observed qualitatively within the ‘O.’ *excavata* hypodigm, such that this variation cannot be partitioned into one dominant component by the PCA.

The loadings in Table 4 indicate the amount of variance that each character contributes to the variance of each PC; how it “loads” upon each PC. The greater the loading value for a character (regardless of sign), the greater is its contribution to that PC axis. The loading values also indicate whether a variable increases or decreases in value along a PC axis. A variable with a large positive loading will have a high value in elements with a high PC score, and a low value in elements with a low PC score. Conversely, a variable with a large negative loading will have a low value in elements with a high PC score, and a high value in elements with a low PC score. The morphological variables that load most heavily on the component axes, as identified by the PCA, are in bold in Table 4.

PC	eigenvalue	Percent variance explained	Cumulative percent variance explained
1	3.223	36.1	36.1
2	1.959	22	58.1
3	1.621	18.2	76.2

Table 3: Eigenvalues and percentage variance explained for the first three principal components of the PCA conducted on the global sample of ‘O.’ *excavata* P₁ elements.

Variable	Variable loadings		
	PC-1	PC-2	PC-3
VPL	0.4516	-0.3129	0.0177
DPL	0.5099	0.0729	0.0879
IPA	-0.1226	-0.2892	-0.4404
CBW	0.0352	-0.0022	0.0946
VPDP	-0.2584	-0.4643	-0.2949
DPDP	-0.3684	-0.279	0.0259
CBW:VPDW	-0.0469	-0.4243	0.4967
CBW:DPDW	-0.1772	-0.1863	0.659
VPDN	0.2988	-0.5428	-0.1422
DPDN	0.4409	-0.1014	0.0131

Table 4: Variable loadings on the first three principal component axes of the PCA conducted on the global sample of 'O.' excavata P₁ elements. Figures in bold indicate the variables with the heaviest loading on that component. See Table 2 for key to abbreviations.

The first principal component (PC-1) primarily represents a contrast between dorsal process length (DPL) and dorsal process denticle packing (DPDP): elements with high scores on PC-1 have long dorsal processes and wide dorsal process denticle bases, elements with low scores have short dorsal processes and narrow dorsal process denticle bases. The second principal component (PC-2) is a contrast between dorsal process length (DPL) and ventral process denticle number (VPDN): elements with high scores on PC-2 have long dorsal processes and few denticles on the ventral process, elements with low scores have shorter dorsal processes and more denticles on their ventral process. The third principal component (PC-3) is a contrast between ratio of cusp base width to dorsal process denticle width (CBW:DPDW) and inter-process angle (IPA). Elements with high scores on PC-3 have wide cusp bases relative to the average basal width of dorsal denticles, and are more arched; elements with low scores have narrower cusp bases relative to the average basal width of dorsal process denticles, and are less arched.

In order to determine whether there were significant morphological differences between the samples, indicating discontinuities within the range of variation encompassed by the 'O.' excavata hypodigm, a global multivariate analysis of variance (MANOVA) was conducted on the full raw data set. This produced significant results (Wilks' $\lambda = 0.013$, $F = 9.764$, $p < 0.001$),

indicating that highly significant differences in mean morphology are present between the different samples of '*O.*' *excavata*.

Unfortunately, the data display significant deviation from a multi-normal distribution (Mardia multivariate skewness and kurtosis test, $p < 0.001$) and heterogeneous variance (Box's *M* test, $p < 0.001$), violating the MANOVA assumptions. In this instance, a non-parametric MANOVA (NPMANOVA) would have been preferable, but sample number exceeded the maximum allowable for conducting a NPMANOVA on the available software. Consequently, the results of the analysis of the global data set must be treated with caution; however, the high significance of the results represents good evidence of genuine differences between samples. The null hypothesis of continuous morphological variation within the '*O.*' *excavata* hypodigm can thus be rejected, and further analysis of the nature of the discontinuities in the data is justified. This will enable testing of the hypothesis that significant morphological discontinuities within the hypodigm correspond to populations of '*O.*' *excavata* that are separated in space and time.

In order to test this hypothesis, separate investigations were conducted into the spatial and temporal morphological variation in '*O.*' *excavata*. Thus, for each sample, eigenscores from the PCA of multivariate data were plotted to facilitate visual examination of the data. Whilst indicating the presence significant morphological differences between samples of '*O.*' *excavata*, the global MANOVA does not reveal the *pattern* of significant differences between each pair of samples; however, conducting separate classification analyses for each sample pair to establish the pattern of significant differences is unsatisfactory, because each pair-wise classification will discriminate sample pairs based upon different variables (see Jones and Purnell (in press)). PAST Version 1.44 incorporates post-hoc pair-wise tests within the MANOVA. These can provide an indication of the pattern of significance differences in morphology between each pair of samples. Hotelling's T^2 comparisons (multivariate t-tests) were used, and were Bonferroni-adjusted to avoid Type I errors (false rejection of H_0). These post-hoc tests were conducted on the raw data of the samples included in each temporal and spatial investigation. As compensation for the use of a parametric test on non-normally distributed data, results were not considered significant unless $p < 0.01$. The smaller sample number required for the spatial and temporal analyses allowed a non-parametric MANOVA (NPMANOVA) to be conducted on the data using a Bray-Curtis distance measure, following the procedures described by Anderson (2001), which provided an additional safeguard against committing Type I errors from applying a MANOVA to non-parametric data.

Temporal variation in 'O.' excavata hypodigm

Variation through time was investigated through analysis of a stratigraphic sequence of 12 samples derived from a small area (approximately 10 × 50 km) in the southwest of the island of Gotland, Sweden, for which excellent material is available in the collections of Lennart Jeppsson at Lund University. Figure 2 illustrates how the morphology of the elements from these 12 samples varies through time. The specimens are ordinated based on eigenscores on the first three principle component axes that bound the morphospace of the hypodigm. As points of reference, the American topotype elements are also plotted on the same axes; interestingly they lie at the centre of the morphospace. Clusters are evident in the Swedish data, varying through time in both position within the morphospace and in volume of morphospace occupied. No obvious trends are apparent in these patterns of changing morphospace occupation, but a higher sampling density and rigorous testing against a random walk is required to conduct a similar analysis to that in Chapter six of *Pterospathodus*, in order to draw evolutionary conclusions from the data.

The NPMANOVA demonstrates that the morphological differences between the Swedish samples are indeed significant ($F = 18.76, p < 0.01$). Previous conodont studies have considered such a result sufficient to accept the presence of multiple species within a sample (e.g. Girard et al. 2004). However, this result provides limited information in a taxonomic context, since it does not indicate *which* samples differ significantly from which. Furthermore, it is not differences between *all* pairs of samples that are important; rather, it is differences between temporally sequential populations. Post hoc tests on the samples (see Table 5) reveal a complex pattern of significant morphological differences. The oldest population (sample one) is morphologically discontinuous from the sample stratigraphically above it and the topotype specimens. Samples two to seven form a continuous morphological sequence and are not significantly different from the topotype elements. Sample eight is discontinuous from populations stratigraphically above and below, and from the topotype specimens; this may represent an immigration event. Samples nine and ten are continuous and do not differ from the topotype. The three youngest samples are morphologically discontinuous from each other and the topotype material.

These significant morphological discontinuities are not correlated with the major environmental changes occurring during the Silurian which involved switches in oceanic circulation that affected the degree of nutrient up-welling and planktonic abundance (Primo and Secundo Episodes, Aldridge et al. 1993, Jeppsson 1990). For example, three samples from one Primo episode (samples seven, eight and nine from the Sproge Primo episode) differ significantly from one another (NPMANOVA, $F = 20.85, p < 0.01$, see also Figure 2), suggesting that

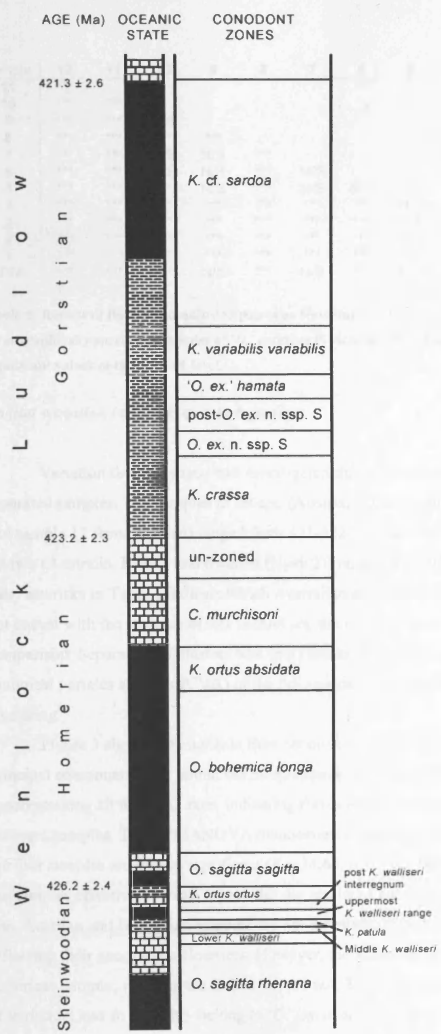
populations do not exhibit consistent morphological changes in response to such broad-scale changes in environment. More parochial effects may be overriding the general environmental influences and producing the differences, raising the possibility of local ecophenotypic responses. However, during the majority of the Ludlow and Wenlock, the southwest region of Gotland represented a distal shelf facies (Bassett et al. 1989, Calner and Jeppsson 2003). All the sample localities themselves are dominated by marls and argillaceous limestones (L. Jeppsson pers. comm. 2006, Jeppsson et al. 2006, Laufeld 1974a, b), with the lithology generally becoming more carbonaceous during Secundo episodes, and more clay-rich during Primo episodes, reflecting the primary sedimentation style of the episode. The pattern of changing morphology in P_1 elements through time in spite of the similarity of the environmental setting between the samples indicates that the changes are facies-independent and argues against local ecophenotypic response to the abiotic environment as a primary causal factor. Further examination of the biotic context of each would be desirable to further test for environmental influence on morphology, but time constraints prevented such a detailed investigation in the present work.

A potential difficulty in interpreting the results arises from the nature of the sampling. No sample locality provided a sequence covering the complete temporal range of '*O.*' *excavata*, so although the Swedish populations inhabited the same region (an area of approximately 50 by 10 km of present-day southwest Gotland) through time, each is from a different locality. Consequently, the apparent changes through time may represent local spatial differences. For example, morphology may differ between localities and yet be relatively stable at each, so that sampling at different localities through time will produce a false appearance of temporal changes. This possibility was evaluated by analysing three coeval samples from different localities on Gotland, each separated by 5-10 km. An NPMANOVA showed no significant difference between the three samples ($F = 1.839, p > 0.1$). Of course, sampling of multiple populations from different localities at every time horizon is necessary to completely eliminate the confounding effect of spatial variation, but this result suggests that the morphological differences observed through time are not reflecting geographic variation.

If spatial and ecophenotypic variation is unlikely, then the differences between the samples probably represent genuine taxonomic differences between samples. Samples two to seven, which form a morphological continuum through time, overlapping with the American topotype material probably do belong to '*O.*' *excavata*; conversely, populations one, eight, 11 and 12 exhibit significantly different morphology from the topotype specimens, and so do not appear to be part of '*O.*' *excavata*. The non-directional and continuous nature of the morphological change in the sequence of older populations (two to seven) would suggest stasis

within a single species, in accordance with the null hypothesis. However, the morphological continuity is also compatible with anagenetic speciation, perhaps also reflected in the significance of the morphological differences between sample seven and sample two, at the beginning and end of the two-to-seven sequence.

Figure 2 (following page): Ordinations of ‘*O.*’ *excavata* P₁ elements from 12 stratigraphically sequential samples from Gotland, Sweden, based on principal component scores from PCA of the global dataset. Circles represent the Swedish samples, crosses indicate the topotype material. Elements within global dataset showing extreme eigenscores are illustrated. A simplified conodont zonation and lithostratigraphy is also shown. The latter indicates oceanic state: Primo episodes are dominated by clay-rich sedimentation, Secundo episodes by limestone deposition. Black sections denote Events, generally dominated by clays. Radiometric ages are also indicated with error. Stratigraphic information from Jeppsson and Aldridge (2000), Jeppsson et al. (2006) and L. Jeppsson pers. comm. 2006. Abbreviations: *Kockolella ortus*, ‘*Ozarkodina*’ *excavata*, *Ctenonathodus murchisoni*.



SAMPLES

Gerete 2

Alsvik 7

Alsvik 4

Lukse 1

Smissarve-strand

Urgude

Sigdarve 1

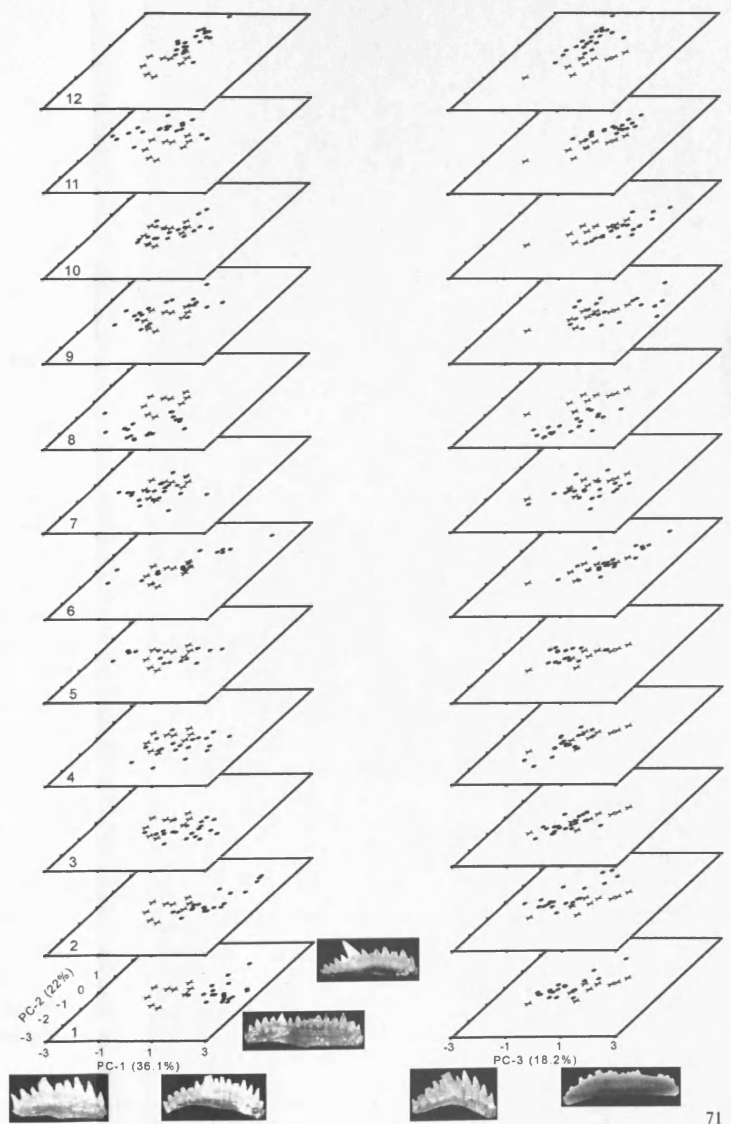
Sudervik 2

Svarvare 3

Svarvare

Östergårde 2

Östergårde 1



sample	12	11	10	9	8	7	6	5	4	3	2	1
11	***											
10	***	***										
9	***	***	N/S									
8	***	***	***	***								
7	***	***	N/S	N/S	***							
6	***	***	N/S	N/S	***	N/S						
5	***	***	***	N/S	***	N/S	N/S					
4	***	***	***	***	***	***	***	N/S				
3	***	***	***	***	***	***	***	N/S	N/S			
2	***	***	***	***	***	***	***	N/S	N/S	N/S		
1	***	***	***	***	***	***	***	***	***	N/S	***	
USA	***	***	***	N/S	***	N/S	***	N/S	***	***	***	***

Table 5: Results of Bonferroni-adjusted pair-wise Hotelling's T^2 tests for comparisons between 12 stratigraphically successive samples of 'O.' excavata P₁ elements from Gotland, Sweden. Asterisks indicate significant values at the $p < 0.01$ level.

Spatial variation in 'O.' excavata hypodigm

Variation through space was investigated through analysis of two sets of four spatially separated samples. The samples in set one (Austria, Bohemia, the American toptype material and sample 12 from Sweden) ranged from 421-422 Ma (see Table 1 for age data). The samples in set two (Australia, Britain and Sweden (Nyan 2)) ranged from 418-419 Ma (see Table 1 for age data; asterisks in Table 1 indicate which Australian and British samples were analysed). Although not coeval with the samples of this second set, the toptype material was also included for comparison. Separation of clusters was less clear in the spatially separated samples, so a global canonical variates analysis (CVA) of the full raw data set was also undertaken to optimise any clustering.

Figure 3 shows the elements from set one (421-422 Ma) ordinated on the first three principal components that bound the morphospace of the hypodigm. Some degree of clustering is apparent along all three PC axes, indicating that complex patterns of variation characterise the different samples. The NPMANOVA demonstrates that the morphological differences between the four samples are indeed significant ($F = 24.66, p < 0.01$). The CVA plot in Figure 4 separates the samples effectively. Table 6 provides the results of the post hoc tests conducted on sample set one. Austrian and Bohemian samples did not differ significantly in their morphology, perhaps reflecting their geographic closeness. However, the Austrian population differed from the American sample, whereas the Bohemian did not. These three samples form an overlapping range of variation, and so probably belong to 'O.' excavata. However, the Swedish population differed significantly from all samples, suggesting it may represent a different species.

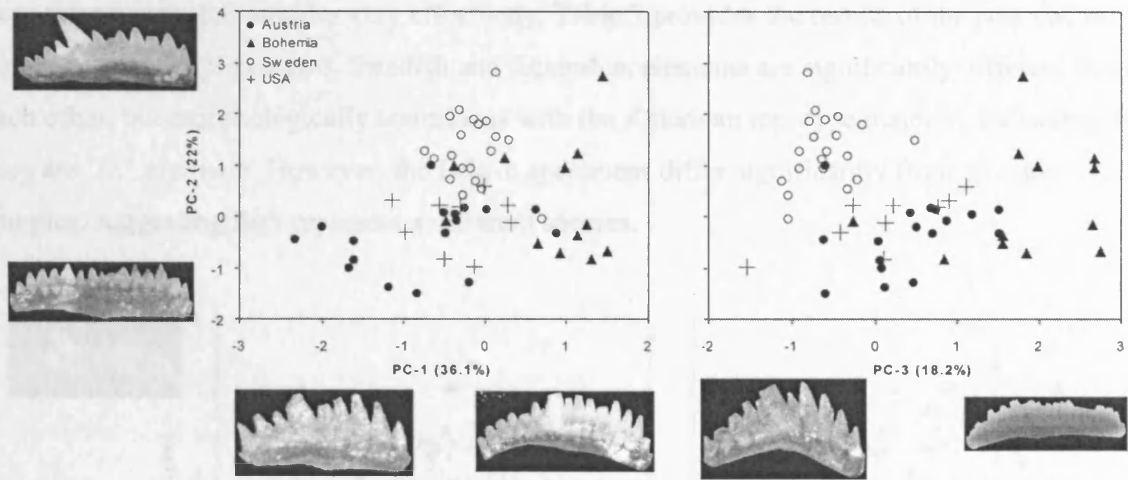


Figure 3: Ordinations of four coeval samples (421-422Ma) of '*O.*' *excavata* P₁ elements on the first three PC axes, based on PC scores from global PCA. End-member elements with extreme eigenscore values are illustrated.

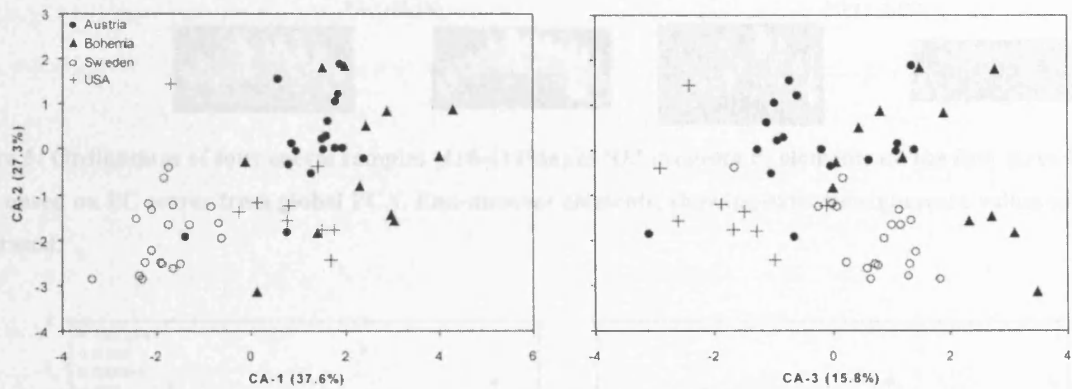


Figure 4: '*O.*' *excavata* P₁ elements from four coeval samples (421-422Ma), ordinated on the first three canonical axes, based on scores from global CVA of multivariate data.

sample	USA	Austria	Bohemia
Austria	***		
Bohemia	N/S	N/S	
Sweden	***	***	***

Table 6: Results of Bonferroni-adjusted pair-wise Hotelling's T^2 tests for comparisons between set one (421-422Ma) of '*O.*' *excavata* P₁ elements. Asterisks indicate significant values at the $p < 0.01$ level.

Figure 5 shows the results for elements from set two (418-419 Ma) ordinated on the first three principal components. Less separation of clusters is apparent in this set of samples, but the NPMANOVA suggests that there are significant morphological differences between the four

spatially separated populations ($F = 15.21, p < 0.01$). Unfortunately, the CVA plot in Figure 6 does not separate the samples very effectively. Table 7 provides the results of the post hoc tests conducted on sample set two. Swedish and Australian elements are significantly different from each other, but morphologically continuous with the American topotype material, indicating that they are '*O.*' *excavata*. However, the British specimens differ significantly from all other samples, suggesting they represent a different species.

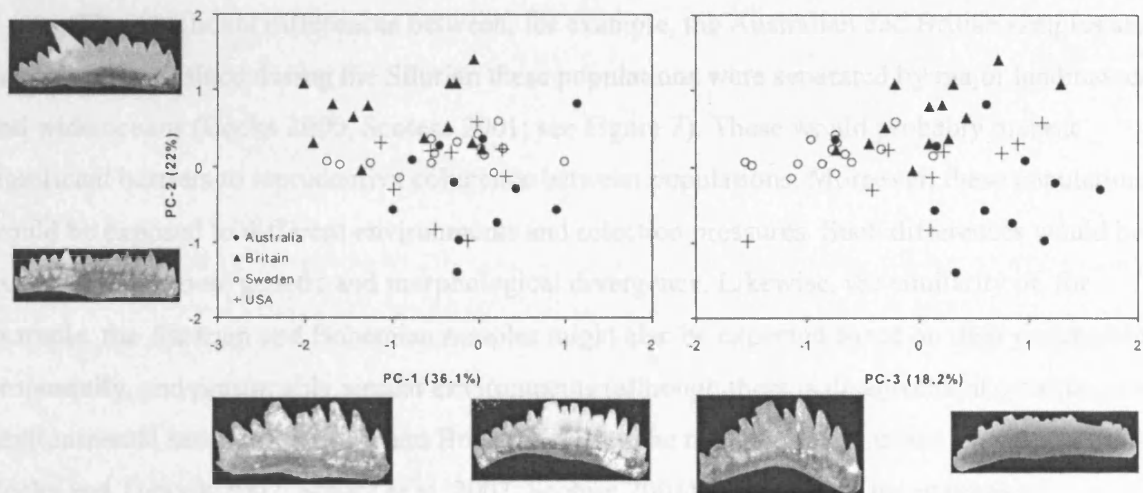


Figure 5: Ordinations of four coeval samples (418-419Ma) of '*O.*' *excavata* P₁ elements on the first three PC axes, based on PC scores from global PCA. End-member elements, showing extreme eignescore values are illustrated.

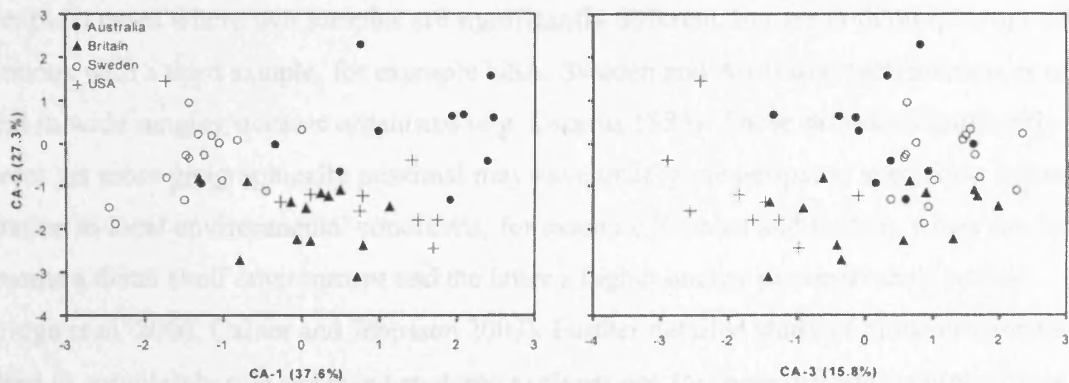


Figure 6: '*O.*' *excavata* P₁ elements from four coeval samples (418-419Ma), ordinated on the first three canonical axes, based on scores from global CVA of multivariate data.

sample	USA	Australia	Britain
Australia	N/S		
Britain	***	***	
Sweden	***	N/S	***

Table 7: Results of Bonferroni-adjusted pair-wise Hotelling's T^2 tests for comparisons between set two (418-419Ma) of '*O.* *excavata* P₁ elements. Asterisks indicate significant values at the $p < 0.01$ level.

The significant differences between, for example, the Australian and British samples are not unexpected, since during the Silurian these populations were separated by major landmasses and wide oceans (Cocks 2000, Scotese 2001; see Figure 7). These would probably present significant barriers to reproductive coherence between populations. Moreover, these populations would be exposed to different environments and selection pressures. Such differences would be expected to promote genetic and morphological divergence. Likewise, the similarity of, for example, the Austrian and Bohemian samples might also be expected based on their geographic propinquity, and presumably similar environments (although there is disagreement over the exact environmental setting of Austria and Bohemia during the mid Silurian; e.g. see Cocks et al. 1997, Cocks and Torsvik 2002, Schatz et al. 2002, Scotese 2001). Yet some of the patterns of significant differences between samples in set one and two are not easily explicable in terms of geographic vicariance, with widely separated samples exhibiting a continuous morphological range, and geographically adjacent population displaying significant differences. Clinal variation may explain cases where two samples are significantly different, but are both morphologically continuous with a third sample, for example USA, Sweden and Australia; such patterns as often present in wide ranging oceanic organisms (e.g. Lazarus 1983). Those samples significantly different yet more geographically proximal may have undergone peripatric speciation following adaptation to local environmental conditions; for example Sweden and Britain, where the former represents a distal shelf environment and the latter a higher energy proximal shelf setting (Aldridge et al. 2000, Calner and Jeppsson 2003). Further detailed study of biotic environment is required to completely rule out ecophenotypic explanations for these differing morphologies.

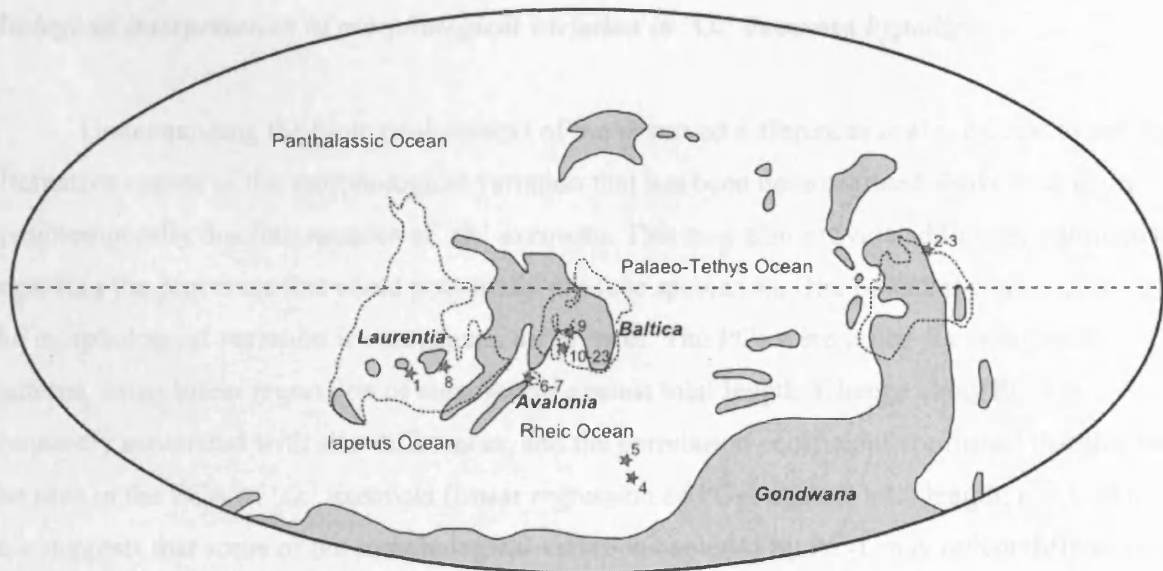


Figure 7: Palaeogeographic map for the mid Silurian (c. 425 Ma), showing ancient landmasses (grey), outlines of selected modern continents (dashed lines) and location of samples listed in Table 1: America (1), Australia (2-3), Austria (4), Bohemia (5), Britain (6-7), Canada (8), Estonia (9) and Sweden (10-23). Map based on reconstruction by Scotese (2001) with additional information from Cocks (2000). Relative proximity of Bohemia and Austria (samples 4 and 5) to Gondwana and the Avalonia-Baltica landmass is uncertain (Cocks et al. 1997, Cocks and Torsvik 2002, Schatz et al. 2002).

Biological interpretation of morphological variation in 'O.' excavata hypodigm

Understanding the biological context of the observed differences is also critical to test for alternative causes of the morphological variation that has been demonstrated above to exist in spatiotemporally discrete samples of '*O.*' *excavata*. This may also provide additional information regarding the processes that could potentially produce speciation. One potential explanation for the morphological variation is ontogenetic differences. The PCs were tested for ontogenetic patterns, using linear regression of eigenscores against total length. Change along PC-1 is frequently associated with size differences, and the correlation coefficient confirmed that this was the case in the PCA of '*O.*' *excavata* (linear regression of PC-1 against total length: $r^2 = 0.76$); this suggests that some of the morphological variation captured by PC-1 may reflect differences between the ages of individuals within each sample. However, the other PC axes had values of $r^2 \ll 0.5$, suggesting that these axes are capturing shape variation that is not primarily ontogenetic.

Principal component two is dominated by variation in dorsal process length and ventral process denticle number. In conodont taxa for which function has been investigated rigorously, the dorsal process is the food handling process of the P_1 element (Donoghue and Purnell 1999). Increasing the length of the process has the obvious potential advantage of increasing length for shearing of food particles. Thus the morphological variation may reflect differences in diet between the different populations. Such resource partitioning in extant populations is known to lead to divergent natural selection and morphological differentiation (see Dayan and Simberloff 2005 for a review with examples). Variations in diet can be tested for using other lines of evidence, for example examining whether element microwear differs between populations (Purnell 1995), indicating that different foodstuffs are being processed. Also, the different morphologies could be modelled (Evans and Sanson 2003) to investigate how observed changes in element structure might affect function, helping to constrain the efficiency with which elements of different configurations could process various hypothesized food types. The latter approach may also provide indications of how other characters of the element contribute to food processing or element articulation, particularly the other variables loading heavily on the component axes; to determine, for example, the effects of changing denticle width on the articulating ventral process, or of altering the overall curvature of the element.

Conclusions

This work has presented new, standardised and widely-applicable morphometric protocols and utilised them to test the hypothesis that the taxonomically problematic conodont species '*Ozarkodina*' *excavata* is monospecific. This has determined that significant morphological discontinuities are present between '*O.*' *excavata* populations which were separated in time and space. Moreover, many of these populations have been shown to differ significantly in their morphology from the topotype material of '*O.*' *excavata*. Analysis of the data produced by the protocol has also revealed which morphological characters in '*O.*' *excavata* best characterise these discontinuities. This permits interpretation of the variation in a biological context, which suggests that these differences are most probably associated with variations in diet.

Biological and spatiotemporal interpretation of the morphological discontinuities suggests that there may be multiple species present in the '*O.*' *excavata* hypodigm. Further independent tests are outlined which could more rigorously test these hypotheses, but they are beyond the scope of the work presented here. If the morphotypes identified here actually represent multiple species, then the high discriminatory power of the protocols to distinguish between them suggests that these techniques have potential to provide a generalised tool for conodont species identification that is methodologically standardised and can produce repeatable and reproducible results.

The results of analyses conducted here also have potentially significant biostratigraphic implications. The global distribution of '*O.*' *excavata* renders this species an ideal taxon for stratigraphic purposes; however morphs and subspecies of '*O.*' *excavata* are currently employed to a very limited extent in establishing biozonation (e.g. Jeppsson and Aldridge 2000). The morphometric protocols utilised here have revealed discrete, temporally separated clusters within the morphospace of '*O.*' *excavata*; these clusters can furthermore be repeatedly and objectively recognised using the variables identified by the analysis. If equivalent morphological clusters can be as rigorously identified at other localities using these protocols, then this holds the potential of far more widespread use of '*O.*' *excavata* morphologies in refining Silurian biostratigraphy.

Hopefully the methods and results presented in this chapter will also catalyse more comprehensive morphometric analysis of conodonts using these protocols; such engagement with morphometrics is a crucial for realising the potential of the rich fossil record of conodonts.

Chapter four: Testing species hypotheses in conodonts – outline analysis of ‘*Ozarkodina*’ *excavata*

Abstract

Conodonts are an extinct group of early vertebrates that possess an exceptionally good fossil record. This record has potential for numerous applications, including phylogenetics, palaeobiological investigation and evolutionary analysis. Exploiting this potential requires both rigorous delineation of conodont morphology and establishment of a stable taxonomic framework. Morphometric analysis provides an effective means of accomplishing these goals. This work presents new, standardised morphometric protocols, suitable for examining morphological variation in conodonts, which extend and complement those outlined and successfully employed in Chapter three and Jones and Purnell (in press). The new protocols presented here incorporate two different outline analyses to capture aspects of general conodont element shape. They are applied to the taxonomically problematic conodont species ‘*Ozarkodina*’ *excavata*, to further test the hypothesis that this morphologically variable taxon is monospecific. Results support some of the significant morphological discontinuities previously identified within samples assigned to this taxon (Jones and Purnell in press). Analysis of these discontinuities in their spatiotemporal and biological context reveals significant differences between spatially separated populations of ‘*Ozarkodina*’ *excavata*, suggesting that multiple species are currently accommodated within this taxon. The protocols have also identified a possible trend in P_1 element morphology of increasing differentiation from P_2 elements, which may provide insights into apparatus evolution within ozarkodinids. The results of this work demonstrate that together, the methods presented here and in Jones and Purnell (in press), constitute an effective suite of morphometric protocols for analysis of morphological variation in conodonts, with great potential for wide across-taxon application.

Introduction

Conodonts are a large, extinct clade of stem gnathostomes, possessing a skeleton composed of phosphatic tooth-like elements, which formed an oropharyngeal feeding apparatus (Aldridge and Purnell 1996, Donoghue et al. 1998). The conodont fossil record consists dominantly of disarticulated elements; the huge abundance of these elements throughout the 300 million year span of the clade's existence has made them invaluable biostratigraphic tools for establishing and constraining relative ages in the geologic record (Higgins and Austin 1985, Sweet and Donoghue 2001). The exceptionally high quality of the conodont fossil record also offers an unparalleled opportunity to study evolutionary rates, patterns and processes within a vertebrate group. Additionally, by virtue of their phylogenetic position, conodonts have a key role to play in elucidating the sequence of character acquisition in the vertebrate clade (Purnell 2001).

Exploiting the potential of the conodont fossil record obviously requires a stable taxonomic foundation. However, conodont taxonomy is frequently problematic: as with many palaeontological studies, species boundaries must be delineated based solely on partial skeletal material that often displays extensive and complex morphological variation. This would seem an ideal problem for the application of morphometric analysis, and yet comparatively few studies have adopted such a quantitative approach to taxonomy; most of these have been based upon outline analysis and are discussed below.

Klapper and Foster (1986, 1993) examined the oral outline of *Palmatolepis* P₁ elements to test whether species identified using distinctive M and P₂ element morphology also displayed characteristic P₁ element morphology, with the aim of refining the biostratigraphy based upon *Palmatolepis* species. They utilised a "non-standard" outline analysis technique, which divided a profile into tangent segments and measured their angles. Unfortunately, "standard" outline techniques, such as Fourier or eigenshape analysis, were not used to compare their efficiency. Klapper and Foster's (1986, 1993) method produced tight clustering of elements in a canonical variates analysis, and showed close correspondence between morphological clusters identified using outline analysis and elements grouped based on qualitative discrimination. Interestingly, although the type specimens often ordinated within the clusters of the species they represented, some plotted well outside; this clearly illustrates the potential pitfalls of a strictly type-based approach to taxonomy in ignoring the morphological variation within a taxon.

The aim of Sloan's (2003) study was to compare different methods of acquiring and analysing outline data from various conodont taxa. Strangely, neither eigenshape nor Fourier analysis was applied; instead, several "non-standard" approaches were tested, including a method akin to that of Klapper and Foster (1986, 1993, see above). The elements analysed were taxonomically assigned *a priori*, and pair-wise comparisons conducted to search for significant differences between the outline data for each pair. Only two-thirds of the contrasts yielded significant results, and the majority of these derived from the cross-generic contrasts, rather than from the congeneric species comparisons. Sloan (2003) presented his work as discriminatory, contrasting it to previous research, but like the studies above, the elements examined are taxonomically assigned *a priori*. No blind tests were undertaken to assess the discriminatory power of the techniques when the specific assignment of the elements was unknown. Thus, the morphometric techniques provided a means to test existing qualitative schemes, rather than being presented as an alternative discriminatory tool.

In contrast, Girard et al. (2004) conducted elliptic Fourier analysis of the oral surface of *Palmatolepis* P₁ elements, primarily to examine evolution and ontogeny within the genus, but also morphometrically to classify elements of uncertain specific assignment, by comparing them with elements of known species affinity. Results for this taxonomic aspect of their work are difficult to interpret since no actual elements are figured, but the *Palmatolepis* species were poorly discriminated by the analysis, so that identification of indeterminate specimens remained equivocal.

The goal of the open outline analysis of Roopnarine et al. (2004) was also primarily evolutionary but they also examined potential taxonomic boundaries at each of the stratigraphic levels they sampled. Roopnarine et al. (2004) used a cubic spline to describe the basal margin of *Wurmiella* P₁ elements; however, restricting the analysis to the basal margin assumes that the most useful information is present in this region. This may be true from a purely taxonomic perspective (e.g. Murphy et al. 1981), but this unsystematic sampling of form is a criticism levelled at traditional methods, because its biological significance may be open to question. A canonical variates analysis of their morphometric data revealed some clustering of elements into three possible taxonomic groupings, although their statistical testing of these groups consisted only of a single MANOVA, which does indicate the pattern of significance differences between the three clusters.

In Jones and Purnell (in press), new, standardised morphometric protocols incorporating multivariate analysis of traditional variables (comprising lengths, angles, etc.) were presented. These protocols were utilised to test whether multiple species existed within the taxonomic

boundaries of '*Ozarkodina excavata*' (Branson and Mehl 1933). The protocols proved highly effective at identifying and discriminating statistically significant morphological differences between populations of '*O.*' *excavata* that were separated in space and time, strongly suggesting that '*O.*' *excavata* is not monospecific.

The goals of the current work are twofold: first, to introduce additional morphometric protocols, based around more sophisticated outline analysis, to analyse aspects of conodont element morphology not captured by analysis of traditional variables; second, to further characterise morphological variation within '*O.*' *excavata*, and to test whether multiple species are currently accommodated within this species. This is the first study to examine the general shape of the rostral profile of conodont elements, recognising that useful shape variability may be present in areas of the element hitherto not considered. This will extend and complement the morphometric methods presented in Jones and Purnell (in press), provide additional tests for the hypothesis that multiple species are currently accommodated within '*O.*' *excavata*, and reveal trends of morphological variation that may offer general insights into element differentiation and apparatus evolution within ozarkodinid conodonts.

The species concept and '*Ozarkodina excavata*'

This species has a global distribution (Jeppsson 1974) and a stratigraphic range extending from at least the mid Silurian to the Early Devonian (Murphy and Cebecioglu 1986), perhaps originating far earlier (Aldridge and Mabillard 1985, Cooper 1975, 1976, Jeppsson 1974). Most authorities currently consider '*O.*' *excavata* to be a single species displaying a high degree of continuous morphological variation, which appears not to vary systematically through time. However, the degree of morphological variation that can be incorporated within '*O.*' *excavata* is uncertain (Jeppsson 1974). This problem is difficult to address using traditional methods of qualitative observation: the relative morphological simplicity of the elements within the '*O.*' *excavata* skeleton and the complex yet subtle variation they display has led to considerable subjectivity and inconsistency in determining the taxonomic boundaries of the species (Jeppsson 1974). These uncertainties surrounding the morphology and taxonomy of '*O.*' *excavata* make it an ideal choice of species for morphometric analysis.

These protocols are used here to further test the hypothesis articulated in Chapter three and Jones and Purnell (in press): that the '*O.*' *excavata* hypodigm represents a single species (use of the term hypodigm follows Mayr et al. 1953: p.237, "A hypodigm is all the available material

of a species"). Testing the morphological boundaries of a species raises the question of what a species is. In order to justify the approach to the specific problem of '*O. excavata*' some theoretical considerations of species concepts are required. These were outlined in Chapter three and Jones and Purnell (in press), but are re-iterated here because of their importance to the current work.

In this work, a general species concept was chosen *a priori*, as recommended by Wiens (2004); hypotheses are framed and the results interpreted within this concept. Full discussion of the continuing debate over the various merits of different species concepts is beyond the scope of this work, but one fact seems unequivocal: despite implicit suggestions to the contrary by many authors (e.g., see contributions to Wheeler and Meier 2000) no single species concept is universally applicable. So rather than selecting a particular concept, and inevitably its associated conceptual baggage, a pragmatic approach is taken, delineating species as follows.

Extinct and most extant sexually reproducing species are operationally identified through morphological features, or phenetic clusters in a quantitative sense (Sokal and Crovello 1970). Yet such morphospecies are often implicitly, if not explicitly, considered as proxies for biological species (Benton and Pearson 2001). This is because biological species are composed of reproductively isolated populations (Mayr 1942, 1969) and the sharing of morphological characters is taken to indicate a shared, common gene pool. In this theoretical definition, biological species are deemed significant because this genetic coherence means that they approach closest to real entities or individuals (Baum 1998, Mishler and Donoghue 1982), in comparison with somewhat arbitrary supra-specific taxa.

Unfortunately, identification of biological species is not simply a question of discerning morphological differences; the use of morphology alone is frequently insufficient because often there is not an exact correspondence between morphological distinctiveness and reproductive isolation. Numerous instances of morphologically indistinguishable sibling species are now known in a range of animal groups (see Knowlton 1993 for a review of marine examples), and intra-specific differences can exceed those between species (e.g., Bell et al. 2002).

Polymorphisms such as ecophenotypy can also produce a range of morphologies within one species (e.g., Peijnenburg and Pierrot-Bults 2004). Moreover, delineating biological species is problematic because the biological species concept is ahistorical and emphasises intrinsic reproductive isolation mechanisms for species maintenance. Reproductive isolation is obviously impossible to test for in fossil populations, and the inapplicability of species concepts based around potential interbreeding is clear where populations are separated in time, perhaps by millions of years. Of course, in the case of fossils, determining where the boundaries between

potential species may lie must be based on recognition of morphological discontinuities. But evaluating the biological significance of these discontinuities requires them to be interpreted within their spatial, temporal and ecological contexts. Only then can the likelihood that distinct morphologies represent reproductively isolated biological species be assessed.

Spatial information can be incorporated by considering the geographic distribution of morphologically distinct fossil populations; extrinsic spatial separation can prevent gene flow between populations, creating the potential for phenotypic differentiation. Moreover, such vicariance is easier to demonstrate in fossil populations than the intrinsic reproductive barriers required by the biological species concept. Environments will also vary across a species' geographic range, and the contrasting selection pressures that result will favour genetic and morphological divergence (the former enhancing reproductive isolation, the latter producing visible change) potentially reflecting the evolution of new species.

Initially, temporal information need only consist of whether a fossil population differs significantly in its morphology from those stratigraphically above or below, where all are initially considered to be the same species. Induction of these patterns explicitly as ancestor-descendent relationships through time is not necessary (but may be undertaken). Nevertheless, these patterns can be assessed to determine whether they would be most sensibly interpreted as the evolving sequence of populations forming a single species or, for example, as an anagenetic pathway, where one species evolves gradually into another. Other factors (sampling density, stratigraphic completeness, etc) will heavily influence any decision as to which of these alternative evolutionary-taxonomic scenarios is determined to be most probable.

Ecological and biological interpretations, including functional morphology, are also required to better assess the taxonomic significance of observed differences, aiding for example, in the identification of confounding intra-specific variation caused by ontogenetic change or ecophenotypy. A population-based rather than strictly type-based approach to taxonomy is endorsed here. This is complementary to the application of quantitative analysis involving a large number of specimens and provides a clearer picture of the variation within the population by better constraining non-taxonomic aspects of variation. Moreover, previous morphometric studies have clearly demonstrated the pitfalls of strictly typological taxonomy (Ritter 1989, see above). If the morphological differences between a given population and the type specimens are statistically significant to a standardised level, this is justification for assigning those morphotypes to different species.

Based on the foregoing discussion, two levels of hypotheses have been formulated. The initial null hypothesis is that the morphological variation within the '*O.*' *excavata* hypodigm is

continuously distributed, supporting the general consensus that the hypodigm is a single morphospecies. The alternative hypothesis is that morphological variation within the hypodigm displays discrete or semi-discrete clustering. If the null hypothesis is falsified and multiple morphological clusters are detected, then if the morphological clusters correspond to temporally and/or spatially discrete populations, and if characters that define them have adaptive biological significance, then the most parsimonious interpretation is that these populations represent separate species.

Materials

As in Jones and Purnell (in press), the focus of this work is elements that are thought to have occupied the P_1 position in the skeleton. This is partly because P_1 elements are regarded as taxonomically useful (Sweet 1988), but particularly because this element has a comparatively two-dimensional structure, providing an appropriate profile for the two-dimensional outline techniques utilised here. P_1 and P_2 elements were differentiated in many samples using protocols similar to those outlined in Chapter two. Other samples had well differentiated P_1 and P_2 elements, which did not require quantitative differentiation.

In order to capture as much of the potential variation within the '*O.*' *excavata* hypodigm as possible, the samples analysed included P_1 elements of '*O.*' *excavata* from most of its spatiotemporal range (see Table 1). The full data set is provided in Appendix 1. All the samples analysed using outline methods were also analysed in Chapter three and, except for one Swedish sample, in Jones and Purnell (in press). However, time constraints prevented the analysis of every sample incorporated in these previous studies. Sample size was limited because only elements with complete aboral margins could be included within the outline analyses. Nevertheless, 169 specimens from 16 samples of '*O.*' *excavata* P_1 elements were analysed.

Including such a "global" sample of the hypodigm produces an empirical morphospace for '*O.*' *excavata* within which individual samples lie. The use of empirical morphospaces has been criticised because of their potential instability with changing sample number and size. However, the robustness of empirical morphospace with changing sample size was assessed in Chapter three and Jones and Purnell (in press), which found that results differed little even when the global sample size was changed by as much as 15%. This supports the interpretation that the empirical hyperspace generated by the analysis does approach the stability of a theoretical morphospace.

Method

The outline of the P₁ element's rostral surface was prepared for digitisation in Adobe Photoshop. Denticles and cusp are frequently worn, broken or absent, and so required elimination from the outline: a mask was drawn around the top of the element, from nadir to nadir, and the denticles and cusp obscured. The dashed line in Figure 1 illustrates the path of this mask, creating the oral portion of the element outline. Although denticle fusion affects the smoothness of this line, in most cases it was insufficient to prevent the general shape of the element from being captured. The positions of the terminals of the basal cavity were marked on (represented by points labelled V and D in Figure 1) and the contrast of the image was increased to delineate the base of the element, producing a silhouette. The thick line in Figure 1 represents this aboral portion of the element outline.

Small irregularities in the outline, such as mineral encrustation, occasionally required elimination. The outline was extended across these irregularities parsimoniously, using a straight line produced with a polygonal mask. This retouching, defined by Bengtson (2000) as adding what was not in the original image, is understandably advised against in most instances: for example where the fine details of internal features are of interest. It is not problematic in this situation where only the general form of the outline is under investigation and retouching is limited. Many elements were still not used if even such simple interpolation of the outline was considered unjustified. An automated "action" can be set up in Photoshop to complete the final enhancements:

1. Application of a Gaussian blur filter, radius 1.2 pixels, to smooth the outline and reduce digitisation noise. The filter decreases the frequency of irregularities in the outline by averaging the pixels next to the hard edge. The radius dictates the area of pixels sampled for this averaging.
2. Rotation of the silhouette by 90° anticlockwise so that the ventral basal cavity terminus is in the top right hand corner, to maintain geometric equivalence during digitisation. If the ventral process of the element initially faced left, then the image was horizontally flipped.
3. Conversion of the image to greyscale to conserve memory. The image was then saved as a tif file.

The silhouette file was then opened within the tpsDig software (Rohlf 2003). Starting at the ventral basal cavity terminus (V) the outline was digitised anticlockwise to 200 Cartesian (x,

y) coordinates and the dorsal basal cavity terminus (D) landmark registered. The data was saved as a tps file. The number of coordinates used will determine how closely the digitisation follows the outline, and consequently how much of the original detail in the outline will be fed into the outline analyses: more points results in lower signal to noise ratio. For any outline analysis that involves this kind of digitisation, the initial choice is somewhat arbitrary. The 200 value was selected after first considering other workers' choice (e.g. Klapper and Foster 1986), and then using a degree of trial and error. If too many points are included, variation for small irregularities swamps the signal; too few point results in major feature being lost, such as the curvature of the aboral margin. Adjusting the outline tolerance during the EES analysis can further fine-tune the degree of shape variation incorporated in the analysis. Similar refinement can be achieved in EFA by varying the number of harmonics incorporated into the final principal components analysis.

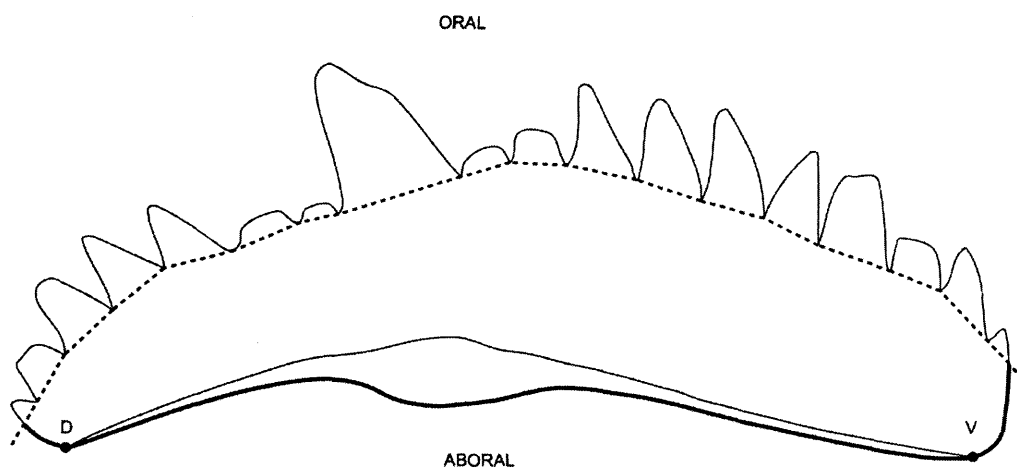


Figure 1: 'O.' excavata P₁ element in rostral view. Dashed line illustrates path of mask to obscure denticles, delineating oral margin of element outline to be analysed. Thick line represents aboral margin of outline. Points V and D mark the positions of the landmark points on the ventral and dorsal terminals of the basal cavity.

Two outline techniques were applied to the rostral profile of 'O.' excavata P₁ elements: extended eigenshape (EES) analysis (MacLeod 1999) and elliptic Fourier analysis (EFA: Ferson et al. 1985, Giardina and Kuhl 1977, Kuhl and Giardina 1982). The latter analysis produced 40 Fourier coefficients, which were input as variables to a PCA. No *a priori* clustering was assumed by either outline analysis. EES analysis was conducted using MacLeod's (1999) EES software. EFA was undertaken in PAST Version 1.44 (Hammer et al. 2001). All graphs were produced in Microsoft Excel.

Locality	Age	Age data reference	N
Lithium, Missouri, USA	mid Ludlow	Boucot (1958); Rexroad and Craig (1971)	7
Broken River, Queensland, Australia	Latest Silurian	A. Simpson pers. comm. 2005	9
Carnic Alps, Austria	Ludlow, mid Gorstian	Walliser (1964)	20
Muslovka Quarry, Bohemia	Upper Přídolí	Walmsley et al. (1974)	8
Netherton, Britain *	Ludlow, Ludfordian	Aldridge et al. (2000)	13
Ludlow, Britain	Ludlow, Ludfordian	Aldridge et al. (2000)	10
Hepworth, Ontario, Canada	Wenlock	von Bitter and Purnell (2005)	20
Pusku, Estonia	Llandovery, late Rhuddanian	P. Mannik pers. comm. 2005	14
Nyan 2, Gotland, Sweden	Ludlow, Ludfordian		8
Gerete 2, Gotland, Sweden (12)	Ludlow, Gorstian		10
Lukse 1, Gotland, Sweden (9)	Ludlow, Gorstian		9
Urgude, Gotland, Sweden (7)	Ludlow, Gorstian	L. Jeppsson pers. comm. 2004	8
Svarvare 3, Gotland, Sweden (4)	Wenlock, Homerian	Jeppsson et al. (2006)	9
Svarvare 1, Gotland, Sweden (3)	Wenlock, Homerian		9
Östergårde 2, Gotland, Sweden (2)	Wenlock, Sheinwoodian		7
Östergårde 1, Gotland, Sweden (1)	Wenlock, Sheinwoodian		8

169

Table 1: Locality, age and number of elements sampled (N) for each sample of ‘*O.*’ excavata P₁ elements analysed in this work. Swedish samples are ordered according to relative age at a series of intervals through the Ludlow and Wenlock. Numbers in brackets on left-hand column refer to sample notation in Figures 2 and 3. Asterisk indicates which British sample was used in the analyses of spatially separated samples (see below).

Results and discussion

The results from the outline analyses of the global dataset are provided below. Table 2 shows eigenvalues and percentage variance captured for the first three eigenshape vectors produced by the EES analysis; Table 3 shows eigenvalues and the percent variance captured for the first three principal components (PCs) from the PCA of Fourier coefficients. The shape differences captured by each outline analysis are discussed below in the context of the sample comparisons.

EES	eigenvalue	% variance	cumulative % variance
1	471.252	98.6	98.6
2	1.65	0.3	98.9
3	0.96	0.2	99.1

Table 2: Eigenvalues, percentage of variance explained and cumulative percent variance explained for first three extended eigenshapes (EESs) produced by EES analysis of the global dataset of ‘*O.*’ excavata P₁ elements.

PC	eigenvalue	% variance	cumulative % variance
1	0.0030	51.1	51.1
2	0.0019	33.2	84.3
3	0.0003	5	89.3

Table 3: Eigenvalues, percentage of variance explained and cumulative percent variance explained for first three principle components (PCs) produced by PCA of Fourier coefficients from the EFA of the global dataset of ‘*O.*’ excavata P₁ elements.

In order to determine whether there were significant morphological differences between the samples, indicating discontinuities within the range of variation encompassed by the ‘*O.*’ excavata hypodigm, a multivariate analysis of variance (MANOVA) was conducted on the eigenscores from each of the two outline analyses. The MANOVA of eigenscores for both the first three extended eigenshapes (Wilks’ $\lambda = 0.225$, $F = 6.51$, $p < 0.001$) and first three principle component scores from the PCA of Fourier coefficients (Wilks’ $\lambda = 0.168$, $F = 8.234$, $p < 0.001$) both indicate highly significant differences in mean morphology are present between the different samples of ‘*O.*’ excavata.

Unfortunately, the outline data display significant deviation from a multi-normal distribution (Mardia multivariate skewness and kurtosis test, $p < 0.01$) and heterogeneous variance (Box's M test, $p < 0.01$), violating the MANOVA assumptions. In this instance, a non-parametric MANOVA (NPMANOVA) would have been preferable, but sample number exceeded the maximum allowable for conducting a NPMANOVA on the available software. Consequently, the results of the analysis must be treated with caution; however, the high significance of the results represents good evidence that the differences are genuine. The null hypothesis of continuous morphological variation within the '*O.*' *excavata* hypodigm can thus be rejected, and further analysis of the nature of the discontinuities in the data is justified. This allows testing the hypothesis that significant morphological discontinuities within the hypodigm correspond to populations of '*O.*' *excavata* that are separated in space and time.

In order to test this hypothesis, spatial and temporal variation in '*O.*' *excavata* was investigated separately. For each sample, elements were ordinated based on eigenscores from the EES analysis and the PCA of Fourier coefficients to facilitate visual examination of the data. Since the aim of this work is to identify morphological discontinuities between '*O.*' *excavata* populations, elements were only plotted on eigenscore axes along which samples were consistently maximally separated: eigenshape axes two and three, and PC axes one and two. In these plots, approximations of the analysed outlines of end-member elements (with extreme eigenscore values), are figured to aid visualisation and interpretation of the shape variation associated with each eigenscore axis. For the eigenshape ordinations, outlines are based on (x, y) coordinate pairs produced by transformation of the extended phi shape functions upon which the EES analysis is based, rounded to a set tolerance threshold (here 99%; the greater the tolerance, the greater the quantity of the outline's detail that is incorporated). For the PCA of Fourier coefficients, outlines were generated using the inverse Fourier function based on ten harmonics (the maximum available in PAST; the more harmonics included, the greater the quantity of the outline's detail that is incorporated). The elements represented by these outlines are illustrated, to relate the variation captured by the outline analyses to actual elements.

The global MANOVA conducted above does not reveal the pattern of significant differences between samples; however, conducting separate classification analyses for each sample pair to establish the pattern of significant differences is unsatisfactory, because each pair-wise classification will discriminate sample pairs based upon different variables (see Jones and Purnell (in press)). PAST Version 1.44 incorporates post-hoc pair-wise tests within the MANOVA. These can provide an indication of the pattern of significance differences in morphology between each sample. Hotelling's T^2 comparisons (multivariate t-tests) were used,

and were Bonferroni-adjusted to avoid Type I errors (false rejection of H_0). As compensation for the use of a parametric test on non-normally distributed data, results were not considered significant unless $p < 0.01$. The smaller sample number required for the spatial and temporal analyses allowed a non-parametric MANOVA (NPMANOVA) to be conducted on the data using a Bray-Curtis distance measure, following the procedures described by Anderson (2001). The NPMANOVA provides an additional safeguard against committing Type I errors from applying a MANOVA to non-parametric data (see above).

Temporal variation in the ‘O.’ excavata hypodigm

Variation through time was investigated through analysis of a stratigraphic sequence of seven samples derived from a small area (approximately 10×50 km) in the southwest of the island of Gotland, Sweden, for which excellent material is available in the collections of Lennart Jeppsson at Lund University. These seven samples were selected from the 13 used in Chapter three because they contained the maximum number of complete elements suitable for outline analysis. Sample numbering is the same as Chapter three and Jones and Purnell (in press), to allow easy comparison. Figure 2 and 3 illustrate how the shape of P_1 elements from the Swedish samples varies through time, within the morphospace of the ‘O.’ *excavata* hypodigm. Figure 2 shows the elements ordinated on eigenshape axes two and three, based on eigenscores from the EES analysis. Figure 3 shows the same elements plotted on the principle component axes one and two, based on eigenscores from the PCA of Fourier coefficients. In both figures, the American topotype elements are plotted on the same axes as points of reference.

The pattern of element distribution is similar in both analyses. Clusters are evident in the Swedish data, varying through time in both position within the morphospace and in volume of morphospace occupied. A possible trend detected by both outline analyses, is a shift from more arched P_1 elements in stratigraphically older samples, to straighter P_1 elements in stratigraphically younger samples, although sample 12 does not conform to this trend, and may, for example, represent an immigration event. P_1 elements in older populations therefore more closely resemble classic P_2 element morphology, than P_1 elements in later populations. Sample size and number are small, so the veracity of this pattern must be accepted with caution; nevertheless, it may reflect a broad-scale shift from poorly- to well-differentiated element morphology within the ‘O.’ *excavata* apparatus through time. There are hints of this trend in the multivariate analysis of Swedish samples (Chapter three; Figure 2), which further indicates that this represents a genuine pattern. Moreover, the oldest sample within the global dataset, from Estonia, displays P_1 elements

with morphology most similar to classic '*O.*' *excavata* P₂ morphology in qualitative observation. Better sampling is required to rigorously test this apparent trend.

The NPMANOVA suggests that the morphological differences between the Swedish samples captured by the outline analyses are significant (EFA: $F = 5.75$, $p < 0.01$; EES analysis: $F = 5.81$, $p < 0.01$). Post hoc tests of the EES eigenscores showed that several samples differed significantly from each other, but no significant differences between stratigraphically adjacent samples were present (see Table 4). Only two populations differed from the American topotype material, both older samples; however, these were morphologically continuous with other samples not differing significantly from the topotype specimens. Post hoc tests on the eigenscores from the PCA of Fourier coefficients (see Table 5) detected more significant differences between stratigraphically adjacent samples: both oldest and youngest populations were significantly different from those stratigraphically above and below, respectively. However, these samples were morphologically continuous with other samples not differing significantly from the topotype specimens. Therefore, although significant differences are present between the populations, the shape of rostral outline of the Swedish P₁ elements falls within the range of variation of *O. excavata* topotype material. Despite this, the results of the multivariate analysis (see Chapter three) strongly suggest that two of the temporally separated populations (samples 1 and 12) do not belong to '*O.*' *excavata*. The trend of increasing angularity within P₁ elements through time may therefore be occurring in a sequence of separate species.

Unfortunately, sample number was too small to test either for correlation with the major environmental changes occurring through the Silurian (see Aldridge et al. 1993, Jeppsson 1990) or control for the limited spatial variation resulting from samples being derived from different localities within present day southwest Gotland. However, morphological changes in the multivariate measures showed no correlation with environmental shifts and nor were any significant differences found between three coeval but spatially separated samples, suggesting the morphological variation in the Swedish samples does not reflect ecophenotypic or geographic differences.

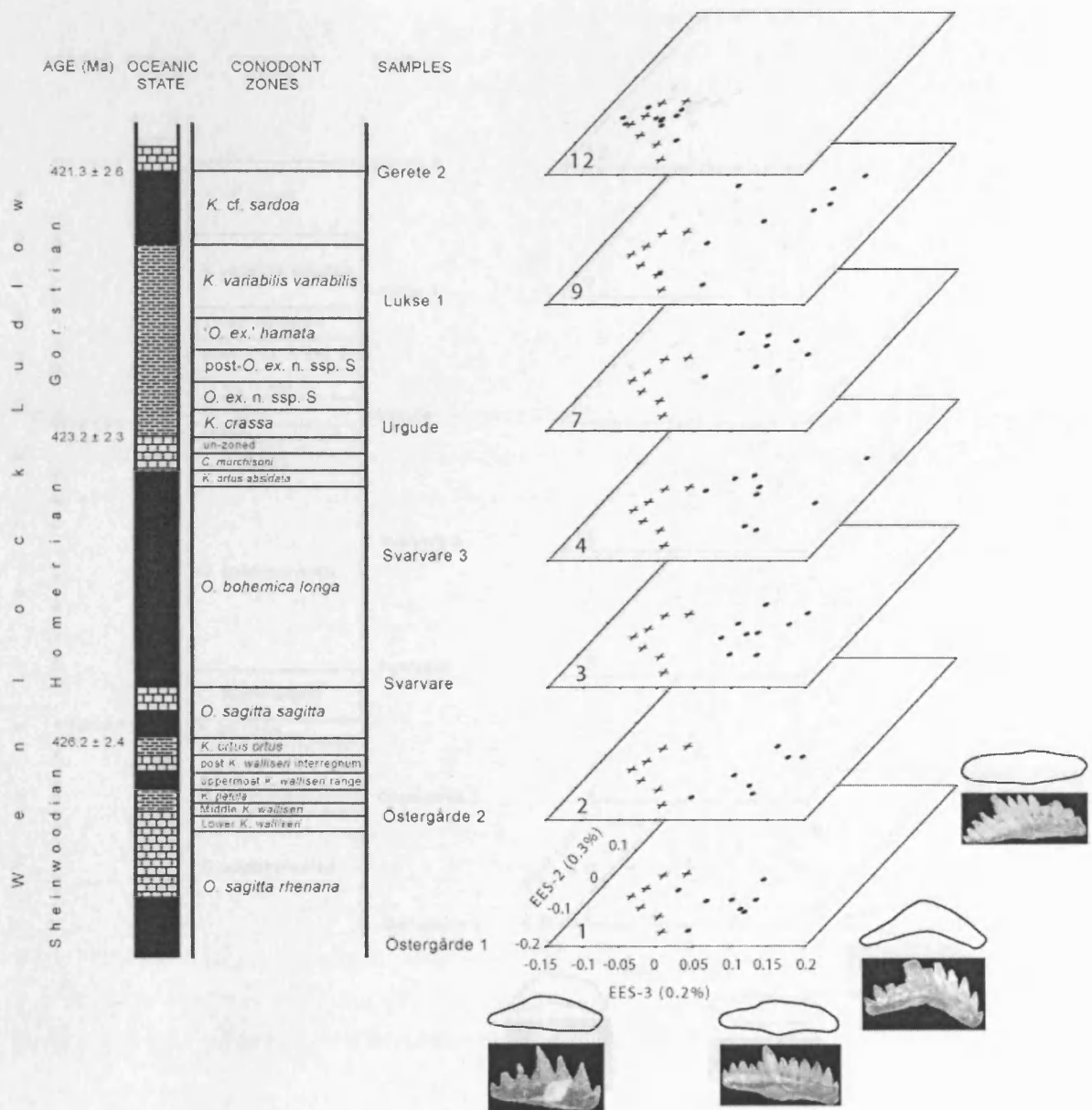


Figure 2: Ordinations of '*O.* excavata P₁ elements from seven stratigraphically sequential samples from Gotland, based on eigenshape scores from EES analysis. Elements are plotted on EES axes two and three, which display maximum separation between samples. Circles represent the Swedish samples, crosses indicate the topotype material. Outlines show elements within global dataset showing extreme eigenscores for each axis. Elements represented by those outlines are figured. A simplified conodont zonation and lithostratigraphy is also shown. The latter indicates oceanic state: Primo episodes are dominated by clay-rich sedimentation, Secundo episodes by limestone deposition. Black sections denote Events, generally dominated by clays. Radiometric ages are also indicated with error. Stratigraphic information from Jeppsson and Aldridge (2000), Jeppsson et al. (2006) and L. Jeppsson pers. comm. 2006. Abbreviations: *Kockolella ortus*, '*Ozarkodina*' *excavata*, *Ctenonathodus murchisoni*.

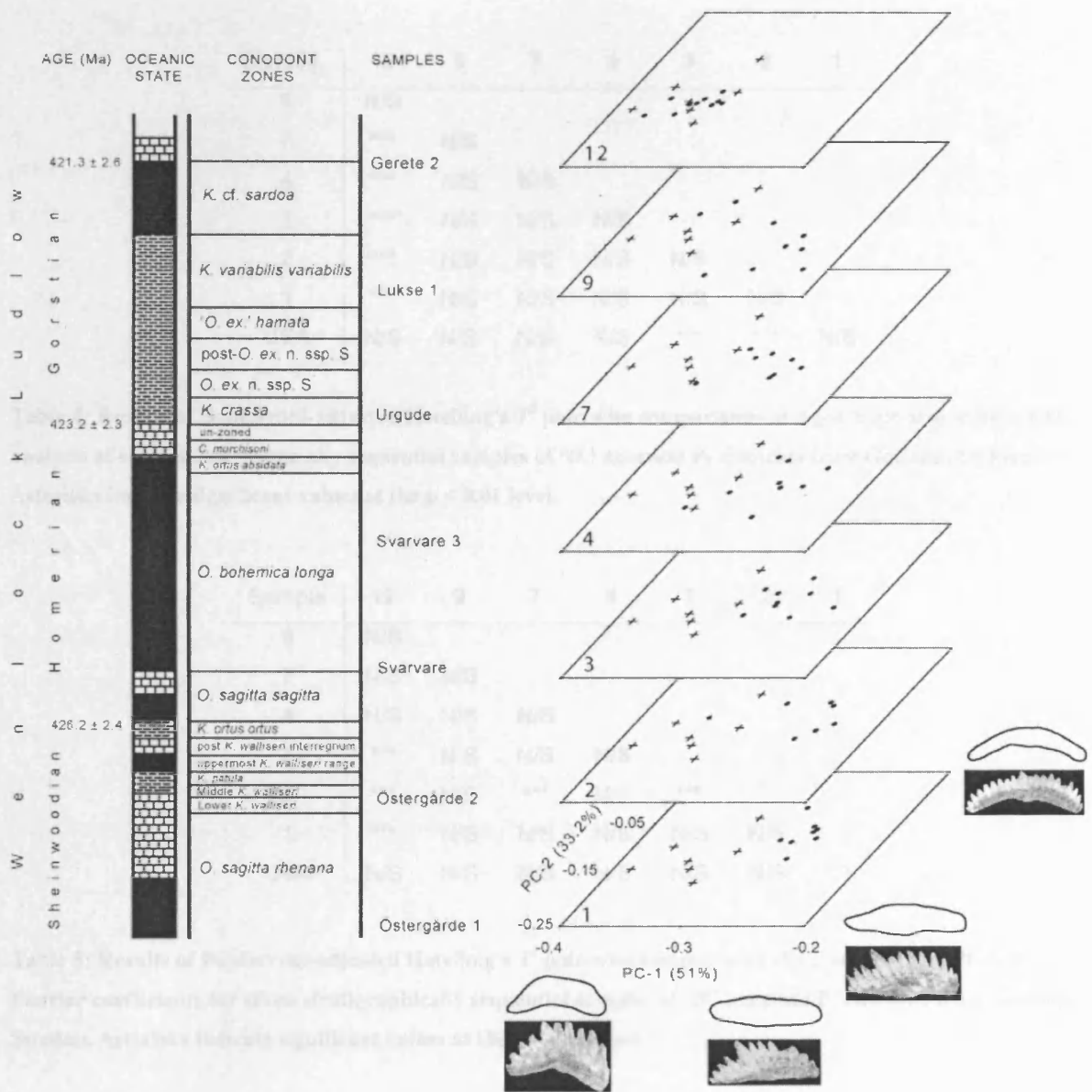


Figure 3: Ordinations of '*O.*' *excavata* P₁ elements from seven stratigraphically sequential samples from Gotland, based on principal component scores from PCA of Fourier coefficients. Elements are plotted on PC axes one and two, which displaying maximum separation between samples. Circles represent the Swedish samples, crosses indicate the toptype material. Outlines show elements within global dataset showing extreme eigenscores for each axis. Elements represented by those outlines are figured. Stratigraphic information is as Figure 2.

Sample	12	9	7	4	3	2	1
9	N/S						
7	***	N/S					
4	***	N/S	N/S				
3	***	N/S	N/S	N/S			
2	***	N/S	N/S	N/S	N/S		
1	***	N/S	N/S	N/S	N/S	N/S	
USA	N/S	N/S	N/S	N/S	***	***	N/S

Table 4: Results of Bonferroni-adjusted Hotelling's T^2 pair-wise comparisons of eigenshape scores from EES analysis of seven stratigraphically sequential samples of 'O.' excavata P₁ elements from Gotland, Sweden. Asterisks indicate significant values at the $p < 0.01$ level.

Sample	12	9	7	4	3	2	1
9	N/S						
7	N/S	N/S					
4	N/S	N/S	N/S				
3	***	N/S	N/S	N/S			
2	***	N/S	***	N/S	***		
1	***	N/S	N/S	N/S	N/S	N/S	
USA	N/S	N/S	N/S	N/S	N/S	N/S	***

Table 5: Results of Bonferroni-adjusted Hotelling's T^2 pair-wise comparisons of PC scores from PCA of Fourier coefficients for seven stratigraphically sequential samples of 'O.' excavata P₁ elements from Gotland, Sweden. Asterisks indicate significant values at the $p < 0.01$ level.

Spatial variation in the 'O.' excavata hypodigm

Variation through space was investigated through analysis of the same two sets of four spatially separated samples as analysed in Chapter three. The samples in set 1 (Austria, Bohemia, the American topotype material and sample 12 from Sweden) ranged from 421-422 Ma (see Table 1 for age data). The samples in set 2 (Australia, Britain, the American topotype material and Sweden (Nyan 2)) ranged from 418-419 Ma (see Table 1 for age data; asterisk in Table 1 indicates which British sample was analysed), except for the American topotype material, which is older.

The results the outline analyses of sample set 1 are discussed first. Figure 4A shows elements plotted on extended eigenshape axes, based on eigenshape scores. Figure 4B shows principal component axes, based on PC scores from the PCA of Fourier coefficients. The pattern produced by both analyses is similar. The data form two clear groups: the first cluster is composed of the Austrian and Bohemian samples, which overlap completely. The second cluster comprises the Swedish and American populations, which also overlap. The two clusters overlap with each other very little.

The end-member outlines in Figure 4 show that the Swedish and American elements are more arched, particularly along the aboral margin, in contrast to the Austrian and Bohemian elements, which are straighter and possess a more convex aboral margin. The EES analysis also indicates that the Bohemian populations tend to possess more flared basal cavities. The NPMANOVA shows that significant morphological differences are revealed by the outline analyses (EFA: $F = 8$, $p < 0.01$; EES analysis: $F = 12.9$, $p < 0.01$). The post hoc tests on eigenscores from both the EES analysis and the PCA of Fourier coefficients are shown in Table 6. Identical patterns of significant morphological differences were present in the results for both analyses, and support the graphical pattern: Austrian and Bohemian populations are not significantly different, and neither are Swedish and American samples; however there are significant differences between these two pairs of samples.

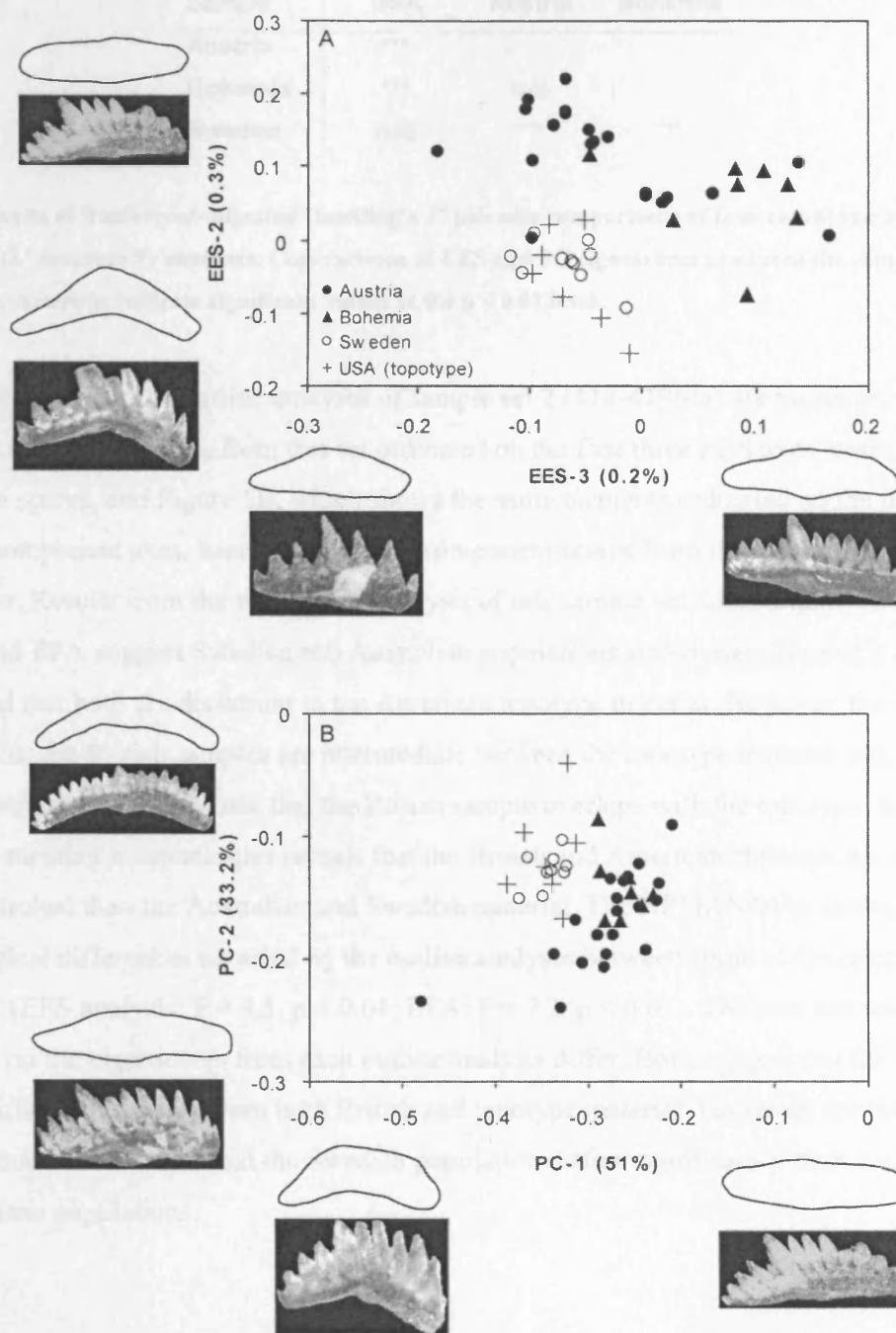


Figure 4: Ordinations of '*O.*' *excavata* P₁ elements from four coeval samples (421-422Ma) based on A) eigenshape scores from EES analysis and B) PC scores from PCA of Fourier coefficients. Elements are plotted on axes displaying maximum separation between samples. Outlines show elements within global dataset showing extreme eigenscores on each axis. Elements represented by those outlines are figured.

Sample	USA	Austria	Bohemia
Austria	***		
Bohemia	***	N/S	
Sweden	N/S	***	***

Table 6: Results of Bonferroni-adjusted Hotelling's T^2 pairwise comparisons of four coeval samples (421-422Ma) of '*O.* excavata P₁ elements. Comparisons of EES and PC eigenscores produced the same pattern of significance. Asterisks indicate significant values at the $p < 0.01$ level.

The results of the outline analyses of sample set 2 (418-419Ma) are presented in Figure 5A, which shows specimens from this set ordinated on the first three EES axes, based on eigenshape scores, and Figure 5B, which shows the same elements ordinated on the first three principal component axes, based on principal component scores from the PCA of Fourier coefficients. Results from the two outline analysis of this sample set differ slightly. Both EES analysis and EFA suggest Swedish and Australian populations are similar, forming a loose cluster, and that both are dissimilar to the American topotype material. However, the EES indicates that the British samples are intermediate between the topotype material and the other samples, whereas EFA indicates that the British sample overlaps with the topotype. Examination of the end-member morphologies reveals that the British and American elements are narrower and more arched than the Australian and Swedish material. The NPMANOVA shows that the morphological differences revealed by the outline analyses between some of the samples are significant (EES analysis: $F = 4.1$, $p < 0.01$; EFA: $F = 7.2$, $p < 0.01$). The post hoc tests conducted on the eigenscores from each outline analysis differ. Both suggest that the Australian samples differ significantly from both British and topotype material. However, the tests of PC scores furthermore indicate that the Swedish population differs significantly from both British and American populations.

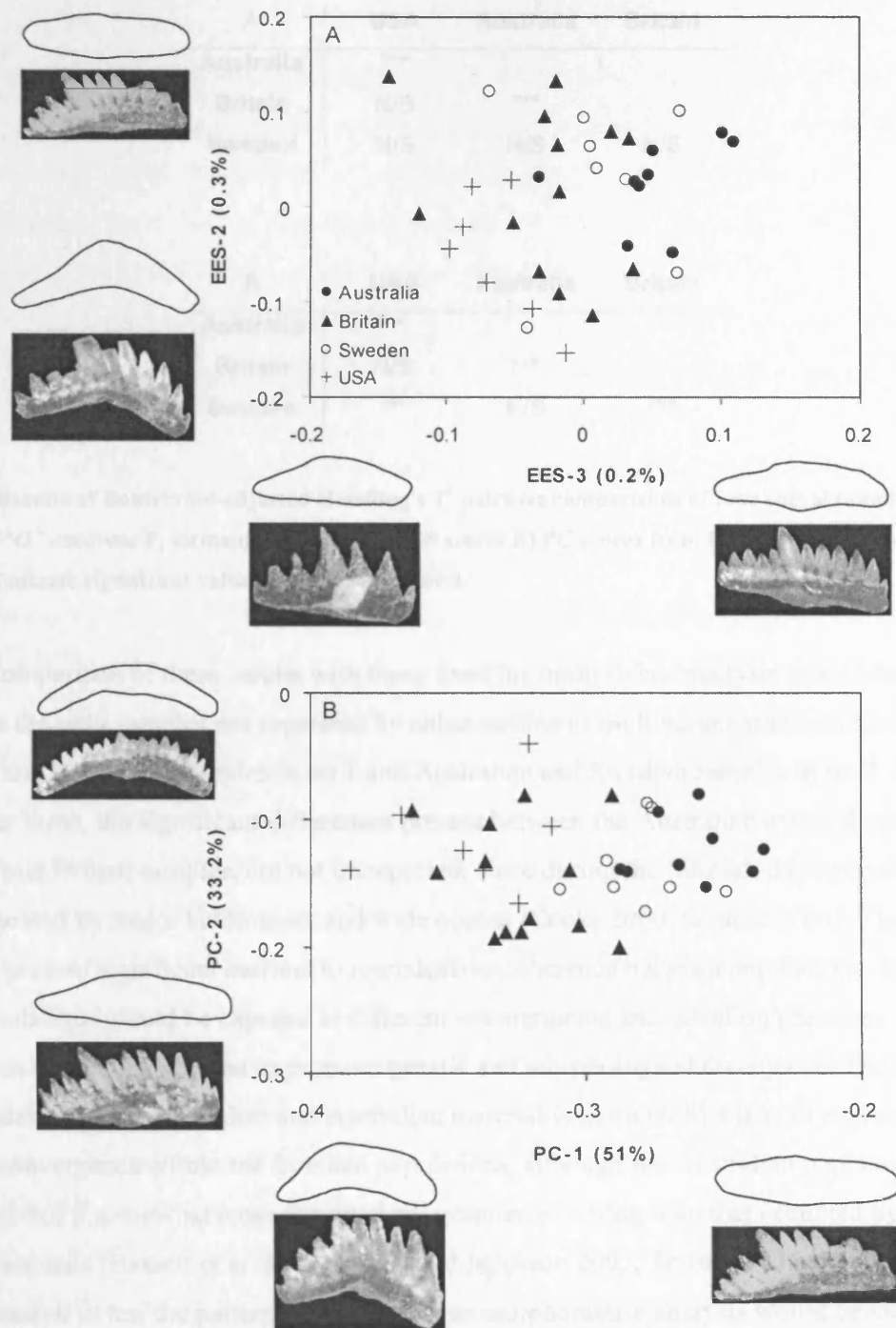


Figure 5: Ordinations of '*O.* *excavata* P₁ elements from four coeval samples (418-419Ma) based on A) eigenshape scores from EES analysis and B) PC eigenscores from PCA of Fourier coefficients. Elements are plotted on axes displaying maximum separation of samples. Outlines show elements within global dataset showing extreme eigenscores on each axis. Elements represented by those outlines are figured.

A	USA	Australia	Britain
Australia	***		
Britain	N/S	***	
Sweden	N/S	N/S	N/S

B	USA	Australia	Britain
Australia	***		
Britain	N/S	***	
Sweden	***	N/S	***

Figure 6: Results of Bonferroni-adjusted Hotelling's T^2 pairwise comparisons of four coeval samples (418-419Ma) of '*O.* excavata P₁ elements based on A) EES scores B) PC scores from PCA of Fourier coefficients. Asterisks indicate significant values at the $p < 0.01$ level.

Comparison of these results with those from the multivariate analysis (see Chapter three) show that the only samples not separated by either outline or multivariate methods are the Austrian and Bohemian samples in set 1 and Australian and Swedish samples in set 2. As noted in Chapter three, the significant differences present between the Australian material and both topotype and British samples, are not unexpected, since during the Silurian these populations were separated by major landmasses and wide oceans (Cocks 2000, Scotese 2001). These would probably present significant barriers to reproductive coherence between populations. Moreover, these populations would be exposed to different environments and selection pressures. Such differences would be expected to promote genetic and morphological divergence. The similarity of the widely separated Swedish and Australian material is more problematic to explain, and may indicate convergence within the Swedish populations, although the Australian population may have inhabited a somewhat more proximal environmental setting than that occupied by the Swedish animals (Bassett et al. 1989, Calner and Jeppsson 2003, Telford 1975). A fruitful line of future research to test the patterns revealed by this morphometric analysis would be vicariance studies with large numbers of coeval samples of varying geographic separation, combined with more detailed study of local conditions to rule out ecophenotypic explanations for the differing morphologies.

Biological interpretation of morphological variation in 'O'. excavata hypodigm

Understanding the biological context of the observed differences is also critical to test for alternative causes of the morphological variation that has been demonstrated above to exist in spatiotemporally discrete samples of '*O.*' *excavata*. It may also provide additional information regarding the processes that could potentially produce speciation. The eigenscores for each axis were tested for ontogenetic shape change, using linear regression against total length: all the regressions had correlation coefficients (r^2) \ll 0.5, except for PC-2 where $r^2 = 0.635$. This suggests that the shape variation captured by the outline analysis is not predominantly ontogenetic.

The most apparent shape difference between populations was the degree of arching between P_1 elements, which appeared to display a systematic temporal trend: P_1 elements became gradually straighter with time. The results of this study and of the analysis in Chapter three suggest this trend of shape change may reflect progressively increasing differentiation of P_1 and P_2 elements within the apparatus in a series of sequential species. The basal phylogenetic position of '*O.*' *excavata* within the ozarkodinid clade (Donoghue et al. in review), means that further investigation of this trend may offer general insights into apparatus evolution within the ozarkodinids.

Interpreting the biological context of changes in element arching is difficult, because although function of conodont elements as food processing structures has been investigated (Donoghue and Purnell 1999), we have yet to constrain the precise adaptive significance of changes in the configuration of the element, such as variation in overall arching. The morphological variation may reflect differences in diet between the different populations. Such resource partitioning in extant populations is known to lead to divergent natural selection and morphological differentiation (see Dayan and Simberloff 2005 for a review with examples). Variations in diet can be tested-for using other lines of evidence, for example examining whether element microwear differs between populations (Purnell 1995), indicating that different foodstuffs are being processed. Also, the different morphologies could be modelled (Evans and Sanson 2003) to investigate how observed changes in element structure might affect function, helping to constrain the efficiency with which elements of different configurations could process various hypothesized food types. Using independent approaches such as these is crucial to properly understand the biological context of the morphological changes captured by the outline analysis.

Conclusions

This work has presented new, standardised, morphometric methods based around outline analysis, to extend and complement those presented in Jones and Purnell (in press). These new protocols have been applied to test the hypothesis that the taxonomically problematic conodont species '*Ozarkodina excavata*' is monospecific. The results have demonstrated the efficiency of the protocol in constraining the nature of the morphological variation within the '*O.*' *excavata* hypodigm. Significant morphological discontinuities have been detected between spatially separated '*O.*' *excavata* populations. Moreover, many of these populations have been shown to differ significantly in their morphology from the topotype material of '*O.*' *excavata*. Analysis of the data produced by the protocol has also revealed which aspects of shape variation in '*O.*' *excavata* best characterise these discontinuities. The interpretation of this variation in a biological context is problematic, owing to our lack of detailed knowledge regarding how changes in element shape influence element function, but these differences are presumably associated with variations in diet. Interpretation of the morphological discontinuities in their biological and spatial context provide further evidence, combined with that presented in Chapter three, that there may be multiple species present within the '*O.*' *excavata* hypodigm. Independent tests are outlined that could more rigorously test these new taxonomic hypotheses. Although beyond the scope of the work presented here, they offer promising directions for future research. If the morphotypes identified here actually represent multiple species, then the high discriminatory power of the protocols to distinguish between them suggests that these techniques have potential to provide a generalised tool for conodont species identification that is methodologically standardised and can produce repeatable and reproducible results. The morphometric protocols have also identified a possible trend of increasing morphological differentiation between P₁ and P₂ elements, which may provide insights into apparatus evolution within ozarkodinids.

It is worth noting that the lack of complete agreement between the results presented here and those in Chapter three does not cast doubt on the power of the analyses. The differences between samples identified using multivariate morphometrics exist regardless of any "conflicting" similarities indicated by the results presented in Chapter four. The results of the outline analyses have simply revealed additional patterns of variation within the morphologically distinct groupings highlighted in Chapter three, as well as distinguishing further differences. Taken as a whole, these results have, for the first time, furnished quantitative hypotheses relating

to the pattern of morphological variation within the '*O.*' *excavata* hypodigm, which can be easily and rigorously tested through further sampling and morphometric analysis.

Hopefully the methods and results presented in this work will also catalyse more comprehensive morphometric analysis of conodonts using these protocols. Such engagement with morphometrics is a crucial to produce more objective and biologically meaningful taxonomic schemes, improve biostratigraphic schemes and realise the potential of the rich fossil record of conodonts for testing broad evolutionary hypotheses.

Chapter five: The autecology of an ozarkodinid conodont

Abstract

A thorough knowledge of a fossil species' autecology including the testing of hypotheses of apparatus growth and function and can elucidate many aspects of its taxonomy, population biology and evolution. The excellent fossil record of conodonts allows us to obtain this information for a successful clade of early vertebrates. The Eramosa Lagerstätte (Silurian, Wenlock) preserves both discrete elements and natural assemblages of articulated apparatuses of '*Ozarkodina*' *excavata*. P₁ elements of this species were utilised to test the hypothesis, based on taphonomic evidence, that the Eramosa Lagerstätte preserves a single natural population of this species. The size frequency distribution of '*O.*' *excavata* P₁ elements revealed a pattern virtually identical to that of extant populations of mussels; strong evidence in support of the hypothesis. The Eramosa Lagerstätte therefore provides an opportunity, exceptional even within conodont studies, to rigorously test autecological hypotheses and examine population biology within a basal ozarkodinid. Cluster analysis identified clear groupings within size distributions of P₁ and P₂ elements, most parsimoniously interpreted as generational cohorts. Population structure was compared to other studies of conodont autecology, revealing inter-specific plasticity in population structure within ozarkodinids. Survivorship analysis of P₁ elements based on generational cohorts produced convex-upward curves, suggesting increasing mortality rates with age. The natural population provides the biologically rigorous evidence that conodont dentition was permanent, and that M and S elements were not used for suspension feeding.

Introduction

Aside from its intrinsic value in facilitating detailed reconstruction of an extinct organism, a thorough knowledge of a fossil species' autecology can elucidate aspects of its taxonomy, population biology and evolution. Unfortunately, the nature of the fossil record generally prohibits our obtaining detailed information regarding an extinct species' population structure, survivorship and growth patterns and the relationship between them; in contrast, the excellent quality of the conodont fossil record (Foote and Sepkoski 1999) renders it highly amenable to autecological studies. Although progress has been made in understanding element function and growth, relatively little work has been conducted in this area; consequently we still possess a comparatively poor understanding of autecology within this successful clade of early vertebrates.

The first detailed quantitative analysis of conodont autecology was by Jeppsson (1976) who measured length in isolated *Ozarkodina* P₁ elements. He identified size clusters within *O. confluens*, which he interpreted as possible generational cohorts, and survivorship analysis of the same taxon revealed increasing mortality rates through time. Purnell (1993, 1994) examined the ontogeny of the conodont skeleton in *Idiognathodus* and *Gnathodus bilineatus*, using both discrete and bedding-plane assemblage elements, to test hypotheses of feeding mechanisms. He demonstrated that growth rates of elements in these taxa supported a tooth-like food processing mode for P elements, and did not support the hypothesis of filter feeding for M and S elements, but rather suggested a raptorial function for these elements. Neither qualitative nor quantitative evidence was found to support element shedding. Tolmacheva and Purnell (2002) investigated growth and survivorship in *Paracordylodus gracilis* using element clusters, and concluded that apparatus growth was isometric and that survivorship was dictated in part by predation of certain size ranges. Using cluster analysis, Armstrong (2005) examined ontogeny in *Idiognathodus* to further test the hypothesis that elements were shed. He identified size clusters within S elements, and survivorship analysis revealed increasing mortality through time. Survivorship curves also refuted the apparatus shedding hypothesis and allowed tentative conclusions to be drawn regarding conodont autecology.

The current work focuses on the conodont '*Ozarkodina*' *excavata* (Branson and Mehl 1933). This species is represented by perhaps the best fossil material hitherto utilised for exploring conodont autecology: the fossil Konservat-Lagerstätte of the Eramosa Member (Silurian, Wenlock) on the Bruce Peninsula of southern Ontario, which preserves both articulated conodont apparatuses and isolated skeletal elements. The Eramosa Lagerstätte is hypothesised, based on taphonomic evidence (von Bitter and Purnell 2005), to preserve a

natural population of '*O.*' *excavata*. Evidence provided herein from comparison of size distributions in '*O.*' *excavata* and extant populations provides strong support for this hypothesis. This is significant, because conclusions drawn from a natural population have greater biological power than those drawn from samples subject to the usual biases of the fossil record. This natural population of '*O.*' *excavata* is thus exploited in this work to further test autecological hypotheses of conodont element function and apparatus shedding, and to elucidate population biology in a basal ozarkodinid at a level of detail rarely achieved even within conodont studies.

Materials and method

This work was based exclusively on material from the Konservat-Lagerstätte of the Eramosa Member. Most of the discrete elements and all of the articulated skeletons were prepared at the Royal Ontario Museum (ROM), Toronto, and are housed in the ROM collections. Discrete elements were extracted using standard rock dissolution techniques, with some additional processing required owing to the nature of the Eramosa lithology (see Chapter one). Apparatuses were removed intact from bedding planes by undercutting with a small, carborundum-coated rotary blade on a Dremel electric tool (P. von Bitter pers. comm. 2005). Some isolated elements were acquired from two Eramosa sub-samples (of samples 01PB1 and 02PB1, see von Bitter and Purnell 2005) provided by the ROM and prepared at the Micropalaeontology laboratories in the Department of Geology, University of Leicester (see Jones and Purnell (in press) and Chapter one for methodology); these sub-samples were split through, and some articulated apparatuses removed, prior to acid processing. The sub-samples were predominantly carbonate lithologies. Density of elements within the sub-samples of 01PB1 and 02PB1 respectively is approximately 96 kg^{-1} and 50 kg^{-1} . Preservation of elements within the Eramosa Lagerstätte is good: isolated specimens generally have complete processes, and frequently retain intact denticles; elements preserved in apparatuses are generally fragmented, but fragments remain correctly juxtaposed in most cases. All elements are pale amber in colour. Further details of the lithology, preservation and biota of the Eramosa Lagerstätte are given in von Bitter and Purnell (2005).

Obviously, the dimensions of a natural assemblage are a function of element size and collapse angle, but apparatuses and their constituent elements range from small examples, where the entire assemblage is $\leq 0.5 \text{ mm}$ across (e.g. ROM assemblage 197) to large individuals several millimetres in diameter (e.g. ROM assemblage 172). Unfortunately, the smallest assemblages are generally too small to measure using light microscopy. They represent a small proportion of the total count of apparatuses, presumably owing to collection

bias: small assemblages are more difficult to locate when splitting through the host rock. The collections of isolated elements are dominated by smaller specimens, suggesting that a larger number of small assemblages may indeed have been present, but were disarticulated during acid preparation, and that larger elements were collected as natural assemblages when splitting through the rock. Consequently, the measurements of elements from bedding-plane assemblages were obtained almost exclusively from larger apparatuses.

Many of the articulated skeletons are associated with patches of dark coloured organic material, interpreted by comparison with other exceptionally preserved conodont material as the remains of eyes (von Bitter et al. in review), e.g. ROM assemblage 64. Generally individual apparatuses are well separated from each other on their bedding surfaces, but there is an example of multiple apparatuses preserved together on one surface in such close proximity as to be virtually in contact (ROM assemblage 178). Single elements also occur, apparently separated on their bedding surface from any articulated apparatuses, sometimes in considerable numbers (e.g. ROM assemblage 247).

The taphonomy of the Eramosa Lagerstätte is outlined in von Bitter and Purnell (2005). There is negligible bioturbation in the deposit; this, the presence of the articulated apparatuses and the wide size range of elements, suggests very limited current activity and little transport or sorting of elements. Elements and bedding-plane assemblages are preserved in a thin, non-bioturbated horizon, suggesting limited time-averaging, although modelling and empirical studies indicate that sample variance is not significantly increased by time-averaging where population structure changes little through time (Bush et al. 2002, Hunt 2004a, b). Consequently, the lagerstätte is currently hypothesised to approximate a single biological population. Elements and natural assemblages were morphometrically analysed to test this hypothesis. If the hypothesis is supported, the material will allow analysis of population variation within '*O.*' *excavata* at a level of detail rarely possible in conodont studies.

A deposit with so little disturbance comes with a potential difficulty: a high probability of multiple discrete elements deriving from single individuals (Gilinsky and Bennington 1994), which would, for example produce inaccurate census counts, confuse any asymmetry with other patterns of variation and violate the criterion of independence in statistical tests. Of course, this is irrelevant to measurements taken from bedding-plane assemblages, since the context of elements is known. But it should be considered for the isolated elements, particularly if isolated elements originate from small assemblages disarticulated during acid preparation.

Since most elements are paired and those from the left and right side of the skeleton differ in curvature, separation into sinistral and dextral elements is straightforward and

ensures their provenance is from different animals. Although distinguishing sinistral and dextral M and S elements is thus unproblematic, differentiating between S₃ and S₄, and between S₁ and S₂ elements, has proved impracticable in this work; quantifiable morphological differences may exist, but sample sizes are too small to detect them. Distinguishing dextral and sinistral P elements based on morphology is harder. Two criteria may be used. Articulated skeletons reveal that, as in other ozarkodinid conodonts, '*O.*' *excavata* P element cusps are directed dorsally and that the elements are concave caudally, convex rostrally. However, the curvature pattern is not universal; frequently elements show a sinusoidal curvature in oral view. In those elements where curvature is a simple curve, the flare of the basal cavity is always greatest caudally and medially. Thus, basal cavity flare is also used here to differentiate sinistral and dextral elements. Isolated P₁ and P₂ elements were differentiated based on multivariate discrimination (see Chapter two).

A total of 289 isolated elements were measured and 73 apparatuses examined. Varying numbers of elements were measured from each apparatus, depending on element completeness and the number of elements unobscured by matrix; where feasible, matrix was carefully removed with a fine needle to provide better exposure. Nevertheless, measuring elements within apparatuses remains difficult, limiting sample sizes. Elements on which preparation was conducted are recorded. Data were acquired using the morphometric protocols outlined in Chapter one and Jones and Purnell (in press). Figure 1 illustrates the measured variables and the biological anatomical notation used in this work (Purnell et al. 2000). Table 1 provides descriptions of the measured variables and their abbreviations. Details of the variables measured and their abbreviations are also given there. Specific statistical methods are outlined before each analysis. All analyses were conducted in PAST version 1.44 (Hammer et al. 2001), SPSS version 14 and MINITAB version 14. Graphs were produced in PAST, Microsoft Excel and MINITAB version 14.

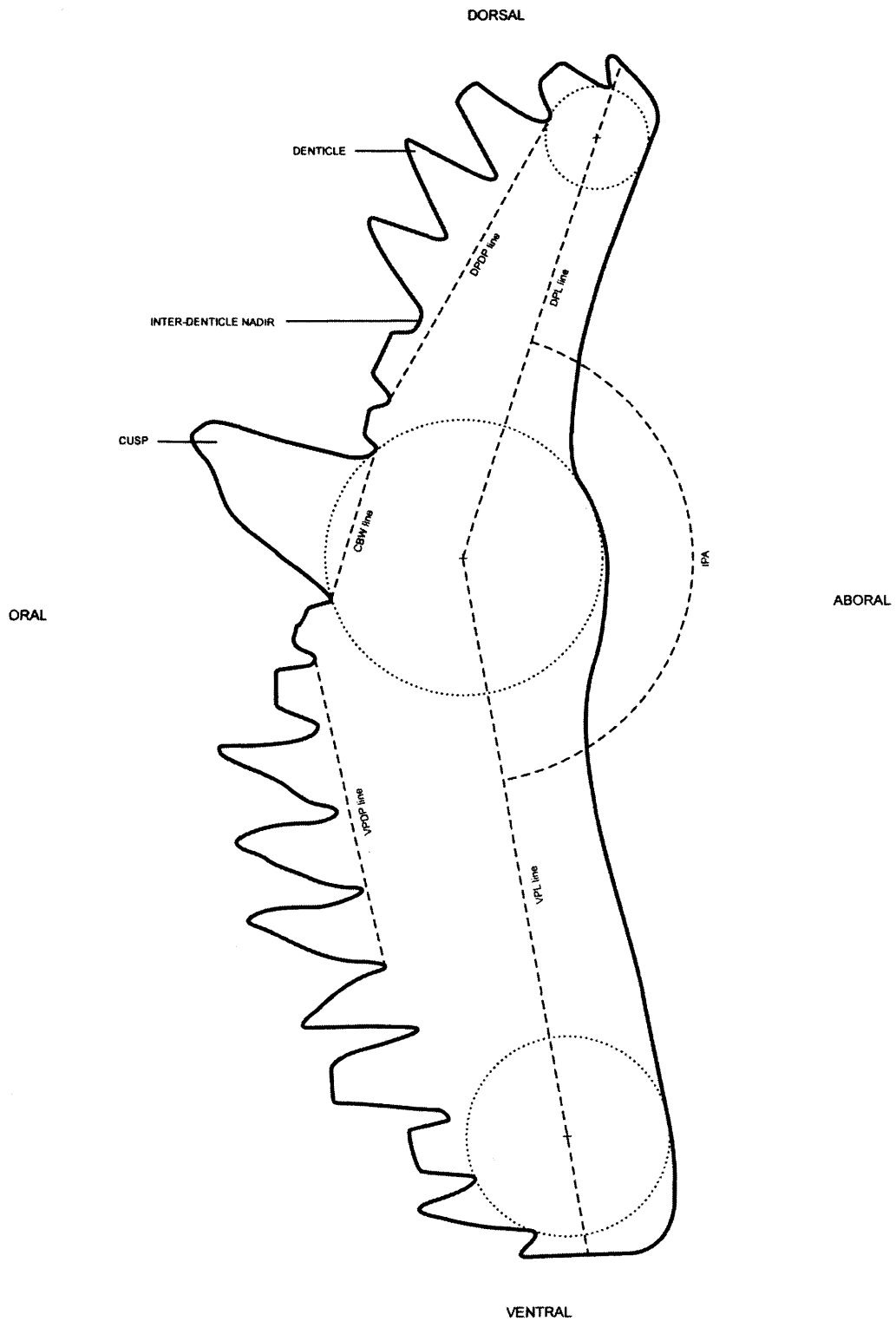


Figure 1: '*O.* *excavata* P₁ element in rostral view. Anchored circles are dotted. Dashed lines represent the measures used in the morphometric analysis, as outlined in Table 1. See Table 1 for key to abbreviations.

Name	Abbreviation	Description
Ventral process length	VPL	Linear distance from the cusp anchored point to the distal process terminus, measured along a line passing through the anchored point of the penultimate denticle.
Dorsal process length	DPL	
Total length	TL	Sum of dorsal and ventral processes lengths.
Inter-process angle	IPA	Angle between the dorsal and ventral process length lines.
Cusp base width	CBW	Linear distance between inter-space nadirs immediately adjacent to cusp.
Ventral process denticle packing	VPDP	Linear distance from the inter-space nadir proximal but one from cusp, along the base of four denticles distally. The value is divided by four to calculate the average denticle width of the process.
Dorsal process denticle packing	DPDP	
Ratio of cusp base width : mean denticle base width for ventral process	CBW:VPDW	Ratio of cusp base width to mean denticle width.
Ratio of cusp base width : mean denticle base width for dorsal process	CBW:DPDW	
Ventral process denticle number	VPDN	Enumeration of denticles on the process.
Dorsal process denticle number	DPDN	

Table 1: Summary of morphometric variables measured on ‘*O.*’ excavata P₁ elements. Variables are illustrated in Figure 1. See Chapter one and Jones and Purnell (in press) for discussion of measured variables.

Analysis and discussion

Testing the Eramosa Lagerstätte

The taphonomy of the Eramosa Lagerstätte suggests that it preserves a single population of '*O.* excavata', based on the limited time- and space-averaging (see materials and method), the high quality preservation of elements and the close agreement between observed ratios of discrete element types and those expected based on skeletal architecture (von Bitter and Purnell 2005). Population structure can be compared to extant populations to test this hypothesis. P₁ elements provide large samples of elements, and P₁ total length can be used as a surrogate for conodont body size on death, because available data suggest a linear relationship between body length and P₁ element length (Purnell 1994). Examination of distributions of P₁ elements therefore offers the clearest window on population structure in '*O.* excavata'. Figure 2 shows a size frequency histogram based on '*O.* excavata' P₁ element total length. Bin widths were optimised using the Freedman and Diaconis equation, a method summarised in Izenman (1991), since arbitrary selection of bin width can have a major influence on distribution shape in a histogram; optimisation allows histograms to provide a more objective indication of the nature of any discontinuities within a continuous dataset.

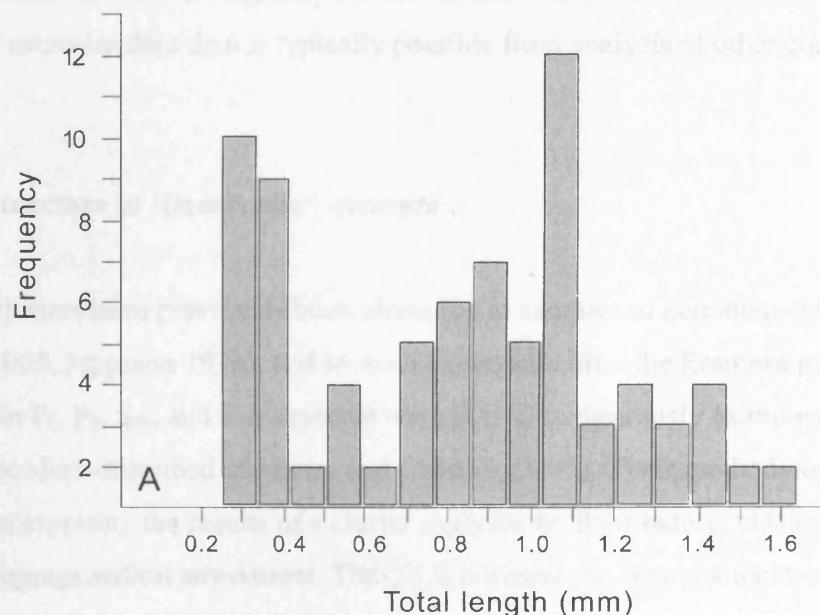


Figure 2: Size frequency distribution of discrete and natural assemblage '*O.* excavata' P₁ elements from the Eramosa Lagerstätte.

As noted by Raup and Stanley (1978, p. 79), caution must be exercised when utilising size-frequency distributions to ascertain the degree of taphonomic bias within a fossil sample,

and thus the reliability of conclusions drawn from the sample regarding the dynamics of the population that it represents. Nevertheless, the size-frequency distribution of the 'O.' *excavata* P₁ elements in the Eramosa Lagerstätte in Figure 2 is strikingly reminiscent of the pattern observed in the extant mussel *Mytilus edulis* measured by Craig and Hallam (1963, Text-Fig. 1d.). In their study, the peak of smaller individuals represented that year's newly settled spatfall and the spread of larger individuals the adults of the previous years' spatfalls. The sampling of the new spatfall was a product of fortuitous timing and thus introduced a somewhat anomalous pattern; the distribution of the larger individuals, and of individuals sampled at subsequent times in the year, all show normal to slightly right skewed distributions (Craig and Hallam 1963, Text-Fig. 1a-c). This same pattern is visible in the larger 'O.' *excavata* elements from the Eramosa in Figure 2, and the peak of smaller 'O.' *excavata* individuals may indicate a mass mortality event occurring immediately subsequent to a new cohort either migrating into the area (as Jeppsson (1976) has hypothesised for some Swedish populations) or originating *in situ* through hatching, birth or metamorphosis.

This close agreement of characteristic size distributions between the *M. edulis* population sampled by Craig and Hallam (1963) and the 'O.' *excavata* sample from the Eramosa Lagerstätte strongly suggests that analogous population dynamics are generating the patterns in both cases. It provides good support for the hypothesis that the Eramosa Lagerstätte preserves a single biological population of 'O.' *excavata*. This is significant, because it permits far more biologically robust conclusions to be drawn from analysis of the Eramosa 'O.' *excavata* data than is typically possible from analysis of other conodont element samples.

Population structure in 'Ozarkodina' *excavata*

Size clusters have previously been identified in samples of conodont elements (Armstrong 2005, Jeppsson 1976), and so were expected within the Eramosa population. Size distributions in P₁, P₂, S_{3/4} and S_{1/2} elements were therefore rigorously examined using the clustering procedure described in Jerram and Cheadle (2000). Their methodology addresses a difficulty in interpreting the results of a cluster analysis: by their nature, clustering algorithms will form groupings within any dataset. Thus, it is necessary to obtain a more objective determination of (1) whether the data show greater clustering than would be expected by chance, and (2) if so, into how many clusters the data should be divided. Jerram and Cheadle's (2000) procedure for accomplishing these goals was successfully employed by Armstrong (2005) to search for size clusters in *Idiognathodus* S element dimensions. It is summarised briefly below in the context of the current work.

Cluster analysis, here using a Euclidian distance measure, was first conducted on the measured dataset of element dimensions, and on ten sets of uniform random numbers (where all numbers within a range have identical probabilities of selection) with the same range as the measured data. Each cluster analysis returned a distance level for each cluster number; the latter was converted to cluster frequency to allow comparison of different sized samples, using the following:

$$[n_c / (N-1)] \times 100$$

where n_c is cluster number and N is sample size. Towards the base of a cluster hierarchy, every observation forms its own cluster, so cluster number and frequency are highest, and distance levels between adjacent clusters are lowest. Near the top of the hierarchy, all the data form one cluster, so cluster number and frequency are lowest, and distance levels are highest. A mean was taken of the ten sets of distance levels from the random datasets. This mean distance was then subtracted from the distance levels of the measured dataset, and from the distance levels of each random set, producing a series of residual distances, normalised to a random distribution. All the residuals were then plotted against cluster frequency. If the curve from the measured dataset falls below zero and predominantly outside the envelope of the random data, this indicates that significant clustering is present within the data. If significant clustering is present, residual distance values for the measured data gradually decrease with decreasing cluster frequency, until the optimum cluster number is reached. This will form a trough in the measured data curve, because it will be most dissimilar to the random distributions, and the next residual distance (working left along the curve) will be considerably higher, reflecting a large separation between clusters.

There appears to be no overwhelming justification for selecting one clustering algorithm over all others. Complete linkage (=furthest neighbour) cluster analysis has been used to analyse conodonts previously (Armstrong 2005), however, this algorithm performed poorly when applied to '*O. excavata*' P₁ and P₂ elements; specifically, it separated many adjacent points into different clusters. This is a predicted shortcoming of the method by which the algorithm groups data when clusters are more elongated (Shaw 2003). Therefore, two other clustering methods were applied to all element types, and the results compared, as suggested by Johnson and Wichern (2002). Average linkage and Ward (=minimum variance) clustering both generally produce results intermediate between those of complete and single linkage clustering (Shaw 2003), although they function differently from each other: average linkage calculates distances between two clusters as the average distance between all pairs of objects in each cluster, whereas Ward clustering calculates distance between two clusters by

minimising the sum of squares between them. Both methods have been used in previous cluster analyses of *Ozarkodina* P elements, with good results (Croll and Aldridge 1982). Moreover, in empirical assessments of different clustering algorithms, these methods generally outperformed all other hierarchical clustering techniques (see Sharma 1996 for a review). Dendrograms from the cluster analysis were finally compared qualitatively with bivariate plots of the variables to assess whether the clustering solutions were sensible, as recommended by Johnson and Wichern (2002).

For P elements, clustering was based on ventral and dorsal process lengths, rather than total length, because univariate clustering tended to produce results characteristic of distributions that are ordered in some way, for example where there is very even spacing between all points (see Jerram and Cheadle 2000 for discussion of cluster analysis of ordered distributions). Figure 3 illustrates the residual-frequency plot from the cluster analyses of P₁ element ventral and dorsal process length for natural assemblage and sinistral discrete specimens. Both Ward and average linkage P₁ element cluster analyses suggest that significant clustering is present, and produce similar clustering patterns (see Figure 4), differing only in the assignment of the largest individual. It is therefore likely that these clusters represent genuine natural groupings. It is important to note however, that the exact relationship between conodont age and size is at present unknown. Therefore, it currently cannot be demonstrated conclusively whether these groupings in the size distributions represent true generational cohorts, or whether each size cluster includes individuals of a range of ages.

The residual-frequency plots (see Figure 5) from both cluster analyses of 'O.' *excavata* P₂ element process lengths indicate the presence of significant clustering, and both analyses suggest an optimum division into two clusters. The dendrograms in Figure 5 show both Ward and average linkage produce identical clustering patterns. The size-frequency histograms in Figure 7 and 8 plot 'O.' *excavata* S_{1/2} and S_{3/4} elements from the Eramosa Lagerstätte based on anterolateral and posterior process length, respectively. A bimodal distribution is apparent in both plots. In the residual-frequency plot from the cluster analyses of S_{3/4} elements (Figure 7), the measured data curve does fall below zero and is predominantly outside the random data envelope; however the trough in the curve falls marginally inside this envelope. Residual-frequency results for S_{1/2} elements are less clear (Figure 8). The size-frequency histogram suggests two clusters. Average linkage clustering performed poorly, producing results that are difficult to interpret. The measured data curve in the Ward clustering residual-frequency plots below zero but within the random distributions.

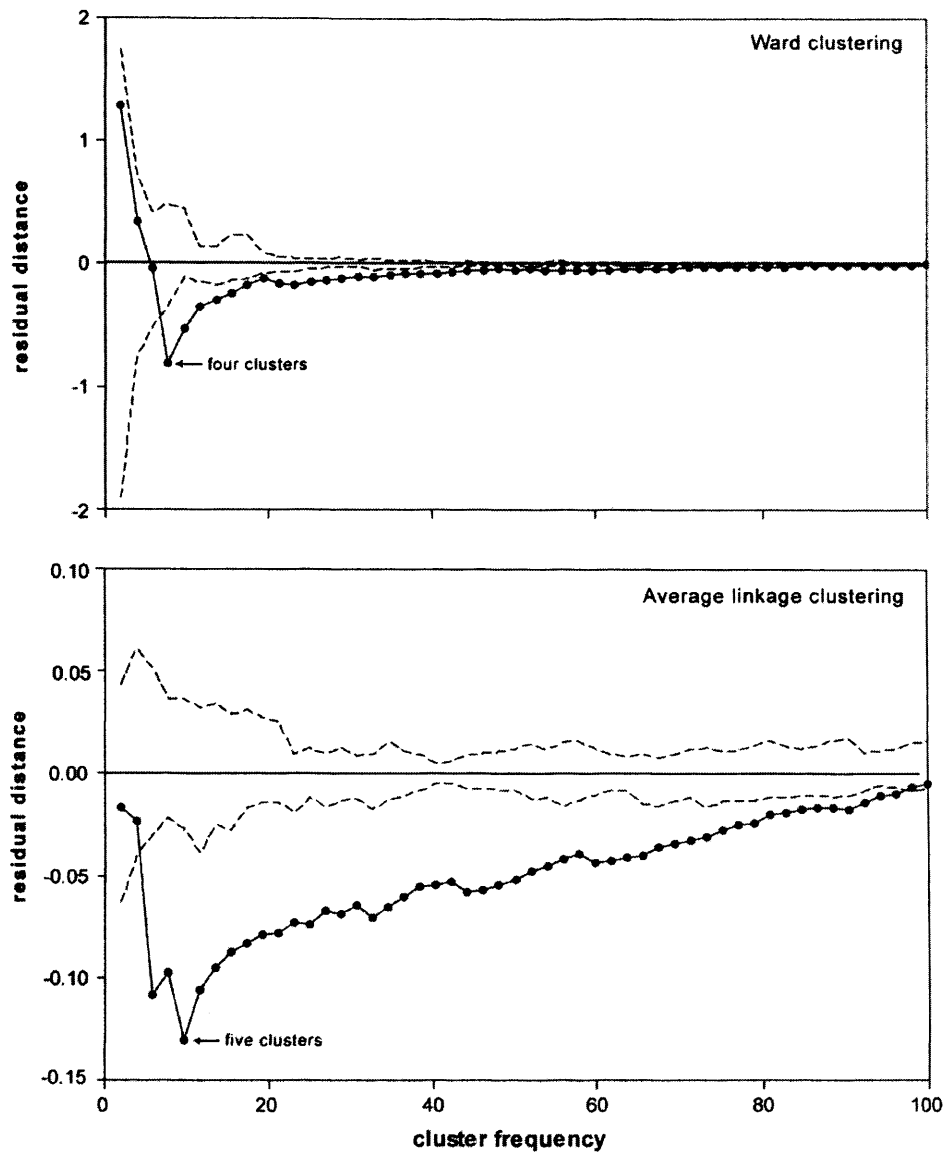


Figure 3: Residual distance against cluster frequency plots for Ward and average linkage cluster analysis of '*O.*' excavata natural assemblage and sinistral discrete P_1 elements from the Eramosa Lagerstätte. Optimal cluster number is indicated. Dashed lines enclose envelope of random data.

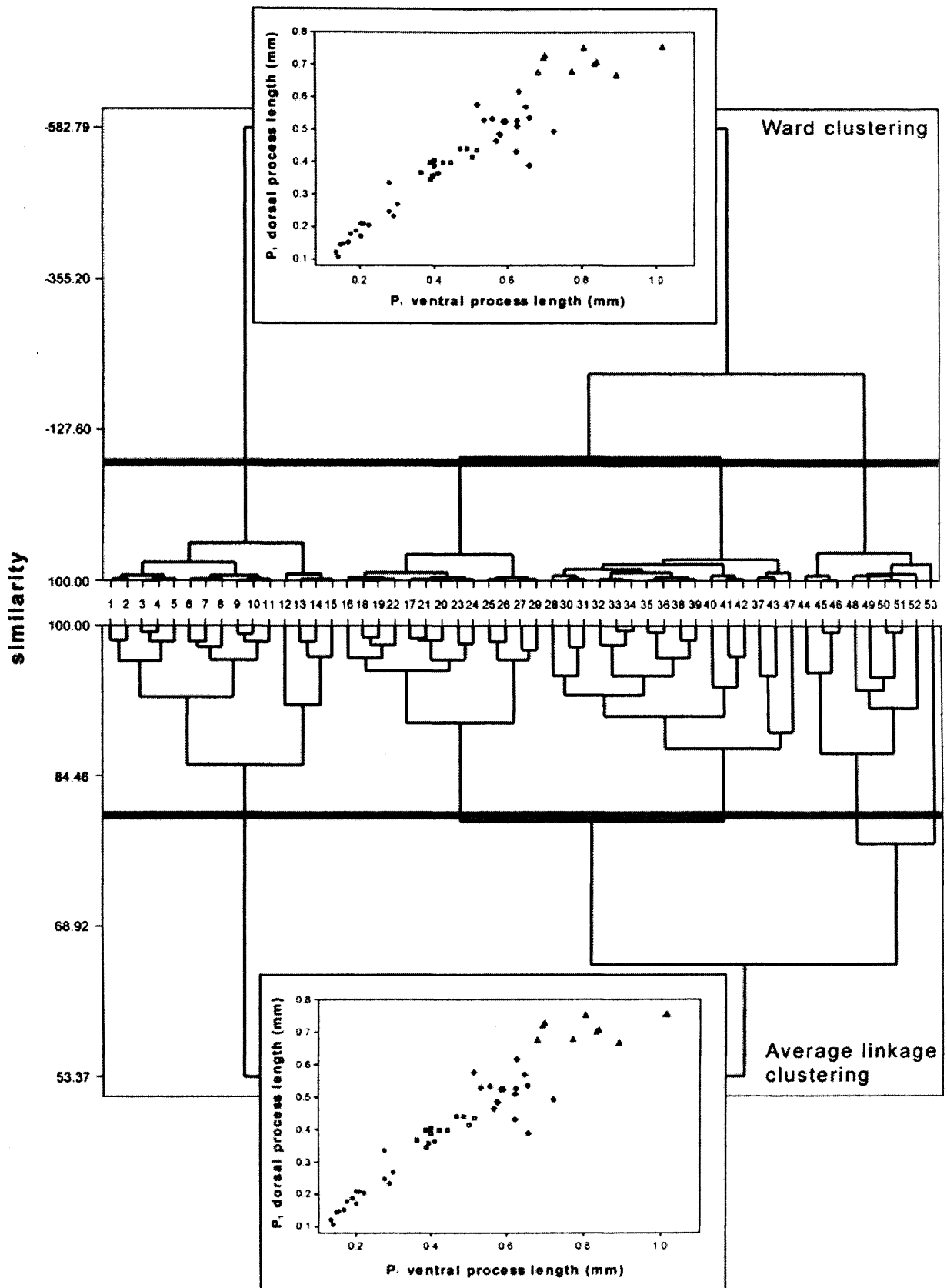


Figure 4: Dendrograms produced by Ward and average linkage cluster analysis of ‘*O.*’ excavata sinistral discrete and natural assemblage P₁ elements from the Eramosa Lagerstätte. Cut-off based on optimal cluster number (see Figure 1 and text) is indicated by grey line. Bivariate ordinations show P₁ elements plotted based on variables used in cluster analyses, with clusters identified indicated by different symbols.

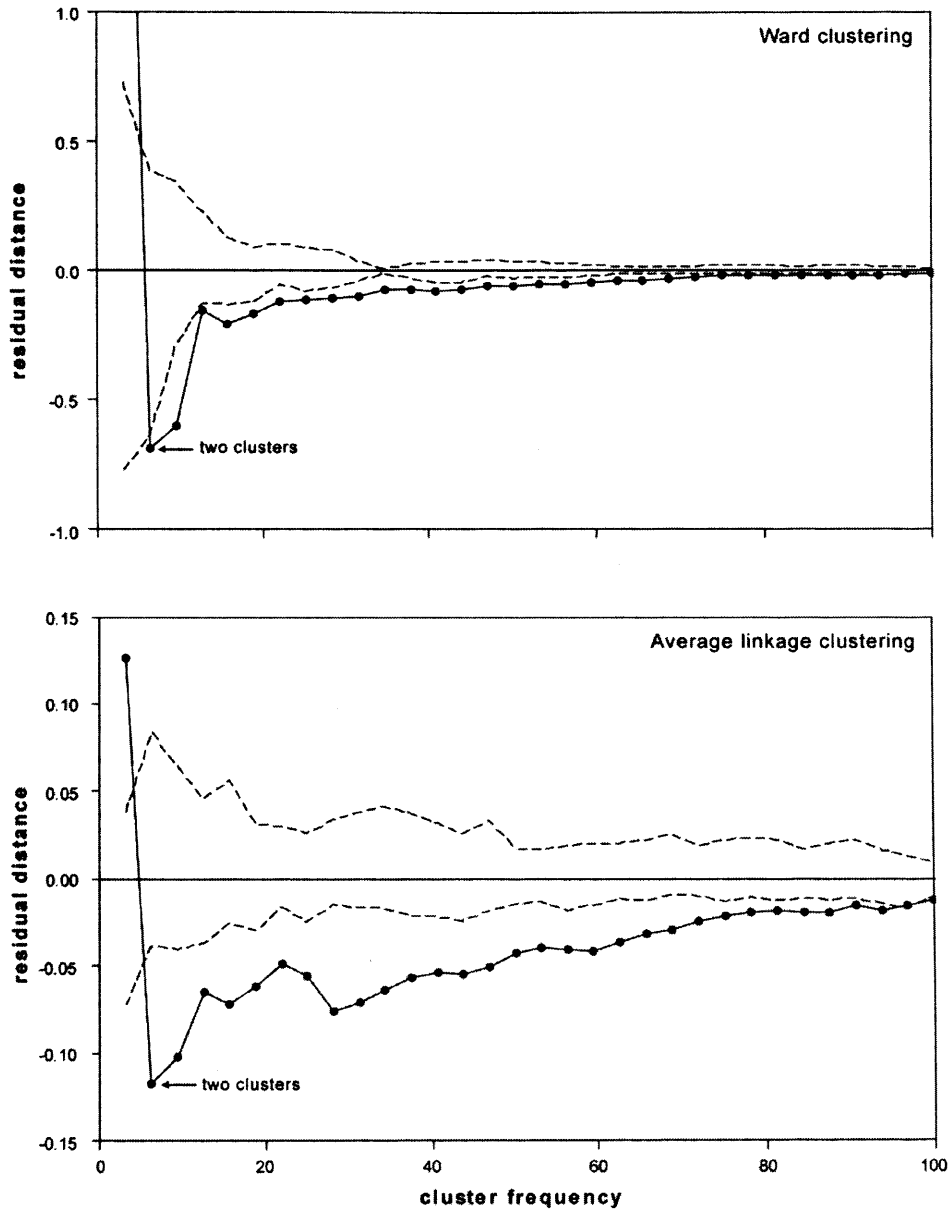


Figure 5: Residual distance against cluster frequency plots for Ward and average linkage cluster analysis of ‘*O.* excavata discrete and natural assemblage P_2 elements from the Eramosa Lagerstätte. Optimal cluster number is indicated. Dashed lines enclose envelope of random data. Size-frequency histogram of P_2 total length is inset based on natural assemblage and dextral discrete specimens.

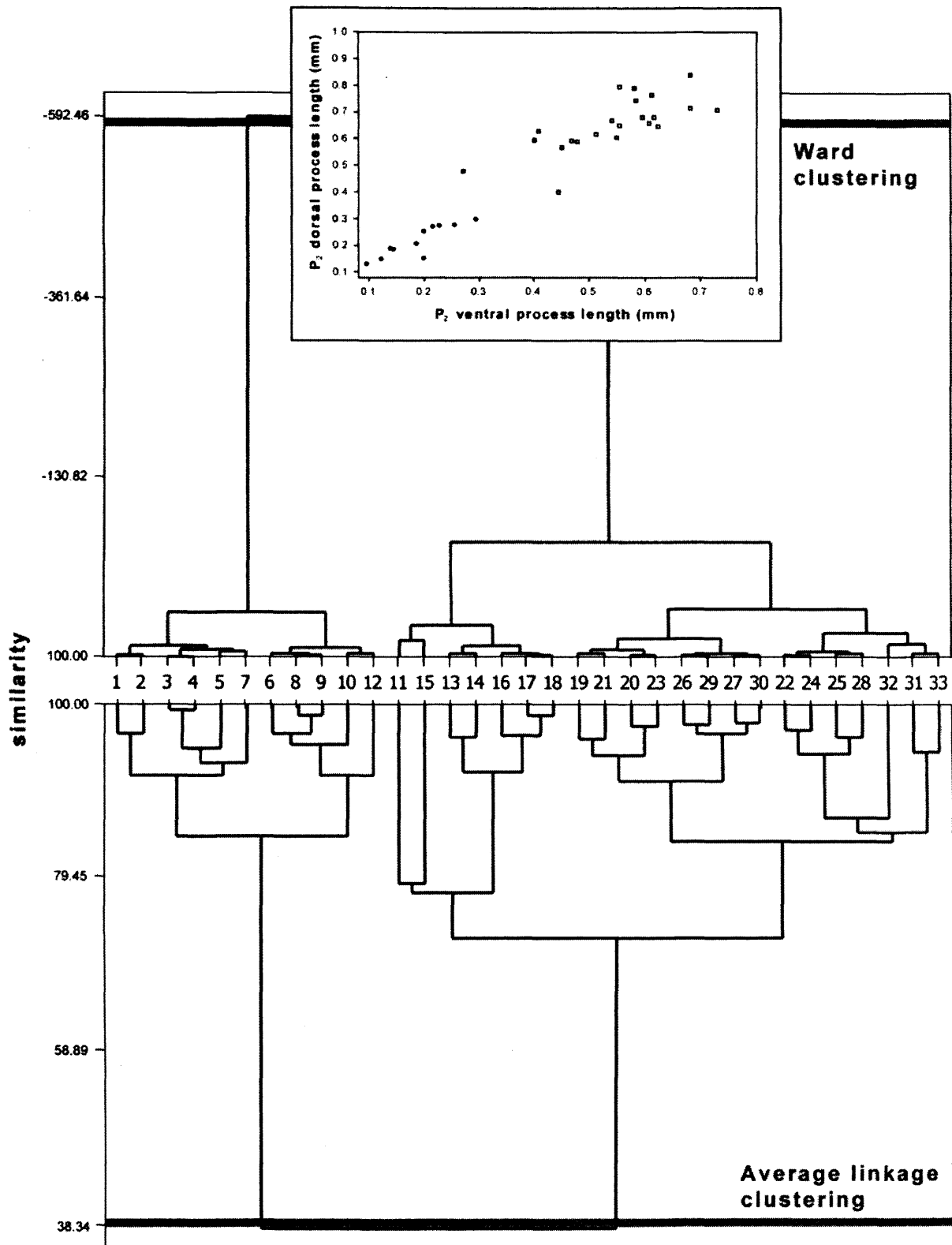


Figure 6: Dendrograms produced by Ward and average linkage cluster analysis of '*O.*' *excavata* dextral discrete and natural assemblage P₂ elements from the Eramosa Lagerstätte. Cut-off based on optimal cluster number (see Figure 3 and text) is indicated by grey line. Bivariate ordination shows P₂ elements plotted based on variables used in cluster analyses, with clusters identified indicated by different symbols. Clustering pattern is identical in both analyses.

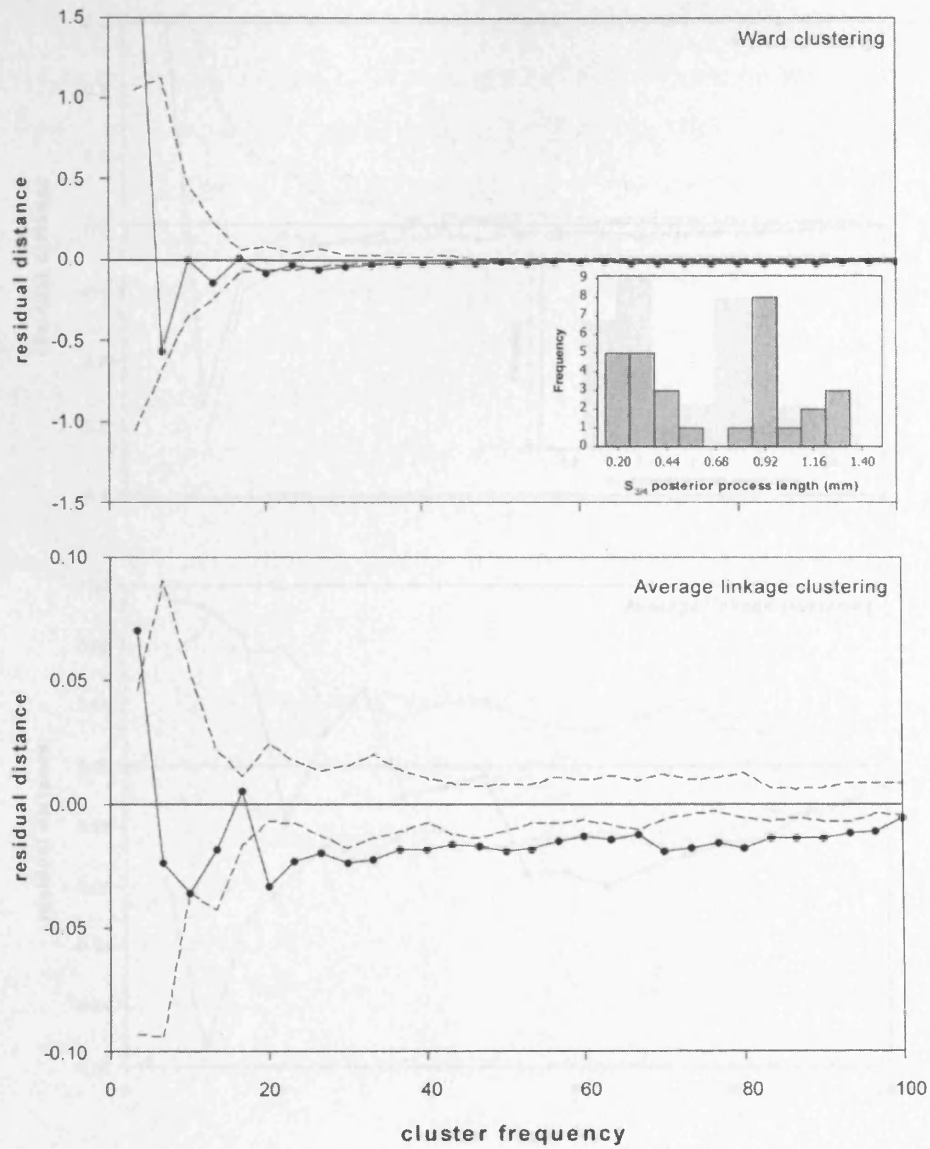


Figure 7: Residual distance against cluster frequency plots for Ward and average linkage cluster analysis of ‘*O.*’ excavata discrete and natural assemblage $S_{3/4}$ elements from the Eramosa Lagerstätte. Dashed lines enclose envelope of random data. Size-frequency histogram of $S_{3/4}$ total length is inset.

which P_1 elements provide the largest sample size, and produced the best clustering solution. Results for the P_2 and P_3 elements were approximately equivalent to those of P_1 . We investigate why the clustering patterns are different in the different elements of the apparatus. The following method was used. P_1 element total length data for the discrete and natural assemblages were used in the cluster analysis with calculated P_2 element length values. These values were then input to the appropriate growth curve model and used to predict the P_2 length of P_1 element length against P_1 element length (see below). The solutions of equivalent clusters that would be predicted in the P_1 and P_2 elements, were then the opposing growth trajectory, can be mapped onto the subset P_1 and P_2 data for comparison. This approach is strengthened by the caveat that the growth curves are not

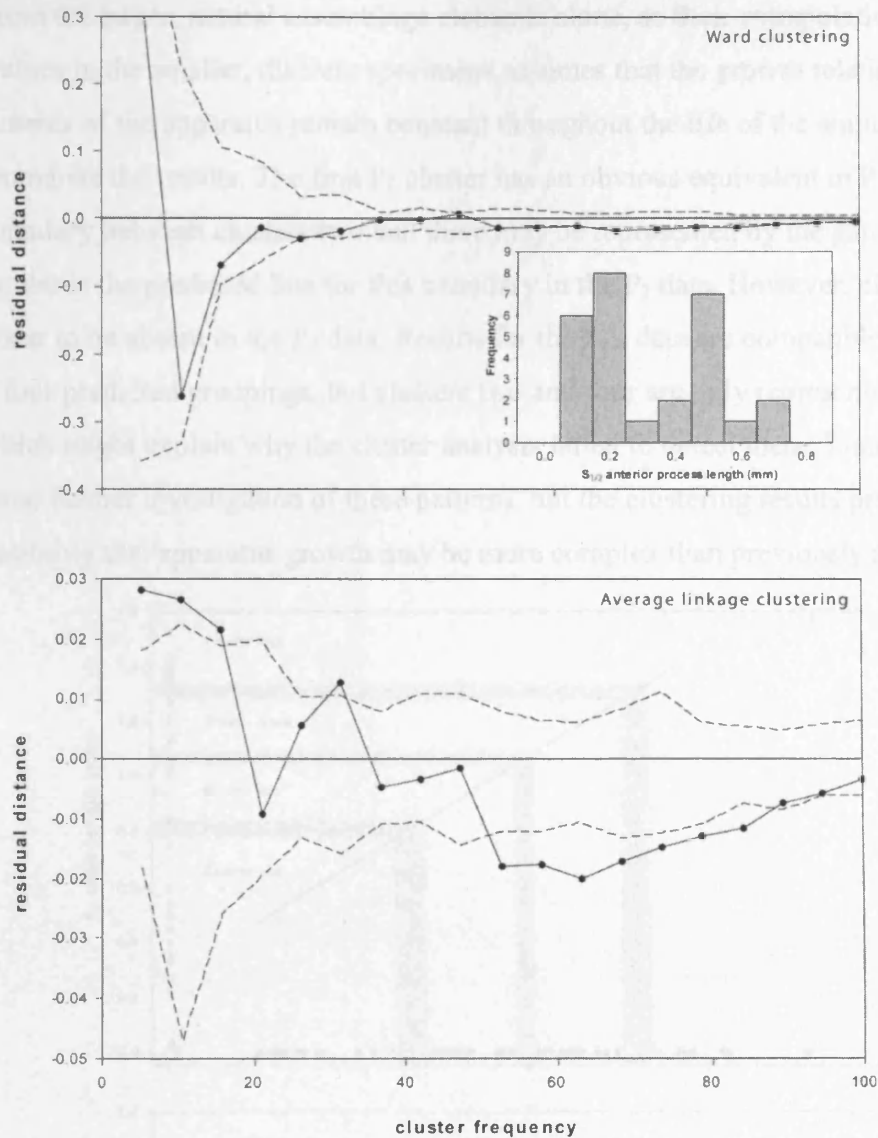


Figure 8: Residual distance against cluster frequency plots for Ward and average linkage cluster analysis of ‘*O.*’ excavata discrete and natural assemblage $S_{1/2}$ elements from the Eramosa Lagerstätte. Dashed lines enclose envelope of random data. Size-frequency histogram of $S_{1/2}$ total length is inset.

Since P_1 elements provide the largest sample size, and produce the best clustering pattern, results for the P_2 and $S_{3/4}$ elements were quantitatively compared to these, to investigate why the clustering patterns are different in the different elements of the apparatus. The following method was used. P_1 element total length data for the discrete and natural assemblage elements used in the cluster analysis were calculated by summing the process lengths. These values were then input to the appropriate growth line equations calculated from the regressions for P_2 length/ $S_{3/4}$ process length against P_1 element length (see below). The positions of equivalent clusters that would be predicted in the P_2 and $S_{3/4}$ elements, based on the apparatus growth trajectory, can be mapped onto the actual P_2 and $S_{3/4}$ data for comparison. This approach is accompanied by the caveat that the growth equations were

calculated from the larger, natural assemblage elements alone, so their extrapolation to predicting values in the smaller, discrete specimens assumes that the growth relationships between elements of the apparatus remain constant throughout the life of the animal. Figures 9 and 10 summarise the results. The first P_1 cluster has an obvious equivalent in P_2 length data. The boundary between clusters two and three may be represented by the gap immediately above the predicted line for this boundary in the P_2 data. However, clusters three and four appear to be absent in the P_2 data. Results for the $S_{3/4}$ data are compatible with the presence of four predicted groupings, but clusters two and four are only represented by a few elements, which might explain why the cluster analysis failed to detect them. Time constraints have prevented further investigation of these patterns, but the clustering results presented here raise the possibility that apparatus growth may be more complex than previously assumed.

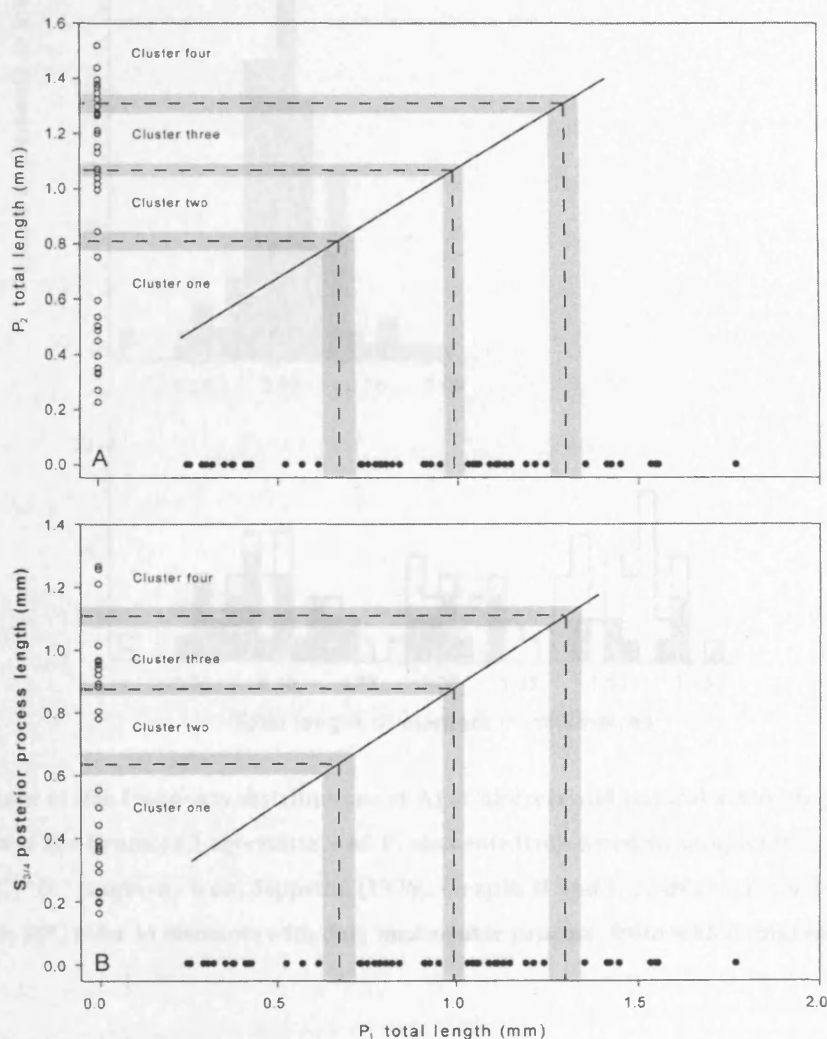


Figure 9: Plots of A) P_2 total length and B) $S_{3/4}$ posterior process length, against P_1 total length for ‘*O.*’ *excavata* natural assemblage and discrete element data from the Eramosa Lagerstätte. Solid line represents growth trajectory for P_2 elements relative to P_1 elements (A) and $S_{3/4}$ elements relative to P_1 elements (B), calculated from natural assemblage elements (see below). Dashed lines indicate centres of predicted cluster boundaries, grey shading indicates qualitative “confidence intervals” for each line.

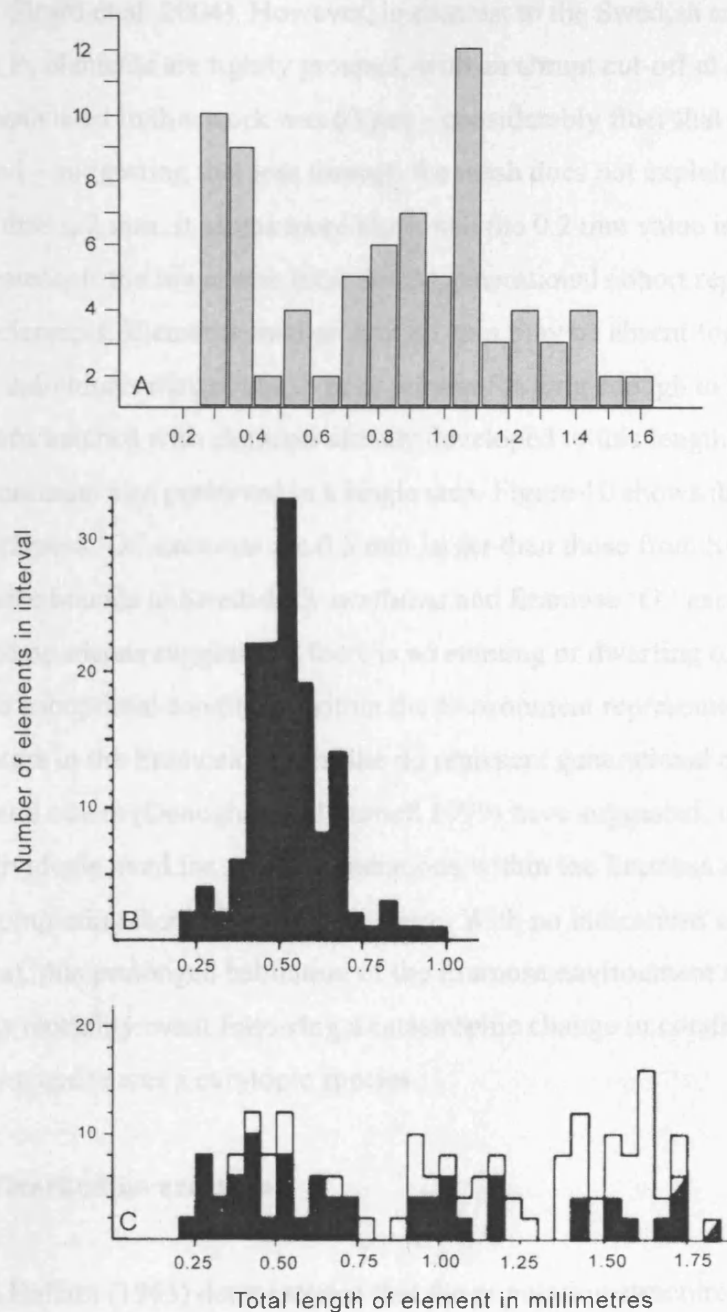


Figure 10: Comparison of size frequency distributions of A) of discrete and natural assemblage *O. excavata* P₁ elements in the Eramosa Lagerstätte, and P₁ elements from Swedish samples (Gogs locality) of B) *O. excavata* and C) '*O.*' *confluens* from Jeppsson (1976). Graphs B and C re-drawn from Jeppsson (1976). White bars in 10C refer to elements with only measurable process, from which total length was calculated.

The size distribution within the '*O.*' *excavata* P₁ elements from the Eramosa Lagerstätte was also compared with those of Jeppsson's (1976) *Ozarkodina* species from Sweden (see Figure 10). The lower bound of total length in the '*O.*' *excavata* specimens from Sweden and Canada is the same, as is the lower size bound in Swedish *O. confluens*. This lower limit has been assumed to be determined by sieve mesh size and so has no biological

significance (e.g. Girard et al. 2004). However, in contrast to the Swedish samples, the smallest Eramosa P₁ elements are tightly grouped, with an abrupt cut-off at approximately 0.2 mm. The finest mesh used in this work was 63 μm – considerably finer than the smallest elements recovered – suggesting that loss through the mesh does not explain the absence of elements smaller than 0.2 mm. It seems more likely that the 0.2 mm value is biologically significant and represents the lower size limit for the generational cohort represented by the group of smaller elements. Elements smaller than 0.2 mm may be absent for a variety of reasons: younger individuals may not have been present for long enough to be fossilised; they may have been born/hatched with elements already developed to this length, or grew their elements to the minimum size preserved in a single step. Figure 10 shows that the largest P₁ elements in the Eramosa '*O.*' *excavata* are 0.5 mm larger than those from Sweden, whereas upper and lower size bounds in Swedish *O. confluens* and Eramosa '*O.*' *excavata* are almost identical. These comparisons suggest that there is no stunting or dwarfing of '*O.*' *excavata* elements owing to suboptimal conditions within the environment represented by the Eramosa.

If the clusters in the Eramosa Lagerstätte do represent generational cohorts, as Jeppsson (1976) and others (Donoghue and Purnell 1999) have suggested, it would imply that '*O.*' *excavata* individuals lived for several generations within the Eramosa environment, before dying or completing their life cycle elsewhere. With no indications of suboptimal growth (see above), this prolonged habitation of the Eramosa environment supports the scenario of a mass mortality event following a catastrophic change in conditions, and may suggest that '*O.*' *excavata* was a eurytopic species.

Survivorship in Ozarkodina excavata

Craig and Hallam (1963) demonstrated that the population structure and size distribution of a population is a function of survivorship and growth rate; therefore survivorship analysis was conducted on '*O.*' *excavata* using the P₁ element size groupings identified by the Ward linkage cluster analysis (see upper bivariate plot in Figure 4), since these appear to represent real groupings that may equate directly to age cohorts.

Survivorship analysis reflects the mortality pattern that produced a fossil assemblage (Kurtén 1964), and is based around a life table. There are two kinds of survivorship analysis. The first assumes that a fossil deposit was created by mass mortality, so that it documents the age structure of the population at a single point in time; so-called time-specific (or static) survivorship. The second assumes that a fossil deposit was created by gradual accumulation of dead organisms: dynamic survivorship (Kurtén 1964). Samples are divided into age groups and three values are recorded: the number of individuals alive at the start of each age interval

(l_z), the number of individuals dying during each age interval (d_z) and the mortality rate during each age interval (q_z). The life table can then be used to plot a survivorship curve: a graph of percent survivors against age, by dividing l_z for each interval by the total number of individuals in the sample.

Figure 11 shows time-specific and dynamic life tables and survivorship curves, with elements divided into size groupings based on the clustering results. Although survivorship analyses cannot be used to test whether a deposit is a census or an accumulation (Raup and Stanley 1978), the taphonomic evidence from the Eramosa Lagerstätte, supported by the similarity between the population structure of '*O.*' *excavata* and that of a modern biological population, strongly suggest that this material represents a census count. Therefore, the time-specific survivorship analysis is a more appropriate representation. The time-specific curve displays somewhat convex-upward configuration (intermediate between the standard Type I and Type II curves of Deevey 1947, Pearl 1928), indicating a slight increase in mortality rates through time. Previous survivorship analyses in conodont taxa, including *O. confluens* (Jeppsson 1976), *Paracordylodus* (Tolmacheva and Löfgren 2000, Tolmacheva and Purnell 2002) and *Idiognathodus* (Armstrong 2005) are all similar to the Eramosa '*O.*' *excavata* in pattern, being concave-upwards, but differ in degree, generally exhibiting a greater increase in mortality rates amongst older individuals than that present in the Eramosa specimens.

Increasing mortality rates with age are typical of organisms that are predominantly K-strategists (Pianka 1970); the broad phylogenetic coverage of previous studies indicates a tendency towards K-selection may be common within conodont populations. Certainly the dynamics of the Eramosa '*O.*' *excavata* population conform to the characteristics of K-selected organisms of 1) a long lifespan, at least four years for '*O.*' *excavata* if the P_1 element size clusters are generational cohorts; 2) few progeny, indicated by the low frequency of elements in the Eramosa (although the large number of younger individuals (see Figure 10) is superficially more typical of r-strategists, the *relative* numbers of younger and older individuals are compatible with K-selection); 3) slow development and late reproduction, possibly suggested by the '*O.*' *excavata* survivorship curve, since the point of inflection on a convex-upwards survivorship curve, probably corresponding to cluster three in Figure 11, frequently indicates the onset of sexual maturity and mortality owing to breeding competition (see Erikson et al. 2006 and references therein). Conodont survivorship curves may therefore hold the potential to differentiate between adult and juvenile individuals.

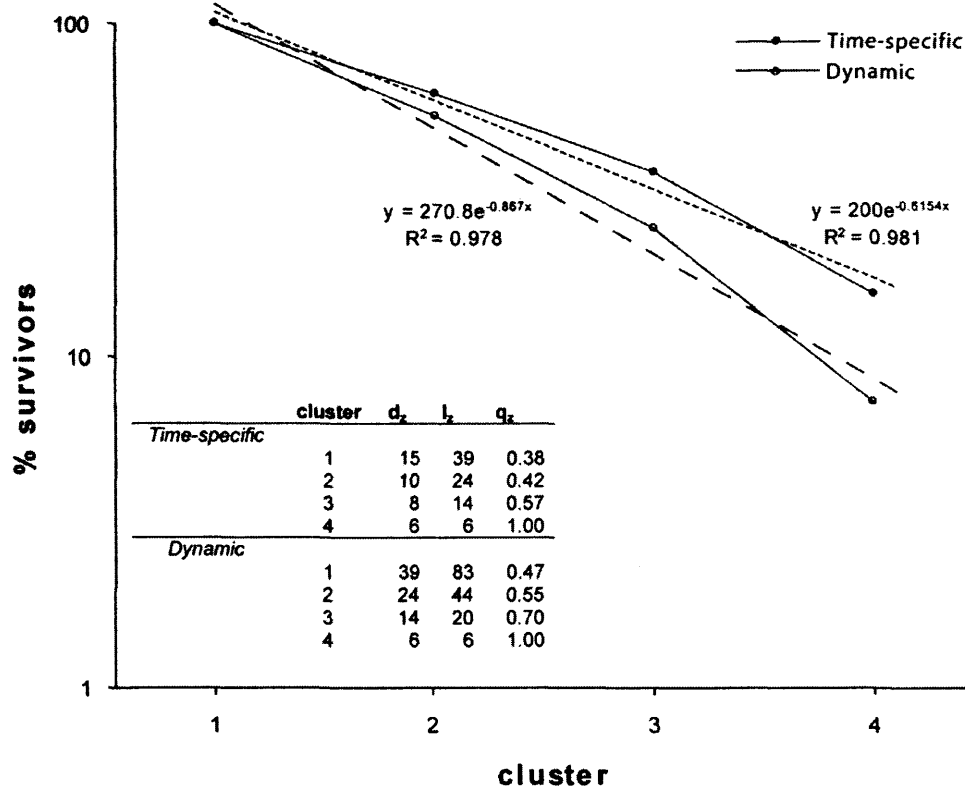


Figure 11: Time-specific and dynamic survivorship curves for ‘*O.* excavata dextral discrete and natural assemblage P₁ elements from the Eramosa Lagerstätte, plotted using the data from the inset life tables, with exponential trend lines. Line equations and correlation coefficients (R^2) are indicated. Clusters are based on groupings identified by cluster analyses (see Figure 4).

Craig and Hallam (1963) demonstrated that the size distribution they observed in *M. edulis* is predicted in an organism displaying essentially constant growth and constantly increasing mortality through time. Bearing in mind the caveats regarding the ‘*O.* excavata survivorship analysis of (1) uncertainties over the extent to which the clusters upon which the survivorship analysis was based represent true age cohorts and (2) that although the time-specific survivorship curve does not show *constantly* increasing mortality rates, the size distribution of the larger ‘*O.* excavata P₁ elements matches the pattern produced by an organism showing (constantly) increasing mortality levels through time. By analogy with *M. edulis*, this therefore suggests that growth in ‘*O.* excavata P elements occurred at a roughly constant rate between prolonged periods of function. This agrees with the even size and spacing of the clusters in Jeppsson’s (1976) *Ozarkodina confluens*, and also those in the current study of Eramosa ‘*O.* excavata. The closer spacing of the Eramosa ‘*O.* excavata size clusters compared to the Swedish *O. confluens* may suggest that periods of growth were shorter in the former species. Cluster size may also reflect how tightly controlled growth is: the more spherical clusters in the Eramosa ‘*O.* excavata are comparable to those in ostracods (e.g. Ruiz et al. 2003) and may indicate that growth was more strictly regulated in this population of conodonts. The morphological plasticity of ‘*O.* excavata (see previous

chapters) and the apparent harshness of the environment (von Bitter et al. in review) in which the Eramosa population lived suggests this regulation may have been driven more by extrinsic than intrinsic forces.

Survivorship analysis was also used to test the apparatus shedding hypothesis (cf. Armstrong 2005). The dissimilarity of mortality rates between time-specific and dynamic analyses of the Eramosa '*O.*' *excavata* population (see Figure 11), contrary to that predicted in a moulting organism (Kurtén 1964), provide no evidence for the hypothesis of apparatus shedding in '*O.*' *excavata* (cf. Armstrong 2005), supporting the hypothesis that conodonts retained their apparatus throughout life.

Apparatus ontogeny in Ozarkodina excavata

The apparatus data from the Eramosa Lagerstätte permit appraisal of the relative ontogenetic relationships between elements within the '*O.*' *excavata* skeleton. P_1 total length is taken as a standardised proxy for conodont body size on death (see above) which also enables comparison with previous tests of apparatus allometry (Purnell 1993, 1994, Tolmacheva and Purnell 2002). However, the method acquiring of total element length data using the new protocols differs slightly to that used in previous studies: here they are calculated as the sum of the processes; previously they are measured as the linear distance between distal terminals of the element (see inset element diagrams in Figures 13-14). Consequently, these results are not directly comparable. Therefore, two sets of ordinations are plotted: one based on the new protocols, the other based on the methods used in previous work. Linear distances between distal process terminals are calculated from process lengths and inter-process angles using the cosine rule.

Sample sizes were insufficient to examine relationships between P_1 elements and either $S_{1/2}$ or S_0 elements. Only in three articulated apparatuses could both $S_{3/4}$ posterior process length and P_1 total length be measured, but posterior process height was more readily measurable in the natural assemblages. Therefore, $S_{3/4}$ posterior process length was calculated using the equation of least-squares regression of isolated and assemblage $S_{3/4}$ elements for which posterior process length and height data were available (see figure 12). The correlation co-efficient for this regression is quite high ($r^2 = 0.77$), indicating that it provides a reasonably accurate estimate of posterior process length in $S_{3/4}$ elements. Moreover, the three measured process lengths plot within the field of calculated values in the regression in Figure 14. When plotted against P_1 total length, other linear measures on assemblage elements, such as cusp and denticle width, produced r-values too low (< 0.5) to meaningfully analyse using a linear model.

Growth was investigated in 'O.' *excavata* elements using the power function $y = bx^a$ (Huxley 1924). Ontogenetic relations within and between elements were analysed through Reduced Major Axis (RMA) regression, to facilitate comparison with previous studies. Allometry was tested for statistical significance by comparing calculated growth exponents with isometric values using Z-tests. Figure 14 illustrates Reduced Major Axis (RMA) ordinations of distance measures in various elements of the apparatus, against P_1 total length as measured between distal process tips, and provides the associated RMA statistics for the comparisons. Figure 14 provides the same results, but for P_1 total length measured as the sum of the process lengths. RMA statistics for both comparisons differ little, justifying comparability between these results and previous work.

No statistically significant difference between the calculated growth coefficients and isometry was found in the RMA analyses of M and $S_{3/4}$ elements. Although sample sizes are small, the p -values for M and $S_{3/4}$ elements are considerably greater than the 0.05 significance level (see Figure 14). This indicates that the M and $S_{3/4}$ elements of *O. excavata* grew isometrically, as found in all previous RMA analyses of apparatus ontogeny in conodont species, including *Idiognathodus* (Purnell 1993), *Gnathodus bilineatus* (Purnell 1994) and *Paracordylodus* (Tolmacheva and Purnell 2002). The absence of significant positive allometry within M and S elements predicted by the hypothesis of a filter-feeding function for these elements (Purnell 1993, 1994) further supports the hypothesis that ozarkodinids did not use their M and S elements for suspension feeding. Rather, a raptorial function remains more probable, supporting the hypothesis that conodonts were predators or scavengers (Purnell 1994, 1995).

In contrast, the P_2 elements displayed slight negative allometry, contrary to the expected pattern of isometry to maintain functional equivalence (Purnell 1993, 1994). This may of course result from inadequate sample size, but it could also reflect the inability of the traditional measures to accurately quantify the curvature of the blade, underestimating the length of the functional cutting edge. A more accurate measure of this cutting edge would perhaps be the sum of all the denticle base widths; unfortunately time constraints prevented this from being conducted in the present study, but it potentially provides a method of testing this explanation.

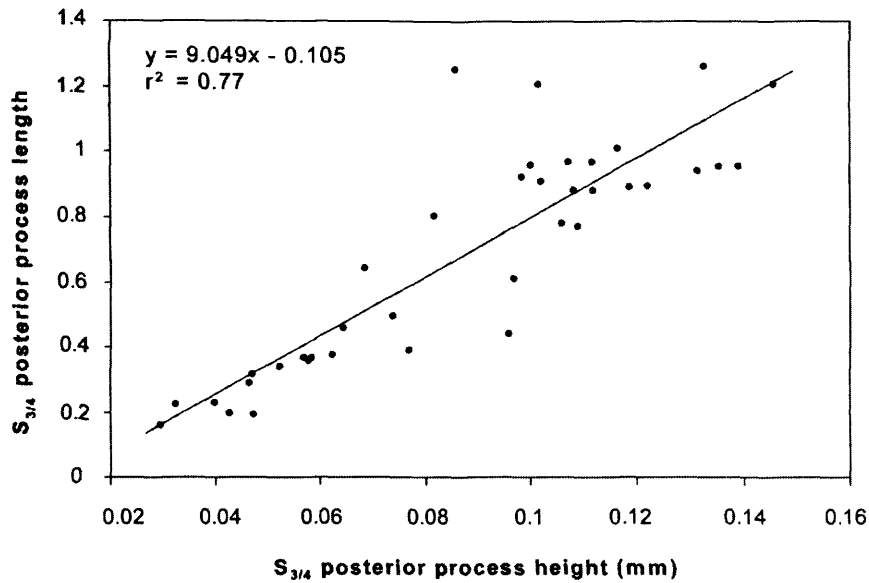


Figure 12: Least-squares regression of posterior process length (PPL) against posterior process height (PPH) for '*O.*' *excavata* discrete and bedding-plane assemblage $S_{3/4}$ elements from the Eramosa Lagerstätte, Ontario.

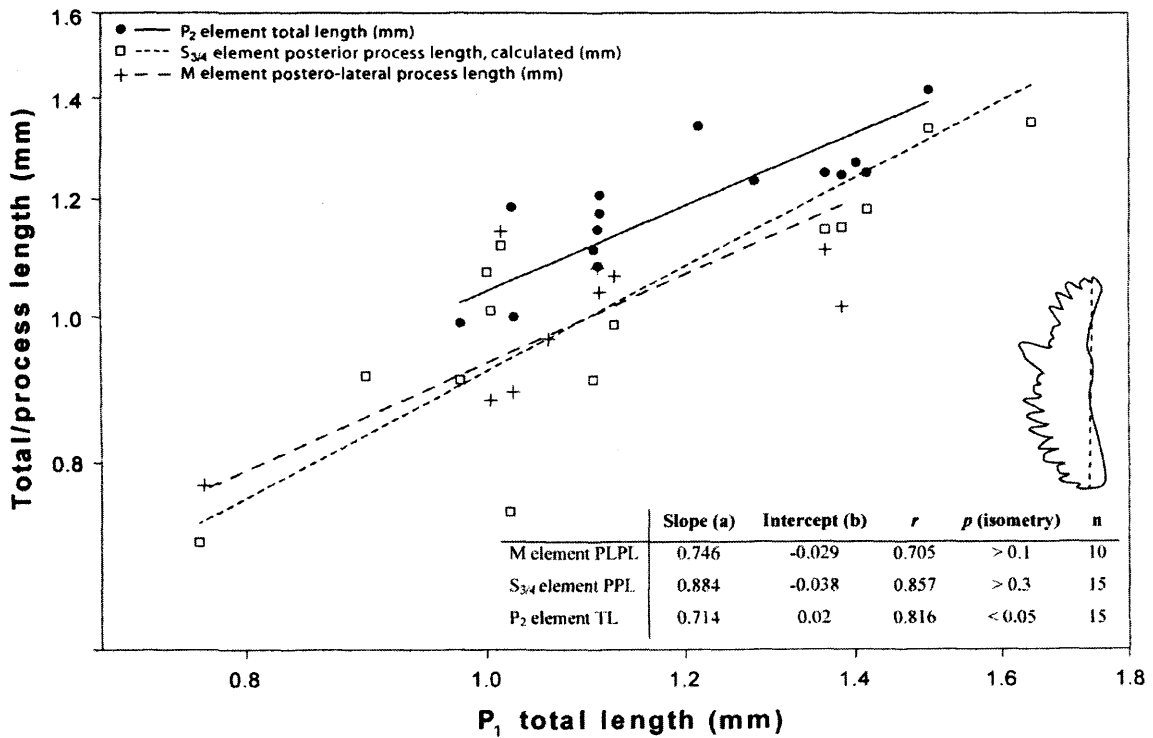


Figure 13: RMA regressions of '*O.*' *excavata* natural assemblage elements from the Eramosa Lagerstätte against P_1 element total element length (TL). TL is measured as the linear distance between distal terminals of the element, as illustrated on inset element diagram. Inset table provides statistics for RMA regressions, showing slope and intercept of RMA regression line, r -value, p -value significance against isometry and sample size.

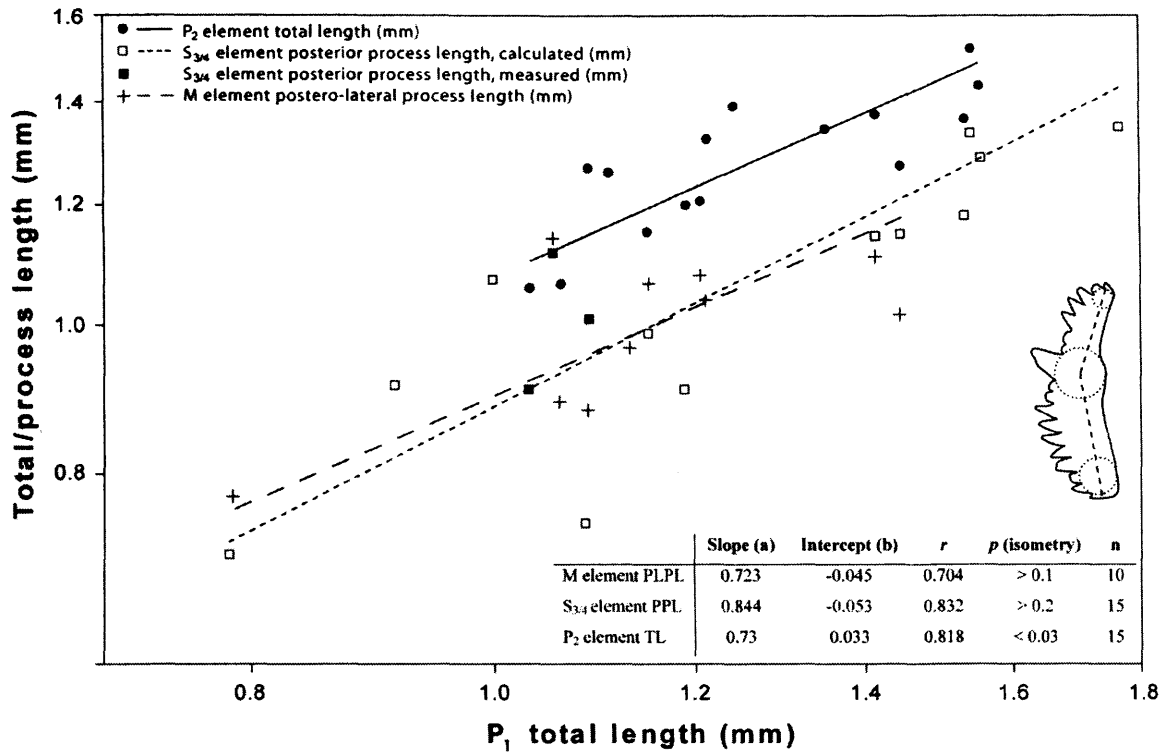


Figure 14: RMA regressions of '*O. excavata*' natural assemblage elements from the Eramosa Lagerstätte against P₁ element total element length (TL). TL is measured as the sum of ventral and dorsal processes, as illustrated on inset element diagram. Inset table provides statistics for RMA regressions, showing slope and intercept of RMA regression line, *r*-value, *p*-value significance against isometry and sample size.

Conclusions

New morphometric protocols, outlined in Jones and Purnell (in press) and Chapter one have been applied to elements from articulated apparatuses and discrete elements of the conodont '*Ozarkodina*' *excavata* from the Eramosa Lagerstätte, Ontario. Size frequency distributions of P elements have produced a characteristic pattern similar to those seen in populations of the extant mussel *Mytilus edulis* (Craig and Hallam 1963). This supports the hypothesis, based on taphonomic evidence (von Bitter and Purnell 2005), that the Eramosa Lagerstätte closely approximates a single biological population of '*O.*' *excavata*. The Eramosa Lagerstätte thus permitted testing of autecological hypotheses and examination of population biology in '*O.*' *excavata* at a level of detail rarely possible in conodont studies.

Size distributions were rigorously examined using cluster analysis, which identified natural groupings within the elements. Comparison of the Eramosa '*O.*' *excavata* size distribution with those revealed by previous work on the genus (Jeppsson 1976), argued against any stunting or dwarfing of '*O.*' *excavata* within the Eramosa; coupled with the wide size range of individuals and probable presence of multiple generations within the harsh environment of the Eramosa Lagerstätte (von Bitter et al. in review), this indicates that '*O.*' *excavata* may have been eurytopic. Accepting the most parsimonious interpretation of the element size clusters as generational cohorts (Donoghue and Purnell 1999, Jeppsson 1976), allowed them to be utilised as the basis of survivorship analysis. Survivorship curves indicate slightly increasing mortality rates through time within the Eramosa population of '*O.*' *excavata*. This pattern is similar to that present in previous analyses of conodont survivorship, which sample both ozarkodinids and prionidinids (Armstrong 2005, Jeppsson 1976, Tolmacheva and Purnell 2002); such wide phylogenetic coverage suggests that this may be a common pattern in conodonts. In modern species with increasing mortality rates through time, sexual maturity can frequently be identified from the survivorship curve (see Erikson et al. 2006 and references therein), and so survivorship analyses may enable differentiation of adult and juvenile conodonts.

The natural population of the Eramosa Lagerstätte has also permitted testing of previously examined hypotheses, but with a greater degree of biological rigour. Differences in mortality patterns between dynamic and time-specific survivorship refutes the hypothesis that '*O.*' *excavata* shed its apparatus (cf. Armstrong 2005). No evidence was found in the Eramosa Lagerstätte for element shedding. This suggests that the dentition of '*O.*' *excavata* was retained through life. Analysis of element length measurements within the '*O.*' *excavata* skeleton has revealed that the M and S_{3/4} elements grew isometrically, as found in previous analyses of conodont apparatus ontogeny (Armstrong 2005, Purnell 1993, 1994, Tolmacheva

and Purnell 2002). This refutes the hypothesis of a suspension feeding function for these elements, where positive allometry of M and S elements would be predicted; a more raptorial function for these elements is more probable (Purnell 1994, Purnell and Donoghue 1997).

The results presented here clearly demonstrate the effectiveness of new morphometric protocols outlined in Jones and Purnell (in press) and Chapter one, in capturing patterns of morphological variation within the conodont skeleton, and hold promise of broad across-taxon application in future quantitative analyses of conodont autecology.

Chapter six: Morphometric analysis of evolutionary rate and pattern in the conodont *Pterospathodus*

Abstract

Conodonts are an extinct clade of vertebrates whose fossil record is one of the best available for studying evolutionary rates and patterns. Yet few studies have hitherto analysed conodont evolution with the necessary quantitative rigour, and consequently the potential of the conodont fossil record as a tool for elucidating the evolutionary process has not been realised. This study applies new standardised morphometric protocols to the Silurian conodont *Pterospathodus* (Walliser 1964), whose morphology is currently understood within a primarily qualitative framework. *Pterospathodus* is an ideal taxon to investigate because it displays one of the best examples of apparent directional morphological evolution in conodonts, and is a biostratigraphically important taxon, species of which define several Silurian biozones. These existing qualitative evolutionary and taxonomic hypotheses are examined and tested using morphometric analysis of *Pterospathodus* skeletal elements from the Viki core (Estonia), which constitutes the best sampled stratigraphic sequence so far analysed quantitatively for evolutionary pattern and rate in conodonts.

Taxonomic hypotheses proved difficult to test owing to ambiguity of characters diagnosing taxa. Little quantitative support was found for the taxa examined, based on analysis of their diagnostic characters. Few continuous variables displayed any discontinuities through the Viki core at which taxonomic boundaries could be placed. Whilst this supports the interpretation of *Pterospathodus* as an anagenetic continuum, it suggests taxa diagnosed by these variables will necessarily be arbitrary constructs, with no biological reality. Hypotheses of directional evolutionary change in *Pterospathodus* were tested using log rate-log interval and rescaled range analysis of stratophenetic series. Analysis of element length increase produced ambiguous results, in part because of increasing variance in length with time. Analysis of process length increase indicated significant directional evolution. Fourier analysis of P₁ lateral outline captured a directional evolutionary shape change, involving a transition from short, wide elements and longer, narrower forms. Evolutionary rates were measured for the first time in a conodont taxon: shape change occurred at 0.033 haldanes; slightly closer to the upper range of rates recorded in other fossil organisms.

Introduction

Conodonts are an extinct group of vertebrates that possess tremendous potential for documenting evolutionary patterns, measuring evolutionary rates and investigating evolutionary processes: they are represented by an excellent fossil record (Foote and Sepkoski 1999), they have endured through extreme environmental fluctuations (Higgins and Austin 1985), exposing them to a variety of potential selection pressures, and they exhibit obvious morphological change through time (Sweet 1988). Yet to realise their potential for studying evolution, a detailed, quantitative understanding of morphology, most rigorously achieved using morphometric methods, is necessary. This is frequently absent in previous discussions of conodont evolution; reviewed below are the few studies that have approached the study of conodont evolution from a quantitative standpoint.

Barnett (1971, 1972) examined temporal trends in quantitative morphological variables for *Spathognathodus remischeidensis*, to examine element ontogeny and evolutionary patterns, the latter primarily for biostratigraphic correlation. He noted patterns of both apparent stasis and directionality within eight morphological characters and hypothesised causal relationships between purported evolutionary change and concurrent environmental shifts. However, because the recorded morphological changes were not tested against a random walk, necessary to avoid erroneously interpreting stochastic change as evolutionary pattern e.g. (Bookstein 1987, Raup 1977, see below), it is difficult to assess the reality of the apparent directional or static patterns of morphology through time.

Murphy and Cebecioglu (1984) focussed upon *Icriodus*, using denticulation and length:width ratio measures to elucidate the biostratigraphy, taxonomy and evolutionary mode within the genus. They found predominantly stasis in measured morphological variables. Murphy and Springer (1989) conducted a similar study of *Amydrotaxis praejohnsoni*, using several variables, concluding that the morphometric results supported the existing qualitative taxonomic framework and again revealed apparent stasis in the majority of characters. In neither study was there statistical comparison of the morphological changes with a random walk, so the conclusion that the patterns truly represent stasis cannot be accepted with confidence.

In an excellent study, Ritter (1989) examined the taxonomy of *Neogondolella mombbergensis* to clarify its evolutionary mode and evaluate its biostratigraphic potential. Although several of the measured variables were of uncertain biological significance, Ritter's (1989) work provides a good example of a thorough and effective sampling strategy, where shifts

through time in measured variables were tested against the null hypothesis of a random walk, which statistically confirmed the apparent qualitative pattern of non-directional change through time.

A series of papers by Girard and others applied elliptic Fourier analysis to platform element outline: Renaud and Girard (1999) investigated the evolution of *Icriodus* and *Palmatolepis* during the late Devonian extinction events, causally relating morphological changes in size and shape to concomitant environmental changes; Girard et al. (2004a) conducted a similar study, concentrating on *Palmatolepis*; Girard et al. (2004b) then investigated the evolutionary taxonomy of *Palmatolepis*. In none of the papers were morphological changes through time tested against a random walk model. Although the most obvious morphological shifts corresponded so closely to probable causative environmental changes as to perhaps render such tests unnecessary, the trends of shape change stratigraphically above and below these abrupt events show a more ambiguous pattern; analysis of evolutionary rate and pattern here would have been informative, particularly if compared to results during periods of morphological change.

Roopnarine et al. (2004) examined the evolutionary taxonomy of *Wurmiella* using a cubic spline analysis to capture the shape of the P₁ element aboral margin. Using rescaled range (R/S) analysis, they demonstrated that some of the temporal shape variation was directional, and that some changes could not be distinguished from a random walk. Although Roopnarine et al. (2005) cite this as evidence for microevolutionary trends in *Wurmiella*, but this is perhaps premature: the analysed sequence is somewhat coarsely and unevenly sampled; it seems probable that more complex morphological patterns are present, and would be detected were a better sampling strategy utilised.

The current study has examined the Silurian conodont *Pterospathodus* (Walliser 1964) using a suite of new, standardised morphometric protocols developed to analyse morphological variation in conodonts. *Pterospathodus* represents an excellent taxon for quantitative analysis because its morphology, taxonomy and evolution have been described in detail (Männik 1998, Männik and Aldridge 1989), but are currently understood within a dominantly qualitative framework. *Pterospathodus* also displays one of the best examples of apparent directional morphological evolution in conodonts (Männik and Aldridge 1989) and is a biostratigraphically important taxon, species of which define several Silurian biozones (Männik 1998). The goal of this work is to rigorously test existing qualitative evolutionary and taxonomic hypotheses through morphometric analysis of *Pterospathodus* elements from the Viki core, Estonia, which represents the longest, most densely and evenly sampled stratigraphic sequence hitherto analysed quantitatively for evolutionary trends and rates in conodonts. Details of samples taken through

the core are given in Table 1; sample numbers are not sequential because of the sampling strategy used, so the sample number and depths are stated in the text, to allow easier identification of specified horizons referred to.

Taxonomic hypotheses

Within the open shelf environment from which material used in this study is derived (see below) Männik (1998, text-fig 3) has divided *Pterospathodus* into a series of non-overlapping, stratigraphically sequential species and subspecies, forming an anagenetic continuum. Figure 1 illustrates these taxa. Several of the taxa define Silurian biozones, and so assessing their boundaries has biostratigraphic implications. Some taxa are not tested here: those diagnosed using obvious qualitative characteristics, or using ambiguous characters that cannot readily be quantified; unfortunately, many of the taxa fall into these categories, and these are discussed below. The few remaining taxonomic boundaries are, however, investigated. Because Männik's (1998) taxonomic descriptions use traditional anatomical notation, this is used throughout the current work.

The oldest species *Pterospathodus* species in the Viki core, *P. eopennatus* is particularly variable, and Männik (1998) has identified two new subspecies within it, which he labels 1 and 2. He also recognises eight morphs within these subspecies, of which seven occur in the Viki core: 1a and 1b, 2a and 2b, 3, 4 and 6. Subspecies 1 is diagnosed by morph 6, subspecies 2 by morphs 2 and 4 (Männik 1998). However, some of the differences between *P. eopennatus* morphs are subtle, making repeated identification by multiple workers of differing experience potentially problematic (see Chapter two for an example of the effect of experience on element identification in '*Ozarkodina*' *excavata*). Primary discriminators between the morphs are denticle height and element length. Denticle height is difficult to describe even qualitatively, and is virtually impossible to quantify accurately, because of denticle breakage and wear, and ambiguity in identifying the boundaries of white matter within the denticle. Therefore morphs differentiated by denticle height cannot be tested with the current protocols. Morphs are also divided into long and short forms. Attempting to discriminate between the short morphs within *P. eopennatus* highlights the problems of adopting a length-based diagnosis: adults of smaller forms can be confused with juveniles of the longer morphs. Here, the adults of short morphs 2 and 6 and juveniles of long morphs 1 and 3 would have the same morphology as diagnosed in Männik (1998): they are short and possess high distal denticles. This could represent an interesting

example of heterochrony within *Pterospathodus*, but without identifying these diagnostic short morphs, Männik's (1998) new subspecies 1 and 2 cannot be objectively delineated and tested.

The origination of *Pterospathodus amorphognathoides* (and its earliest subspecies, *P. a. angulatus*) is marked by the appearance of mature elements with ≥ 20 denticles (Männik 1998), which places the origin of *P. amorphognathoides* between 167.4 and 169.35 m depth (between samples 6 and 27) within the Viki core. The biological significance of this species boundary is, however, uncertain. The origin of the next subspecies, *P. amorphognathoides lennarti*, is marked by the appearance of elements with bifurcated processes (Männik 1998). In the Viki core, bifurcated processes occur sporadically from 167.4 m (sample 6; coinciding with the appearance of elements with 20 denticles), but only start to appear in consecutive horizons between 153.05 and 151.64 m (between samples 12 and 8). Therefore, the origin of *P. a. lennarti* is placed between these horizons. *P. a. lennarti* is distinguished from *P. amorphognathoides lithuanicus* by a reduction in the distance between the first process denticle and the main denticle row (Männik 1998). This boundary has been quantitatively tested. The youngest subspecies, *P. amorphognathoides amorphognathoides*, is diagnosed by the possession of platform ledges. The appearance of this subspecies and the base of its associated biozone are thus unequivocally defined by an obvious qualitative character; in the Viki core, platforms originate between 145.55 and 146.7 m depth (between samples 24 and 14).

Hypotheses of process asymmetry

Männik and Aldridge (1989) and Männik (1998) identified asymmetry in the anterolateral processes of *P. eopennatus* elements: process development was generally greater in dextral elements. Process development was measured in two ways, reflecting the two senses in which the term was used in Männik and Aldridge (1989); The first is frequency of process possession; how often the process is developed on an element. The second is process length; how developed the process becomes if it is present, as measured through length.

Hypotheses of evolutionary pattern

Pterospathodus displays one of the best examples of apparent directional morphological evolution in conodonts (Männik and Aldridge 1989). Two trends occurring through the sequence of *Pterospathodus* P₁ elements, documented by Männik and Aldridge (1989) and Männik (1998), are tested in this study: element size increase and increasing process development. Another trend,

not discussed in detail by either Männik and Aldridge (1989) or Männik (1998), is change in element shape. This is also tested, using both traditional multivariate measures, and outline analysis.

Hypotheses of evolutionary rate

Because of the absence of a quantitative framework for *Pterospathodus*, characterisation of the evolutionary rates at which morphological changes occur are vague, ranging from gradual to rapid (Männik 1998, Männik and Aldridge 1989). These hypotheses of rates were tested, quantifying evolutionary rates in a conodont taxon for the first time.

Sample number	Slide number	Depth interval (m)	N (multivariate)	N (outline)
1	M-593	183.32 - 183.42	34	13
2	M-962	181.29 - 181.40	50	20
3	M-957	182.42 - 182.54	51	-
4	M-6	163.6 - 163.8	56	21
5	M-9	171.6 - 171.8	55	23
6	C95-80	167.3 - 167.4	50	23
7	C95-88	159.9 - 160	54	17
8	M-971	151.54 - 151.64	32	15
9	M-975	150.17 - 150.28	45	-
10	M-979	148.75 - 148.85	25	-
11	C98-1	147.4 - 147.5	33	-
12	M-968	153.05 - 153.2	21	-
13	M-2	155.2 - 155.4	20	12
14	M-368	145.4 - 145.55	33	11
15	M-374	138.95 - 139.1	35	14
16	M-381	130.45 - 130.55	32	12
17	M-387	120.6 - 120.75	12	-
19A	M-996	113.65 - 113.75	18	7
20	M-994	114.05 - 114.2	11	-
21	M-371	142.1 - 142.25	19	8
22	M-378	134.8 - 134.9	19	11
23	M-385	124.6 - 124.75	16	9
24	M-367	146.7 - 146.8	22	-
25	M-3	156.5 - 156.7	19	12
26	C95-82	165.1 - 165.2	42	21
27	C95-78	169.35 - 169.45	33	19
28	C95-73	173.1 - 173.2	40	19
29	M-964	179.82 - 179.95	50	20
30	C95 - 89	159.1 - 159.2	30	14
31	M-1	154.4 - 154.5	18	12
32	M-978	149.07 - 149.17	16	12

Table 1: Summary details for *Pterospathodus* P₁ element samples from the Viki core, Saaremaa, Estonia. N represents number of elements sampled for multivariate and outline analyses. Slide numbers based on catalogue scheme of P. Mannik. Depth values are rounded to the nearest metre in stratophenetic plots.

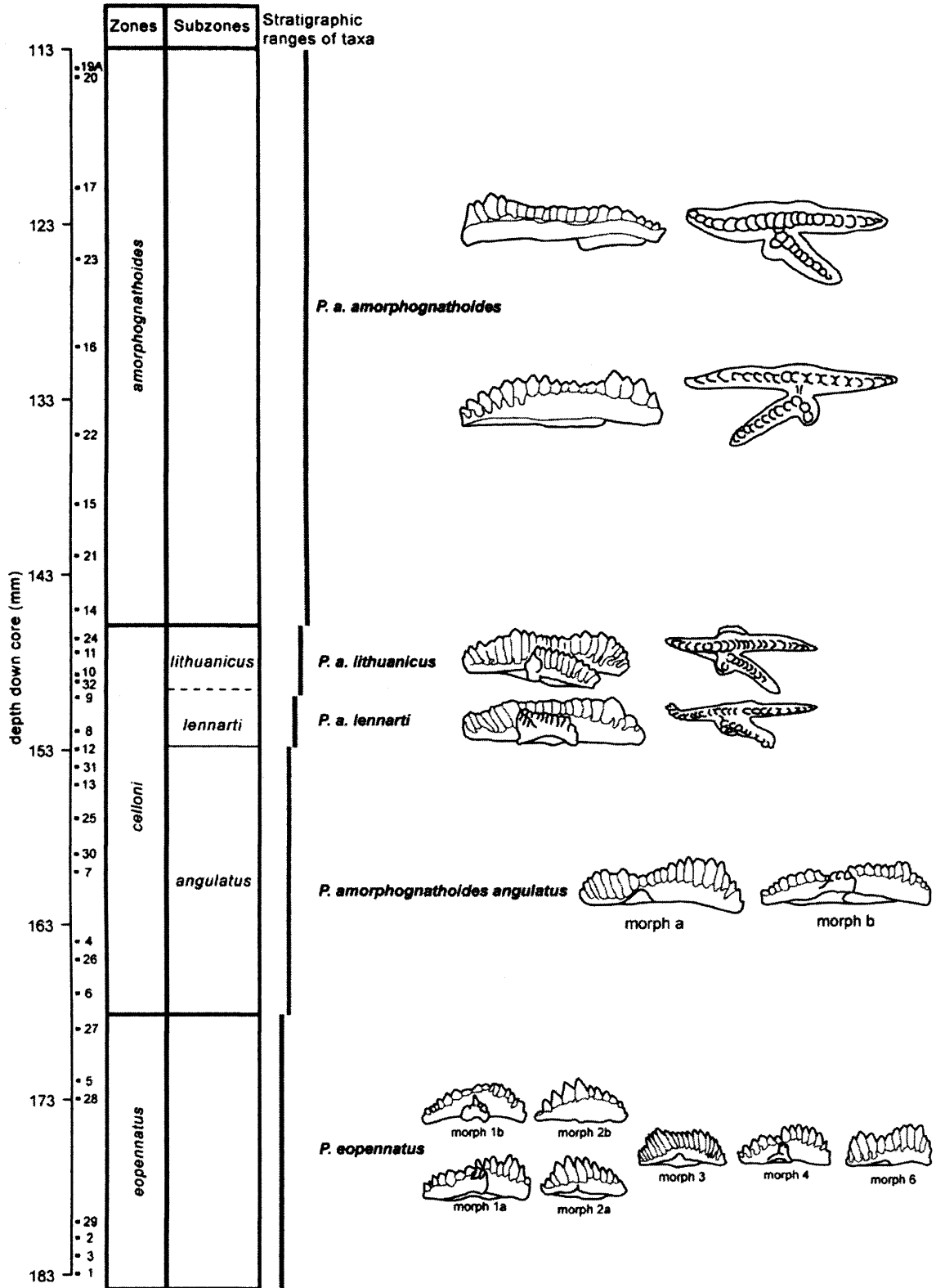


Figure 1: Schematic stratigraphic column, showing zones and subzones based on *Pterospathodus* taxa. Exemplar P₁ elements representing *Pterospathodus* taxa and morphs present during these intervals, within the open shelf environment represented by the Viki core, are also illustrated. Grey lines show taxon ranges. Sample numbers (see Table 1) and approximate stratigraphic positions are shown at left. Position of *lennarti-lithuanicus* boundary relative to samples is uncertain (see text). All elements re-drawn from Mannik (1998).

Materials and method

This study was based on collections of *Pterospathodus* elements from the Institute of Geology at the Tallinn Technical University, Tallinn, Estonia. Over 900 elements were analysed. Element preservation is good (CAI = 1), although many of the large elements are incomplete, frequently missing lateral processes. The material was derived from the Viki core taken on the island of Saaremaa, Estonia. The core samples the marlstone lithology of the Velise Formation (Adavere Stage, upper Llandovery, Nestor 1997), interpreted as an open shelf carbonate-terrigenous environment (P. Männik pers. comm. 2005). The sequence within the core records a gradual marine transgression, beginning in the Rumba Formation at the base of the Adavere Stage, approximately 7.7 m below the sampled section of the core (Nestor and Einasto 1997), although this was probably not eustatic (Loydell et al. 1998, and references therein). No major unconformities are apparent within the sequence (Nestor 1997). Thirty-one stratigraphic levels were sampled through 70.1 m (183.4-113.3 m) of core, covering virtually the entire temporal extent of *Pterospathodus* in Estonia (approximately six million years; Gradstein et al. 2004, P. Männik pers. comm. 2005).

Only the P_1 elements were examined as they have large sample sizes and display more extensive morphological variation than the other elements of the *Pterospthodus* skeleton (Männik and Aldridge 1989). Data were acquired using the morphometric protocols outlined in Chapter one and Jones and Purnell (in press). Figure 2 illustrates the measured variables, and Table 2 provides descriptions of the measured variables and their abbreviations.

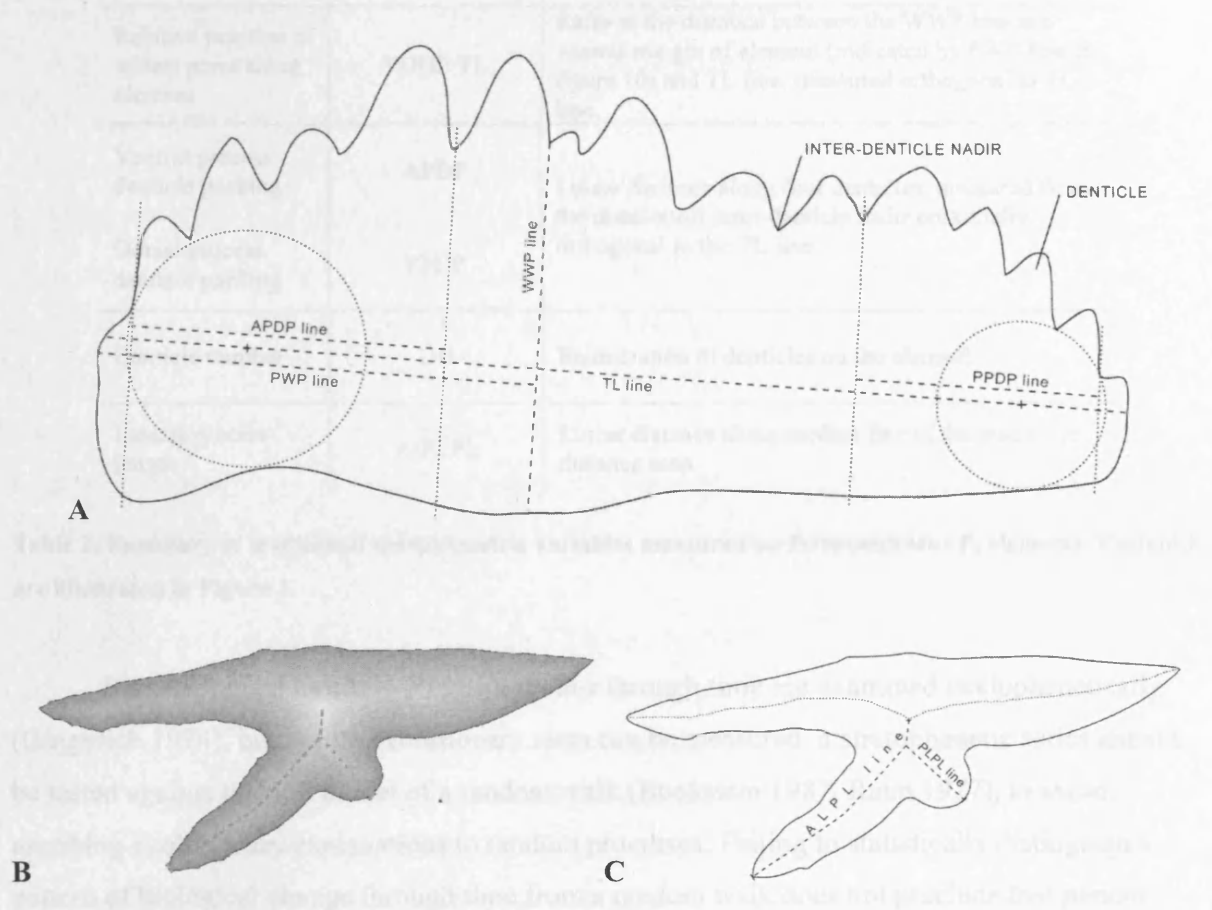


Figure 2: A) Diagram of lateral profile of *Pterospthodus* P_1 element, illustrating measured variables used in the study. Dashed lines indicate measured variables. Dotted lines represent the anchored circles (see Chapter one and Jones and Purnell (in press) for detailed discussion) and construction lines used to consistently place measurement lines. B) Outline of oral surface of *Pterospthodus* P_1 element showing placement of measurement lines relative to distance map C) outline of oral surface of *Pterospthodus* P_1 element illustrating measurement lines. See Table 2 for key to variable abbreviations.

Name	Abbreviation	Description
Total length of element	TL	Linear distance from ventral to dorsal margin, measured along a line passing through the anchored points of penultimate ventral and dorsal denticles.
Width at widest point	WWP	Linear distance from oral-most inter-denticle nadir to the aboral margin of the element, orthogonal to the TL line.
Relative position of widest point along element	VDHP:TL	Ratio of the distance between the WWP line and ventral margin of element (indicated by PWP line in figure 10) and TL line, measured orthogonal to TL line.
Ventral process denticle packing	APDP	Linear distance along four denticles, measured from the distal-most inter-denticle nadir proximally, orthogonal to the TL line.
Dorsal process denticle packing	PPDP	
Denticle number	DN	Enumeration of denticles on the element.
Lateral process length	A/PLPL	Linear distance along median line of the process in distance map.

Table 2: Summary of traditional morphometric variables measured on *Pterospathodus* P₁ elements. Variables are illustrated in Figure 2.

Morphological trends in *Pterospathodus* through time are examined stratophenetically (Gingerich 1974), but before evolutionary rates can be measured, a stratophenetic series should be tested against the null model of a random walk (Bookstein 1987, Raup 1977), to avoid ascribing evolutionary explanations to random processes. Failing to statistically distinguish a pattern of biological change through time from a random walk does not preclude that pattern being generated by directional evolutionary processes, for example through adaptive responses to stochastically varying environmental factors, however rejection of the null hypothesis of randomness can reinforce interpretations that observed changes result from selection (Hendry and Kinnison 1999). Sheets and Mitchell (2001) demonstrated that different methods to test the null model of randomness differ in their statistical power depending on the characteristics of the dataset; therefore, two approaches are utilised in this work to examine temporal sequences of morphological change in *Pterospathodus*, and results compared. These are rescaled range (R/S) analysis and log rate-log interval (LRI) analysis. Roopnarine et al. (1999) have shown them to be computationally equivalent, but whilst R/S analysis is perhaps more flexible in the morphological

data it can analyse, LRI analysis allows evolutionary rate to be quantified in standardised units that facilitate comparison with previous studies.

Rescaled range (R/S) analysis (Hurst 1951) has been utilised previously to analyse conodont evolution (Roopnarine et al. 2004). The method statistically assesses the deviation of a series from a random walk by estimating the Hurst exponent of the sequence. The analysis itself describes the persistence or anti-persistence of a series (Roopnarine et al. 1999). Anti-persistence means that successive steps differ more than would be expected than by chance alone. Conversely, persistence measures the degree to which each step depends on the previous step, over a prolonged time period. The Hurst exponent (H) is estimated through multiple pair-wise comparisons. This involves calculating the differences in any given morphological variable between all pairs of samples in a temporal sequence, and scaling this by the interval of time separating each pair. The time interval may be measured in generations (see below) or years based on thickness of rock separating the samples and estimated sedimentation rates. The reason for adopting this approach is to reveal the relationship between rates of change and the interval over which they are measured, which is generally an inverse correlation (Gingerich 1983). The Hurst exponent can take any value between zero and unity. If $H \approx 0.5$, then the series is random; if $H \gg 0.5$, then the sequence is directional, if $H \ll 0.5$, the sequence is constrained (Roopnarine et al. 1999).

Log rate-log interval (LRI) analysis (Gingerich 1993) is similarly calculated by multiple pairwise comparisons on all possible morphological ranges for all intervals in a sequence, producing a graph of logged evolutionary rate (in haldanes; see below) against logged time interval (in generations). A logarithmic measurement scale is used because proportional rather than absolute change is being examined (Simpson 1944). An iterative maximum-likelihood procedure that minimises absolute deviations is used to fit a line to the points (Gingerich and Gunnell 1995). The slope of this best-fit line varies between zero and minus one, and indicates whether the sequence is random (slope = -0.5), significantly directional (slope \gg -0.5) or significantly constrained (slope \ll -0.5). Bootstrapping is utilised to calculate 95% confidence intervals for the slope and intercept of the best-fit line; in this work, 100 bootstrap re-samples are used to produce confidence intervals. The y-intercept of the maximum-likelihood line also furnishes a prediction of the generational rate of change (Gingerich's intrinsic rate (1993)), providing a standardised value for comparing rates in different taxa at different geological times. Evolutionary rate is measured in haldanes (Gingerich 1983), calculated using the following:

$$((x_2 - x_1)/S_p)/g$$

where x_1 and x_2 represent mean character values in two samples of logged data, S_p represents the pooled standard deviation for the two samples, and g is the number of generations separating the two samples (Gingerich 1993). The haldane is necessarily simplistic, but offers a useful standard for comparison between different studies (although such comparisons should be conducted with caution, Hendry and Kinnison 1999). For the *Pterospathodus* analysis, conodont generation time is assumed to be one year. Sedimentation rates through the Viki core are assumed to be constant on average, which is reasonable based on the lithological uniformity and stratigraphic continuity of the succession suggested by the available evidence (Nestor 1997). LRI analysis is, however, robust to inaccuracies in generation time estimates and time equivalence of different stratigraphic levels (Gingerich and Gunnell 1995).

Rescaled range R/S analysis was conducted using Peter Noble's Hurst Exponent Calculator (<http://stahl.ce.washington.edu/nobleprograms.jsp>) and log rate-log interval (LRI) analysis was undertaken using Philip Gingerich's HALDANEX program. Extended eigenshape analysis was conducted using MacLeod's (1999) EES software. All other analyses were conducted in PAST Version 1.44 (Hammer et al. 2001), SPSS Version 14 and MINITAB Version 14. Graphs were produced in MINITAB Version 14 and Microsoft Excel.

Results and discussion

Testing taxonomic hypotheses

The boundary between *P. eopennatus* and *P. amorphognathoides* is straightforward to examine: it is marked by the appearance of adult elements with ≥ 20 denticles. Simple qualitative inspection of a stratophenetic plot of denticle number shows no obvious discontinuities at which a species boundary could be placed, either at the level where *P. amorphognathoides* is purported to appear (marked with an arrow on Figure 3), or elsewhere. Thus, whilst this taxonomic boundary may have biostratigraphic utility, its biological significance seems doubtful.

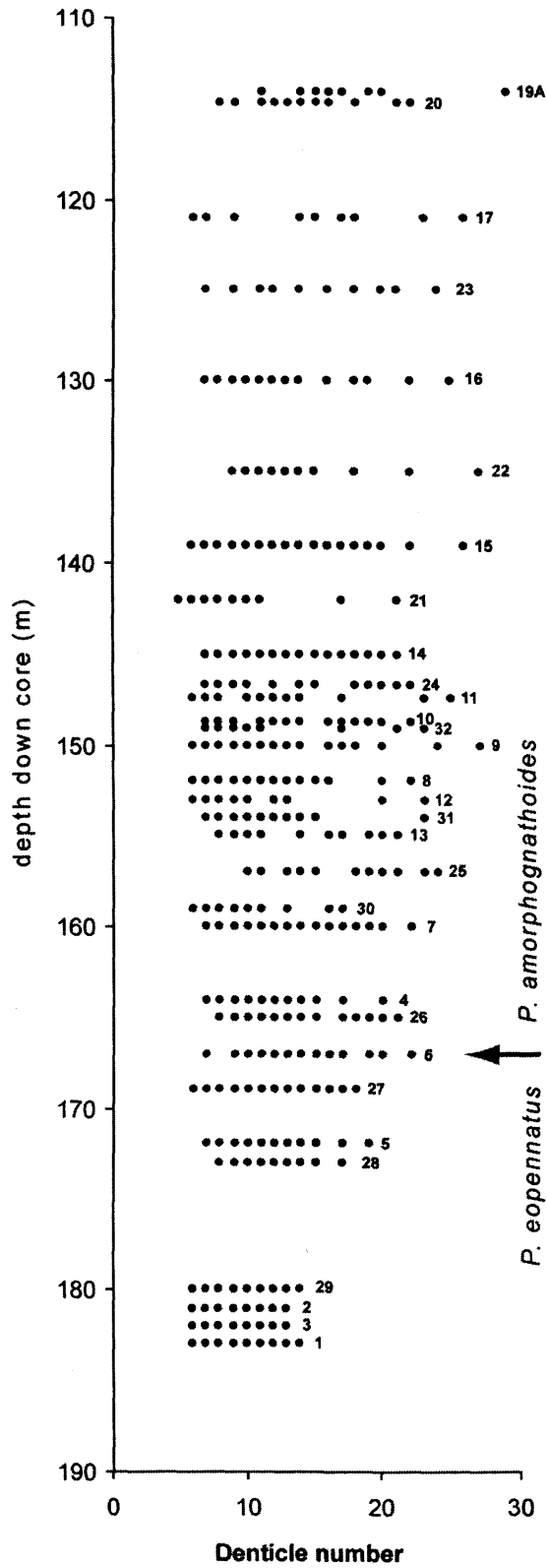


Figure 3: Stratophenetic plot of denticle number in *Pterospathodus* P₁ elements from the Viki core, Estonia. Purported boundary between *P. eopennatus* and *P. amorphognathoides* indicated by arrow. Numbers refer to samples in Table 1.

The character used to differentiate *P. a. lennarti* and *P. a. lithuanicus*, the distance between the first process denticle and the main denticle row (Männik 1998), cannot be measured or observed in elements with broken processes; such incomplete elements represent a large proportion of specimens, at least in the Viki core, so this limits the usefulness of this character. Moreover, quantitative testing offers little support for its discriminatory ability: Figure 4A shows that despite a slight tendency towards an increasing distance between the denticle row and the first denticle of the process with depth down the core, this is a gradational transition, not a sharp division. The histogram in Figure 4B shows the frequency distribution for this distance measure. If the two subspecies differed markedly, the distribution would be expected to show bimodality; however, the pattern more closely resembles a normal distribution. Hence, unless an arbitrary boundary is imposed, the distance between the denticle row and the first denticle of the process does not appear to be reliable diagnostic character for distinguishing *P. a. lennarti* and *P. a. lithuanicus*, and the biological reality of these taxa is suspect.

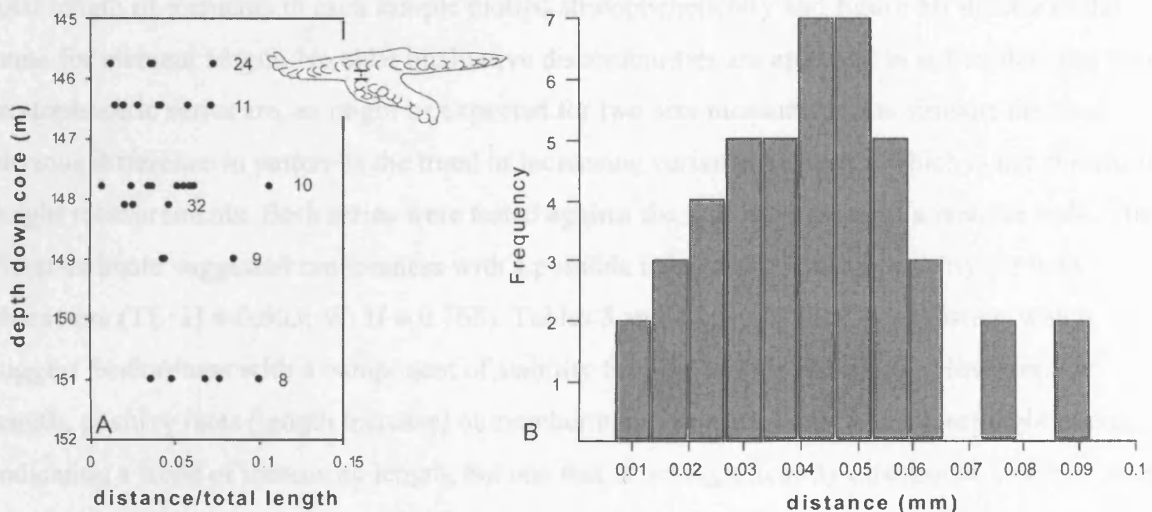


Figure 4: Results of analysis of *Pterospathodus* P₁ elements from 151.64 - 146.7 m (samples 8, 9, 32 10, 11, 24) depth in the Viki core, on which distance between main denticle row and first process denticle can be measured A) Plot of distance between main denticle row and first process denticle against total length (TL) and B) Histogram of distance between main denticle row and first process denticle. Histogram bin widths optimised using the Freedman and Diaconis equation, a method summarised in Izenman (1991).

Testing hypotheses of process asymmetry

Männik and Aldridge (1989) and Männik (1998) identify asymmetry in the anterolateral process of *Pterospathodus*: process development was greater in dextral than sinistral elements. The qualitative observation of asymmetry was tested quantitatively using both frequency and length of processes, and is supported by both characters. Within *P. eopennatus* samples, processes occur almost twice as frequently in dextral than in sinistral elements (dextral:sinistral ratio of 33 : 18) and dextral process length was significantly greater than sinistral (one-tailed t-test: $t = -5.464$, $p < 0.001$, $n = 36$; log-normalised data).

Testing evolutionary hypotheses

The apparent directional size increase within *Pterospathodus* was quantitatively tested through two variables: total element length and element height at highest point. Figure 5A shows total length of elements in each sample plotted stratophenetically and figure 5B illustrates the same for element height. No clear qualitative discontinuities are apparent in either plot. The two stratophenetic series are, as might be expected for two size measures, quite similar; the most obvious difference in pattern is the trend of increasing variance in length, which is not evident in height measurements. Both series were tested against the null hypothesis of a random walk. The Hurst estimate suggested randomness with a possible component of directionality for both characters (TL: $H \approx 0.603$; W: $H \approx 0.763$). Tables 3 and 4 provide the LRI statistics, which suggest randomness with a component of stability for both length and height. However, for length, positive rates (length increase) outnumber negative rates (length decrease) eight to one, indicating a trend of increasing length, but one that is not significantly directional. Intrinsic rates (evolutionary rates on a generational timescale, given by the y-intercept of the best fit line) are high for both variables: 0.07 and 0.23 haldanes respectively for length and height (see predicted rate in Tables 3 and 4). This paradoxically rapid evolution in the absence of a significantly directional trend represents a potential rate of evolutionary change over a single generation, extrapolated by the LRI analysis from rates measured over longer time-frames. These high rates are frequently not sustained over long periods to produce directional evolution, as here, because the extrinsic selective forces driving them do not persist for long periods (Gingerich and Gunnell 1995).

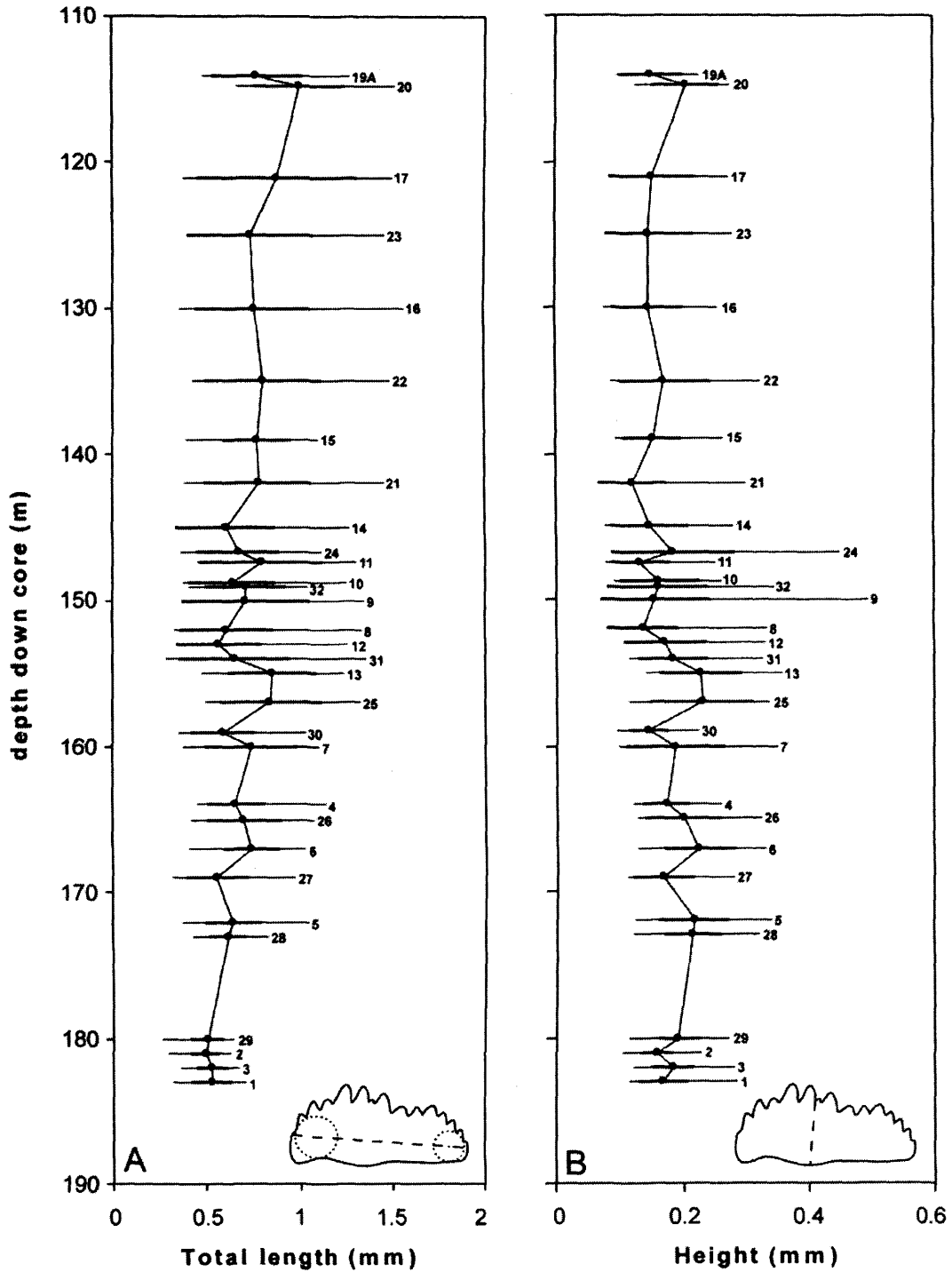


Figure 5: Stratophenetic sequences of A) total length and B) width of *Pterospathodus* P₁ elements within the Viki core, Estonia. Points represent mean values at each horizon, thin bars represent the range of values and thick bars represent the standard deviation of the values. Numbers refer to samples in Table 1. Measured variables are indicated by dashed lines on element diagrams. Dotted circles in A represent the anchored circles used to position the total length line.

			Min.	Median	Max.
Total rates	465	Log interval	2.239	3.984	4.609
Non-zero rates	465	Log rate	-5.307	-3.724	-2.738
Positive rates	207	Slope		-0.785	
Median log interval	4.039	CI	-0.622	-0.775	-0.916
Median log rate	-3.721	Intercept		-1.141	
Negative rates	24	CI	-1.819	-1.174	-0.743
Median log interval	3.438	Predicted rate (haldanes)		0.07	
Median log rate	-3.874	CI	0.02	0.06	0.18

Table 3: Statistics for LRI analysis of total length in *Pterospathodus* P₁ elements from the Viki core, Estonia.

			Min.	Median	Max.
Total rates	465	Log interval	2.239	4.029	4.609
Non-zero rates	465	Log rate	-7.633	-4.242	-2.611
Positive rates	319	Slope		-0.891	
Median log interval	4.080	CI	-0.786	-0.914	-1.039
Median log rate	-4.230	Intercept		-0.646	
Negative rates	146	CI	-1.111	-0.566	-0.102
Median log interval	3.895	Predicted rate (haldanes)		0.23	
Median log rate	-4.279	CI	0.0078	0.272	0.791

Table 4: Statistics for LRI analysis of width in *Pterospathodus* P₁ elements from the Viki core, Estonia.

The weakness of quantitative support for directional evolution in element length despite apparently clear qualitative observation to the contrary may be a consequence of including smaller, immature elements within the samples, because this will both fix the lower length limit at each level, and confuse ontogenetic variation with evolutionary change. In adult populations of *Pterospathodus*, mean or variance or both may be increasing through the Viki core. If variance alone is increasing, as has been observed in other organisms through time (Jablonski 1997), then the degree and pattern of any increase may be obscured as a consequence of including smaller specimens within the samples. If variance is constant and mean alone is increasing, this pattern would be entirely masked by the inclusion of immature elements. Without controlling for this ontogenetic variation, the true pattern and rate of size change cannot be properly quantified.

Unfortunately, excluding immature specimens is problematic in conodonts, since maturation age cannot at present be determined from element morphology. Jablonski (1997) used maximum size to counter the effect of ontogenetic variation, although this too is subject to

sampling bias. The largest elements at the top of the core are around 2.5 times the length of those near the base, so maximum length values were tested against a random walk. LRI analysis cannot be conducted on maximum values; however, the R/S analysis indicated a strongly directional pattern ($H \approx 0.994$). This provides strong statistical support for a clear qualitative trend of directional increase in the upper size bound of *Pterospathodus* P₁ elements, and provides a possible example of peramorphic heterochrony (where descendents develop characters beyond the stage present in the adults of their ancestors; Alberch et al. 1979, McNamara 1986).

Directional increase in *Pterospathodus* process development through the core was quantitatively tested using two variables: length of process (see Figure 6A) and frequency of process possession (see figure 6B). The stratophenetic series of process length was tested against a random walk. LRI analysis indicated no significant deviation from randomness; although there were more negative than positive rates (see Table 5). R/S analysis detected a significantly directional trend ($H \approx 0.88$). The frequency of process possession is measured as the percentage of elements possessing processes within each sample. Figure 6B plots this variable stratophenetically.

			Min.	Median	Max.
Total rates	435	Log interval	2.239	4.033	4.609
Non-zero rates	435	Log rate	-7.432	-4.203	-2.466
Positive rates	122	Slope		-0.629	
Median log interval	3.821	CI	-0.446	-0.616	-0.715
Median log rate	-4.425	Intercept		-1.608	
Negative rates	313	CI	-2.475	-1.670	-1.300
Median log interval	4.114	Predicted rate (haldanes)		0.025	
Median log rate	-4.163	CI	0.003	0.021	0.05

Table 5: Statistics for LRI analysis of anterolateral process length in *Pterospathodus* P₁ elements from the Viki core, Estonia.

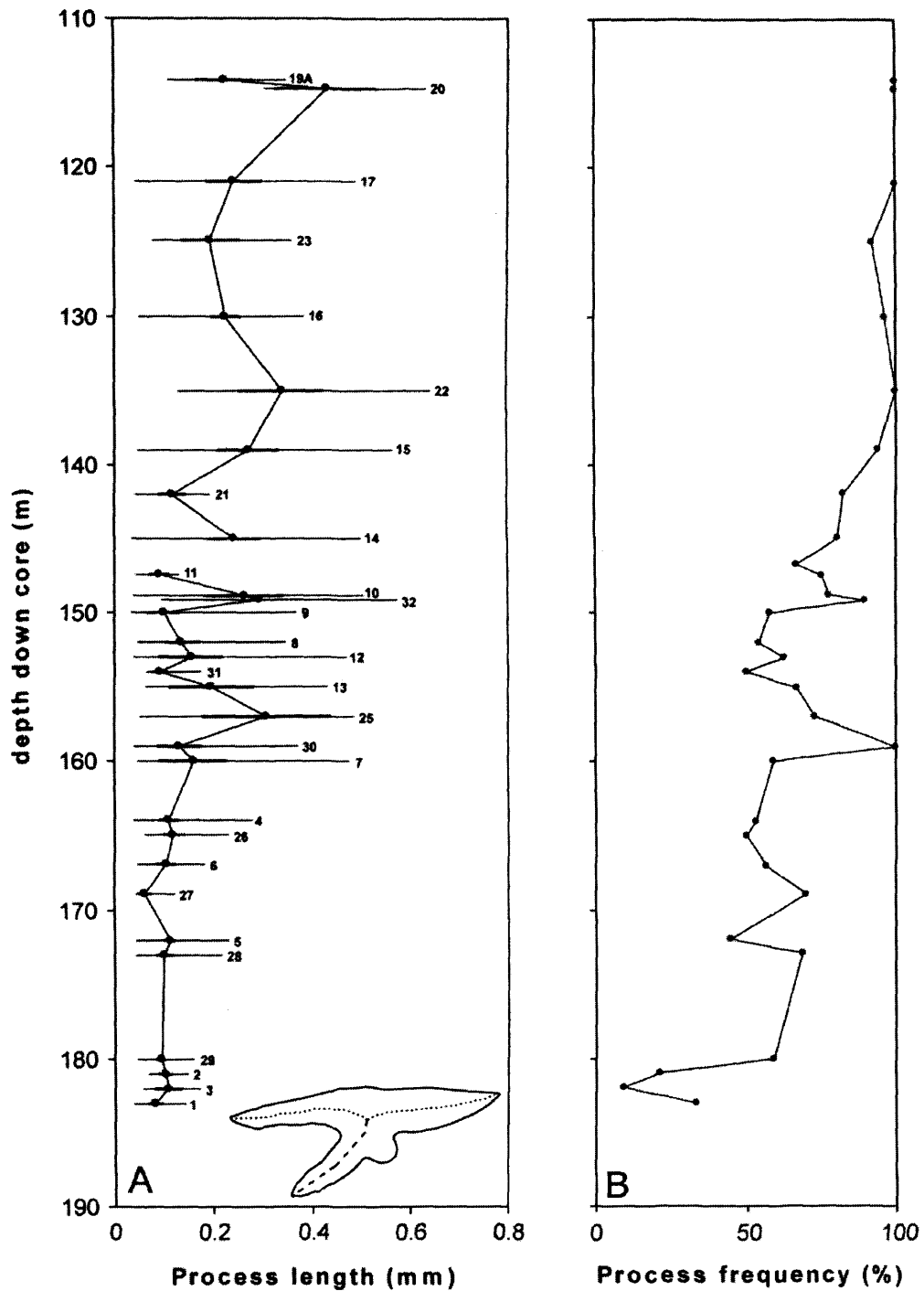


Figure 6: Stratophenetic sequences of A) process length and B) process frequency of *Pterospathodus* P₁ elements within the Viki core, Estonia. Points represent mean values at each horizon, thin bars represent the range of values, thick bars represent the standard deviation of the values. Numbers refer to samples in Table 1. Sample 24 (146.75 m) included no elements with complete processes for measurement. Elements where the presence of a process could not be ascertained were not included in the process frequency counts. Dashed line on element diagram represents measured variable, dotted lines indicate centre-line of distance map.

In pre-*Pterospathodus amorphognathoides amorphognathoides* elements (those below 145.55 m depth in the core, sample 14 in Figure 6), the frequency of process possession seems to increase, but with much fluctuation (see figure 6B). Artificial biases partially contribute to these fluctuations: some of the samples where n is low may not be representative and there is also a degree of subjectivity in deciding whether an element possesses a process. Frequently there is protuberance from the lateral surface of the element, and the point at which this is designated as a process is arbitrary; Männik (1998) refers to this feature variously as a lobe or a process. The onset of process development within pre-*P. a. amorphognathoides* elements also appears not to be strongly associated with a specific stage in ontogeny: specimens lacking a process are present at all size intervals up to around 1.3 mm, by which length all elements have processes. For example, elements 0.4-0.5 mm in length have the same chance of possessing a process as elements 0.5-0.6 mm in length. This plasticity disappears with the origin of *P. a. amorphognathoides*: process frequency within this subspecies increases steadily with little fluctuation up the core until essentially all elements within each sample possess processes, regardless of length. Since the lower size bound for *P. a. amorphognathoides* is similar at all horizons, process development appears to be beginning at progressively earlier stages in ontogeny through the evolutionary sequence, again suggesting possible peramorphosis. Analysis of growth curves based on larger samples at each level could test these potential heterochronic patterns.

When the process length and process frequency plots are considered together, it can be seen that the apparent discontinuity between 160 m and 163.8 m (between samples 7 and 4), where maximum process length almost doubles, occurs less than a metre below a large jump in process frequency at 159.2 m (sample 30). Although there is no sampling immediately below the process length increase, these morphological shifts may reflect a genuine evolutionary response within *Pterospathodus*; they may even offer a more objective taxonomic boundary. This section of the core should be specifically targeted with denser sampling to determine the precise depth at which this potentially significant morphological change occurs, and assess how gradual or abrupt it is.

Another qualitatively obvious pattern of morphological variation through time, not considered in detail in Männik (1998) and Männik and Aldridge's (1989) discussions of *Pterospathodus* evolution, is shape change in the lateral profile of the P_1 element. This apparent directional morphological trend was tested quantitatively first using traditional measures, and then using two outline analyses.

The length:width ratio of *Pterospathodus* P₁ elements was examined stratophenetically through the core (Figure 7). Qualitative observation suggests a directional trend, with elements becoming generally longer and thinner through time. Unfortunately, LRI analysis cannot meaningfully be conducted on ratio variables, since their artificially inflated variances will distort measures based on standard deviations such as the haldane. However, the R/S analysis on the length:width data produced a Hurst estimate of one, demonstrating that the lateral profile of *Pterospathodus* P₁ elements display directional morphological trend through time in the Viki core.

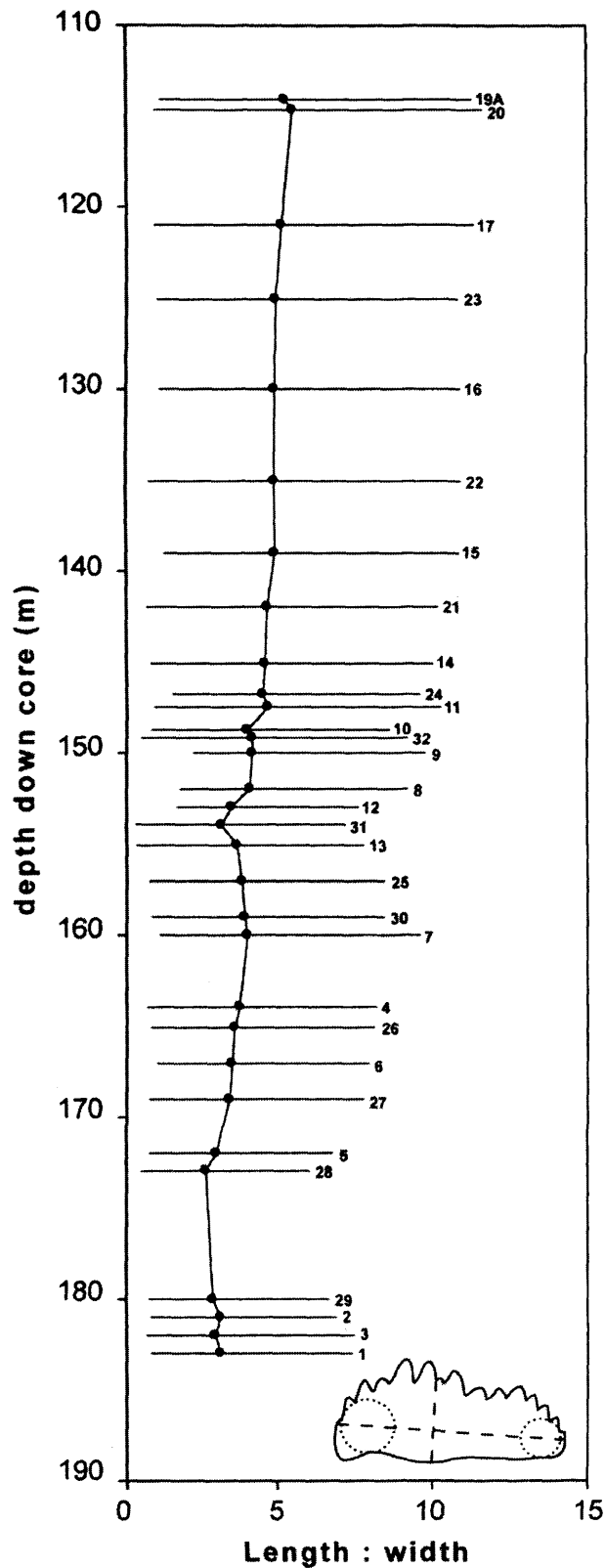


Figure 7: Stratophenetic plot of length:width ratio of *Pterospathodus* P₁ elements from the Viki core, Estonia. Points represent mean values at each horizon; thin bars represent the range of values. Numbers refer to samples in Table 1. Dashed lines on element diagram indicate the two measured variables used to calculate the length : width ratio; Dotted lines represent anchored circles used to position total length line (see Chapter one for methodology).

Outline analysis using extended eigenshape (EES) analysis (MacLeod 1999) and elliptic Fourier analysis (EFA: Ferson et al. 1985, Giardina and Kuhl 1977, Kuhl and Giardina 1982) was also undertaken to examine shape changes in the lateral profile of the P₁ elements more effectively than is possible using a simple length:width ratio. Elements must have a complete aboral margin to be included within the outline analyses, and time constraints prevented the inclusion of elements from every horizon; nevertheless, 325 specimens from 22 relatively evenly spaced horizons were sampled. Table 1 indicates which horizons in the core were sampled, and the sample sizes at each level. Sample sizes were small at some levels, necessitating the caveat that the complete range of variation may not be represented at these horizons. Inequality in sample size may also mask differences in variance between samples, so sample size at each horizon was kept as even as possible.

The results of the EES analysis are discussed first. Table 6 shows eigenvalues for the first three eigenshape vectors, and the percentage variance explained by each eigenshape, for the extended eigenshape (EES) analysis. Figure 8 plots stratophenetically the eigenscores for the first three EES axes for each sample. End-member elements, with extreme eigenscore values, are figured to aid visualisation and interpretation of the shape variation associated with each axis. The outlines are based on (x, y) coordinate pairs produced by transformation of the extended phi shape functions upon which the EES analysis is based, rounded to a set tolerance threshold (here 99%; the higher the threshold, the more details of the outline are captured). The elements represented by these outlines are also illustrated, to relate the shape variation to actual elements

EES	eigenvalue	% variance	cumulative % variance
1	648.762	98.552	98.552
2	1.285	0.195	98.747
3	0.828	0.126	98.873

Table 6: Eigenvalues, percentage of variance explained and cumulative percent variance explained for first three extended eigenshapes (EESs) for EES analysis of *Pterspathodus* P₁ elements from the Viki core, Estonia.

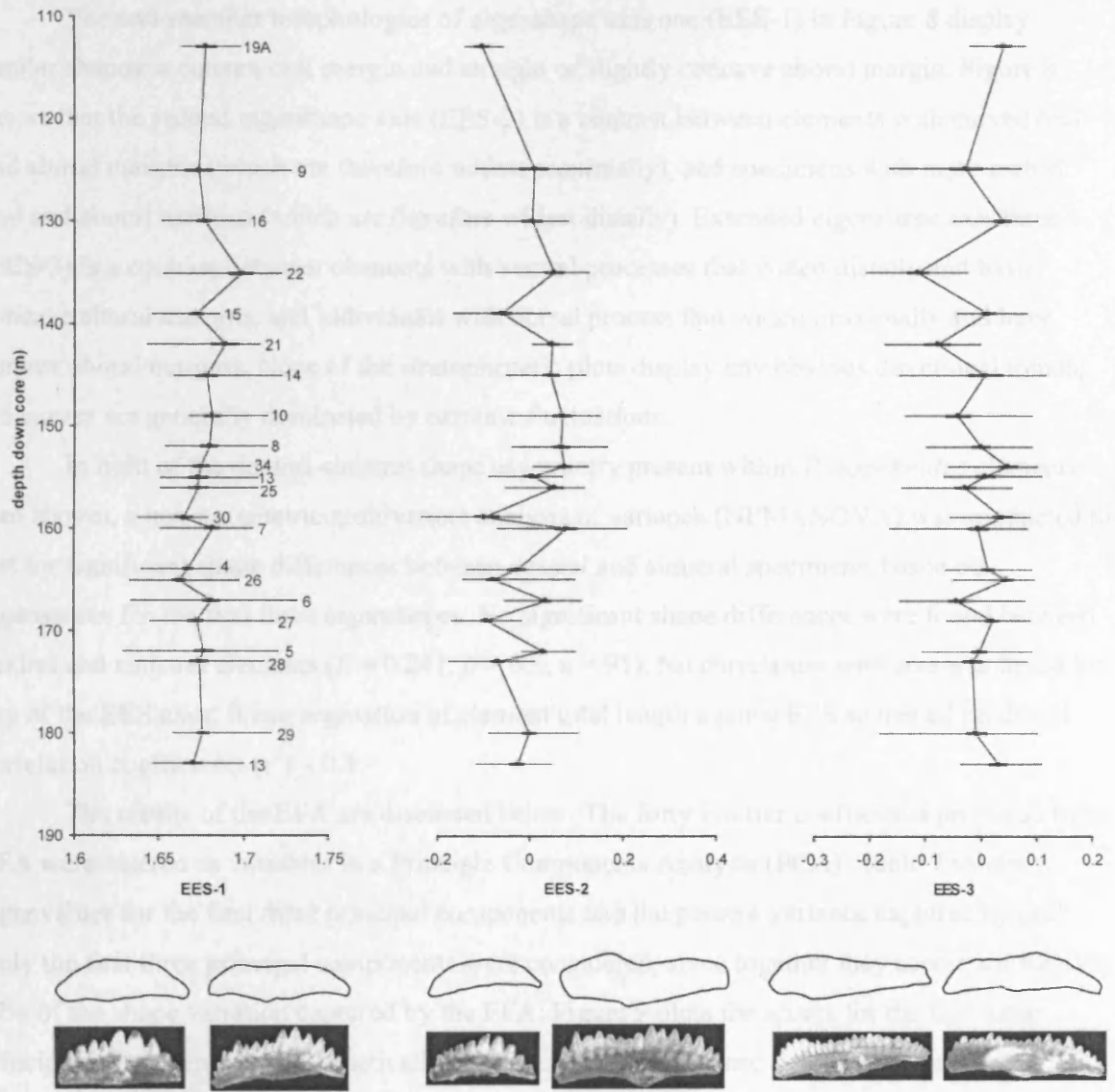


Figure 8: Stratophenetic plots of scores for the first three extended eigenshape (EES) axes for *Pterospathodus* P₁ elements from the Viki core, Estonia. Points represent mean value at each horizon, thick bars the standard error and thin bars the range of values. Numbers refer to samples in Table 1. End-member morphologies, representing elements with extreme eigenscore values, are illustrated by outlines and images of elements they represent.

The end-member morphologies of eigenshape axis one (EES-1) in Figure 8 display similar shapes: a convex oral margin and straight or slightly concave aboral margin. Figure 8 shows that the second eigenshape axis (EES-2) is a contrast between elements with curved oral and aboral margins (which are therefore widest proximally), and specimens with more arched oral and aboral margins (which are therefore widest distally). Extended eigenshape axis three (EES-3) is a contrast between elements with ventral processes that widen distally and have concave aboral margins, and individuals with dorsal process that widen proximally and have convex aboral margins. None of the stratophenetic plots display any obvious directional trends; the curves are generally dominated by extreme fluctuations.

In light of the dextral-sinistral shape asymmetry present within *P. eopennatus* elements (see above), a non-parametric multivariate analysis of variance (NPMANOVA) was conducted to test for significant shape differences between dextral and sinistral specimens, based on eigenscores for the first three eigenshapes. No significant shape differences were found between dextral and sinistral elements ($F = 0.241, p > 0.8, n = 91$). No correlation with size was found for any of the EES axes; linear regression of element total length against EES scores all produced correlation coefficients (r^2) $\ll 0.5$.

The results of the EFA are discussed below. The forty Fourier coefficients produced by an EFA were entered as variables in a Principle Components Analysis (PCA). Table 7 shows eigenvalues for the first three principal components and the percent variance captured by each. Only the first three principal components were considered, since together they accounted for over 87% of the shape variation captured by the EFA. Figure 9 plots the scores for the first three principle components stratophenetically. End-member elements are figured. Outlines were generated using the inverse Fourier function based on ten harmonics (the maximum number available in PAST; the more harmonics included, the greater the quantity of detail incorporated into the outline). The elements represented by these outlines are illustrated.

PC	eigenvalue	% variance	cumulative % variance
1	0.0041	58.412	58.412
2	0.0015	21.379	79.791
3	0.0005	7.6736	87.4646

Table 7: Eigenvalues, percentage of variance explained and cumulative percent variance explained for first three principle components (PCs) of PCA of Fourier coefficients for *Pterspathodus* P₁ elements from the Viki core, Estonia.

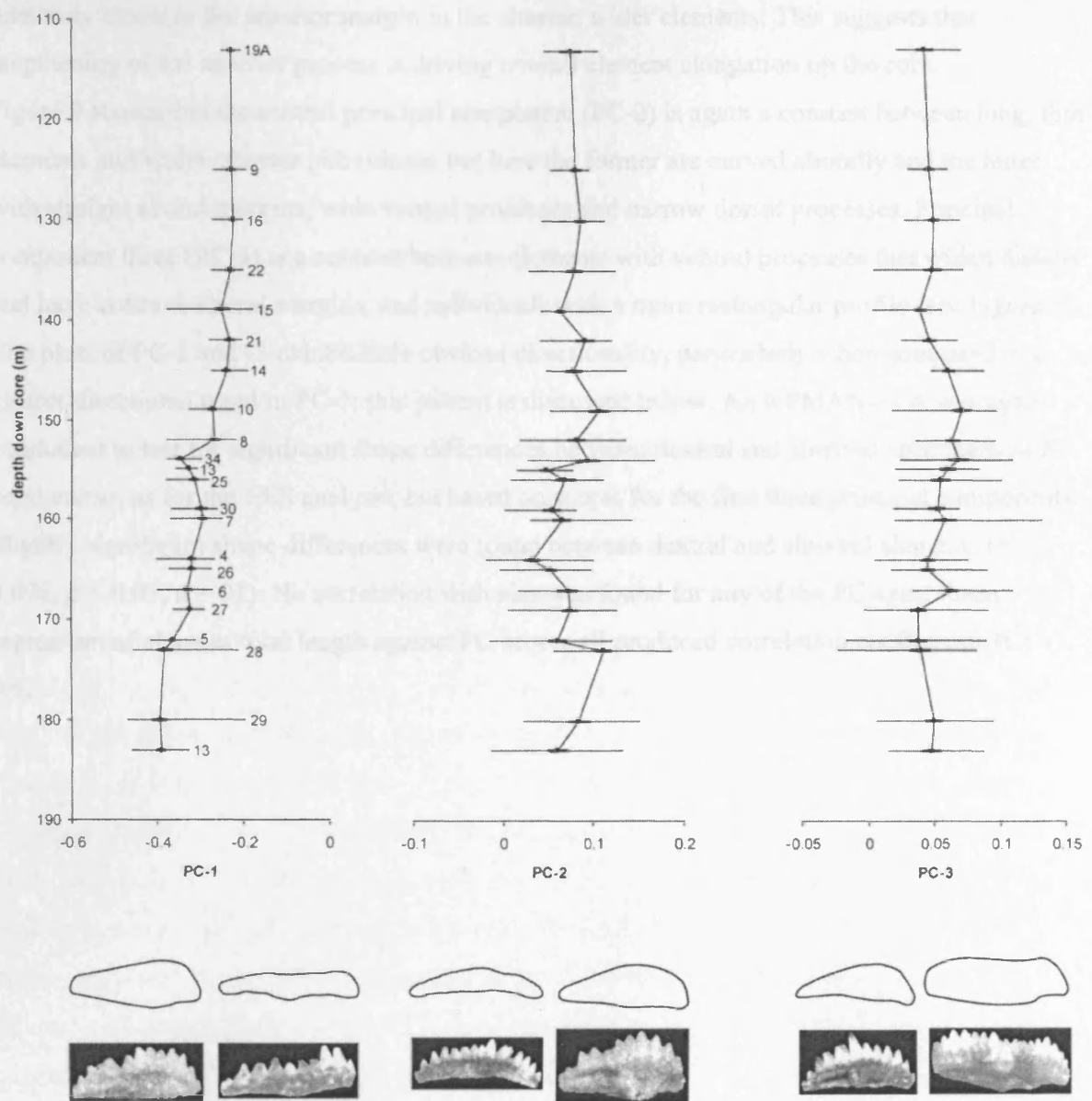


Figure 9: Stratophenetic plots based on principal component scores from a PCA of Fourier coefficients produced by an EFA of *Pterospathodus* P₁ elements from the Viki core, Estonia. Points represent mean values at each horizon, thick bars represent standard error and thin bars represent the range of values. Numbers refer to samples in Table 1. End-member morphologies, representing elements with extreme PC scores, are illustrated by outlines and images of elements they represent.

The end-member morphologies in Figure 9 show that principal component one (PC-1) is a contrast between short, wide elements and long, thin specimens. The change in mean values through the core closely mimics that in the length:width plot in Figure 7. The centre of the basal cavity (approximately indicated by the protuberance on the aboral margin) appears to be situated

relatively closer to the anterior margin in the shorter, wider elements. This suggests that lengthening of the anterior process is driving overall element elongation up the core.

Figure 9 shows that the second principal component (PC-2) is again a contrast between long, thin elements and wider, shorter individuals, but here the former are curved aborally and the latter with straight aboral margins, wide ventral processes and narrow dorsal processes. Principal component three (PC-3) is a contrast between elements with ventral processes that widen distally and have concave aboral margins, and individuals with a more rectangular profile (see Figure 9). The plots of PC-2 and -3 exhibit little obvious directionality, particularly when compared to a clearer directional trend in PC-1; this pattern is discussed below. An NPMANOVA was again conducted to test for significant shape differences between dextral and sinistral specimens of *P. eopennatus*, as for the EES analysis, but based on scores for the first three principal components. Slightly significant shape differences were found between dextral and sinistral elements ($F = 3.678, p < 0.05, n = 91$). No correlation with size was found for any of the PC axes; linear regression of element total length against PC scores all produced correlation coefficients (r^2) « 0.5.

Testing evolutionary rate hypotheses

Directional evolution within *Pterospathodus* has been variously described as rapid and gradual (Männik 1998, Männik and Aldridge 1989). Although directionality was difficult to demonstrate in the univariate stratophenetic series, the qualitative pattern in PC-1 does suggest strong directionality, and appears to be capturing a similar trend to that in the length:height series. It is therefore analysed to test the qualitative observations of rate above. Sample number for the outline analyses is too small to conduct an R/S analysis using the Hurst Calculator, so an LRI analysis was conducted on the PC-1 eigenscores. This confirmed the presence of a directional pattern (see Figure 10) and, for the first time, enabled quantification of evolutionary rates within a conodont taxon. Whilst rates of change in multivariate measurements may be difficult to reify, they have been successfully analysed previously (e.g. Losos et al. 1997) and there appear to be no theoretical reasons for not considering them (Hendry and Kinnison 1999).

Figure 10 provides results from the LRI analysis of PC-1 scores. The maximum likelihood line has a slope of -0.308, with bootstrapped 95% confidence intervals ranging from -0.066 to -0.404. In comparison, the predicted slope for a random pattern is -0.5, which falls outside these confidence limits. The expected slope for a directional trend is 0; these results therefore indicate strong directionality in the data, with a component of randomness. Negative rates of evolutionary change are over eight times as frequent as positive rates; since the PC scores become lower up the core, this indicates a general transition from short, wide morphologies to longer, narrower forms with time. The y-intercept value of the best-fit line corresponds to a generational evolutionary rate of $10^{-2.484}$, or 0.003, haldanes, with a 95% confidence interval ranging from 0.0002 to 0.007 haldanes. This, of course, assumes that conodont generation time is one year; were generation time longer, as may be the case in some populations of '*O.*' *excavata* (see Chapter 5), this would increase the evolutionary rate.

Published evolutionary rates vary widely (see Hendry and Kinnison 1999 for a review), but are generally lower in fossil lineages than in modern populations. The evolutionary rates for *Pterospathodus* do fall within the range recorded for fossil sequences (10^{-2} - 10^{-6} haldanes, Gingerich 2001), and slightly towards the upper bound, demonstrating that directional evolutionary change in element shape within *Pterospathodus* appears to be only marginally faster than that observed within other extinct organisms.

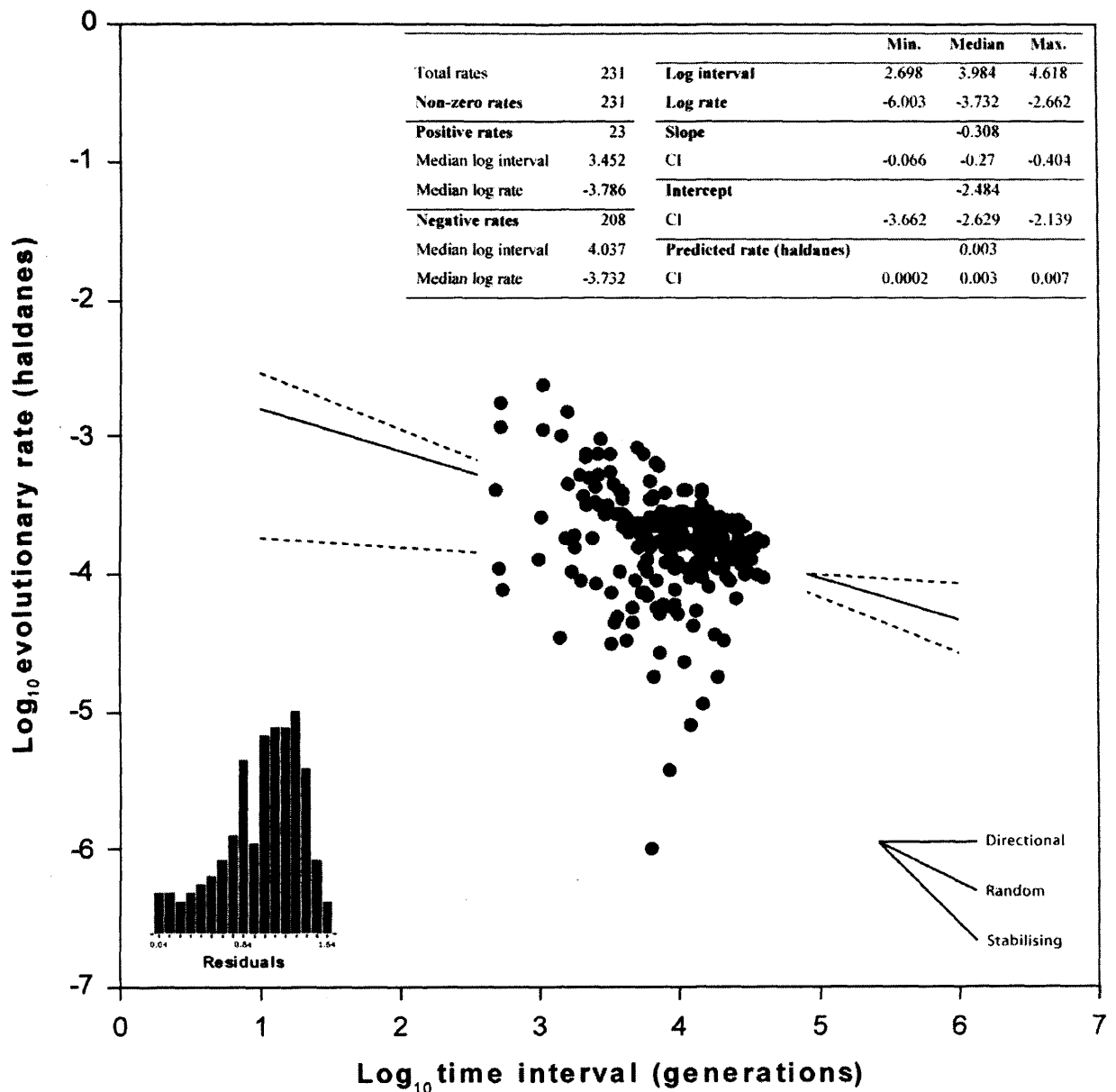


Figure 10: Log rate-log interval (LRI) plot of shape change in *Pterospathodus* P₁ elements from the Viki core, Estonia. Points represent rates of change in haldanes (standard deviations per generation) between each pairwise comparison of samples, for the time intervals (generations) between each pair. Solid line is maximum likelihood best-fit line. Dashed lines represent 95% confidence intervals for the slope, calculated from 100 bootstrap resamplings of log rates and corresponding log intervals. Expected slope of best-fit line under conditions of directional and stabilising selection, and from a random pattern, is illustrated at bottom right. Table provides rate and interval statistics derived from the LRI analysis. Bar chart shows residual deviations from the best-fit line.

Biological interpretations of evolutionary change in *Pterospathodus*

The palaeobiological interpretations of the morphological changes occurring within *Pterospathodus* have yet to be explored. Size increase within a lineage – the most obvious qualitative trend in *Pterospathodus* evolution – is commonly cited as a manifestation of Cope's Rule: the tendency of species within an evolving lineage to increase in body size through time (Cope 1896). Previous studies suggest that P₁ element length is a reliable surrogate for body length, because available data suggest a linear relationship between element size and body length (Donoghue and Purnell 1999a, Purnell 1994), with the caveat that the exact relationship between age and size is at present unknown. Unfortunately, the test results for directional element size increase were ambiguous. Whilst it remains possible that adult populations of *Pterospathodus* are increasing directionally in size through time, the increase in variance observed in the Estonian data, probably resulting from the inclusion of smaller, immature individuals, will obscure this trend if present. Thus, if these data cannot support directional evolutionary size increase in adult elements it cannot be definitively stated that evolution in *Pterospathodus* does conform to Cope's Rule.

Maximum element length has been shown to increase through time; so regardless of potential increases in body size, enlarging the elements alone should have functional implications in terms of food processing. Likewise, the plasticity of P₁ element morphology within *Pterospathodus*, including asymmetry and variations in process development, will have functional repercussions. Finally, the transition from short, wide elements to relatively longer, narrower individuals, possibly driven by increasing the relative length of the anterior process, should have functional significance because in conodont taxa for which function has been investigated rigorously, the anterior process of the P₁ element maintains occlusive precision (Donoghue and Purnell 1999b). Possession of larger elements would presumably enable larger food items to be processed; lengthening of the ventral process, coupled with increasing development of a ventrally directed lateral process, may have been necessary to maintain occlusion in the face of increasing stresses from processing larger foodstuffs. Detailed functional analyses are needed to test this hypothesis.

The morphological plasticity of *Pterospathodus* elements, regardless of whether it reflects ecophenotypic, epigenetic or genetic variation, seems difficult to reconcile with the strong functionality of elements: structures associated with food processing are expected to be highly constrained morphologically (e.g., Evans and Sanson 2003) yet even gross morphological

features such as process development in actuality appear remarkably flexible, apparently displaying few systematic patterns. The precise functional significance of changes in process development and the directional change from short, wide elements to longer, thinner elements, in terms of food processing are currently unknown, and require investigation using additional, independent approaches.

The morphological changes observed within the Estonian sequence of *Pterospathodus* appear to be repeated globally (Männik and Aldridge 1989), presumably in response to world-wide environmental perturbations. *Pterospathodus* appears slightly above the base of the Telychian (P. Männik, pers comm. 2005) and persisted through the Snipklint Primo episode (Jeppsson 1997), a global environmental state characterised by low sea levels, cool oceanic bottom waters upwelling to supporting diverse and prolific planktonic communities, and the organisms dependent upon them (Aldridge et al. 1993, Wenzel and Joachimski 1996). Oceanic conditions were not globally uniform however, to which, for example, the variations in eustatic sea level can attest (Zhang and Barnes 2002). *Pterospathodus* populations underwent comparable and essentially simultaneous morphological changes despite occupying differing environments and, presumably, being exposed to contrasting local selection pressures. A large degree of genetic coherence between populations must have been maintained to counter these conflicting selection pressures. Although there is little research on dispersal patterns even in the modern oceans, animals with effective dispersal abilities exhibit the most genetic continuity between populations (Knowlton 1993, Lazarus 1983), which strongly suggests that *Pterospathodus* species were efficient swimmers.

Conclusions

A series of qualitative hypotheses of evolution and taxonomy within P_1 elements of the Silurian ozarkodinid conodont *Pterospathodus*, as outlined in (Männik 1998, Männik and Aldridge 1989), have been tested quantitatively using a suite of new standardised morphometric protocols, applied to material from the Viki core, Estonia.

Unfortunately, many taxonomic hypotheses could not be tested quantitatively, because of the ambiguity of the characters defining some of the subspecies within *Pterospathodus*. However, little support was found for those taxonomic boundaries that could be tested. No discontinuity was evident in the stratophenetic plot of denticle number, even at the point of appearance of *P. amorphognathoides* with 20 or more denticles. Indeed, with the possible exception of a process

length, none of the stratophenetic plots displayed any abrupt changes at which a taxonomic boundary could be placed which, whilst supporting the hypothesis of *Pterospathodus* as an anagenetic continuum, suggest any taxa or morphs diagnosed by these variables will necessarily be arbitrary constructs, with no biological reality. Morphometric analysis of the character marking the transition from *Pterospathodus amorphognathoides lennarti* to *P. a. lithuanicus*, distance between the first process denticle and main denticle row, similarly suggests that the biological reality of these taxa is uncertain.

Hypotheses of directional evolutionary change in *Pterospathodus* were tested through analysis of stratophenetic series. R/S analysis detected a slight directional trend in P₁ element length and height. The ambiguity probably results from including smaller, immature elements within the analysis. Strong directional trends were statistically confirmed in maximum P₁ length and anterolateral process length. A gradual increase in frequency of process possession was also evident in the stratophenetic plot of this variable; this culminated in *P. a. amorphognathoides* where all elements in each sample had processes. This may represent an example of peramorphorphic heterochrony within *Pterospathodus*.

Directional shape change in the lateral profile of *Pterospathodus* P₁ elements, involving a transition from short, wide elements near the base of the core, to longer, narrower forms near the top, has been captured by elliptic Fourier analysis. Evolutionary rates in *Pterospathodus* have been quantified for the first time in a conodont taxon: LRI analysis demonstrated that P₁ element shape changes at a rate of 0.003 haldanes, slightly closer to the upper range of rates recorded in other fossil organisms. Once evolutionary rates are quantified in other conodonts, useful comparisons can be made, providing an indication of how fast different taxa can respond evolutionarily to environmental change.

The precise functional significance of the evolutionary changes in element size, process development and the directional shift from short, wide elements to longer, thinner elements, in terms of food processing are currently unknown; this represents a fruitful line for future investigation, using additional, independent approaches. This study has clearly demonstrated the efficacy of the morphometric protocols outlined in Chapter one and Jones and Purnell (in press) in characterising conodont element morphology. Wide, across-taxon application of these protocols would enable us to fully exploit the potential of the conodont fossil record as an invaluable resource for understanding the evolutionary process on a broad scale.

Conclusions

The results presented in this work have clearly demonstrated the efficacy of new, standardised morphometric protocols, which were outlined in chapter one, in capturing patterns of morphological variation within the conodont skeleton.

The protocols have formed the basis of a methodology that has enabled identification of homology in discrete element collections of '*Ozarkodina excavata*' based upon morphology alone, which holds promise of broad application to other conodont taxa where morphologically similar elements occupy different positions within the skeleton; for example in prioniodinids (Purnell 1993b). The ability of the methodology to determine quantitatively which variables discriminate between morphologically similar elements also has utility in taxonomy.

The hypothesis that the conodont taxon '*Ozarkodina excavata*' is monospecific has been tested using multivariate morphometrics and outline analysis. Significant morphological discontinuities have been revealed between '*O.*' *excavata* populations, including the topotype material of '*O.*' *excavata*. Biological and spatiotemporal interpretation of the morphological discontinuities indicates that there may be multiple species present in the '*O.*' *excavata* hypodigm. The ability of the morphometric protocols to repeatedly and objectively recognise discrete, temporally separated morphological clusters may allow more widespread use of '*O.*' *excavata* in refining Silurian biostratigraphy.

Comparison of size frequency distributions of '*O.*' *excavata* P elements with extant populations of animals has found strong support for the hypothesis, based on taphonomic evidence (von Bitter and Purnell 2005), that the Eramosa Lagerstätte preserves a single biological population of '*O.*' *excavata*. This has allowed testing of hypotheses of apparatus shedding and growth with a greater degree of biological rigour than in previous work. It has also elucidated population biology within '*O.*' *excavata* at a level of detail rarely possible in conodont studies.

Qualitative hypotheses of evolution and taxonomy within P₁ elements of the conodont *Pterospathodus*, as outlined in Männik (1998) and Männik and Aldridge (1989) were also tested using the new protocols. Little support was found for the presence of any taxonomic boundary based on quantitative variables, which all showed continuous variation through the core. Some of the hypothesised directional trends in element and process length were statistically confirmed. Possible examples of heterochrony were identified, which require further analysis. Evolutionary rates have been quantified for the first time in conodonts.

Finally, the analyses have also highlighted, particularly in chapters two and six, how morphologically flexible conodont elements could be: from variation in the degree of P

element differentiation within apparatuses of a single population, to plasticity in the development of major structural features such as processes. The precise functional significance of these morphological changes in terms of food processing are currently unknown; this represents an important and exciting area for future research into developmental plasticity, specialisation and functionality within the earliest vertebrate feeding structures, and holds the key to understanding the relationship between evolutionary pattern and process within conodonts.

References

- Alberch, P., S. J. Gould, G. F. Oster, and D. B. Wake. 1979. Size and Shape in Ontogeny and Phylogeny. *Paleobiology* 5:296-317.
- Aldridge, R. J., D. E. G. Briggs, M. P. Smith, E. N. K. Clarkson, and N. D. L. Clark. 1993a. The anatomy of conodonts. *Philosophical Transactions of the Royal Society, London, Series B* 340:405-421.
- Aldridge, R. J., L. Jeppsson, and K. J. Dorning. 1993b. Early Silurian oceanic episodes and events. *Geology* 150:501-513.
- Aldridge, R. J., and J. E. Mabillard. 1985. Microfossil distribution across the base of the Wenlock Series in the type area. *Palaeontology* 28:89-100.
- Aldridge, R. J., and M. A. Purnell. 1996. The conodont controversies. *Trends in Ecology & Evolution* 11:463-468.
- Aldridge, R. J., D. J. Siveter, D. J. Siveter, P. D. Lane, D. Palmer, and N. H. Woodcock, eds. 2000. *British Silurian Stratigraphy (Geological Conservation Review Series)*. Joint Nature Conservation Committee.
- Anderson, M. J. 2001. A new method for non-parametric multivariate analysis of variance. *Austral Ecology* 26:32-46.
- Armstrong, H. A. 2005. Modes of growth in the euconodont oral skeleton: implications for bias and completeness in the fossil record. Pp. 27-38. *In* M. A. Purnell, and P. C. J. Donoghue, eds. *Conodont Biology and Phylogeny: interpreting the fossil record*. Palaeontological Association, London.
- Barnes, C. R., D. J. Kennedy, A. D. McCracken, G. S. Nowland, and G. A. Tarrant. 1979. Structure and evolution of Ordovician conodont apparatuses. *Lethaia* 12:125-151.
- Barnett, S. G. 1970. A new stage for orientating microfossils. *Journal of Paleontology* 44:1133-1144.
- Barnett, S. G. 1971. Biometric determination of the evolution of *Spathognathodus remischeidensis*: a method for precise intrabasinal time correlations in the Northern Appalachians. *Journal of Paleontology* 45:274-300.
- Barnett, S. G. 1972. The evolution of *Spathognathodus remischeidensis* in New York, New Jersey, Nevada, and Czechoslovakia. *Journal of Paleontology* 46:900-917.
- Bassett, M. G., D. Kaljo, and L. Teller. 1989. The Baltic Region. Pp. 158-170. *In* C. H. Holland, and M. G. Bassett, eds. *A global standard for the Silurian System*. National Museum of Wales Geological Series No.10, Cardiff.
- Baum, D. A. 1998. Individuality and existence of species through time. *Systematic Biology* 47:641-653.

- Bell, A. S., C. Sommerville, and D. I. Gibson. 2002. Multivariate analyses of morphometrical features from *Apatemon gracilis* (Rudolphi, 1819) Szidat, 1928 and *A. annuligerum* (v. Nordmann, 1832) (Digenea : Strigeidae) metacercariae. *Systematic Parasitology* 51:121-133.
- Bengtson, P. 1988. Open Nomenclature. *Palaeontology* 31:223-227.
- Bengtson, S. 2000. Teasing fossils out of shales with cameras and computers. *Palaeontologia Electronica* 3:article 4.
- Benton, M. J., and P. N. Pearson. 2001. Speciation in the fossil record. *Trends in Ecology & Evolution* 16:405-411.
- Blum, H. 1973. Biological shape and visual science (Part 1). *Journal of Theoretical Biology* 38:205-287.
- Bookstein, F. L. 1987. Random-walk and the existence of evolutionary rates. *Paleobiology* 13:446-464.
- Bookstein, F. L. 1991. *Morphometric Tools for Landmark Data: Geometry and Biology*. Cambridge University Press, Cambridge.
- Bookstein, F. L., R. E. Strauss, J. M. Humphries, B. Chernoff, R. L. Elder, and G. R. Smith. 1982. A comment upon the uses of Fourier methods in systematics. *Systematic Zoology* 31:85-92.
- Boucot, A. J. 1958. Age of the Bainbridge Limestone. *Journal of Paleontology* 32:1029-1030.
- Branson, E. B., and M. G. Mehl. 1933. Conodonts from the Bainbridge (Silurian) of Missouri. *University of Missouri Studies* 8:39-53.
- Bush, A. M., M. G. Powell, W. S. Arnold, T. M. Bert, and G. M. Daley. 2002. Time-averaging, evolution, and morphologic variation. *Paleobiology* 28:9-25.
- Calner, M., and L. Jeppsson. 2003. Carbonate platform evolution and conodont stratigraphy during the middle Silurian Mulde Event, Gotland, Sweden. *Geological Magazine* 140:173-203.
- Cocks, L. R. M. 2000. The Early Palaeozoic geography of Europe. *Journal of the Geological Society* 157:1-10.
- Cocks, L. R. M., W. S. McKerrow, and C. R. vanStaal. 1997. The margins of Avalonia. *Geological Magazine* 134:627-636.
- Cocks, L. R. M., and T. H. Torsvik. 2002. Earth geography from 500 to 400 million years ago: a faunal and palaeomagnetic review. *Journal of the Geological Society* 159:631-644.
- Cooper, B. J. 1975. Multielement conodonts from the Brassfield Limestone (Silurian) of southern Ohio. *Journal of Paleontology* 49:984-1008.

- Cooper, B. J. 1976. Multi-element conodonts from the St-Clair Limestone, Silurian of southern Illinois, USA. *Journal of Paleontology* 50:205-217.
- Cooper, C. L. 1935. Ammonium chloride sublimate apparatus. *Journal of Paleontology* 9:357-359.
- Cope, E. D. 1896. *The primary factors of organic evolution*. Open Court Publishing Company, Chicago.
- Craig, G. Y., and A. Hallam. 1963. Size-frequency and growth-ring analysis of *Mytilus edulis* and *Cardium edule*, and their palaeoecological significance. *Palaeontology* 6:731-750.
- Crampton, J. S. 1995. Elliptic Fourier shape-analysis of fossil bivalves - some practical considerations. *Lethaia* 28:179-186.
- Croll, V. M., and R. J. Aldridge. 1982. Computer applications in conodont taxonomy: classificatory methods. *Miscellaneous Paper - Geological Society of London* 14:247-261.
- Croll, V. M., R. J. Aldridge, and P. K. Harvey. 1982. Computer applications in conodont taxonomy: characterisation of blade elements. *Miscellaneous Paper - Geological Society of London* 14:237-246.
- Dayan, T., and D. Simberloff. 2005. Ecological and community-wide character displacement: the next generation. *Ecology Letters* 8:875-894.
- Deevey, E. S. 1947. Life tables for natural populations. *Quarterly Review of Biology* 22:187-220.
- Donoghue, P. C. J. 1998. Growth and patterning in the conodont skeleton. *Philosophical Transactions of The Royal Society of London, Series B* 353:633-666.
- Donoghue, P. C. J., P. L. Forey, and R. J. Aldridge. 2000. Conodont affinity and chordate phylogeny. *Biological Reviews* 75:191-251.
- Donoghue, P. C. J., and M. A. Purnell. 1999a. Growth, function, and the conodont fossil record. *Geology* 27:251-254.
- Donoghue, P. C. J., and M. A. Purnell. 1999b. Mammal-like occlusion in conodonts. *Paleobiology* 25:58-74.
- Donoghue, P. C. J., M. A. Purnell, and R. J. Aldridge. 1998. Conodont anatomy, chordate phylogeny and vertebrate classification. *Lethaia* 31:211-219.
- Donoghue, P. C. J., M. A. Purnell, R. J. Aldridge, and S. Zhang. in review. The interrelationships of complex conodonts (Vertebrata). *Systematic Palaeontology*.
- Erikson, G. M., P. J. Currie, B. D. Inouye, and A. A. Winn. 2006. Tyrannosaur life tables: an example of nonavian dinosaur population biology. *Science* 313:213-217.

- Evans, A. R., and G. D. Sanson. 2003. The tooth of perfection: functional and spatial constraints on mammalian tooth shape. *Biological Journal of the Linnean Society* 78:173-191.
- Ferson, S., F. J. Rohlf, and R. K. Koehn. 1985. Measuring shape variation of two-dimensional outlines. *Systematic Zoology* 34:59-68.
- Foote, M. 1989. Perimeter-based Fourier analysis: a new morphometric method applied to the trilobite cranidium. *Journal of Paleontology* 63:880-885.
- Foote, M., and J. J. Sepkoski. 1999. Absolute measures of the completeness of the fossil record. *Nature* 398:415-417.
- Giardina, C. R., and F. P. Kuhl. 1977. Accuracy of curve approximation by harmonically related vectors with elliptical loci. *Computer Graphics and Image Processing* 6:277-285.
- Gilinsky, N. L., and J. B. Bennington. 1994. Estimating numbers of whole individuals from collections of body parts; a taphonomic limitation of the paleontological record. *Paleobiology* 20:245-258.
- Gingerich, P. D. 1974. Size variability of teeth in living mammals and diagnosis of closely related sympatric species. *Journal of Paleontology* 48:895-902.
- Gingerich, P. D. 1983. Rates of evolution: effects of time and temporal scaling. *Science* 222:159-161.
- Gingerich, P. D. 1993. Quantification and comparison of evolutionary rates. *American Journal of Science* 293-A:453-478.
- Gingerich, P. D. 2001. Rates of evolution on the time scale of the evolutionary process. *Genetica* 112:127-144.
- Gingerich, P. D., and G. F. Gunnell. 1995. Rates of Evolution in Paleocene-Eocene Mammals of the Clarks-Fork Basin, Wyoming, and a Comparison with Neogene Siwalik Lineages of Pakistan. *Palaeogeography Palaeoclimatology Palaeoecology* 115:227-247.
- Girard, C., S. Renaud, and D. Korn. 2004a. Step-wise morphological trends in fluctuating environments: evidence in the Late Devonian conodont genus *Palmatolepis*. *Geobios* 37:404-415.
- Girard, C., S. Renaud, and A. Sérayet. 2004b. Morphological variation of *Palmatolepis* Devonian conodont: species versus genera. *Comptes Rendus Palevol* 3:1-8.
- Gradstein, F. M., J. G. Ogg, A. G. Smith, W. Bleeker, and L. J. Lourens. 2004. A new Geologic Time Scale, with special reference to Precambrian and Neogene. *Episodes* 27:83-100.

- Hammer, Ø., D. A. T. Harper, and P. D. Ryan. 2001. PAST: paleontological statistics software package for education and data analysis. *Palaeontologia Electronica* 4:Article 4.
- Hawkins, J. A., C. E. Hughes, and R. W. Scotland. 1997. Primary homology assessment, characters and character states. *Cladistics* 13:275-283.
- Hendry, A. P., and M. T. Kinnison. 1999. Perspective: The pace of modern life: Measuring rates of contemporary microevolution. *Evolution* 53:1637-1653.
- Higgins, A. C., and R. L. Austin, eds. 1985. A stratigraphical index of conodonts. Ellis Horwood Limited, Chichester.
- Hunt, G. 2004a. Phenotypic variance inflation in fossil samples: an empirical assessment. *Paleobiology* 30:487-506.
- Hunt, G. 2004b. Phenotypic variation in fossil samples: modeling the consequences of time-averaging. *Paleobiology* 30:426-443.
- Hurst, H. E. 1951. Long-term storage capacity of reservoirs. *Transactions of the Society of Civil Engineers* 116:770-808.
- Huxley, J. S. 1924. Constant differential growth-rates and their significance. *Nature* 114:895-896.
- Izenman, A. J. 1991. Recent developments in nonparametric density estimation. *Journal of the American Statistical Association* 86:205-224.
- Jablonski, D. 1997. Body-size evolution in Cretaceous molluscs and the status of Cope's rule. *Nature* 385:250-252.
- Jeppsson, L. 1969. Notes on some Upper Silurian multielement conodonts. *Geologiska Föreningens I Stockholm Förhandlingar* 91:12-24.
- Jeppsson, L. 1974. Aspects of Late Silurian conodonts. *Fossils and Strata* 6:1-54.
- Jeppsson, L. 1976. Autecology of Late Silurian conodonts. Pp. 105-118. *In* C. R. Barnes, ed. *Conodont Paleoecology*, Geological Association of Canada Special Paper 15.
- Jeppsson, L. 1990. An oceanic model for lithological and faunal changes tested on the Silurian record. *Journal of the Geological Society* 147:663-674.
- Jeppsson, L. 1997. A new latest Telychian, Sheinwoodian and Early Homeric (Early Silurian) Standard Conodont Zonation. *Transactions of the Royal Society of Edinburgh* 88:91-114.
- Jeppsson, L., and R. J. Aldridge. 2000. Ludlow (late Silurian) oceanic episodes and events. *Journal of the Geological Society* 157:1137-1148.
- Jeppsson, L., M. E. Eriksson, and M. Calner. 2006. A latest Llandovery to latest Ludlow high-resolution biostratigraphy based on the Silurian of Gotland - a summary. *GFF* 128:109-114.

- Jeppsson, L., D. Fredholm, and B. O. Mattiasson. 1985. Acetic acid and phosphatic fossils; a warning. *Journal of Paleontology* 59:952-956.
- Jerram, D. A., and M. J. Cheadle. 2000. On the cluster analysis of grains and crystals in rocks. *American Mineralogist* 85:47-67.
- Johnson, R. A., and D. W. Wichern. 2002. Applied multivariate statistical analysis. Prentice-Hall Inc, Upper Saddle River.
- Jones, D., and M. Purnell. in press. A new semi-automated morphometric protocol for conodonts and a preliminary taxonomic application. In N. MacLeod, ed. Automated Object Identification in Systematics, Systematic Association Special Volume.
- Klapper, G. 1985. Sequence in conodont genus *Ancyrodella* in lower *asymmetricus* Zone (earliest Frasnian, Upper Devonian) of the Montagne Noire, France. *Palaeontographica. Abteilung A: Palaeozoologie-Stratigraphie* 188:19-34.
- Klapper, G., and C. T. Foster. 1986. Quantification of outlines in Frasnian (Upper Devonian) platform conodonts. *Canadian Journal of Earth Sciences* 23:1214-1222.
- Klapper, G., and C. T. Foster. 1993. The Paleontological Society Memoir 32: Shape analysis of Frasnian species of the Devonian conodont genus *Palmatolepis*. Supplement to *Journal of Paleontology* 67:1-35.
- Knowlton, N. 1993. Sibling species in the sea. *Annual Review of Ecology and Systematics* 24:189-216.
- Kuhl, F. P., and C. R. Giardina. 1982. Elliptic Fourier features of a closed contour. *Computer Graphics and Image Processing* 18:236-258.
- Kurtén, B. 1964. Population Structure in Paleoecology. Pp. 91-106. In J. Imbrie, and N. Newell, eds. *Approaches to Paleoecology*. John Wiley and Sons, Ltd, New York.
- Lambert, L. L. 1994. Morphometric confirmation of the *Mesogondolella idahoensis* to *M. nankingensis* transition. *Permophiles* 24:28-35.
- Laufeld, S. 1974a. Reference localities for palaeontology and geology in the Silurian of Gotland. *Sveriges Geologiska Undersökning, Ser. C* 750:1-172.
- Laufeld, S. 1974b. Silurian Chitinozoa from Gotland. *Fossils and Strata* 5:1-130.
- Lazarus, D. 1983. Speciation in pelagic protista and its study in the planktonic microfossil record: A review. *Paleobiology* 9:327-340.
- Lohmann, G. P. 1983. Eigenshape analysis of micro-fossils - a general morphometric procedure for describing changes in shape. *Journal of the International Association for Mathematical Geology* 15:659-672.
- Lohmann, G. P., and P. N. Schweitzer. 1990. On eigenshape analysis. Pp. 145-166. In F. J. Rohlf, and F. L. Bookstein, eds. *Michigan Morphometric Workshop*. The University of Michigan Museum of Geology, The University of Michigan, Ann Arbor, Michigan.

- Losos, J. B., K. I. Warheit, and T. W. Schoener. 1997. Adaptive differentiation following experimental island colonization in *Anolis* lizards. *Nature* 387:70-74.
- Loydell, D. K., D. Kaljo, and P. Mannik. 1998. Integrated biostratigraphy of the lower Silurian of the Ohesaare core, Saaremaa, Estonia. *Geological Magazine* 135:769-783.
- MacLeod, N. 1999. Generalizing and extending the eigenshape method of shape visualization and analysis. *Paleobiology* 25:107-138.
- MacLeod, N. 2002. Geometric morphometrics and geological form - classification systems. *Earth Science Reviews* 59:27-47.
- MacLeod, N., and T. R. Carr. 1987. Morphometrics and the analysis of shape in conodonts. Pp. 168-187. *In* R. L. Austin, ed. *Conodonts: investigative techniques and applications*. Ellis Horwood Limited, Chichester.
- Männik, P. 1998. Evolution and taxonomy of the Silurian conodont *Pterospirifer*. *Palaeontology* 41:1001-1050.
- Männik, P., and R. J. Aldridge. 1989. Evolution, taxonomy and relationships of the Silurian conodont *Pterospirifer*. *Palaeontology* 32:893-906.
- Marcus, L. F. 1988. Traditional morphometrics. Pp. 179-200. *In* F. J. Rohlf, and F. L. Bookstein, eds. *Michigan Morphometrics Workshop*. University of Michigan Museum of Zoology, University of Michigan, Ann Arbor, Michigan.
- Mayr, E., E. G. Linsley, and R. L. Usinger. 1953. *Methods and principles of systematic zoology*. McGraw-Hill, New York.
- Mayr, E. E. 1942. *Systematics and the Origin of Species*. Columbia University Press, New York.
- Mayr, E. E. 1969. *Principles of systematic zoology*. McGraw-Hill, New York.
- McClain, C. R., N. A. Johnson, and M. A. Rex. 2004. Morphological disparity as a biodiversity metric in lower bathyal and abyssal gastropod assemblages. *Evolution* 58:338-348.
- McNamara, K. J. 1986. A Guide to the Nomenclature of Heterochrony. *Journal of Paleontology* 60:4-13.
- Merrill, G. K., and S. M. Merrill. 1974. Pennsylvanian nonplatform conodonts, IIa: The dimorphic apparatus of *Idioprioniodus*. *Geologica et Palaeontologica* 8:119-130.
- Mishler, B. D., and M. J. Donoghue. 1982. Species concepts: a case for pluralism. *Systematic Zoology* 31:491-503.
- Murphy, M. A., and M. K. Cebecioglu. 1984. The *Icriodus steinachensis* and *I. claudia* lineages (Devonian conodonts). *Journal of Paleontology* 58:1399-1411.

- Murphy, M. A., and M. K. Cebecioglu. 1986. Statistical study of *Ozarkodina excavata* (Branson and Mehl) and *O. tuma* Murphy and Matti (Lower Devonian, *delta* Zone, conodonts, Nevada). *Journal of Paleontology* 60:865-869.
- Murphy, M. A., and M. K. Cebecioglu. 1987. Morphometric study of the genus *Ancyrodelloides* (Lower Devonian, Conodonts), Central Nevada. *Journal of Paleontology* 61:583-594.
- Murphy, M. A., J. C. Matti, and O. H. Walliser. 1981. Biostratigraphy and Evolution of the *Ozarkodina-Remscheidensis-Eognathodus-Sulcatus* Lineage (Lower Devonian) in Germany and Central Nevada. *Journal of Paleontology* 55:747-772.
- Murphy, M. A., and K. B. Springer. 1989. Morphometric study of the platform elements of *Amydrotaxis praejohnsoni* n.sp. (Lower Devonian, Conodonts, Nevada). *Journal of Paleontology* 63:349-355.
- Murphy, M. A., J. I. Valenzuela-Rios, and P. Carls. 2004. On classification of Přídolí (Silurian)-Lochkovian (Devonian) Spathognathodontidae (conodonts). University of California, Riverside campus Museum Contribution 6.
- Nestor, H. 1997. Sediment tray cover: Silurian. Pp. 89-106. *In* A. Raukas, and A. Teedumäe, eds. *Geology and mineral resources of Estonia*. Estonian Academy Publishers, Tallinn.
- Nestor, H., and R. Einasto. 1997. Formation of the territory: Ordovician and Silurian carbonate sedimentation basin. Pp. 192-204. *In* A. Raukas, and A. Teedumäe, eds. *Geology and mineral resources of Estonia*. Estonian Academy Publishers, Tallinn.
- Pearl, R. 1928. *The rate of living*. Knopf, New York.
- Peijnenburg, K., and A. C. Pierrot-Bults. 2004. Quantitative morphological variation in *Sagitta setosa* Muller, 1847 (Chaetognatha) and two closely related taxa. *Contributions to Zoology* 73:305-315.
- Pianka, E. R. 1970. On r and K selection. *American Naturalist* 102:592-597.
- Purnell, M. A. 1993a. Feeding mechanisms in conodonts and the function of the earliest vertebrate hard tissues. *Geology* 21:375-377.
- Purnell, M. A. 1993b. The *Kladognathus* apparatus (Conodonts, Carboniferous) - Homologies with Ozarkodinids, and the Prioniodinid Bauplan. *Journal of Paleontology* 67:875-882.
- Purnell, M. A. 1994. Skeletal ontogeny and feeding mechanisms in conodonts. *Lethaia* 27:129-138.
- Purnell, M. A. 1995. Microwear on conodont elements and macrophagy in the first vertebrates. *Nature* 374:798-800.

- Purnell, M. A. 2001. Scenarios, selection and the evolution of early vertebrates. Pp. 187-208. In P. E. Ahlberg, ed. Major events in vertebrate evolution: palaeontology, phylogeny, genetics, and development. Taylor and Francis, London.
- Purnell, M. A., and P. C. J. Donoghue. 1997. Architecture and functional morphology of the skeletal apparatus of ozarkodinid conodonts. Philosophical Transactions of the Royal Society of London Series B-Biological Sciences 352:1545-1564.
- Purnell, M. A., and P. C. J. Donoghue. 1998. Skeletal architecture, homologies and taphonomy of ozarkodinid conodonts. Palaeontology 41:57-102.
- Purnell, M. A., P. C. J. Donoghue, and R. J. Aldridge. 2000. Orientation and anatomical notation in conodonts. Journal of Paleontology 74:113-122.
- Raup, D., and S. M. Stanley. 1978. Principles of Paleontology. W. H. Freeman, San Francisco.
- Raup, D. M. 1977. Probabilistic models in evolutionary paleobiology. American Scientist 65:50-57.
- Renaud, S., and C. Girard. 1999. Strategies of survival during extreme environmental perturbations: evolution of conodonts in response to the Kellwasser crisis (Upper Devonian). Palaeogeography Palaeoclimatology Palaeoecology 146:19-32.
- Rexroad, C. B., and W. W. Craig. 1971. Restudy of conodonts from the Bainbridge Formation (Silurian) at Lithium, Missouri. Journal of Paleontology 45:684-703.
- Ritter, S. M. 1989. Morphometric patterns in Middle Triassic *Neogondolella mombergensis* (Conodonts), Fossil Hill, Nevada. Journal of Paleontology 63:233-245.
- Rohlf, F. J. 1986. Relationships among eigenshape analysis, Fourier analysis, and analysis of coordinates. Mathematical Geology 18:845-854.
- Rohlf, F. J. 2003a. tps Utility program, Version 1.26.
- Rohlf, F. J. 2003b. tpsDIG, Version 1.37.
- Roopnarine, P. D., G. Byars, and P. Fitzgerald. 1999. Anagenetic evolution, stratophenetic patterns, and random walk models. Paleobiology 25:41-57.
- Roopnarine, P. D., M. A. Murphy, and N. Buening. 2004. Microevolutionary dynamics of the Early Devonian conodont *Wurmiella* from the Great Basin of Nevada. Palaeontologia Electronica 8:Article 3.
- Ruiz, F., M. L. Gonzalez-Regalado, J. M. Munoz, J. G. Pendon, A. Rodriguez-Ramirez, L. Caceres, and J. R. Vidal. 2003. Population age structure techniques and ostracods: Applications in coastal hydrodynamics and paleoenvironmental analysis. Palaeogeography Palaeoclimatology Palaeoecology 199:51-69.

- Schatz, M., J. Tait, V. Bachtadse, H. Heinisch, and H. Soffel. 2002. Palaeozoic geography of the Alpine realm, new palaeomagnetic data from the Northern Greywacke Zone, Eastern Alps. *International Journal of Earth Sciences* 91:979-992.
- Scotese, C. R. 2001. Atlas of Earth History, Volume 1, Paleogeography, PALEOMAP Project. <http://www.scotese.com/>.
- Sharma, S. 1996. Applied multivariate techniques. John Wiles & Sons, Inc, New York.
- Shaw, P. A. J. 2003. Multivariate statistics for the environmental sciences. Hodder Arnold, London.
- Sheets, H. D., and C. E. Mitchell. 2001. Why the null matters: statistical tests, random walks and evolution. *Genetica* 112:105-125.
- Simpson, G. G. 1944. Tempo and mode in evolution. Columbia University Press, New York.
- Sloan, T. R. 2003. Results of a new outline-based method for the differentiation of conodont taxa. Pp. 389-404. *In* R. Mawson, and J. A. Taylor, eds. Second Australian conodont Symposium (AUSCOS II). Courier Forschungsinstitut Senckenberg, Orange, Australia.
- Smith, G. R. 1988. Homology in morphometrics and phylogenetics. Pp. 325-338. *In* F. J. Rohlf, and F. L. Bookstein, eds. Michigan Morphometrics Workshop. University of Michigan Museum of Zoology, University of Michigan, Ann Arbor, Michigan.
- Sokal, R. R., and T. J. Crovello. 1970. The biological species concept: a critical review. *American Naturalist* 104:127-153.
- Stone, J. 1987. Review of investigative techniques used in the study of conodonts. Pp. 17-34. *In* R. L. Austin, ed. Conodonts: investigative techniques and applications. Ellis Horwood Ltd, Chichester.
- Straney, D. O. 1988. Median axis methods in morphometrics. Pp. 179-200. *In* F. J. Rohlf, and F. L. Bookstein, eds. Michigan Morphometrics Workshop. University of Michigan Museum of Zoology, University of Michigan, Ann Arbor, Michigan.
- Sweet, W. C. 1988. The Conodonta: morphology, taxonomy, paleoecology, and evolutionary history of a long-extinct animal phylum. Clarendon Press, Oxford.
- Sweet, W. C., and P. C. J. Donoghue. 2001. Conodonts: Past, present, future. *Journal of Paleontology* 75:1174-1184.
- Telford, P. G. 1975. Lower and middle Devonian conodonts from the Broken River embayment North Queensland, Australia. Special Papers in Palaeontology Number 15. Palaeontological Association, London.
- Tolmacheva, T., and A. Löfgren. 2000. Morphology and paleogeography of the Ordovician conodont *Paracordylodus gracilis* Lindström, 1955. *Journal of Paleontology* 74:1114-1121.

- Tolmacheva, T. Y., and M. A. Purnell. 2002. Apparatus composition, growth, and survivorship of the lower Ordovician conodont *Paracordylodus gracilis* Lindström, 1955. *Palaeontology* 44:209-228.
- Velhagen, W. A., and V. L. Roth. 1997. Scaling of the mandible in squirrels. *Journal of Morphology* 232:107-132.
- Villier, L., and G. J. Eble. 2004. Assessing the robustness of disparity estimates: the impact of morphometric scheme, temporal scale, and taxonomic level in spatangoid echinoids. *Paleobiology* 30:652-665.
- von Bitter, P. H., and M. A. Purnell. 2005. An experimental investigation of post-depositional taphonomic bias in conodonts. Pp. 39-56. *In* M. A. Purnell, and P. C. J. Donoghue, eds. *Conodont Biology and Phylogeny: interpreting the fossil record*. Palaeontological Association, London.
- von Bitter, P. H., M. A. Purnell, C. A. Stott, and D. K. Tetreault. in review. A fossil Lagerstätte with exceptional preservation of 'typical' marine and nearshore biotas. *Geology*.
- Walliser, O. H. 1964. Conodonten des Silurs. *Abhandlungen des Hessischen Landesamtes für Bodenforschung* 41:1-106.
- Walmsley, V. G., R. J. Aldridge, and R. L. Austin. 1974. Brachiopod and conodont faunas from the Silurian and lower Devonian of Bohemia. *Geologica et Palaeontologica* 8:39-47.
- Wenzel, B., and M. M. Joachimski. 1996. Carbon and oxygen isotopic composition of Silurian brachiopods (Gotland/Sweden): Palaeoceanographic implications. *Palaeogeography Palaeoclimatology Palaeoecology* 122:143-166.
- Wheeler, Q. D., and R. Meier. 2000. *Species concepts and phylogenetic theory: a debate*. Columbia University Press, New York.
- Wiens, J. J. 2004. What is speciation and how should we study it? *American Naturalist* 163:914-923.
- Willig, M. R., R. D. Owen, and R. L. Colbert. 1986. Assessment of morphometric variation in natural populations - the inadequacy of the univariate approach. *Systematic Zoology* 35:195-203.
- Zhang, S., and C. R. Barnes. 2002. Late Ordovician-Early Silurian (Ashgillian-Llandovery) sea level curve derived from conodont community analysis, Anticosti Island, Quebec. *Palaeogeography Palaeoclimatology Palaeoecology* 180:5-32.